THE CHEMISTRY OF η-CYCLOHEPTATRIENYL DERIVATIVES OF MOLYBDENUM AND TUNGSTEN

by

Kee-Pui Dennis Ng

A thesis submitted in part fulfillment of the requirements
for the degree of Doctor of Philosophy at the University of Oxford.

Balliol College
Oxford

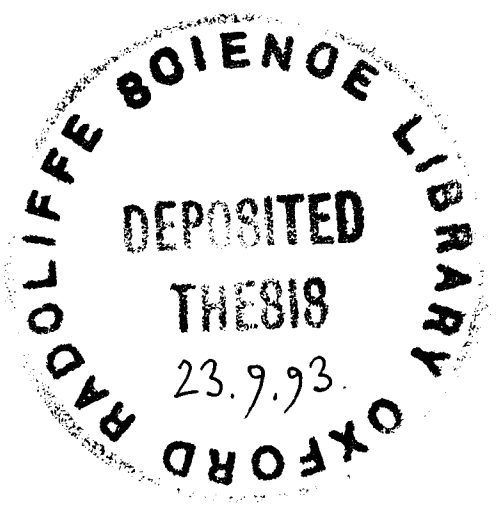

June, 1993

ABSTRACT

The Chemistry of η-Cycloheptatrienyl Derivatives of Molybdenum and Tungsten

Kee-Pui Dennis Ng
Balliol College

D. Phil.
Trinity Term, 1993

This thesis describes the synthetic, structural and reactivity studies of η-cycloheptatrienyl-molybdenum and -tungsten chemistry.

Chapter 1 presents an overview of the chemistry of η-cycloheptatrienyl derivatives of transition metals, in particular group 6 metals. The functional group properties of the η-cycloheptatrienyl ligand are also discussed.

Chapter 2 describes the synthesis of $[Mo(\eta\text{-}C_7H_7)(\eta^5\text{-}C_7H_9)]$ from $MoCl_5$ or $[MoCl_4(thf)_2]$, which provides a convenient route to η-cycloheptatrienyl-molybdenum compounds, such as $[Mo(\eta\text{-}C_7H_7)LX_2]$ and $[Mo(\eta\text{-}C_7H_7)L_2X]$, where L = tertiary phosphines or acetonitrile and X = halogen, $[NBu_4][Mo(\eta\text{-}C_7H_7)I_3]$, $[Mo(\eta\text{-}C_7H_7)(\eta\text{-}C_5H_4R)]$ (R = H or Me) and $[Mo(\eta\text{-}C_7H_7)(\eta^5\text{-}C_9H_7)]$. The X-ray crystal structures of $[Mo(\eta\text{-}C_7H_7)(MeCN)I_2]$, $[NBu_4][Mo(\eta\text{-}C_7H_7)I_3]$ and $[Mo(\eta\text{-}C_7H_7)(\eta\text{-}C_5H_4Me)]$ are presented. The compound $[Mo(\eta\text{-}C_7H_7)(MeCN)I_2]$, mixed with Me_3SiCH_2MgCl, is a catalyst for ring-opening polymerisation of norbornene giving *trans* polymer exclusively. The electron-transfer complexes $[Mo(\eta\text{-}C_7H_7)(\eta\text{-}C_5H_4Me)][tcne]$ and $\{[Mo(\eta\text{-}C_7H_7)(\eta\text{-}C_5H_5)]_2[tcnq]\}$ and the intercalation compound $\{ZrS_2[Mo(\eta\text{-}C_7H_7)(\eta\text{-}C_5H_4Me)]_{0.22}\}$ are also described.

An extension of these synthetic pathways to tungsten is described in **chapter 3**. Reduction of WCl_6 with sodium amalgam in the presence of cycloheptatriene gives $[W(\eta\text{-}C_7H_7)(\eta^5\text{-}C_7H_9)]$, which is a precursor to the compounds $[W(\eta\text{-}C_7H_7)(MeCN)I_2]$, $[W(\eta\text{-}C_7H_7)(PMe_3)X_2]$ (X = Br or I), $[W(\eta\text{-}C_7H_7)(dmpe)I]$, $[W(\eta\text{-}C_7H_7)(\eta\text{-}C_5H_4R)]$ (R = H or Me) and $[Mo(\eta\text{-}C_7H_7)(\eta^5\text{-}C_9H_7)]$. The $[W(\eta\text{-}C_7H_7)(MeCN)I_2]$ / Me_3SiCH_2MgCl system is an active catalyst for ring opening polymerisation of norbornene. The electronic

structures of [W(η-C_7H_7)(η-C_5H_4R)] (R= H or Me) are discussed on the basis of their He I and He II photoelectron spectra. The intercalation of [W(η-C_7H_7)(η-C_5H_4Me)] into ZrS_2 is also described.

The magnetic properties of the 17-electron compounds [Mo(η-C_7H_7)(MeCN)I_2], [Mo(η-C_7H_7)(PMe_3)I_2], [W(η-C_7H_7)(MeCN)I_2], [W(η-C_7H_7)(PMe_3)I_2] and [W(η-C_7H_7)(PMe_3)Br_2] are discussed in **chapter 4**. They behave as one-dimensional antiferromagnets which was suggested by magnetic model fittings and the crystal structure of [Mo(η-C_7H_7)(MeCN)I_2].

Chapter 5 comprises of two parts. The first part describes a new series of binuclear thiolato-bridged molybdenum complexes [(η-$C_7H_3R^1{}_4$)Mo(μ-SR^2)$_3$Mo-(η-$C_7H_3R^1{}_4$)][BF_4] (R^1 = H or Me; R^2 = Et, Pr, Bu, Ph or CH_2Ph). Dynamic NMR studies reveal that all of these complexes (except for R^2 = Ph) are fluxional due to inversion at the pyramidal sulfur centre. Cyclic voltammetric studies show that they undergo two reversible one-electron reductions. Second part of this chapter describes the new bridging-imido compound [(η-C_7H_7)Mo(μ-NAr)$_2$Mo(η-C_7H_7)] (Ar = 2,6-diisopropylphenyl).

Chapter 6 discusses the η-1,2,4,6-tetramethylcycloheptatrienyl-molybdenum system. The new η-tetramethylcycloheptatriene molybdenum compounds [M'(η-$C_7H_4Me_4$-1,3,5,7)], [M'(η-$C_7H_4Me_4$-1,2,4,6)] and [M'(η-$C_7H_4Me_4$-1,3,4,6)], M' = $Mo(CO)_3$, and new η-tetramethylcycloheptatrienyl-molybdenum compounds [M"$(CO)_3$]$^+$, [M"$(CO)_2$Cl], [M"(dmpe)Cl], [M"(η-C_6H_5Me)]$^+$ and [M"(acac)(PPh_3)], M" = Mo(η-$C_7H_3Me_4$-1,2,4,6), and [Mo(η^3-$C_7H_3Me_4$-1,2,4,6)(dmpe)$(CO)_2$Cl] are described.

Chapter 7 gives the experimental details for the work described in preceeding chapters. **Appendix A** presents characterising data for all the new compounds and previously unreported data for known compounds. Crystallographic details for the X-ray structure determinations and X-ray powder diffraction data are listed in **Appendix B** and **C** respectively.

The work described in this thesis was carried out in the Inorganic Chemistry Laboratory, South Parks Road, Oxford, from October 1990 to April 1993 under the supervision of Professor M. L. H. Green F. R. S.. All the work is my own unless stated to the contrary, and has not previously been submitted for a degree at this, or any other, University.

ACKNOWLEDGEMENTS

Firstly, I would like to express my deepest gratitude to my supervisor, Prof. M. L. H. Green F. R. S. for his inspiration, support and help during the past three years.

This research work was made possible only with the efforts of many brainy people. Dr. Andy Hughes showed me various aspects of NMR and Dr. Peter Scott introduced me cyclic voltammetry. Dr. Paddy McGowan collected the X-ray data of [Mo(η-C_7H_7)(MeCN)I_2]. Despo Michaelidou and Adam Stephens measured some of the mass spectra and Richard Douthwaite ran some of the EPR spectra. Sherman Fung ran some emergency NMR spectra in the Dyson Perrins Laboratory. Dr. Philip Wiseman and Dr. Anjana Chaudhuri helped with magnetic susceptibility measurements. Frank Arnold initiated the electron-transfer complex project. Dr. Dermot O'Hare was responsible for helpful discussions in organometallic solid state chemistry. To all these people I acknowledge my gratitude.

Of the co-workers who made specific contributions, I would like to thank Dr. Andrew Harrison, who passed me some of his knowledge in magnetism and Dr. Philip Mountford and Dr. Alexander Chernega for solving the crystal structures. I also owe Philip for teaching me a bit of crystallography. Thanks are due to Dr. Jenny Green and Christian Whitaker for measuring the PE spectra and helpful discussion. Dr. Wa-Hung Leung and Vee Wong are also thanked for their collaboration in preparing the bridging-imido and intercalation compounds, respectively.

The whole manuscript was painstakingly reviewed by Prof. Malcolm Green, John Turner, Adam Stephens, Richard Douthwaite and Neil Popham. Their comments and criticisms are gratefully acknowledged.

My thanks also go to the other members of Green's groups and O'Hare's group, past and present, who have created such an enjoyable environment to work in.

Particular thanks are due to the Croucher Foundation of Hong Kong for offering me a scholarship.

Finally, I owe heartfelt thanks to my wife, Jessica, for her constant understanding, support and encouragement.

To Mum, Dad and Jessica

CONTENTS

LIST OF FIGURES

LIST OF TABLES

ABBREVIATIONS

General :

Me	methyl
Et	ethyl
Pr	propyl
Pr^{i}	isopropyl
Bu	butyl
Bu^{t}	tert-butyl
Ph	phenyl
acacH	pentane-2,4-dione
dme	1,2-dimethoxyethane
dmpe	1,2-bis(dimethylphosphino)ethane
dppe	1,2-bis(diphenylphosphino)ethane
dppm	bis(diphenylphosphino)methane
en	ethylenediamine
tmen	N,N,N',N'-tetramethylethylenediamine
tcne	tetracyanoethene
tcnq	7,7,8,8-tetracyanoquinodimethane
thf	tetrahydrofuran
L	2-electron donor ligand
X	1-electron donor ligand
r.t.	room temperature

Nuclear Magnetic Resonance (NMR) data :

{^{1}H}	proton decouple	δ	chemical shift
J	coupling constant in Hz	ppm	parts per million
s	singlet	d	doublet
t	triplet	q	quartet
sep	septet	m	multiplet
br s	broad signal	vt	virtual triplet
DEPT	distortionless enhancement by polarization transfer		

Electron Paramagnetic Resonance (EPR) data :

A^{Mo}	hyperfine splitting constant due to ^{95}Mo and ^{97}Mo

Mass Spectrometric (MS) data :

m/z	mass/charge	M+	molecular ion
FAB	fast atom bombardment	EI	electron impact

Infra-red (IR) data :

vs	very strong	s	strong
sh	shoulder	m	medium
w	weak		

Cyclic Voltammetric (CV) data :

SCE	saturated calomel electrode	$E_{1/2}$	half-wave potential
Fc	ferrocene	ΔE_p	peak separation

CHAPTER ONE

Introduction

1.1 General

Organotransition metal chemistry has continued to grow rapidly during the past decade. A rich abundance of new metal complexes with a variety of ligands have been synthesised and structurally characterised; they have contributed to the development of areas such as homogeneous catalysis,[1] organic synthesis,[1] new materials[2] and biological sciences.[3]

Among the ligands being studied, the η-cyclopentadienyl group (η-C_5R_5) is one of the most common classes of ligand encountered in organotransition metal chemistry. Complexes of this ligand class are known for all the transition metals. There are many methods for preparing η-cyclopentadienyl-metal complexes[4] but perhaps the most general one is the treatment of substitution-labile metal halides with salts of the $C_5R_5^-$ anion. The η-C_5H_5 ligand and its substituted derivatives, such as η-C_5H_4Me and η-C_5Me_5, are normally inert and behave as spectator ligands during reactions at the metal centre.

The chemistry of benzenoid-metal complexes has also been studied extensively[5,6] since the first preparation of [Cr(η-C_6H_6)$_2$] by Fischer and Hafner.[7] The recent advances in metal vapour synthesis technique stimulated the development in this area and many M(η-arene) complexes which as yet cannot be prepared by other methods can be synthesised by means of co-condensation techniques.[8]

Although η-cycloheptatrienyl-transition metal complexes have been known for over thirty years,[9] surprisingly, the organometallic chemistry of cycloheptatrienyl ligand has been largely neglected in comparison with that of cyclopentadienyl and arene ligands. A substantial barrier to the development of η-cycloheptatrienyl-transition metal chemistry has been the difficulty of finding convenient synthetic routes. The objective of the work described in this thesis was to explore new synthetic pathways to η-cycloheptatrienyl-molybdenum and -tungsten derivatives so as to extend our knowledge of the chemistry of this potentially useful ligand class.

This chapter comprises a brief review of the chemistry of η-cycloheptatrienyl derivatives of transition metals, in particular the group 6 metals. A comprehensive review of this area has appeared,[10] thus in the following sections, no attempt has been made to cover all the material; only a selection of the work most relevant to this thesis will be presented and evidence for the functional group properties of the η-cycloheptatrienyl ligand will be reviewed.

1.2 η-Cycloheptatrienyl Complexes of the Group 4 Metals

A number of η-cycloheptatrienyl derivatives of group 4 metals have been reported which are summarised in Table 1.1.

Table 1.1 η-Cycloheptatrienyl derivatives of the group 4 metals

Compound		Reference
$[M(\eta\text{-}C_7H_7)(\eta\text{-}C_5R_5)]$	M = Ti, R = H or Me	11, 12, 14a
	M = Zr, R = H or Me	13,14
	M = Hf, R = Me	14
$[M(\eta\text{-}C_7H_7)(\eta^5\text{-}C_7H_9)]$	M = Ti, Zr or Hf	15, 16, 17, 18
$[Zr(\eta\text{-}C_7H_7)(\eta^5\text{-}C_7H_9)(PMe_3)]$		17
$[(\eta\text{-}C_7H_7)(\eta^5\text{-}C_7H_9)Zr(\mu\text{-dmpe})Zr(\eta^5\text{-}C_7H_9)(\eta\text{-}C_7H_7)]$		17
$[M(\eta\text{-}C_7H_7)(\eta^5\text{-}C_9H_7)]$	M = Ti, Zr or Hf	19, 20
$[M(\eta\text{-}C_7H_7)(\eta^5\text{-}C_9H_7)(PMe_3)]$	M = Zr or Hf	20
$[(\eta\text{-}C_7H_7)(\eta^5\text{-}C_9H_7)Hf(\mu\text{-dmpe})Hf(\eta^5\text{-}C_9H_7)(\eta\text{-}C_7H_7)]$		20
$[M(\eta\text{-}C_7H_7)(thf)(\mu\text{-}Cl)]_2$	M = Ti or Zr	15, 17
$[(\eta\text{-}C_7H_7)(PMe_3)Ti(\mu\text{-}Cl)_2Ti(\eta\text{-}C_7H_7)]$		15
$[M(\eta\text{-}C_7H_7)L_2X]$	M = Ti, L = PMe_3, X = Cl	15
	M = Ti, L_2 = bidentate phosphine, dme or tmen	
	X = Cl, Me, Et or H→BH_3	15
	M = Zr, L = thf or PMe_3, X = Cl or I	17, 21
	M = Zr, L_2 = dmpe, dme or tmen, X = Cl	17

The mixed sandwich compounds [M(η-C_7H_7)(η-C_5R_5)] (M = Ti, Zr or Hf; R = H or Me) can be prepared by reduction of the corresponding metal halides in the presence of cycloheptatriene. For example, treatment of [M(η-C_5H_5)Cl_3] (M = Ti or Zr) with isopropylmagnesium bromide in the presence of C_7H_8 gives the diamagnetic 16-electron complexes [M(η-C_7H_7)(η-C_5H_5)] (M = Ti or Zr) (Scheme 1.1).[11a,13] Other reducing agents such as magnesium, aluminium and zinc can also be used.[11b]

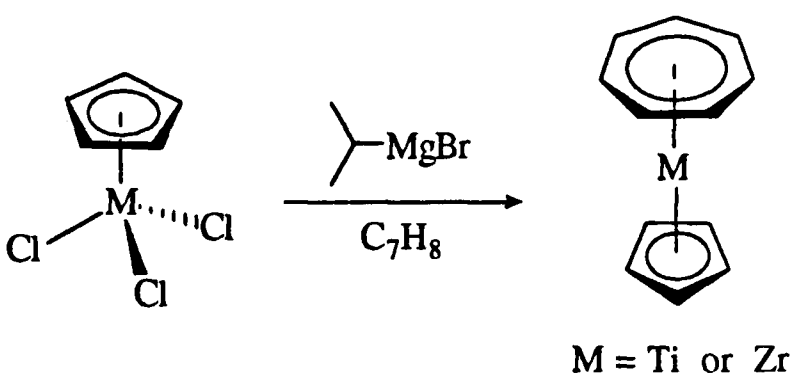

Scheme 1.1

Similar reactions carried out on $TiCl_3$ yield the isoelectronic complex [Ti(η-C_7H_7)(η^5-C_7H_9)].[16a,b] An improved route to this compound has been reported by Timms and Turney which involves the co-condensation of titanium vapour and cycloheptatriene.[16c] The Zr and Hf congeners have been prepared similarly.[18] It has been found that heating [Ti(η-$C_6H_5Me)_2$], which is only available from metal vapour synthesis,[8d] with $(AlEt_2Cl)_2$ and two equivalents of cycloheptatriene in thf at 80^{0}C for 2 h affords [Ti(η-C_7H_7)(η^5-C_7H_9)] in gram quantities and the yield is excellent. However, when the reaction is carried out at room temperature over a period of weeks, with the minimum quantity of solvent and $(AlEt_2Cl)_2$, together with a considerable excess of cycloheptatriene, the novel dimer [Ti(η-C_7H_7)(thf)(μ-Cl)]$_2$ can be isolated in *ca.* 30 % yield (Scheme 1.2).[15] The dimer is an excellent precursor to other Ti(η-C_7H_7) derivatives. For example, it reacts with an excess of PMe_3 to give [Ti(η-C_7H_7)(PMe_3)$_2$Cl]. It also reacts with bidentate ligands, such as dme, tmen, dppe or dmpe

to afford the 16-electron complexes [Ti(η-C_7H_7)L_2Cl], which upon alkylation with Grignard reagents (RMgX) yield the corresponding [Ti(η-C_7H_7)L_2R].[15]

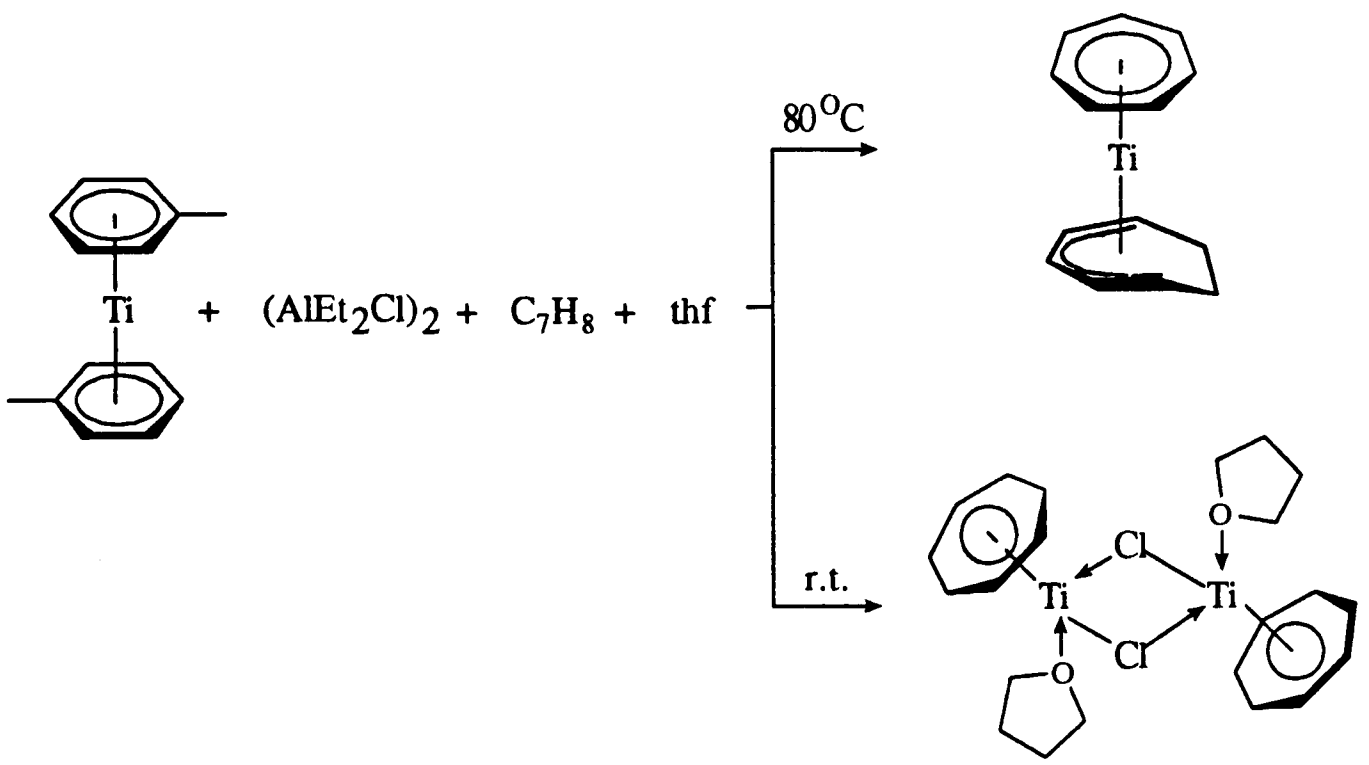

Scheme 1.2

Recently, Green and Walker have reported a one-pot synthesis of [Zr(η^6-C_7H_8)$_2$] by reducing $ZrCl_4$ with sodium amalgam in the presence of cycloheptatriene at < -10 °C (Scheme 1.3).[17] When this reaction is carried out at room temperature an inseparable mixture of [Zr(η^6-C_7H_8)$_2$] and [Zr(η-C_7H_7)(η^5-C_7H_9)] is formed which is in contrast to the related titanium chemistry.[16a,b] In the absence of Lewis bases, the compound [Zr(η^6-C_7H_8)$_2$] is stable to hydrogen migration. It has also been demonstrated that the compound [Zr(η^6-C_7H_8)$_2$] has high reactivity and can be used to prepare other Zr(η-C_7H_7) compounds. For example, treatment of [Zr(η^6-C_7H_8)$_2$] with $(AlEt_2Cl)_2$ in thf gives the dimer [Zr(η-C_7H_7)(thf)(μ-Cl)]$_2$, which has a similar reaction pattern to the titanium analogue.[17] Oxidation of [Zr(η^6-C_7H_8)$_2$] with iodine in thf yields the compound [Zr(η-C_7H_7)(thf)$_2$I] (Scheme 1.3), which on addition of PMe_3 affords [Zr(η-C_7H_7)(PMe_3)$_2$I].[21]

Reduction of MCl_4 (M = Zr or Hf) with two equivalents of sodium amalgam in the presence of two equivalents of PR_3 and an excess of cycloheptatriene gives $[M(\eta^6\text{-}C_7H_8)(PR_3)_2Cl_2]$ (M = Zr or Hf) in moderate yield. These react with lithium indenide to give the mixed sandwich compounds $[M(\eta\text{-}C_7H_7)(\eta^5\text{-}C_9H_7)]$ (M = Zr or Hf) (Scheme 1.4). Upon treatment with PMe_3 or dmpe, they give the 18-electron compounds $[M(\eta\text{-}C_7H_7)(\eta^5\text{-}C_9H_7)(PMe_3)]$ (M = Zr or Hf) or $[(\eta\text{-}C_7H_7)(\eta^5\text{-}C_9H_7)Hf(\mu\text{-dmpe})Hf(\eta^5\text{-}C_9H_7)(\eta\text{-}C_7H_7)]$, respectively.[20]

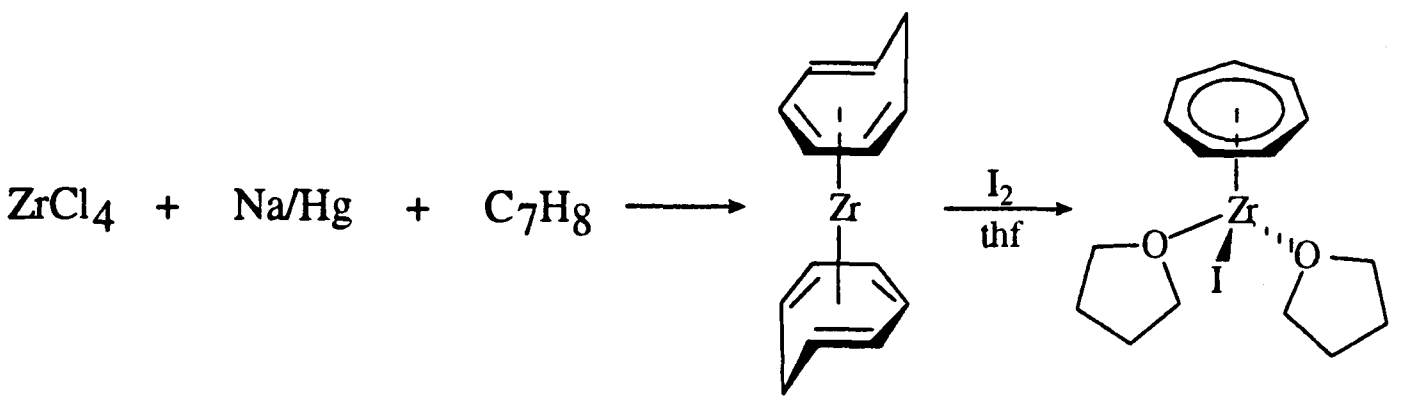

Scheme 1.3

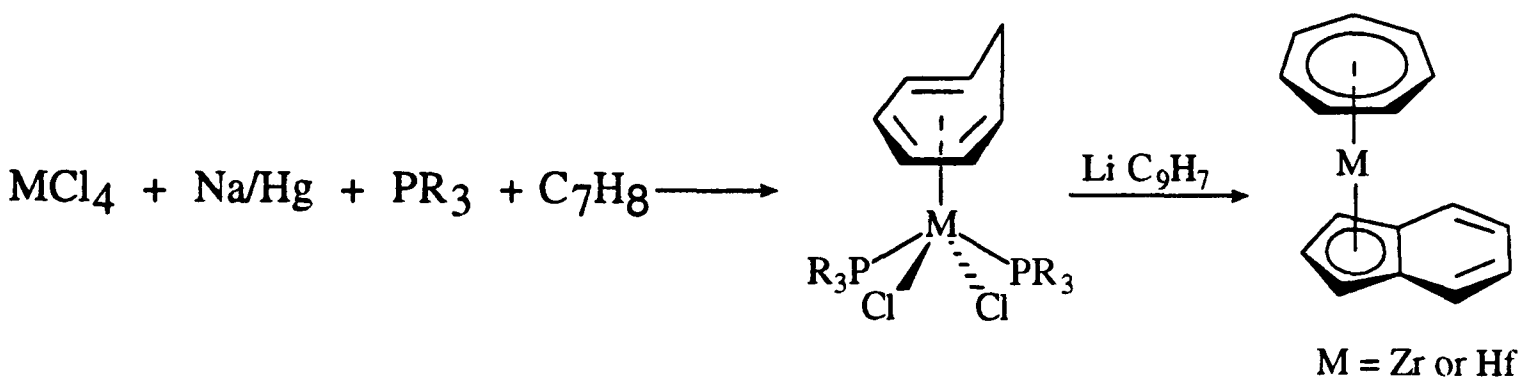

Scheme 1.4

1.3 η-Cycloheptatrienyl Complexes of the Group 5 Metals

Table 1.2 summarises the known η-cycloheptatrienyl derivatives of group 5 metals.

Table 1.2 η-Cycloheptatrienyl derivatives of the group 5 metals

Compound		Reference
$[V(\eta^6\text{-}C_7H_8)_2]$		16b, 16c, 22
$[V(\eta\text{-}C_7H_7)(\eta^5\text{-}C_7H_9)]$		16b, 16c
$[V(\eta\text{-}C_7H_7)(\eta^6\text{-}C_7H_8)]^+$		22
$[V(\eta\text{-}C_7H_7)_2]^{2+}$		22
$[M(\eta\text{-}C_7H_7)(CO)_x(PMe_3)_{3-x}]$	M = V; x = 3	23
	M = Nb; x = 1, 2 or 3	24, 25
$[Nb(\eta\text{-}C_7H_7)(CO)(dmpe)]$		25
$[Nb(\eta\text{-}C_7H_7)(\eta^4\text{-}C_7H_8)L]$	L = CO or PMe_3	24, 25
$[Nb(\eta\text{-}C_7H_7)(\eta^4\text{-}C_4H_6)(PMe_3)]$		25
$[Nb(\eta\text{-}C_7H_7)(\eta^5\text{-}C_7H_9)(PMe_3)]^+$		25
$[M(\eta\text{-}C_7H_7)(\eta\text{-}C_5H_4R)]$	M = V, R = H	26
	M = Nb, R = H or Me	13, 25
	M = Ta, R = Me	27
$[Nb(\eta\text{-}C_7H_7)(\eta\text{-}C_5H_4R)Br]$	R = H or Me	25
$[V(\eta\text{-}C_7H_7)(\eta\text{-}C_5H_5)]^+$		28
$[Nb(\eta\text{-}C_7H_7)(\eta\text{-}C_5H_4Me)(thf)]^+$		27
$[Nb(\eta\text{-}C_7H_7)(\eta\text{-}C_5H_5)]^-$		27
$[Nb(\eta\text{-}C_7H_7)(PMe_3)_2I]$		25

Treatment of $[V(CO)_6]$ with cycloheptatriene produces $[V(\eta\text{-}C_7H_7)(CO)_3]$.[23] Several monosubstituted η-cycloheptatrienyl-vanadium compounds have also been obtained by reaction of $[V(CO)_6]$ with C_7H_7R (R = Me, Ph, CN, OMe, OEt, OPr or CO_2Et).[29]

The paramagnetic compound $[V(\eta^6\text{-}C_7H_8)_2]$ has been prepared by reduction of VCl_4 with isopropylmagnesium bromide in the presence of cycloheptatriene.[16b,22] The co-condensation of vanadium vapour with cycloheptatriene gives a thermally stable compound which was formulated as $[V(\eta\text{-}C_7H_7)(\eta^5\text{-}C_7H_9)]$.[16c] However, these two compounds have not been structurally characterised. It has been reported that compound $[V(\eta^6\text{-}C_7H_8)_2]$ reacts with $[CPh_3][BF_4]$ in two successive steps to yield eventually the dication $[V(\eta\text{-}C_7H_7)_2]^{2+}$ (Scheme 1.5).[22]

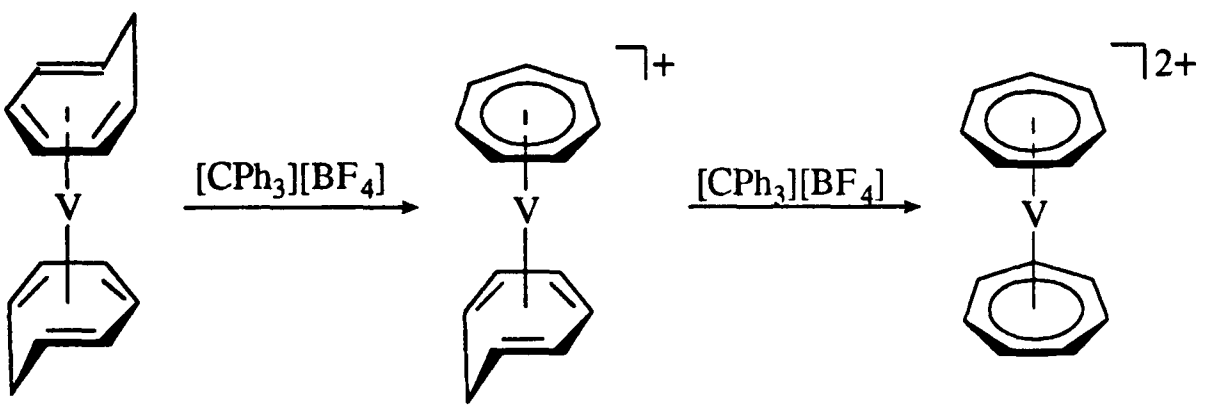

Scheme 1.5

Recently, Green and Scott have developed new routes to η-cycloheptatrienyl derivatives of niobium.[25] By the reduction of $[NbCl_4(thf)_2]$ with sodium amalgam or magnesium turnings in the presence of cycloheptatriene and other ligands, such as PMe_3 or carbon monoxide, $[Nb(\eta^6\text{-}C_7H_8)(PMe_3)_2Cl_2]$, $[Nb(\eta\text{-}C_7H_7)(\eta^4\text{-}C_7H_8)(PMe_3)]$ or $[Nb(\eta\text{-}C_7H_7)(CO)_3]$ can be isolated (Scheme 1.6). These compounds can be used to prepare other $Nb(\eta\text{-}C_7H_7)$ derivatives, such as $[Nb(\eta\text{-}C_7H_7)L_2L']$ (L_2 = dmpe, $\eta^4\text{-}C_7H_8$, $\eta^4\text{-}C_4H_6$; L, L' = CO or PMe_3), $[Nb(\eta\text{-}C_7H_7)(\eta^5\text{-}C_7H_9)(PMe_3)]^+$, $[Nb(\eta\text{-}C_7H_7)(PMe_3)_2I]$, $[Nb(\eta\text{-}C_7H_7)(\eta\text{-}C_5H_4R)Br]$ and $[Nb(\eta\text{-}C_7H_7)(\eta\text{-}C_5H_4R)]$ (R = H or Me).

The sandwich compounds $[M(\eta\text{-}C_7H_7)(\eta\text{-}C_5H_4R)]$ (M = V, Nb or Ta; R = H or Me) can also be prepared by a reductive method, but in general the yields of these reactions are low.[13,26c,27] For example, the first η-cycloheptatrienyl-tantalum compound, namely $[Ta(\eta\text{-}C_7H_7)(\eta\text{-}C_5H_4Me)]$ has been synthesised in 12 % yield by treating $[Ta(\eta\text{-}C_5H_4Me)Cl_4]$ with magnesium turnings in the presence of cycloheptatriene.[27] The mixed sandwich compounds are redox active and some of the products of oxidation and reduction have been isolated[28] and structurally characterised.[27]

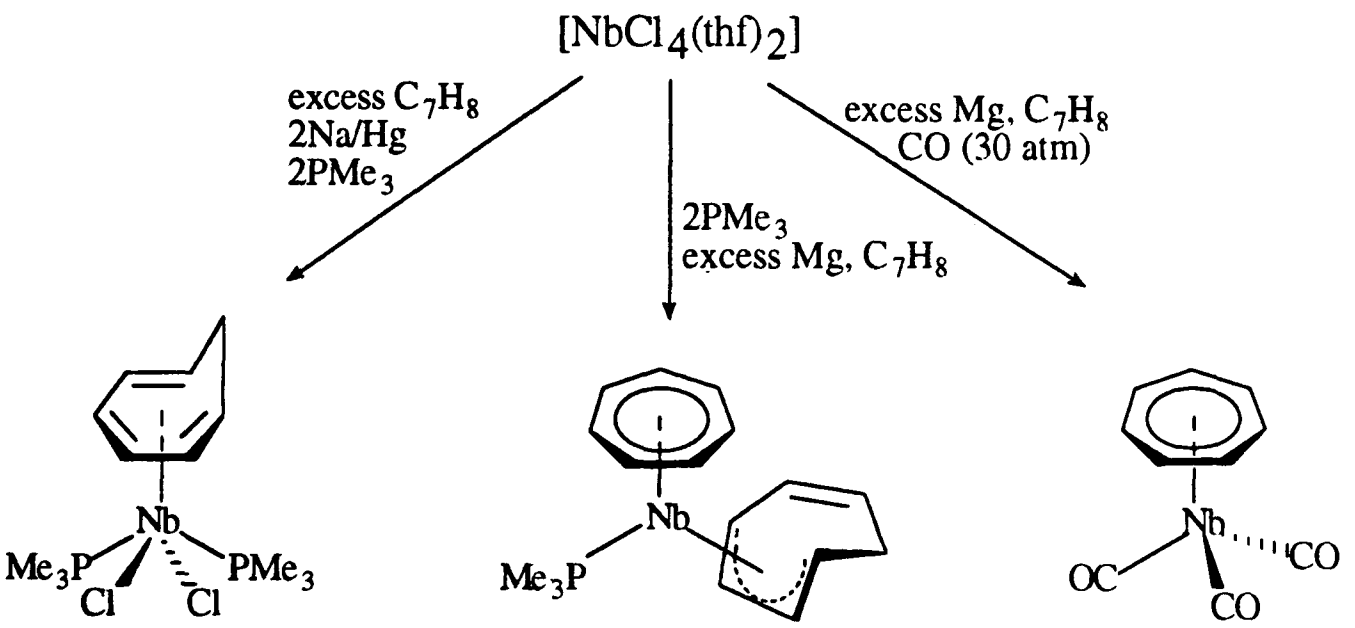

Scheme 1.6

1.4 η-Cycloheptatrienyl Complexes of the Group 6 Metals

The chemistry of η-cycloheptatrienyl complexes of group 6 metals is more developed in comparison with that of other transition metals. Generally speaking, there are three main synthetic pathways to $M(\eta\text{-}C_7H_7)$ (M = Cr, Mo or W) derivatives which employ metal carbonyls, metal atoms or metal chlorides as the starting materials. In this section, the chemistry will be outlined under these headings where M represents Cr, Mo or W, unless stated otherwise.

1.4.1 From metal carbonyls

Metal carbonyls $[M(CO)_6]$ are good starting materials to some synthetically useful compounds, such as $[M(\eta\text{-}C_7H_7)(CO)_3]^+$, $[M(\eta\text{-}C_7H_7)(CO)_2X]$ (X = halogen) and $[Mo(\eta\text{-}C_7H_7)(\eta\text{-}C_6H_5R)]^+$ (R = H or Me), which can generate most of the known η-cycloheptatrienyl derivatives of group 6 metals.

1.4.1.1 $[M(\eta^6\text{-}C_7H_8)(CO)_3]$

The compounds $[M(\eta^6\text{-}C_7H_8)(CO)_3]$ have been long known. They can be prepared by refluxing $[M(CO)_6]$ in pure cycloheptatriene[30] or in high boiling solvent.[31] However, the complex $[W(\eta^6\text{-}C_7H_8)(CO)_3]$ is much more conveniently prepared from $[W(CO)_3(MeCN)_3]$ (Scheme 1.7).[32]

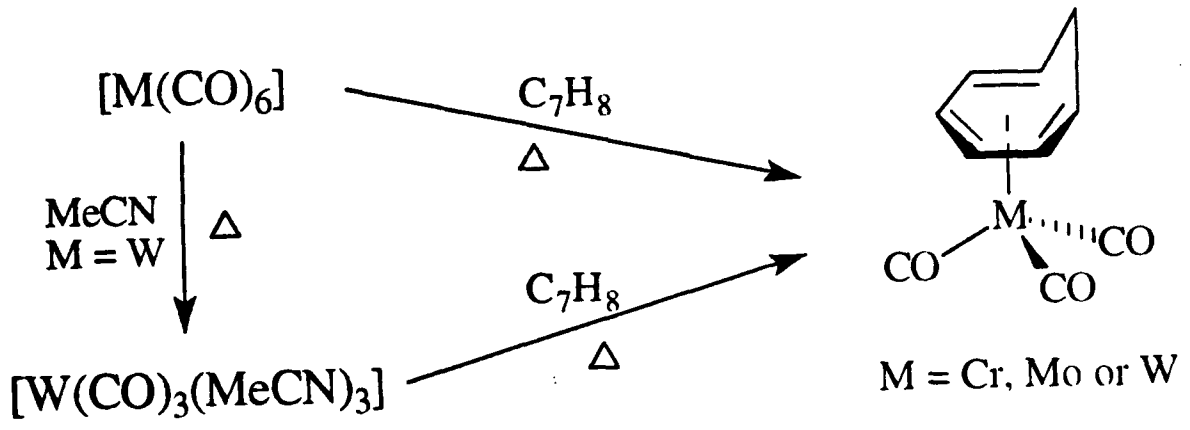

Scheme 1.7

The molecular structure of [Mo(η^6-C_7H_8)$(CO)_3$] has been determined,[33] which shows alternate single and double carbon-carbon bonds with an approximate symmetry plane passes through the molybdenum atom, one carbonyl group and the methylene group.

The ^{13}C NMR spectra of [M(η^6-C_7H_8)$(CO)_3$] give only one signal corresponding to all three carbonyl resonances at room temperature. However, at -60^{0}C, two distinct signals of relative intensity 2 : 1 appear which are due to the hindered rotation about the M-ring bond. The activation energies for M-C_7H_8 rotation in these complexes have been estimated to be 47.3 - 53.1 kJ/mol.[34]

Several $M(CO)_3$ derivatives of substituted cycloheptatrienes, such as [M(η^6-C_7H_7R-7)$(CO)_3$] (M = Cr or Mo, R = Me or Ph),[30] [Mo(η^6-$C_7H_5Me_3$-3,7,7)$(CO)_3$],[31a] [Mo(η^6-$C_7H_4Me_4$-2,3,7,7)$(CO)_3$][31a] and [Cr(η^6-$C_7H_4Ph_4$-1,2,6,7)$(CO)_3$][35c] have also been prepared from the corresponding substituted cycloheptatriene and [$M(CO)_6$] or [$Cr(CO)_3(MeCN)_3$]. It has been found that methyl substituted cycloheptatriene compounds have higher thermal stability than the complexes with electronegative substituents.

The *exo*-isomers of compounds [M(η^6-C_7H_7R-7)$(CO)_3$] (M = Cr or Mo) have been shown to undergo thermal 1,5-hydrogen shifts.[35] The 7-*endo*-hydrogen migrates in a stereospecific manner as shown in Scheme 1.8 which probably involves the transition state **1**. The activation energy for rearrangement of [Cr(η^6-C_7H_7Me-7)$(CO)_3$] has been estimated to be 101.3 kJ/mol,[35c] which is significantly lower than that of the free ligand (139.3 kJ/mol).[36] This indicates the 1,5-sigmatropic shift is metal-assisted.

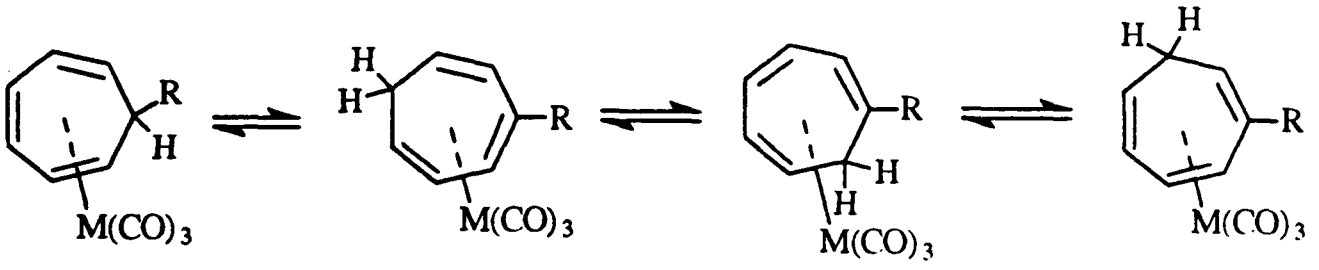

Scheme 1.8

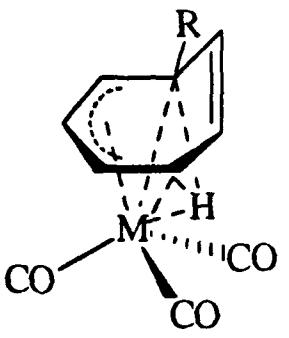

1

Some of the chemistry of $[M(\eta^6\text{-}C_7H_8)(CO)_3]$ is summarised in Scheme 1.9. The cycloheptatriene ligand in these complexes can be thermally displaced by a wide range of σ-donor ligands L such as amines, phosphines, phosphine oxides, phosphites, arsines, stibines and nitriles giving the compounds *fac*-$[M(CO)_3L_3]$.[30,37] The ligand can also be photochemically displaced by ^{14}C-labelled cycloheptatriene.[38] Although microcalorimetric studies of the thermal decomposition of $[M(\eta^6\text{-}C_7H_8)(CO)_3]$ showed that the M-C_7H_8 bond-strengths decreased in the order W > Mo > Cr,[39] the ease of release of the C_7H_8 group in these reactions was observed to decrease down the series Mo > W > Cr.[37d,38,40]

Substitution of CO ligand in $[M(\eta^6\text{-}C_7H_8)(CO)_3]$ is uncommon.[41] However photochemically induced substitutions at low temperature occur for the chromium complex giving $[Cr(\eta^6\text{-}C_7H_8)(CO)_2L]$ [L = PPh_3, PMe_3, $AsMe_3$, $P(OMe)_3$ or $P(OPh)_3$].[41b,c] Protonation of $[M(\eta^6\text{-}C_7H_8)(CO)_3]$ (M = Mo or W) with HBF_4 produces the 16-electron cations $[M(\eta^5\text{-}C_7H_9)(CO)_3]^+$ whilst protonation with HCl leads to the formation of neutral complexes $[M(\eta^5\text{-}C_7H_9)(CO)_3Cl]$.[42] An historically important reaction of $[M(\eta^6\text{-}C_7H_8)(CO)_3]$ was hydride abstraction by $[CPh_3]^+$ to yield the η-cycloheptatrienyl-metal complexes $[M(\eta\text{-}C_7H_7)(CO)_3]^+$.[9,32,43]

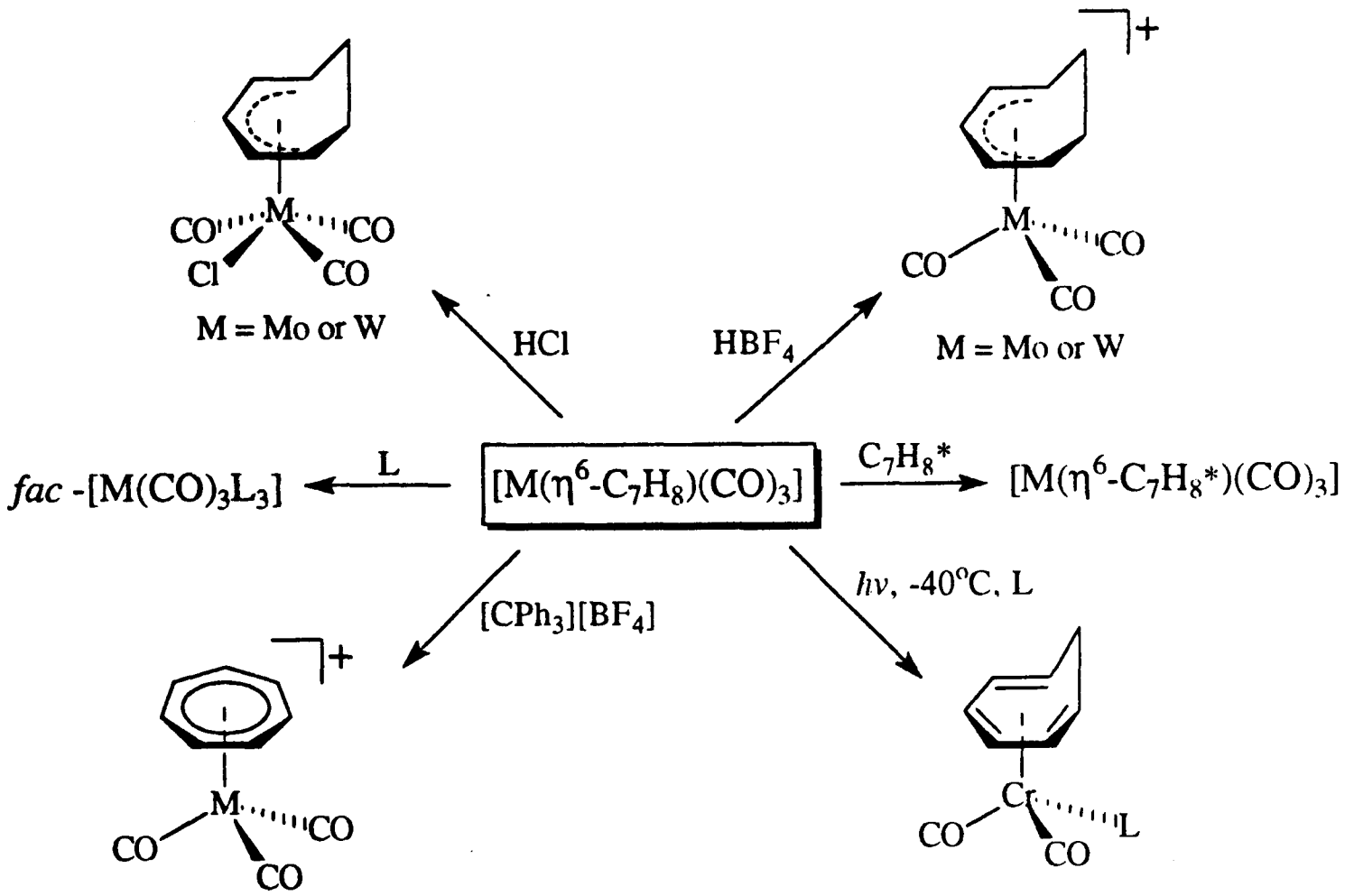

Scheme 1.9

1.4.1.2 $[M(\eta\text{-}C_7H_7)(CO)_3]^+$

The X-ray structure of $[Mo(\eta\text{-}C_7H_7)(CO)_3][BF_4]$ has confirmed that the planar C_7H_7 ring binds symmetrically to the metal.[44] The Mo-C(carbonyl) distance of 2.032 Å is substantially longer than in other $Mo(CO)_3$ complexes whilst the Mo-C(ring) distance of 2.314 Å is one of the shortest found in Mo-aromatic ring compounds. These imply that the Mo-CO bond is reasonably weak and the Mo-ring bond is strong. Comparison of the X-ray powder diffraction patterns for the Cr, Mo and W complexes suggested that these complexes are isostructural.[45]

The activation energies for ring rotation in solid $[M(\eta\text{-}C_7H_7)(CO)_3][BF_4]$ (M = Cr or Mo) have been determined by proton spin-lattice relaxation time measurements.[45] These values are quite similar (Cr, 12.8; Mo, 13.6 kJ/mol) which may reflect the fact that these complexes are isostructural with similar packing densities.

As expected, the carbonyl groups in these cationic compounds can be readily displaced by other ligands. For example, the reaction of $[M(\eta\text{-}C_7H_7)(CO)_3]^+$ (M = Mo or W) with halide or pseudohalide anions gives $[M(\eta\text{-}C_7H_7)(CO)_2X]$ (X = Cl, Br, I, OCN, SCN or N_3) (Scheme 1.10).[32,46] IR studies showed that in the X = OCN and SCN complexes the ligands are N-bonded to the metal. Interestingly, the reaction of $[W(\eta\text{-}C_7H_7)(CO)_3]^+$ with $Na_2[NCN]$ yields the unexpected product $[W(\eta\text{-}C_6H_6)(CO)_3]$ in 15 % yield as a result of ring contraction.[46]

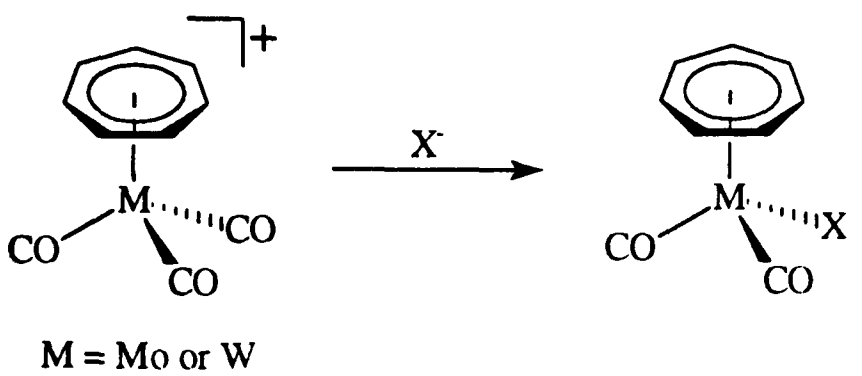

M = Mo or W

Scheme 1.10

Treatment of $[M(\eta\text{-}C_7H_7)(CO)_3]^+$ (M = Mo or W) with certain σ-donors L such as PPh_3, $AsPh_3$ or $SbPh_3$ produces mono-substituted cations $[M(\eta\text{-}C_7H_7)(CO)_2L]^+$.[47] Reaction of $[Mo(\eta\text{-}C_7H_7)(CO)_2L]^+$ with $NaBH_4$ or RLi gives the otherwise inaccessible L-substituted species $[Mo(\eta^6\text{-}C_7H_7R\text{-}7)(CO)_2L]$ (R = H, Me or Bu^t) (Scheme 1.11).[47a,b]

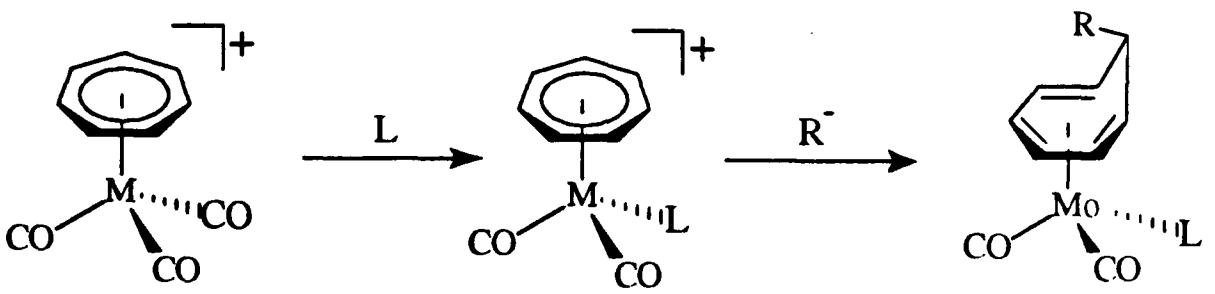

M = Mo or W

Scheme 1.11

Stone and co-workers have shown that $[Mo(\eta\text{-}C_7H_7)(CO)_3]^+$ is an useful precursor to other $Mo(\eta\text{-}C_7H_7)$ compounds. The transformations also involve the displacement of carbonyl ligand(s) and are summarised in Scheme 1.12. Reaction of $[Mo(\eta\text{-}C_7H_7)(CO)_3][BF_4]$ with Me_3SiX (X = Cl, Br or I) in thf at *ca.* 50°C provides an alternative pathway to $[Mo(\eta\text{-}C_7H_7)(CO)_2X]$. However, the use of excess Me_3SiX in refluxing thf gives instead the binuclear molybdenum complexes $[(\eta\text{-}C_7H_7)Mo(\mu\text{-}X)_3Mo(\eta\text{-}C_7H_7)]$.[48] These binuclear compounds can be readily oxidised with mild oxidising agents such as diazonium salts or iodine to give the corresponding cations. The

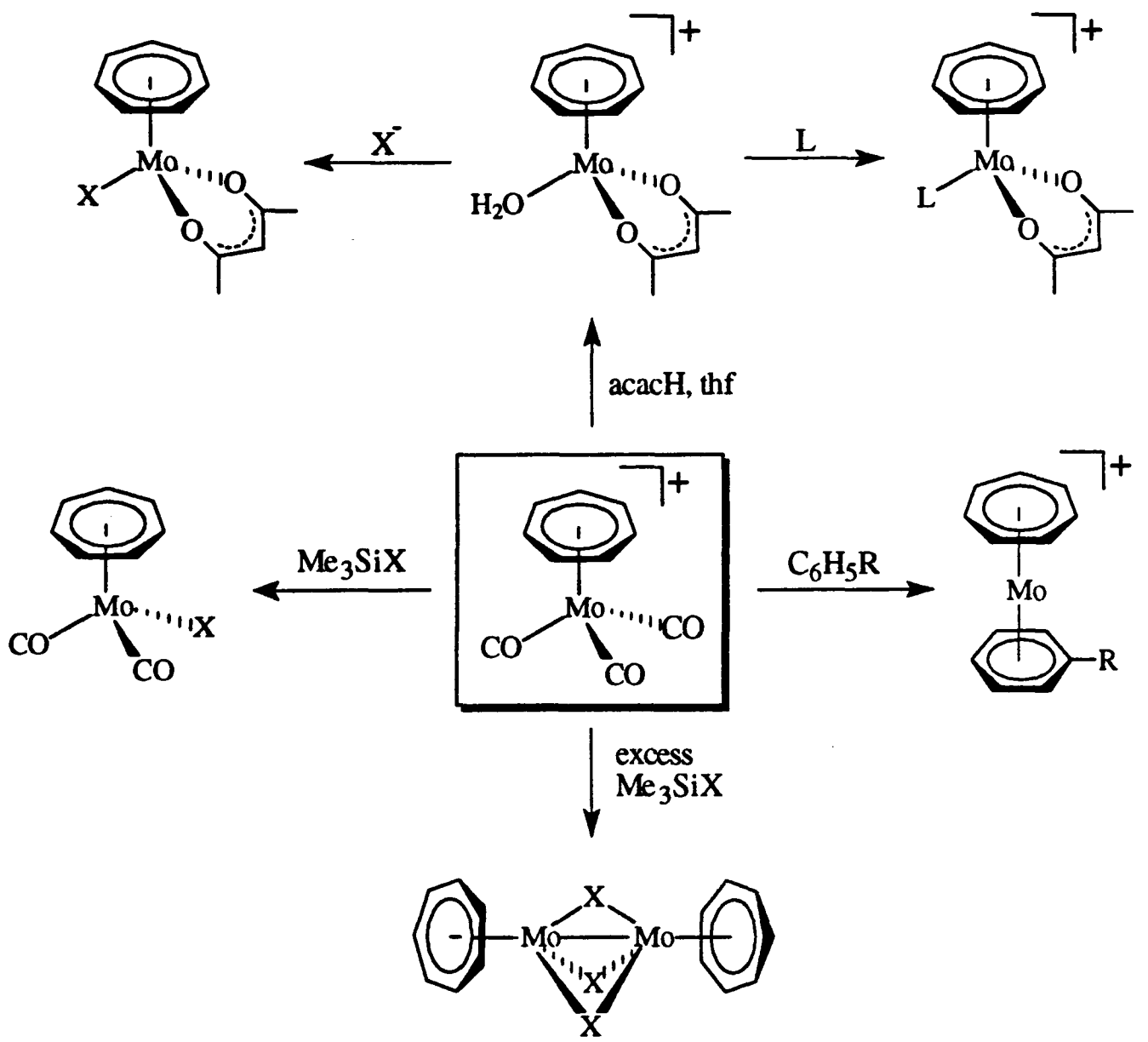

Scheme 1.12

X-ray structure of the chloro cation has been reported which confirms the presence of symmetrical planar η-C_7H_7 rings, a weak Mo-Mo bond and three bridging chloro ligands.[49]

[Mo(η-C_7H_7)$(CO)_3$][BF_4] also reacts with pentane-2,4-dione (acacH) in dry thf to afford the 17-electron complex [Mo(η-C_7H_7)(acac)(H_2O)][BF_4]. It has been suggested that the coordinated water molecule arises from aldol condensation of the pentane-2,4-dione. The aquo ligand can be displaced by a variety of neutral (L) and anionic (X-) ligands to give [Mo(η-C_7H_7)(acac)L][BF_4] and [Mo(η-C_7H_7)(acac)X] respectively.[48a,50]

The three CO ligands in [Mo(η-C_7H_7)$(CO)_3$]+ can also be displaced by arenes to give the mixed sandwich cations [Mo(η-C_7H_7)(η-arene)]+,[48a] which are excellent precursors to other η-cycloheptatrienyl derivatives of molybdenum (see section 1.4.1.4).

Other types of reaction of [M(η-C_7H_7)$(CO)_3$]+ include nucleophilic addition to and displacement of the C_7H_7 ligand. For example, some phosphonium adducts [M(η^6-$C_7H_7PR_3$-7)$(CO)_3$]+ have been isolated from the reaction of [M(η-C_7H_7)$(CO)_3$]+ with stoichiometric amounts of PR_3. The use of an excess of PR_3, however, causes ring displacement and isolation of *fac*-[$M(CO)_3(PR_3)_3$] (for M = Mo or W) (Scheme 1.13).[51]

Reaction of [M(η-C_7H_7)$(CO)_3$]+ with certain anions A-, such as OMe^-, Bu^{t-} or [Fe(η^3-C_7H_7)$(CO)_3$]-, yields the *exo*-isomer of [M(η^6-C_7H_7A-7)$(CO)_3$].[43,52] However, ring contraction occurs when [M(η-C_7H_7)$(CO)_3$]+ (M = Cr or Mo) is treated with $C_5H_5^-$ or diethyl malonate anion (Scheme 1.13).[53]

Displacement of C_7H_7 ring in [M(η-C_7H_7)$(CO)_3$]+ by acetonitrile has been reported (Scheme 1.13).[54] The ease of release of the ring decreases markedly in the order Mo > W >> Cr which is similar to the order in displacement of C_7H_8 from [M(η^6-C_7H_8)$(CO)_3$].[40] However, the former reactions proceed more slowly because of the stronger M-C_7H_7 bond.

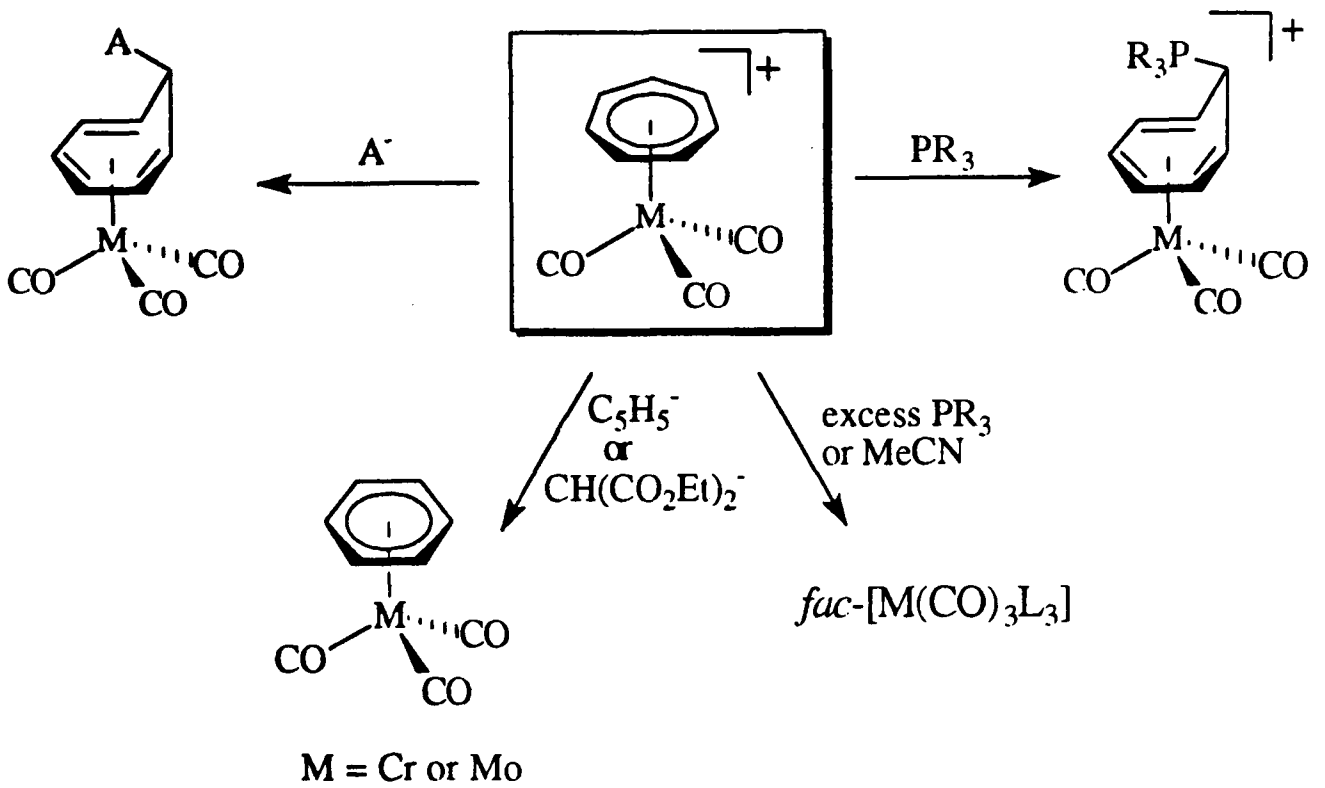

Scheme 1.13

1.4.1.3 [M(η-C7H7)(CO)2X]

The compounds [M(η-C7H7)(CO)2X] (M = Mo or W; X = Cl, Br or I) can be prepared by treating [M(η-C7H7)(CO)3]+ with halide anions X-.[32,46] The X-ray crystal structures of [Mo(η-C7H7)(CO)2X] (X = Cl or Br) have been reported.[55] These complexes are useful precursors to other M(η-C7H7) derivatives *via* CO and halide substitution.

Reactions of [M(η-C7H7)(CO)2X] (M = Mo or W) with monodentate phosphines or phosphites simply displace one CO ligand to give the monosubstituted compounds [M(η-C7H7)(CO)(PR3)X].[56] However, the reactions of [Mo(η-C7H7)(CO)2I] with bi- or tri-dentate group V ligands may displace both CO ligands and iodide depending on the reaction conditions and the nature of the ligand (Scheme 1.14).[57]

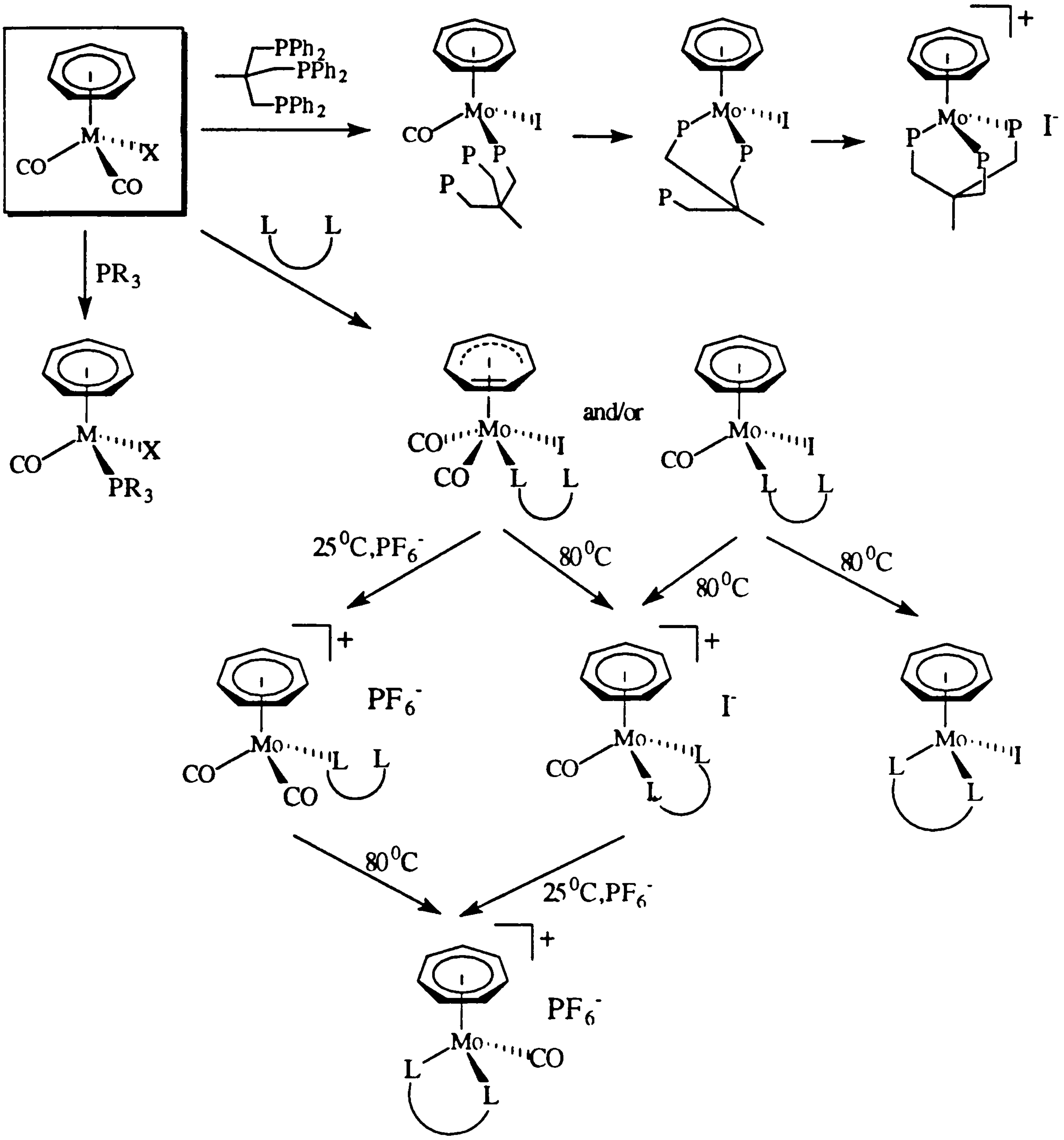

PPh2
PPh2
PPh2
M
CO
X
CO
Mo
I
P
PR3
L L
and/or
25°C,PF6-
80°C
+
PF6-
I-
CO
25°C,PF6-

Scheme 1.14

Several halide displacement reactions have been reported on the molybdenum compounds (Scheme 1.15). For example, $[Mo(\eta\text{-}C_7H_7)(CO)_2I]$ reacts with pentafluorophenylmagnesium bromide to give a stable σ-aryl complex $[Mo(\eta\text{-}C_7H_7)(CO)_2(\sigma\text{-}C_6F_5)]$, which has been structurally characterised by X-ray studies.[58] The bi-metallic compound $[Mo(\eta\text{-}C_7H_7)(CO)_2Mn(CO)_5]$ has been prepared by treating $[Mo(\eta\text{-}C_7H_7)(CO)_2I]$ with $Na[Mn(CO)_5]$.[59] Other metal-metal bonded derivatives (Mo-M; M = Si, Ge or Sn) have also been prepared by the reactions with NEt_3 and $HSiCl_3$, $HGeCl_3$ or $SnCl_2$, or through the anion $[Mo(\eta\text{-}C_7H_7)(CO)_2]^-$.[60]

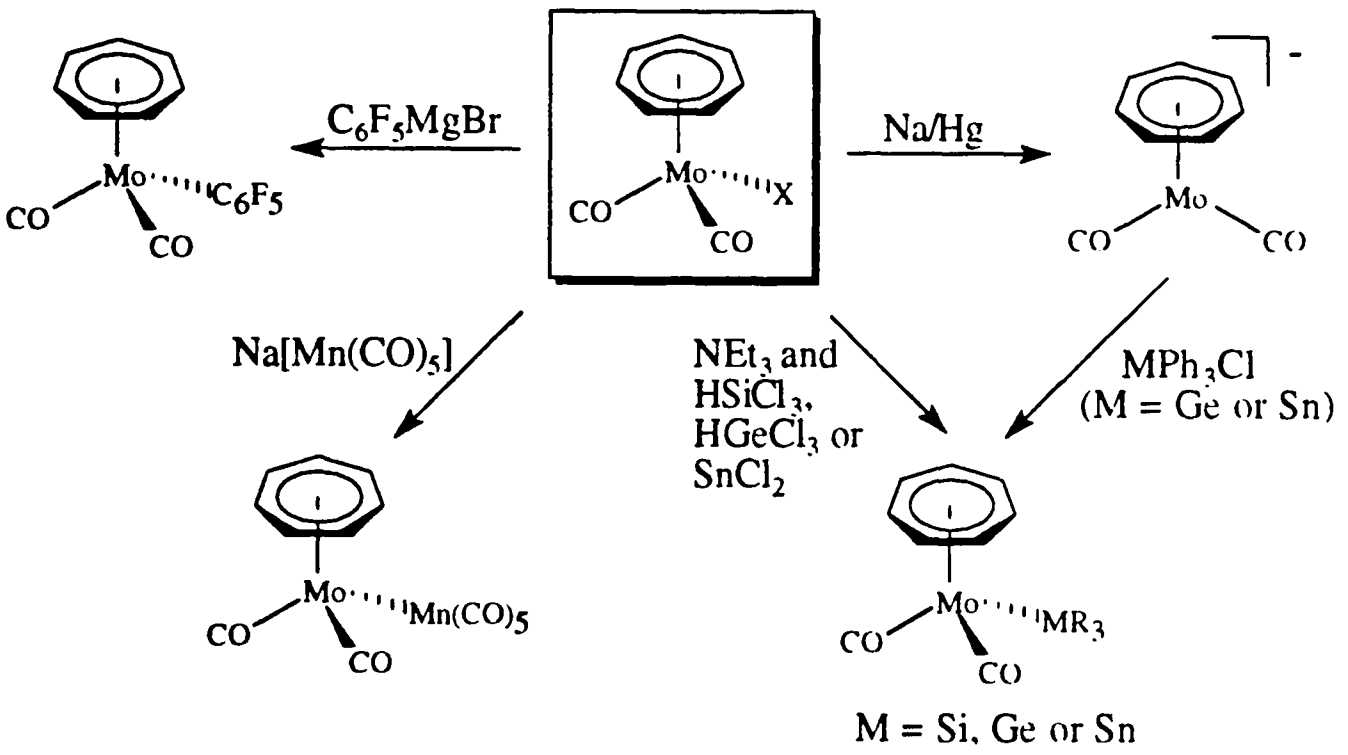

Scheme 1.15

The reactions of $[Mo(\eta\text{-}C_7H_7)(CO)_2X]$ with chalcogen ligands have been studied. Treatment of $[Mo(\eta\text{-}C_7H_7)(CO)_2X]$ with arenethiols (ArSH) gives a mixture of products $[Mo(\eta\text{-}C_7H_7)(CO)_2(SAr)]$ and $[Mo(\eta\text{-}C_7H_7)(CO)(\mu\text{-}SAr)]_2$.[61] However, the corresponding reaction with thiolates SR^- (R = alkyl) produces the unsymmetrical triply SR-bridged complexes $[(\eta\text{-}C_7H_7)Mo(\mu\text{-}SR)_3Mo(CO)_3]$.[62,63] The structure for R = Bu^t has been confirmed by X-ray crystallographic study. The analogous SeR-bridged dimers can also be prepared similarly using RSeMgBr. The reaction of $[Mo(\eta\text{-}C_7H_7)(CO)_2Br]$ with PhTeLi or PhTeMgBr yields exclusively the symmetrical doubly bridged species $[Mo(\eta\text{-}C_7H_7)(CO)(\mu\text{-}TePh)]_2$ (Scheme 1.16).[62]

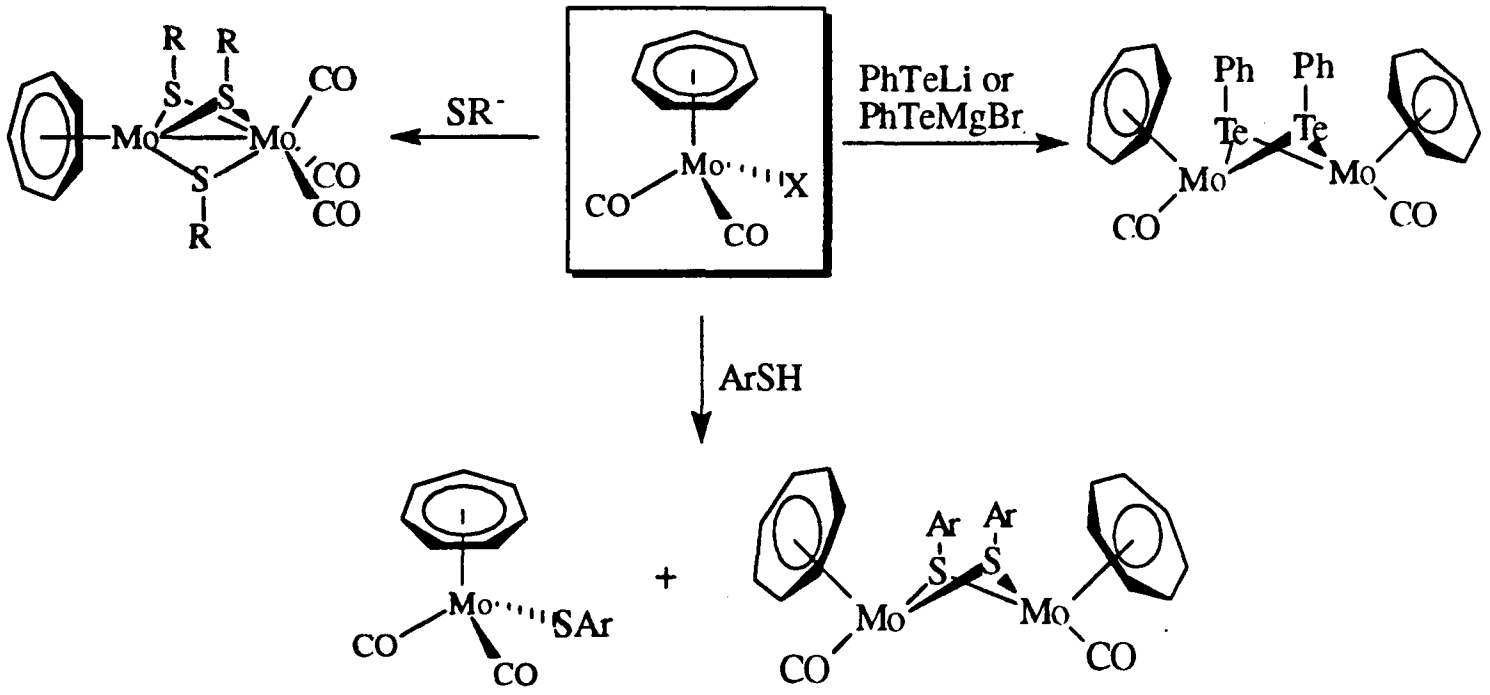

Scheme 1.16

Knox and co-workers have demonstrated that the binuclear compounds [(η-C_7H_7)Mo(μ-SR)$_3$Mo(CO)$_3$] (R = Me, Et, Pr^i or Bu^t) have interesting fluxional behaviour.[63] They exist as a mixture of two isomeric forms **2** and **3** (viewed along the Mo-Mo axis). The IR spectrum of each complex exhibits six carbonyl bands at room temperature showing that both isomers are present. ^{1}H NMR studies show that these isomers interconvert rapidly at or above this temperature through inversion at sulfur. The molecular structure of the related complex {(η-C_7H_7)Mo(μ-SBu^t)$_3$Mo(CO)$_2$[P(OMe)$_3$]} has also been reported. It shows that the sulfur bridges are unsymmetrical, favouring the molybdenum bound to P(OMe)$_3$.[63]

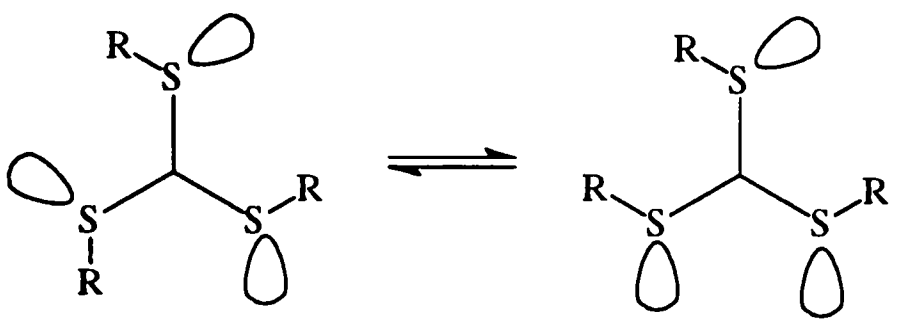

2 **3**

The reaction of [M(η-C_7H_7)(CO)$_2$I] (M = Mo or W) with NaC_5H_5 affords the interesting trihapto-cycloheptatrienyl complexes [M(η^3-C_7H_7)(η-C_5H_5)(CO)$_2$] (Scheme 1.17).[32,59,64] Their ^{1}H NMR spectra at room temperature show only two sharp singlets with 7 : 5 ratio, but several bands appear at lower temperature which is consistent with the η^3-C_7H_7 structure.[65] It has been shown that the principle pathway of rearrangement is a 1,2-shift of the metal about the cycloheptatrienyl ring.[65d]

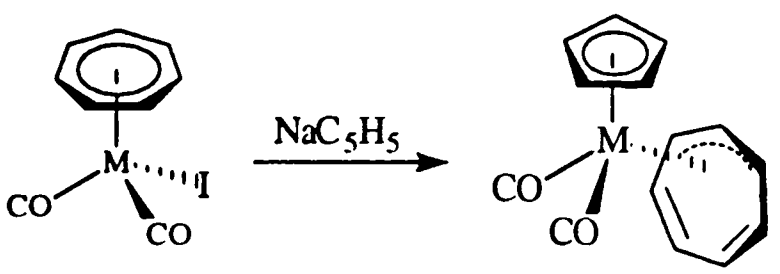

M = Mo or W

Scheme 1.17

Other type of reaction of $[M(\eta\text{-}C_7H_7)(CO)_2X]$ (M = Mo or W) involves a change in hapticity of the C_7H_7 ligand without breaking the M-CO and M-X bonds. Treatment of the halides with some bidentate ligands, such as dppm, dppe or en, give the trihapto-cycloheptatrienyl complexes $[M(\eta^3\text{-}C_7H_7)(L\text{-}L)(CO)_2X]$ (Scheme 1.18).[66] These complexes are fluxional due to the trigonal twist rearrangement illustrated in Scheme 1.19.

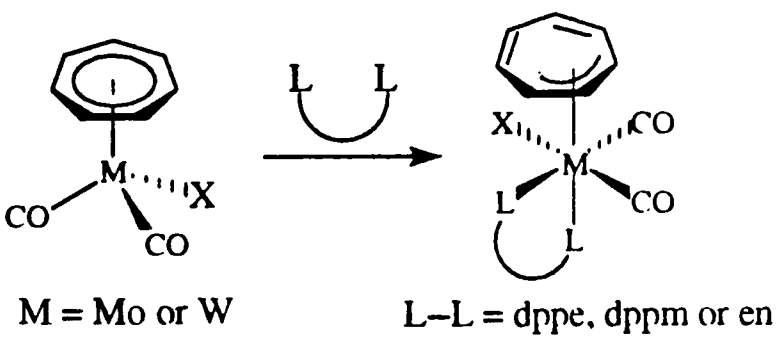

Scheme 1.18

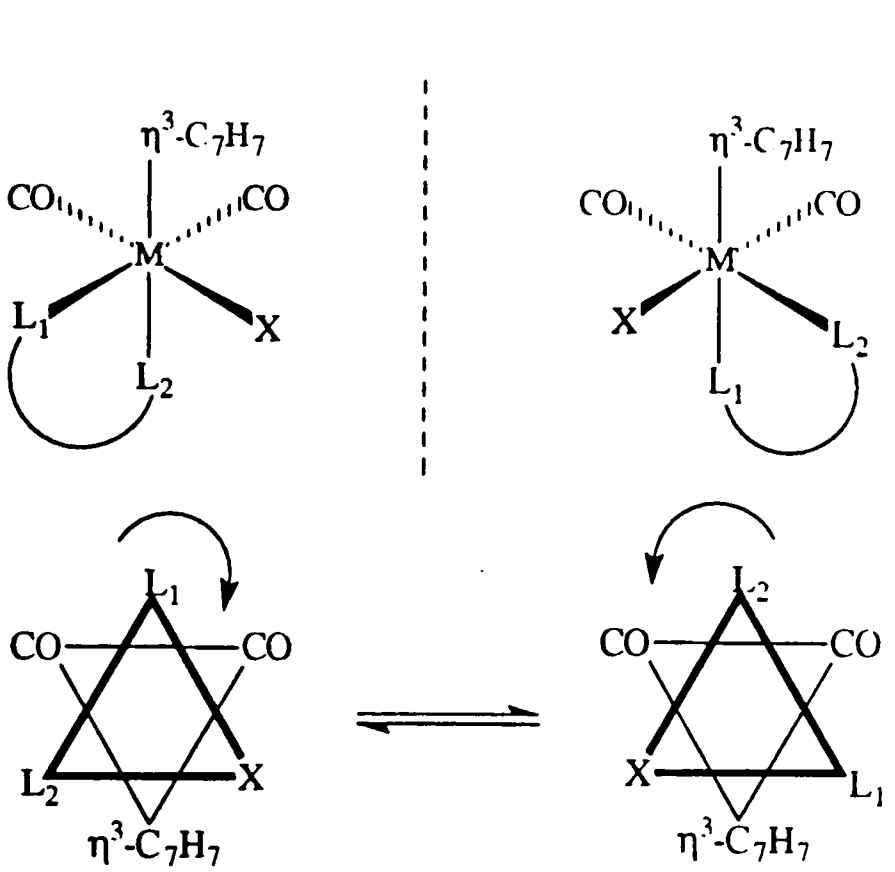

Scheme 1.19

Recent works by Whiteley and co-workers further enrich the chemistry of these complexes. Reaction of $[M(\eta\text{-}C_7H_7)(CO)_2I]$ (M = Mo or W) with $AgBF_4$ in nitriles produces the cations $[M(\eta\text{-}C_7H_7)(CO)_2(RCN)]^+$ which are also useful precursors to other $M(\eta\text{-}C_7H_7)$ derivatives.[67] Some of the chemistry is summarised in Scheme 1.20. The nitrile ligand of these cations can be displaced by monodentate or bidentate phosphines to give the corresponding monosubstituted product. The hapticity of the C_7H_7 ligand can be changed from heptahapto to trihapto in the presence of an excess of acetonitrile. Thus, an equilibrium exists between the cations $[W(\eta\text{-}C_7H_7)(CO)_2(dppm)]^+$ and $[W(\eta^3\text{-}C_7H_7)(CO)_2(dppm)(MeCN)]^+$ and between $[M(\eta\text{-}C_7H_7)(CO)_2(MeCN)]^+$ and $[M(\eta^3\text{-}C_7H_7)(CO)_2(MeCN)_3]^+$. Under photolysis in acetonitrile, $[Mo(\eta\text{-}C_7H_7)(CO)_2(MeCN)]^+$ gives the bisacetonitrile cation $[Mo(\eta\text{-}C_7H_7)(CO)(MeCN)_2]^+$. A series of metal-metal bonded complexes $[(\eta\text{-}C_7H_7)(CO)_2M\text{-}M'(CO)_3(\eta\text{-}C_5R_5)]$ have also been prepared from $[M(\eta\text{-}C_7H_7)(CO)_2(MeCN)]^+$ and the appropriate anions $[M'(\eta\text{-}C_5R_5)(CO)_3]^-$ (M' = Mo or W; R = H or Me).[67a,68] The X-ray crystal structure of $[(\eta\text{-}C_7H_7)(CO)_2Mo\text{-}Mo(CO)_3(\eta\text{-}C_5H_5)]$ has been determined.[69]

The chemistry of the related $[M(\eta\text{-}C_7H_7)(CO)(PPh_3)I]$ (M = Mo or W) species has also been studied. Treatment of the M = Mo compound with CN- anion leads to iodide displacement; with $AgBF_4$ in the presence of acetonitrile or pyridine, the cations $[Mo(\eta\text{-}C_7H_7)(CO)(PPh_3)L]^+$ (L = MeCN or C_6H_5N) are formed.[70] Reaction of the M = W compound with dppe gives the cation $[W(\eta\text{-}C_7H_7)(CO)(dppe)]^+$ (Scheme 1.21).[56c]

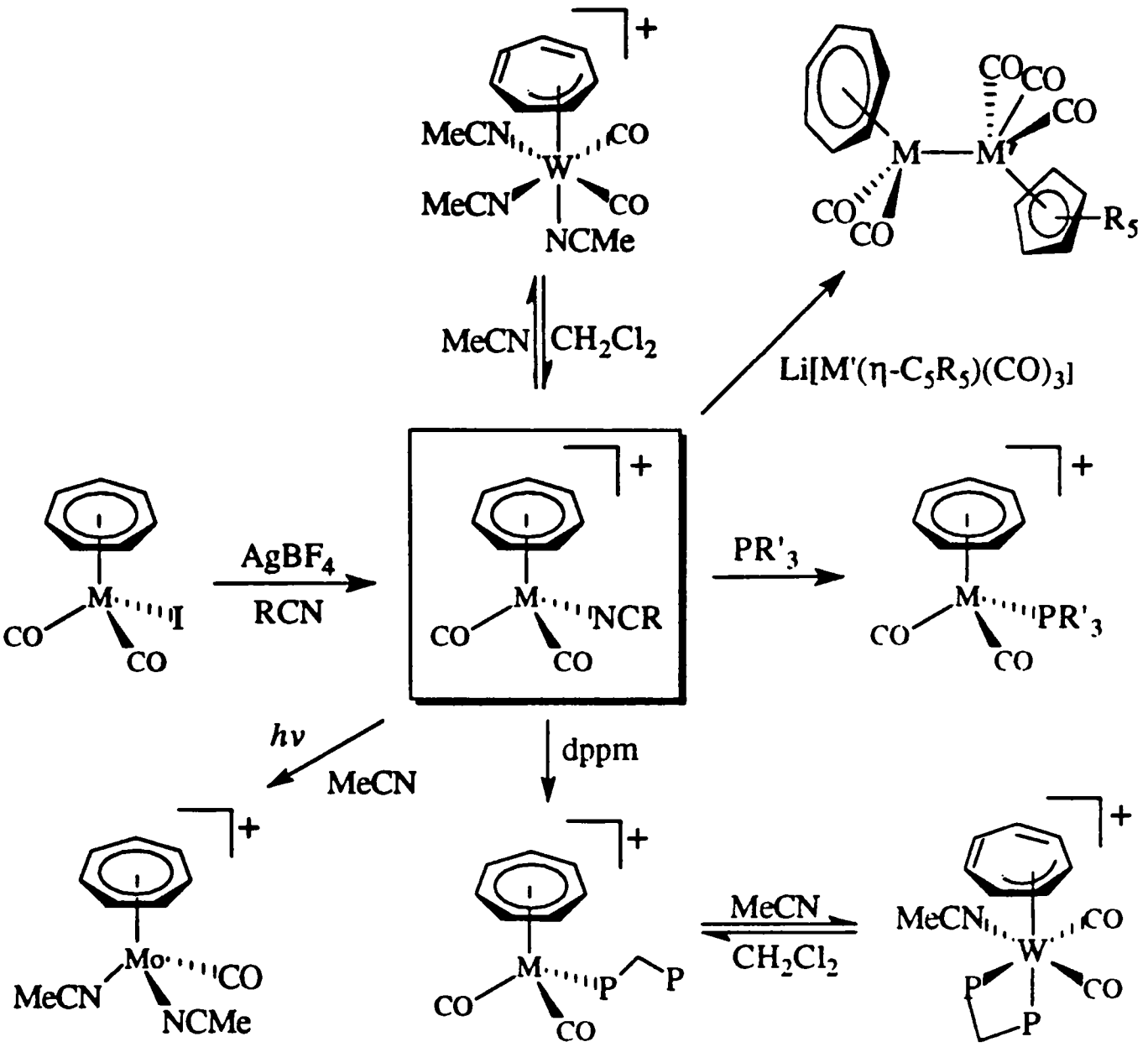

Scheme 1.20

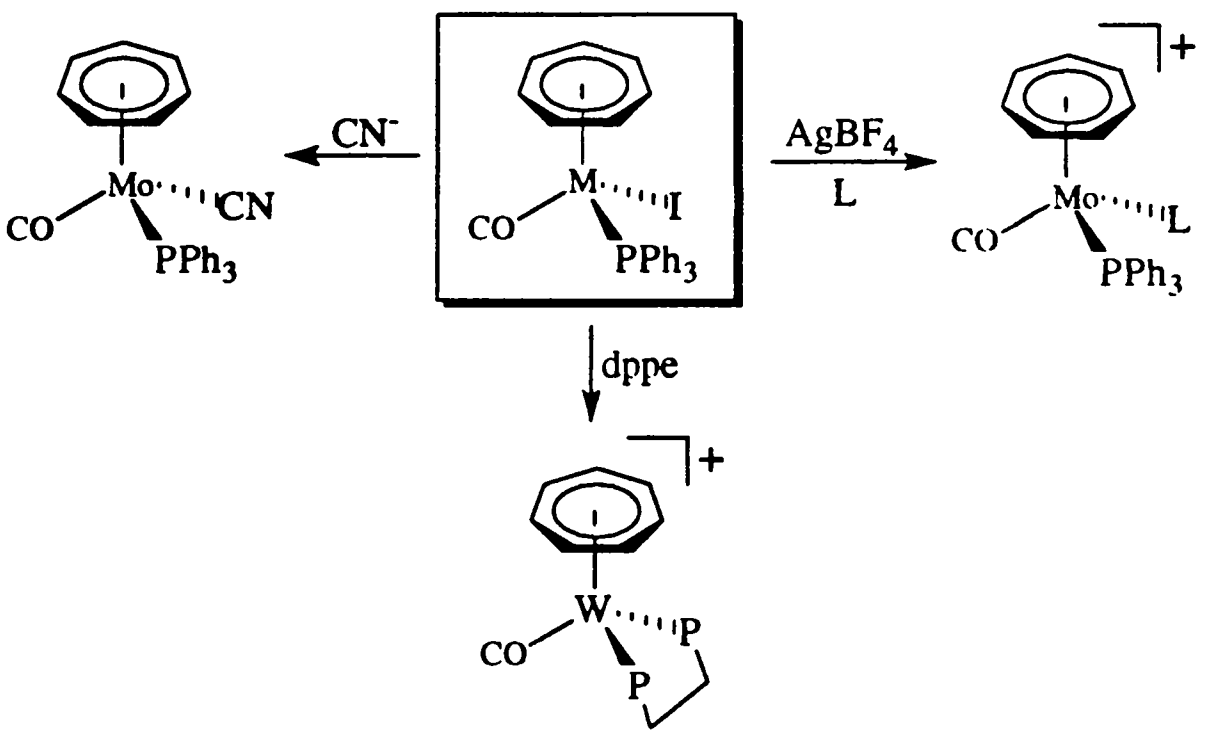

Scheme 1.21

1.4.1.4 [Mo(η-C_7H_7)(η-C_6H_5R)]+

The mixed sandwich cations [Mo(η-C_7H_7)(η-C_6H_5R)]+ (R = H or Me) were first prepared by Green and co-workers by the reaction of [Mo(η-arene)(η-C_3H_5)Cl]$_2$ with [AlEtCl$_2$]$_2$ in the presence of cycloheptatriene (Scheme 1.22).[71] An alternative route was reported independently by Stone and co-workers by refluxing [Mo(η-C_7H_7)(CO)$_3$]+ with the corresponding arenes.[48a] The X-ray structure of the related compound [Mo(η-C_7H_7)(η-$C_6H_5BPh_3$)] has been reported, which confirms the sandwich structure, although the Mo-C distance to the arene carbon bound to the boron atom is significantly longer than the other five Mo-C(phenyl) distances.[72]

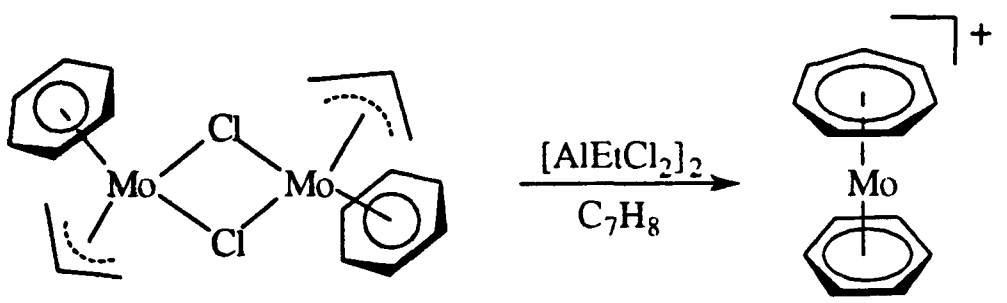

Scheme 1.22

The arene ligands of these cations are labile and can be displaced by a variety of ligands, making them useful precursors for the synthesis of other Mo(η-C_7H_7) derivatives. For example, [Mo(η-C_7H_7)(η-C_6H_5R)]$^+$ (R = H or Me) reacts with donor ligand L (L = MeCN, PMe_2Ph or $PMePh_2$) causing smooth displacement of the arene ligand to form the cations [Mo(η-C_7H_7)L_3]$^+$ in excellent yield.[73] Further ligand substitutions give the cations [Mo(η-C_7H_7)L_2L']$^+$ as shown in Scheme 1.23. Treatment of [Mo(η-C_7H_7)(η-C_6H_5Me)]$^+$ in ethanol with an excess of dppe gives the novel cation [Mo(η-C_7H_7)(dppe)$_2$)]$^+$, which reacts with carbon monoxide (1 atm) to give [Mo(η-C_7H_7)(dppe)(CO)]$^+$.

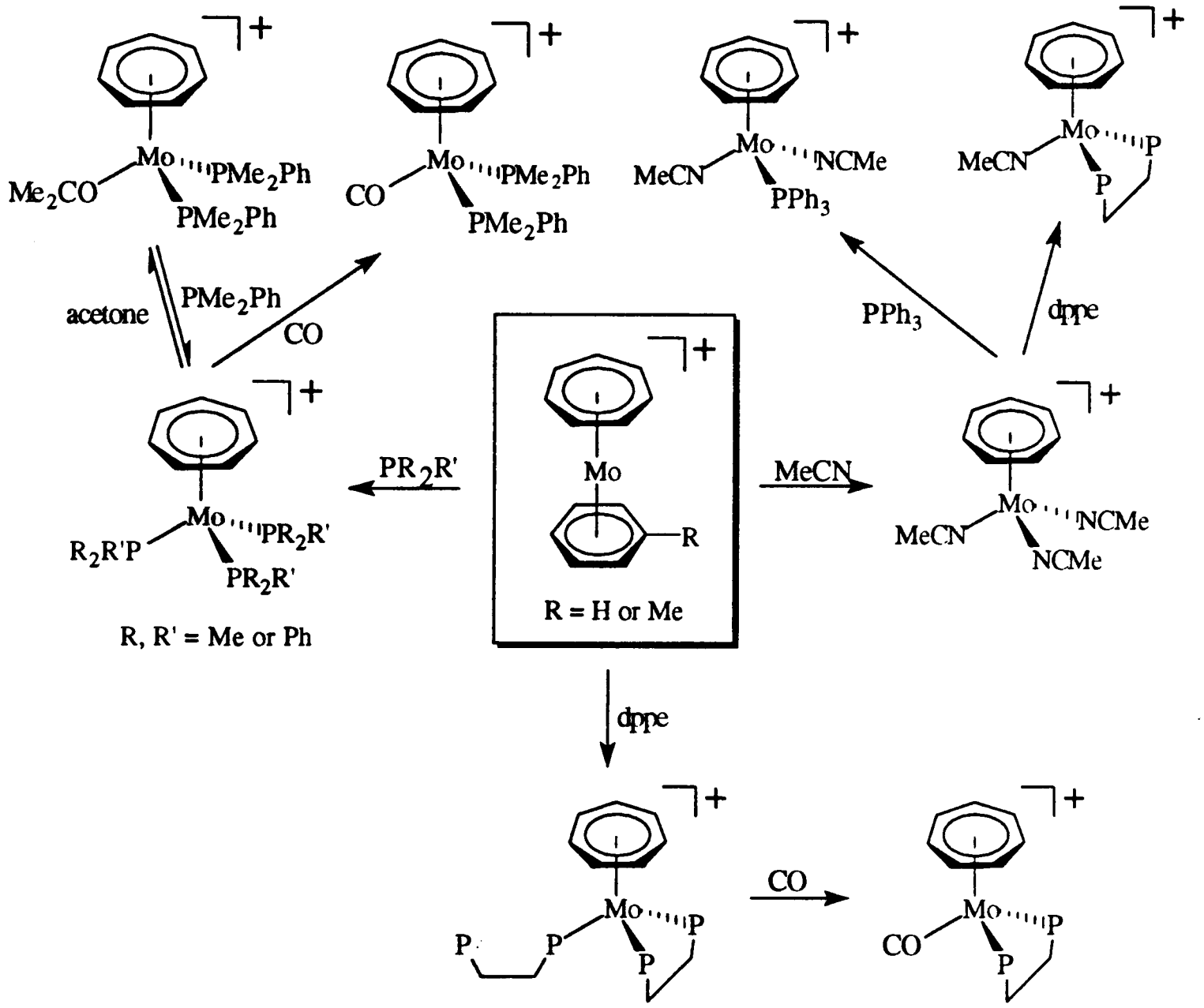

Scheme 1.23

Treatment of the compound $[Mo(\eta\text{-}C_7H_7)(\eta\text{-}C_6H_5Me)][PF_6]$ with one equivalent of dppe in acetone or acetonitrile also causes displacement of toluene to give $[Mo(\eta\text{-}C_7H_7)(dppe)(Me_2CO)][PF_6]$ or $[Mo(\eta\text{-}C_7H_7)(dppe)(MeCN)][PF_6]$, respectively (Scheme 1.24).[74] These compounds react with halide anions X^- producing the diamagnetic compounds $[Mo(\eta\text{-}C_7H_7)(dppe)X]$. Interestingly, the reaction of the acetone complex $[Mo(\eta\text{-}C_7H_7)(dppe)(Me_2CO)][PF_6]$ with CH_2Cl_2 or allylchloride affords the paramagnetic compound $[Mo(\eta\text{-}C_7H_7)(dppe)Cl][PF_6]$. The neutral compounds $[Mo(\eta\text{-}C_7H_7)(dppe)X]$ and their respective cations can be interconverted through simple oxidation and reduction process. The related hydride and methyl complexes $[Mo(\eta\text{-}C_7H_7)(dppe)R]$ (R = H or Me) have also been described (Scheme 1.24).

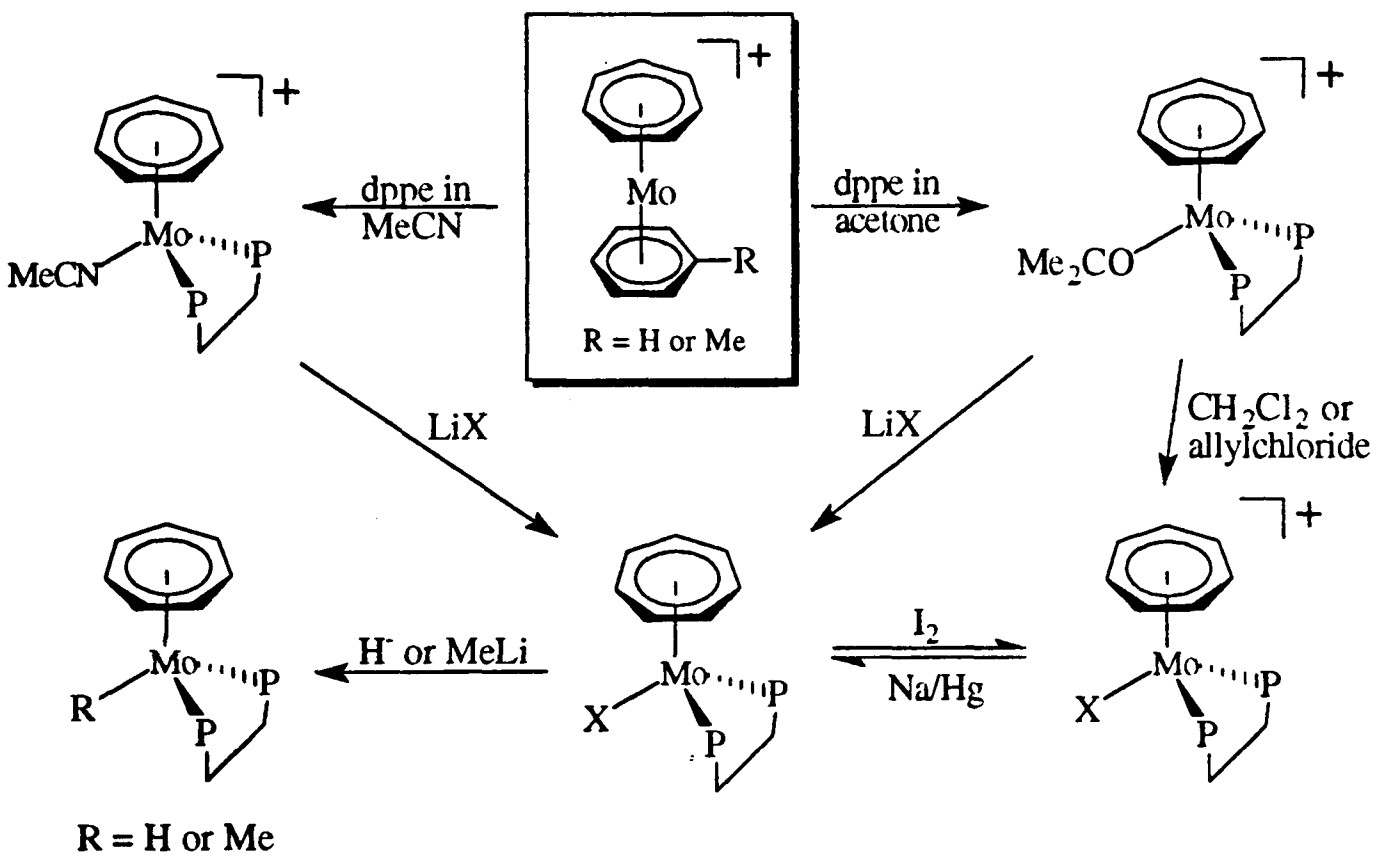

Scheme 1.24

The novel phenylvinylidene complex $[Mo(\eta\text{-}C_7H_7)(dppe)(C{=}CHPh)][PF_6]$ has been prepared by Whiteley and co-workers by treating $[Mo(\eta\text{-}C_7H_7)(dppe)(solvent)][PF_6]$ (solvent = acetone or acetonitrile) with phenylacetylene (Scheme 1.25).[75] Deprotonation of the vinylidene complex gives the alkynyl complex $[Mo(\eta\text{-}C_7H_7)(dppe)(C{\equiv}CPh)]$, which can be protonated with $HBF_4{\cdot}Et_2O$ to regenerate the vinylidene complex.[75] The alkynyl complex can be oxidised with $[Fe(\eta\text{-}C_5H_5)_2]^+$ to give the corresponding cation which undergoes coupling at C_β of the alkynyl ligand to afford the divinylidene-bridged, dimeric product $[(\eta\text{-}C_7H_7)(dppe)Mo(C{=}CPhPhC{=}C)Mo(\eta\text{-}C_7H_7)(dppe)]^{2+}$ (Scheme 1.25).[76] The structure of this dication has been confirmed by crystallography.

Reaction of the sandwich compound $[Mo(\eta\text{-}C_7H_7)(\eta\text{-}C_6H_5Me)][PF_6]$ with two equivalents of $P(OMe)_3$, instead of one equivalent of dppe, in refluxing acetonitrile affords the related compound $\{Mo(\eta\text{-}C_7H_7)[P(OMe)_3]_2(MeCN)\}\{PF_6\}$. This reacts with NaI in acetone giving the neutral compound $\{Mo(\eta\text{-}C_7H_7)[P(OMe)_3]_2I\}$. However, reaction with LiCl in acetone produces the paramagnetic cation $\{Mo(\eta\text{-}C_7H_7)[P(OMe)_3]_2Cl\}^+$.[56c]

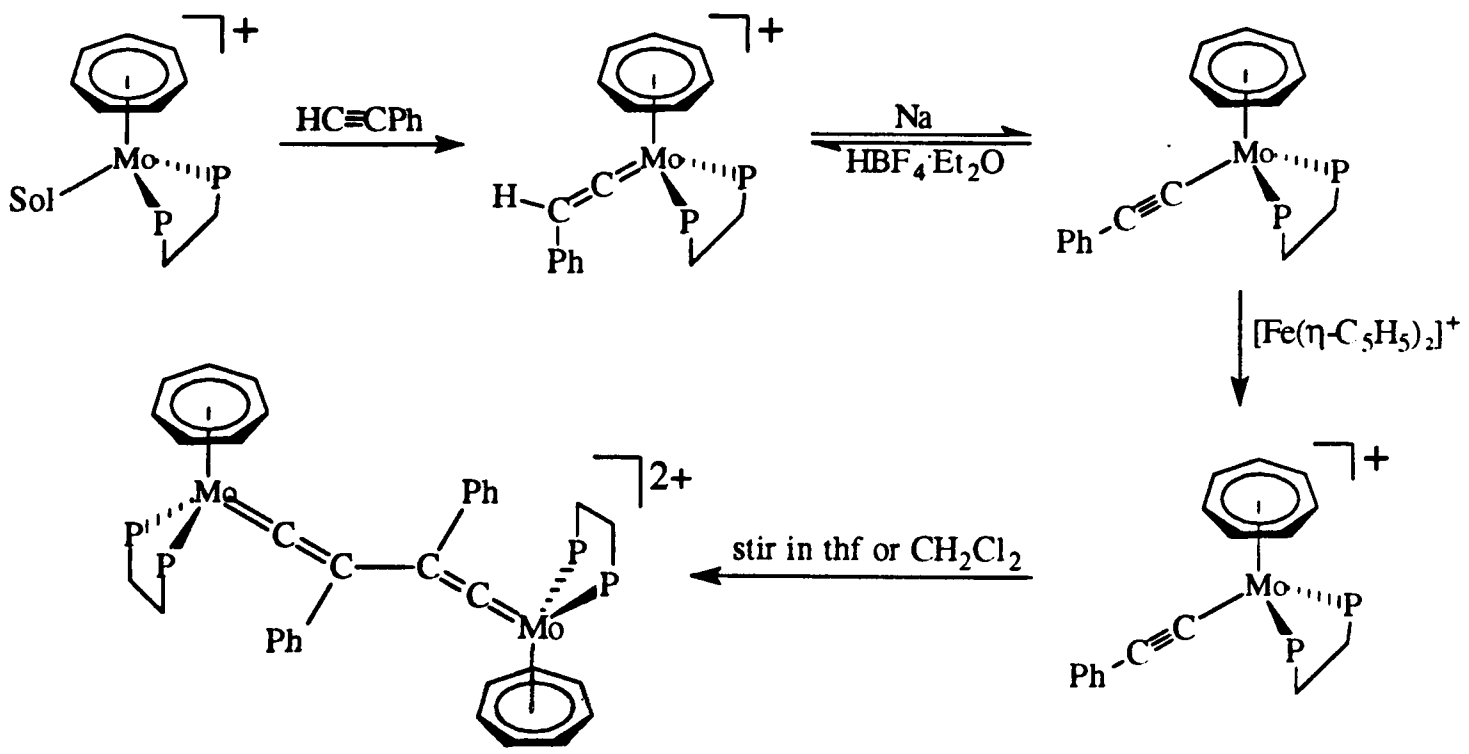

Scheme 1.25

With sodium tetrahydroborate, the cation $[Mo(\eta\text{-}C_7H_7)(\eta\text{-}C_6H_6)]^+$ undergoes hydride addition at the benzene ring[73] as predicted by the Davies-Green-Mingos rules.[77] The reaction of $[Mo(\eta\text{-}C_7H_7)(\eta\text{-}C_6H_5Me)]^+$ with sodium methoxide or lithium halides leads to the formation of the binuclear compounds $[(\eta\text{-}C_7H_7)Mo(\mu\text{-}OMe)_3Mo(\eta\text{-}C_7H_7)]$ or $[(\eta\text{-}C_7H_7)Mo(\mu\text{-}X)_3Mo(\eta\text{-}C_7H_7)]$, respectively. The latter compound (X = Cl) can be prepared from the former by the action of hydrogen chloride. These neutral compounds are readily oxidised to the corresponding cations. Alternatively, treatment of $[Mo(\eta\text{-}C_7H_7)(\eta\text{-}C_6H_5Me)]^+$ with alcohol or hydrochloric acid and tetrafluoroboric acid gives the binuclear cations $[(\eta\text{-}C_7H_7)Mo(\mu\text{-}OR)_3Mo(\eta\text{-}C_7H_7)]^+$ or $[(\eta\text{-}C_7H_7)Mo(\mu\text{-}Cl)_3Mo(\eta\text{-}C_7H_7)]^+$, respectively. These can be reduced to the corresponding neutral compounds by appropriate reducing agents (Scheme 1.26).[73]

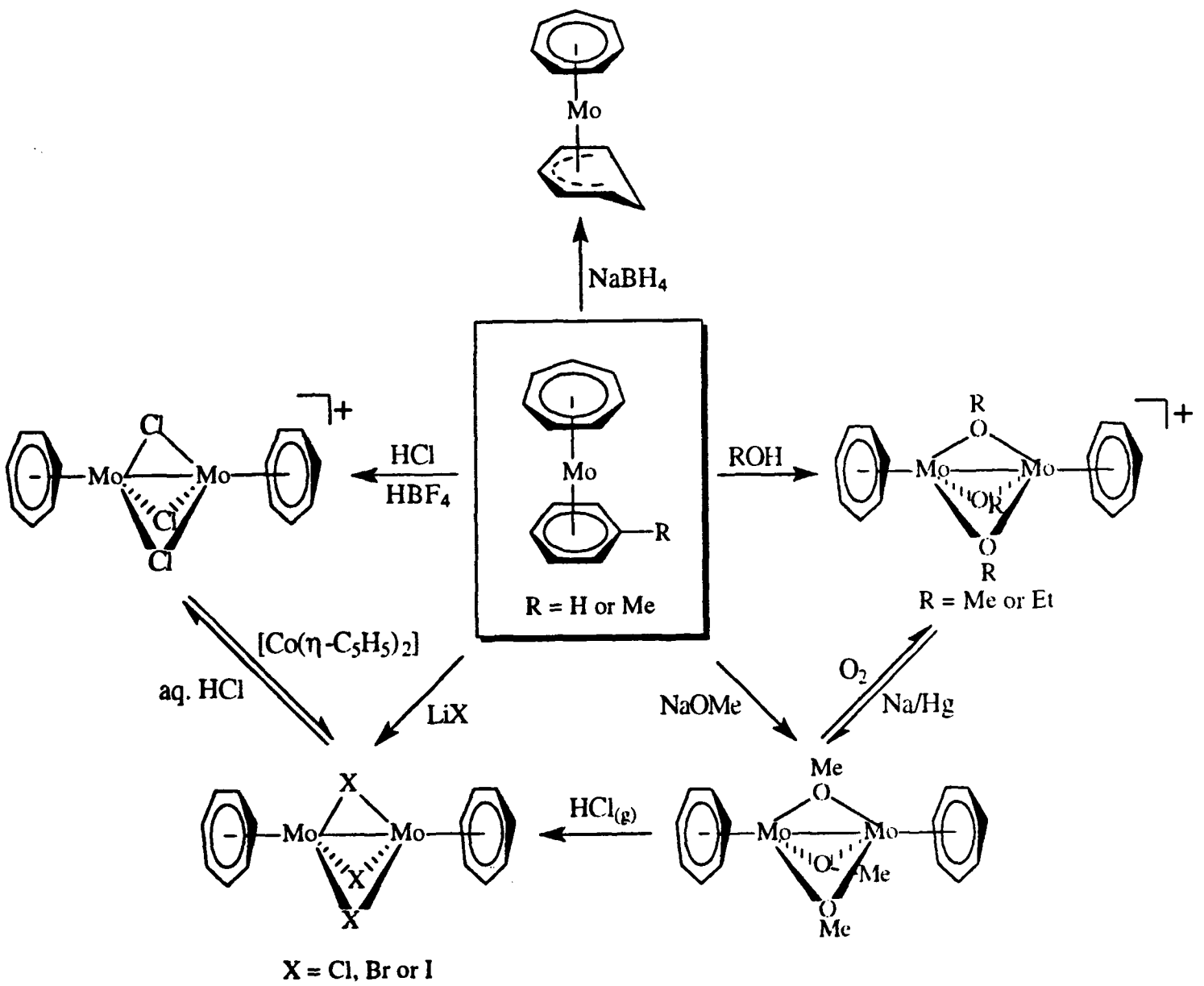

Scheme 1.26

Similar to the cation $[Mo(\eta\text{-}C_7H_7)(CO)_3]+$, $[Mo(\eta\text{-}C_7H_7)(\eta\text{-}C_6H_5Me)]+$ reacts with an excess of pentane-2,4-dione in dry thf to afford the 17-electron cation $[Mo(\eta\text{-}C_7H_7)(acac)(H_2O)]+$.[48a,50] However, treatment of $[Mo(\eta\text{-}C_7H_7)(\eta\text{-}C_6H_5Me)]+$ with PPh_3 and sodium pentane-2,4-dionate gives the 18-electron compound $[Mo(\eta\text{-}C_7H_7)(acac)(PPh_3)]$, which reacts with allylmagnesium bromide to give the corresponding allyl complex (Scheme 1.27).[73]

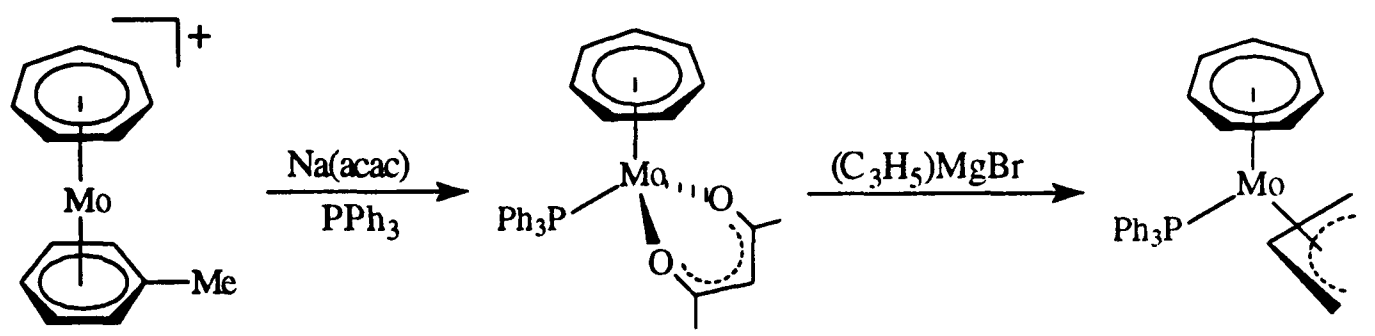

Scheme 1.27

1.4.2 From metal vapour synthesis

Another general route to $M(\eta\text{-}C_7H_7)$ derivatives is through the metal vapour synthesis. Skell and co-workers were the first to report the co-deposition of molybdenum and tungsten vapour with cycloheptatriene.[78] They isolated the compounds $[M(\eta\text{-}C_7H_7)(\eta^5\text{-}C_7H_9)]$ in 52 % (for M = Mo) and *ca.* 20 % (for M = W) yield (Scheme 1.28). When a solution of cycloheptatriene in hexane or methylcyclohexane was co-condensed with chromium vapour, the only product isolated was $[Cr(\eta\text{-}C_7H_7)(\eta^4\text{-}C_7H_{10})]$.[16c,79] However, it was found later that co-deposition of chromium vapour with neat cycloheptatriene gives $[Cr(\eta\text{-}C_7H_7)(\eta^5\text{-}C_7H_9)]$ in 45 % yield together with small amount of $[Cr(\eta\text{-}C_7H_7)(\eta^4\text{-}C_7H_{10})]$.[80]

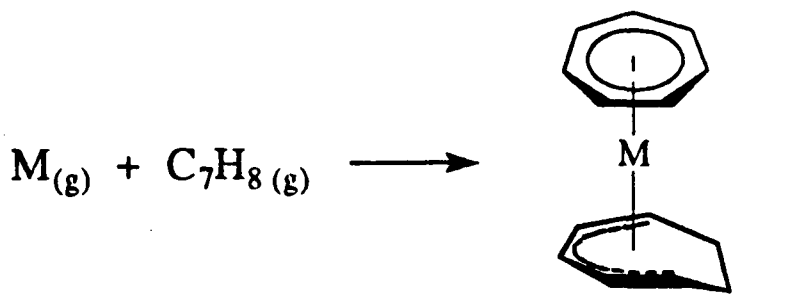

Scheme 1.28

It has been demonstrated later by Green and Newman that the actual first product of co-condensation of molybdenum atoms and cycloheptatriene is [Mo(η^6-C_7H_8)$_2$].[81] This compound is thermally unstable and isomerises quantitatively to give the compound [Mo(η-C_7H_7)(η^5-C_7H_9)]. Both of these compounds can be oxidised by silver tetrafluoroborate to give their corresponding cations [Mo(η^6-C_7H_8)$_2$]$^+$ and [Mo(η-C_7H_7)(η^5-C_7H_9)]$^+$ respectively. The former cation also rearranges to the latter cation but the rate is slower than that for their neutral analogue (Scheme 1.29). Kinetic and crossover studies have shown that the rearrangements are intramolecular.

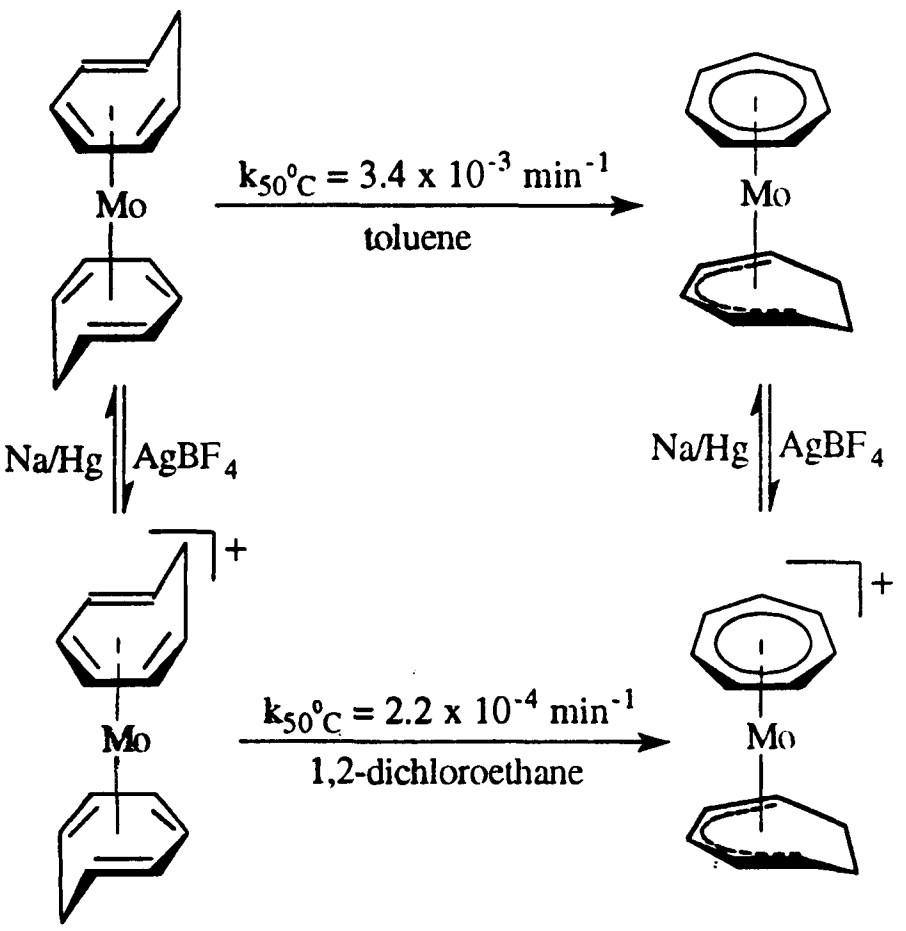

Scheme 1.29

Treatment of $[Mo(\eta\text{-}C_7H_7)(\eta^5\text{-}C_7H_9)]$ with a 15-fold excess of sodium cyclopentadienide in refluxing thf gives $[Mo(\eta\text{-}C_7H_7)(\eta\text{-}C_5H_5)]$. However, the yield of this reaction was not reported.[78] The analogous reaction to prepare the mixed sandwich compound of tungsten failed to obtain a pure product; only mass spectral evidence could be obtained for its presence. The synthetic utilities of $[Mo(\eta\text{-}C_7H_7)(\eta^5\text{-}C_7H_9)]$ has been further explored by Green and Tovey.[80] Oxidation with a half equivalent of iodine or tetrafluoroboric acid gives the cation $[Mo(\eta\text{-}C_7H_7)(\eta^5\text{-}C_7H_9)]^+$. The $\eta^5\text{-}C_7H_9$ ring of this cation is labile and can be displaced by ethanol or iodine to afford the known binuclear cations $[(\eta\text{-}C_7H_7)Mo(\mu\text{-}OEt)_3Mo(\eta\text{-}C_7H_7)]^+$ or $[(\eta\text{-}C_7H_7)Mo(\mu\text{-}I)_3Mo(\eta\text{-}C_7H_7)]^+$, respectively.

Treatment of $[Mo(\eta\text{-}C_7H_7)(\eta^5\text{-}C_7H_9)]$ with one equivalent of iodine in thf gives a mixture of product $[Mo(\eta\text{-}C_7H_7)(thf)I_2]$ and $[Mo(\eta\text{-}C_7H_7)(\eta^5\text{-}C_7H_9)I][I]$ (Scheme 1.30).[80] The 17-electron compound $[Mo(\eta\text{-}C_7H_7)(thf)I_2]$ is air-stable but thermally unstable, losing thf even at room temperature. However, its structure has been determined.[82] Upon heating, the thf adduct gives $[Mo(\eta\text{-}C_7H_7)I_2]_n$ in quantitative yield. Dissolution of $[Mo(\eta\text{-}C_7H_7)I_2]_n$ in thf regenerates the thf complex. Reaction of $[Mo(\eta\text{-}C_7H_7)(thf)I_2]$ with an excess of iodine provides an alternative route to the bridging-iodide complex $[(\eta\text{-}C_7H_7)Mo(\mu\text{-}I)_3Mo(\eta\text{-}C_7H_7)][I_3]$ (Scheme 1.30).[80]

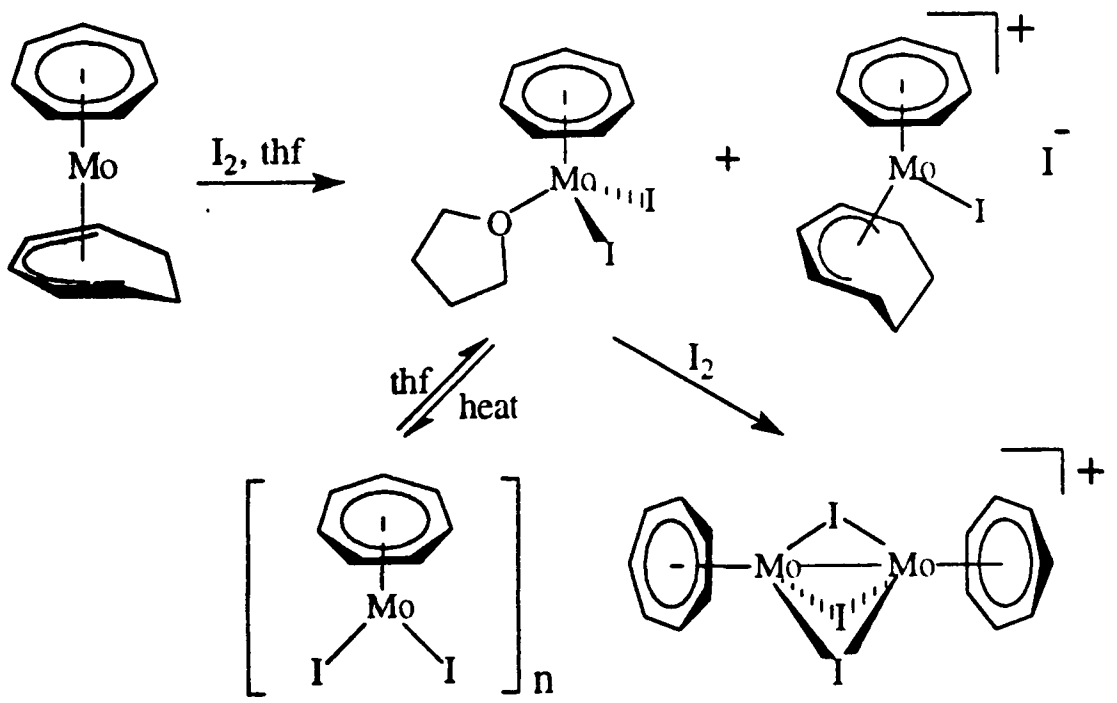

Scheme 1.30

Both $[Mo(\eta\text{-}C_7H_7)(thf)I_2]$ and $[Mo(\eta\text{-}C_7H_7)(\eta^5\text{-}C_7H_9)I][I]$ can be converted to the thermally stable $[Mo(\eta\text{-}C_7H_7)(MeCN)I_2]$ by the action of acetonitrile. With an excess of PMe_3 they give a mixture of product $[Mo(\eta\text{-}C_7H_7)(PMe_3)I_2]$ and $[Mo(\eta\text{-}C_7H_7)(PMe_3)_2I][I]$. Treatment of $[Mo(\eta\text{-}C_7H_7)(MeCN)I_2]$ with an excess of PPh_3 displaces the acetonitrile ligand. Reduction of $[Mo(\eta\text{-}C_7H_7)(PMe_3)I_2]$ with $LiAlH_4$ affords the unexpected product $[Mo(\eta\text{-}C_7H_7)(PMe_3)_2I]$. The compound $[Mo(\eta\text{-}C_7H_7)(PMe_3)I_2]$ also reacts with nucleophiles, such as sodium methoxide, giving the binuclear cation $[(\eta\text{-}C_7H_7)Mo(\mu\text{-}OMe)_3Mo(\eta\text{-}C_7H_7)]^+$. All these reactions are summarised in Scheme 1.31.[80]

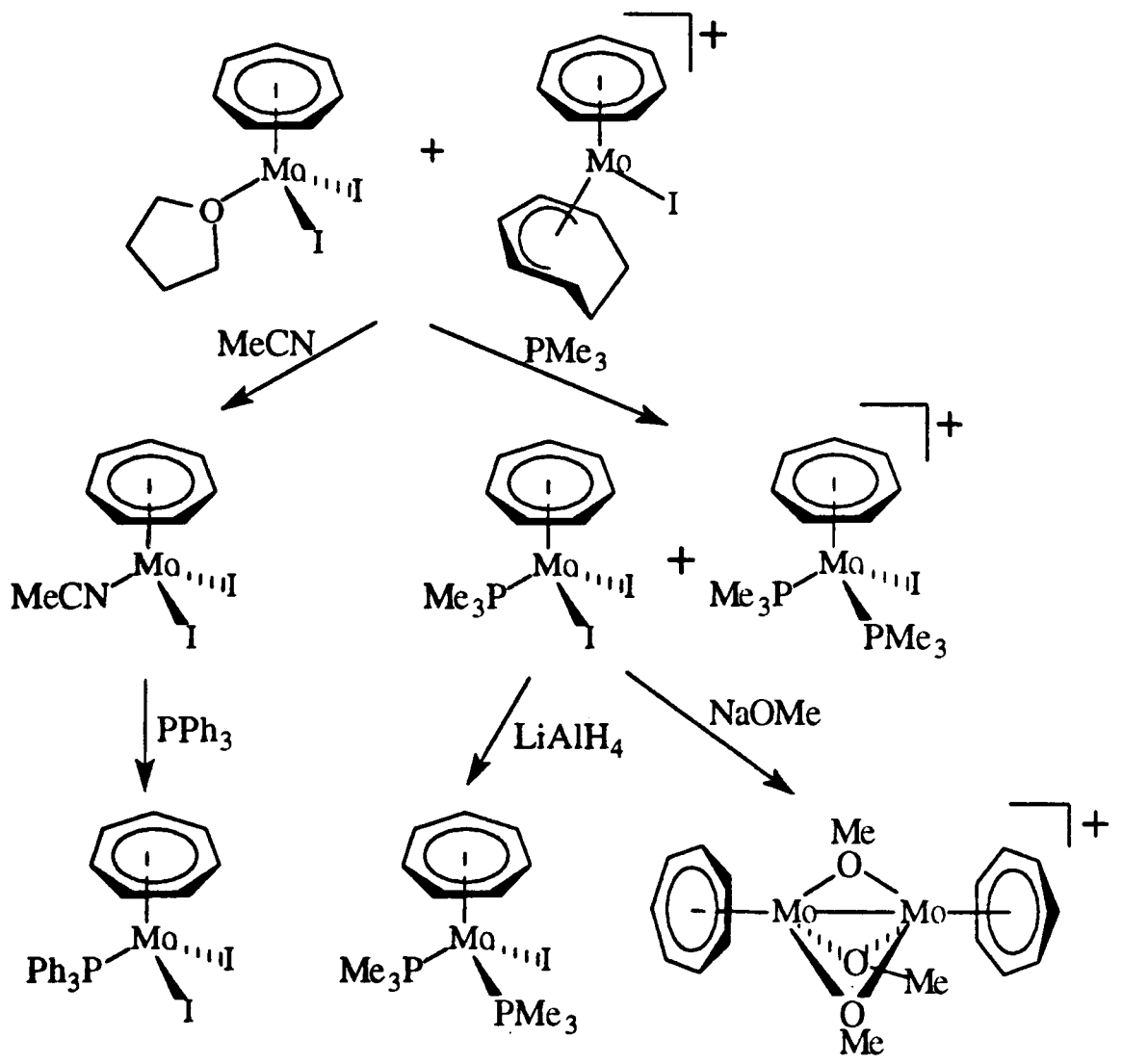

Scheme 1.31

Oxidation of [Mo(η-C_7H_7)(η^5-C_7H_9)] with one equivalent of bromine in thf followed by addition of acetonitrile leads to the formation of [Mo(η-C_7H_7)(MeCN)Br_2]. As expected the MeCN ligand in this compound is also labile and, for example, can be displaced by diethyl sulfide giving [Mo(η-C_7H_7)(Et_2S)Br_2] (Scheme 1.32).[80]

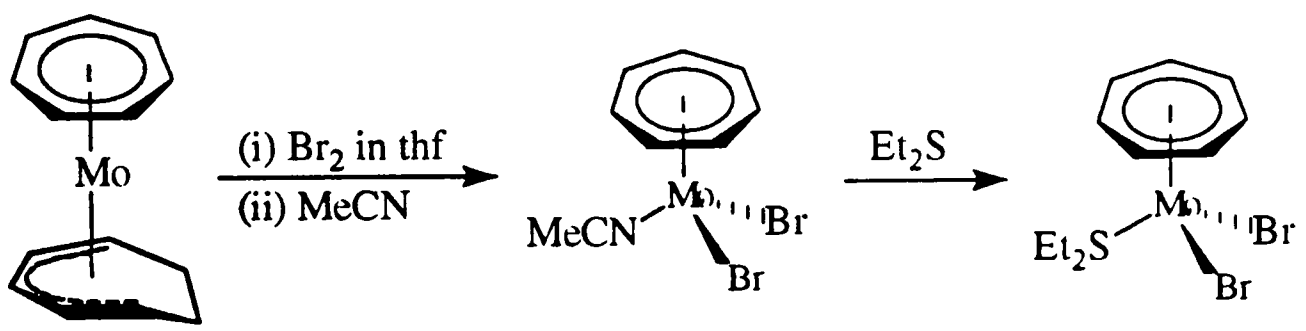

Scheme 1.32

1.4.3 From metal chlorides

Reduction of metal halides in the presence of olefins is a commonly used method to prepare low-valent metal(π-olefin) complexes. Fischer and co-workers have reported the reduction of $CrCl_2$, $MoCl_5$ and WCl_6 with appropriate reducing agents in the presence of cycloheptatriene giving the corresponding mixed sandwich complex [M(η-C_7H_7)(η-C_5H_5)] as shown in Scheme 1.33. However, the yields of these reactions are very low (< 2 %).[83] An improved route to the compound [Mo(η-C_7H_7)(η-C_5H_5)] has been reported which involves the reduction of [$MoCl_3(thf)_3$] with isopropylmagnesium bromide in the presence of cycloheptatriene and cyclopentadiene.[84] The yield of this reaction is 15 %. These sandwich compounds [M(η-C_7H_7)(η-C_5H_5)] can be oxidised with oxygen (for M = Cr) or iodine (for M = Mo or W) to give the corresponding paramagnetic cations [M(η-C_7H_7)(η-C_5H_5)]$^+$.

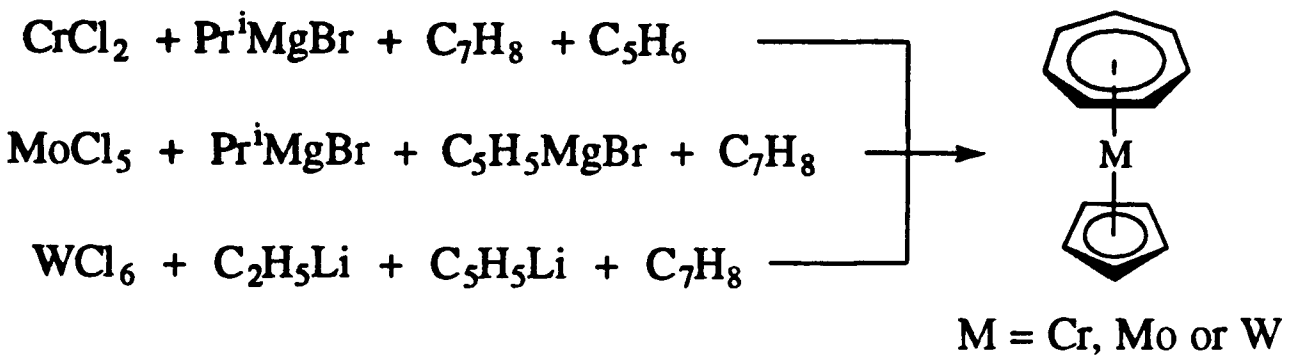

Scheme 1.33

Treatment of $[CrCl_3(thf)_3]$ with isopropylmagnesium bromide in the presence of cycloheptatriene gives $[Cr(\eta\text{-}C_7H_7)(\eta^4\text{-}C_7H_{10})]$ in 6 % yield. However, reaction of $[Cr(Pr^i)_4]$ (previously prepared from $CrCl_3$ with isopropylmagnesium bromide in diethyl ether) with cycloheptatriene yields a mixture of $[Cr(\eta\text{-}C_7H_7)(\eta^4\text{-}C_7H_{10})]$ (42 %) and $[Cr(\eta\text{-}C_7H_7)(\eta^5\text{-}C_7H_9)]$ (22%).[85]

Indirect routes to $M(\eta\text{-}C_7H_7)$ derivatives using metal halides as starting materials have also been reported. Reduction of $MoCl_5$ with $AlCl_3$ / Al in arenes gives the cations $[Mo(\eta\text{-arene})_2]^+$ which, upon alkaline disproportionation, yields the neutral complexes $[Mo(\eta\text{-arene})_2]$.[86] Treatment of $[Mo(\eta\text{-arene})_2]$ with allyl chloride gives the dimeric complexes $[Mo(\eta\text{-arene})(\eta\text{-}C_3H_5)Cl]_2$.[87] As mentioned in the section 1.4.1.4, reaction of this dimer with $[AlEtCl_2]_2$ in the presence of cycloheptatriene gives the cations $[Mo(\eta\text{-}C_7H_7)(\eta\text{-arene})]^+$, which are excellent precursors to $Mo(\eta\text{-}C_7H_7)$ derivatives.[71]

Treatment of $CrCl_3$ with PhMgBr and C_5H_5MgBr gives $[Cr(\eta\text{-}C_6H_6)(\eta\text{-}C_5H_5)]$, which undergoes ring expansion as shown in Scheme 1.34.[88]

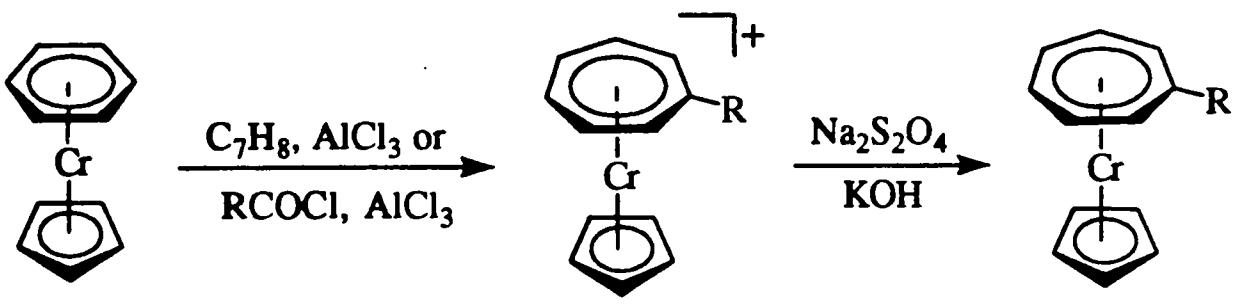

Scheme 1.34

1.4.4 Miscellaneous methods

Recently, it has been demonstrated that the reaction of $[W(PMe_3)_3H_6]$ with cycloheptatriene affords the compounds $[W(\eta\text{-}C_7H_7)(\eta^3\text{-}C_7H_{11})(PMe_3)]$ and $[W(\eta^5\text{-}C_7H_9)(\eta^3\text{-}C_7H_7)(PMe_3)_2]$ in moderate yields. The latter compound reacts with carbon monoxide giving $[W(\eta^5\text{-}C_7H_9)(\eta^3\text{-}C_7H_7)(PMe_3)(CO)]$ (Scheme 1.35).[89]

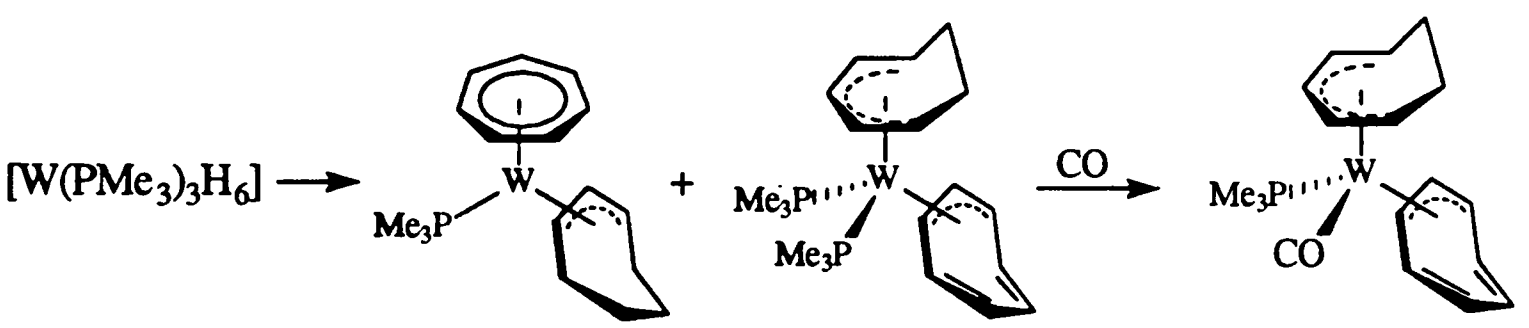

Scheme 1.35

1.5 η-Cycloheptatrienyl Complexes of the Group 7-10 Metals

The cycloheptatrienyl complexes of group 7-10 metals are rare and most of them have trihapto- or pentahapto-bonding mode. The cycloheptatrienyl group sometimes behaves as a bridging ligand. Selected examples are listed in Table 1.3.

Table 1.3 η-Cycloheptatrienyl derivatives of the group 7-10 metals

Compound		Reference
$[Mn(\eta\text{-}C_7H_6R)(\eta\text{-}C_5H_5)]^+$	R = Me or Ph	90, 91
$[Mn(\eta^5\text{-}C_7H_7)(CO)_3]$		92
$[Fe(\eta^5\text{-}C_7H_7)(CO)_3]^+$		93
$[Fe(\eta^3\text{-}C_7H_7)(\eta\text{-}C_5H_5)(CO)]$		94
$[Fe(\eta^3\text{-}C_7H_7)(CO)_3]^-$		95
$[Fe(CO)_3(\eta^3 : \eta^4\text{-}C_7H_7)M(CO)_x]$	M = Mn or Re, x = 3	96
	M = Rh, x = 2	96
$[M(\eta^5\text{-}C_7H_7)(\eta^5\text{-}C_7H_9)]$	M = Fe or Ru	97
$[Os(CO)_3(\eta^3 : \eta^4\text{-}C_7H_7)Os(CO)_2(MMe_3)]$	M = Si or Ge	98
$\{Os(\eta^5\text{-}C_7H_7)(CO)[P(OMe)_3]_2\}^+$		98
$[Co(\eta^3\text{-}C_7H_7)L_3]$	L = CO or PF_3	99, 16c
$[Pt(\eta^3\text{-}C_7H_7)(\eta\text{-}C_8H_{12})]^+$		100

The thermal or photochemical reaction of $[Mn(CO)_5]^-$ with $[C_7H_7][BF_4]$ gives $[Mn_2(CO)_{10}]$ and $C_{14}H_{14}$.[30,92a] The $Mn(\eta\text{-}C_7H_7)$ derivatives, namely $[Mn(\eta\text{-}C_7H_6R)(\eta\text{-}C_5H_5)]^+$(R = Me or Ph) have been prepared, however, by ring expansion of $[Mn(\eta\text{-}C_6H_6)(\eta\text{-}C_5H_5)]$ (Scheme 1.36).[88c,90] An alternative route to these compounds has been reported by Pauson and Segal.[91] Photolysis of a mixture of $[Mn(\eta\text{-}C_5H_4R)(CO)_3]$ (R =

H or Me) and C_7H_7 R'-7 (R' = Me, Ph or Bu^t) gives a mixture of *endo*- and *exo*-isomers of [Mn(η^6-C_7H_7R'-7)(η-C_5H_4R)] in which the *exo*-isomer is generally the predominant species. The *endo*-isomers react with $[CPh_3]^+$ to give [Mn(η-C_7H_6R')(η-C_5H_4R)]$^+$. The *exo*-isomers resist such hydride abstraction but are convertible into other isomers by hydrogen migration on heating. The resulting products, processing an *exo*-hydrogen atom, are then susceptible to hydride abstraction (Scheme 1.37). To the best of our knowledge, these compounds are the only examples of η^7-cycloheptatrienyl derivatives of group 7-10 metals.

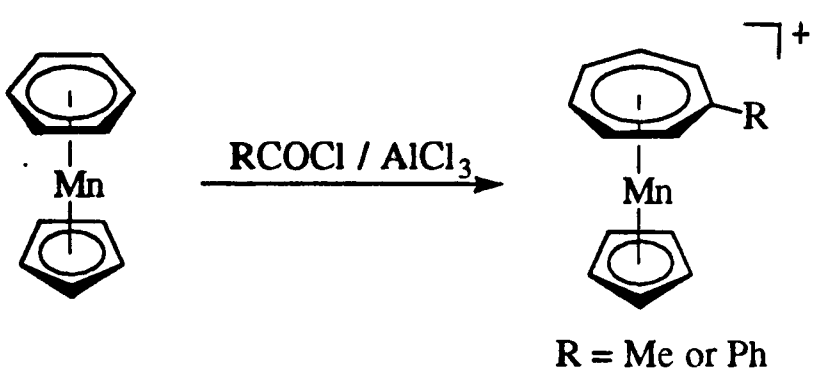

Scheme 1.36

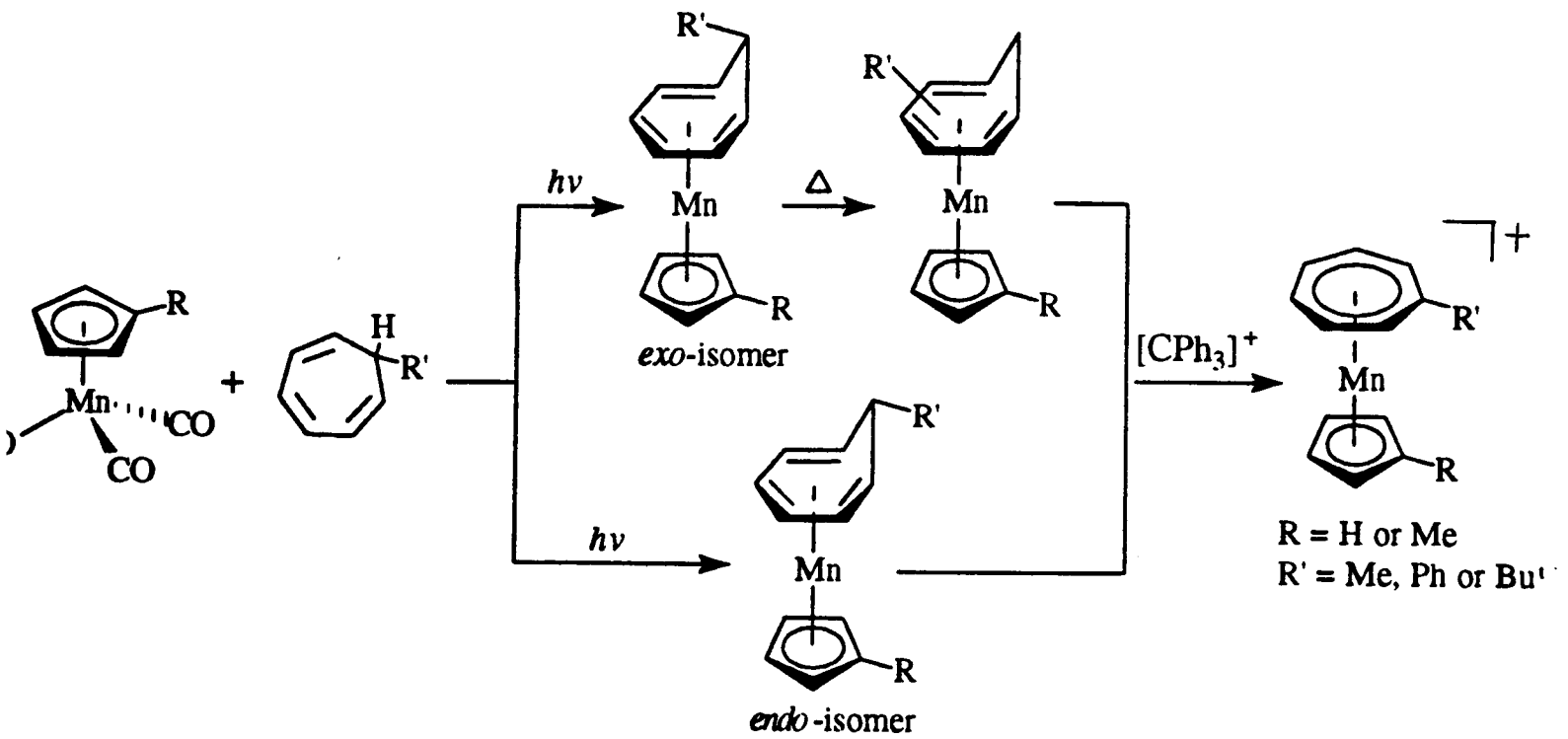

Scheme 1.37

1.6 Functional Group Properties of η-Cycloheptatrienyl Ligand

The η-cycloheptatrienyl ligand is a bulky ligand. It subtends a cone angle of 154°, which is even greater than that of the η-pentamethylcyclopentadienyl ligand (θ = 142°).[15] This ligand is generally regarded as a coordinated aromatic tropylium ion η-$C_7H_7^+$ and thus classified as a 6-electron donor. However, recent studies have shown that the assignment of +1 formal charge to this ligand in its complexes is inappropriate. For example, it gives the misleading impression that the η-C_7H_7 ligand is more susceptible to nucleophilic attack than other coordinated polyenes; in fact, according to the Davies, Green and Mingos rules,[77] it is the least susceptible to nucleophilic attack of all common coordinated polyenes. Moreover, X-ray photoelectron spectroscopy studies on [M(η-C_7H_7)(η-C_5H_5)] (M = Cr, V or Ti) have showed that the oxidation state of the metal increases in the sequence Cr < V < Ti. In the Ti compound, there is greater localisation of the negative charge on the C_7 ring (0.7 - 0.8 electrons) than on the C_5 ring (0.3 - 0.4 electrons).[101] Similar results have been obtained from metallation experiments[102] and ^{13}C NMR studies on this type of compounds.[103]

In an extensive study of Ti(η-C_7H_7) chemistry,[15] Green and co-workers have found that the Ti(η-C_7H_7) moiety is markedly reluctant to form any 18-electron complexes and it prefers to form 16-electron complexes [Ti(η-C_7H_7)L_2X] where L is a two-electron donor ligand and X is a one-electron σ-bonded group. This observation is also not consistent with the common formulation of the cycloheptatrienyl group as $C_7H_7^+$. Since if the η-C_7H_7 group is given a formal charge of +1, the [Ti(η-C_7H_7)]$^+$ group might be expected, by analogy with [V(η-C_5H_5)] which is also by definition d^4, to form 18-electron complexes such as [Ti(η-C_7H_7)$(CO)_4$]$^+$ {*cf.* [V(η-C_5H_5)$(CO)_4$]}. However, no complexes with π-acceptor ligands have been isolated.

In order to reveal the nature of the M-(η-C_7H_7) bond, J. C. Green and co-workers have performed photoelectron spectroscopy (PES) studies on the sandwich compounds [M(η-C_7H_7)(η-C_5H_5)] (M = Ti, V, Nb, Cr or Mo) and [Ta(η-C_7H_7)(η-C_5H_4Me)].[15,27,104,105] Sandwich compounds have been chosen because they give rise to

PE spectra with well-separated bands of metal, ligand, and mixed metal/ligand character. A qualitative molecular orbital (MO) diagram for these sandwich compounds is shown in Fig. 1.1 in which only the e symmetry $p\pi$ orbitals of the ligands are considered.[27] The metal d orbitals split into three sets; d_{z^2} ($1a_1$), d_{xz}, d_{yz} ($3e_1$) and $d_{x^2-y^2}$, d_{xy} ($1e_2$), which are of σ, π and δ symmetry respectively with respect to the metal-ring axes. The $1a_1$ orbital is essentially nonbonding. The $3e_1$ orbitals are strongly antibonding and the $1e_2$ orbitals are metal -> carbon back-bonding in nature. Since the e_1 and e_2 orbitals of C_7 ring are lower than those of C_5 ring, the e_2 interaction will take place primarily via C_7 ring whilst the e_1 involvement remains predominantly with C_5 ring. Thus the localisation of $1e_2$ MOs is of central importance in determining the nature of the M-(η-C_7H_7) bond. If these orbitals are largely metal-localised, this implies that the metal -> carbon back-bonding is relatively weak. If there is a significant contribution from the ligand, the metal-ligand δ interaction is strong.

It has been shown that for [Ti(η-C_7H_7)(η-C_5H_5)], the four least tightly bound electrons in $1e_2$ MOs are substantially localised on the C_7 ring, and have the primary role in forming the covalent bonds between the ring and the metal.[15,104] Formally three of these are derived from the metal and thus the compound is considered to have a Ti(IV) (d^0) metal centre. Consequently, this description redefines the formal charge of the ligand η-C_7H_7 as -3. In which case the Hückel 4n+2 rule for aromaticity is still satisfied. The proposal is in accord with the general pattern of Ti(η-C_7H_7) chemistry. The harder bases, such as ethers and amines, are more tightly bound to [Ti(η-C_7H_7)]$^+$ moiety than the softer bases, such as phosphines, indicating that the metal centre is more d^0 than d^4 in character.

Similar results have been obtained for group 5 sandwich compounds.[27,104] By comparing the relative intensities of the photoelectron bands in the He-I and He-II spectra, it has been shown that there is a significant contribution from both ligand and metal valence orbitals to the M-(η-C_7H_7) bonding MOs and the metal d orbital character of the $1e_2$ MOs decreases in the order Nb > V > Ta.

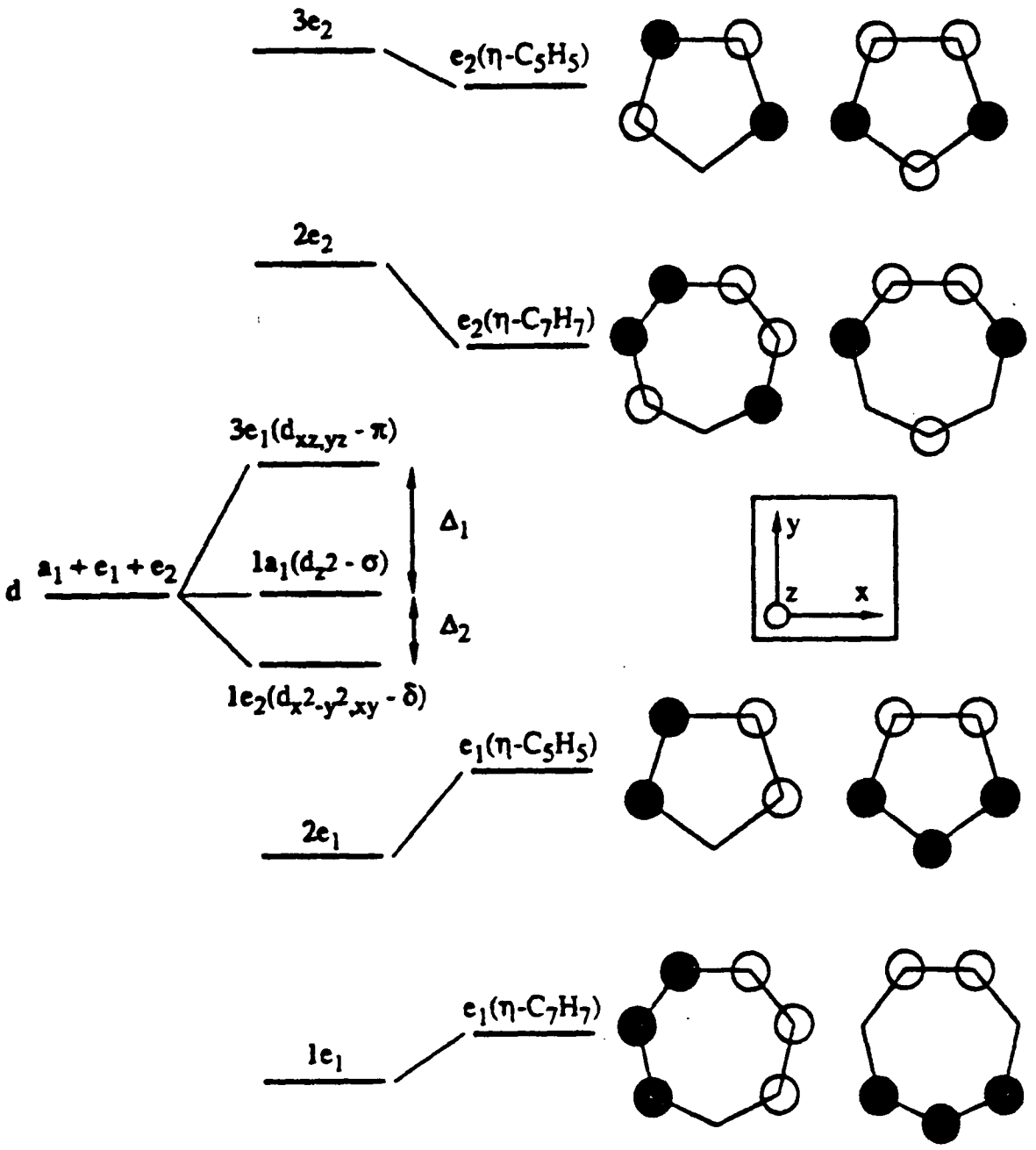

Fig. 1.1 Qualitative molecular orbital diagram for [M(η-C_7H_7)(η-C_5H_5)]

In a systematic PES study of [M(η-C_mH_m)(η-C_nH_n)] (m, n = 5, 6, 7 or 8), it has been found that the ring contribution in the e_2 MOs increases with ring size and decreases with increase in the metal atomic number across the transition series.[104,106] The results are consistent with the observation that the negative charge on the C_7 ring in [M(η-C_7H_7)(η-C_5H_5)] (M = Cr, V or Ti) follows the order : Ti > V > Cr.[101] Although the ligand contribution in the $1e_2$ MOs is smaller in [Cr(η-C_7H_7)(η-C_5H_5)] than in the Ti and V analogues, it has been noted that the a_1-e_2 splitting in [Cr(η-C_7H_7)(η-C_5H_5)] (1.6 eV) is substantially greater than that in [Cr(η-C_6H_6)$_2$] (0.9 eV), suggesting the high contribution the C_7 ring e_2 orbital makes to the e_2 MOs.[104]

These results may come to the conclusion that the metal -> carbon back-bonding is significant in M(η-C_7H_7) moiety where M is a group 4, 5 or 6 metal. Thus, the assignment of -3 to the formal charge of η-cycloheptatrienyl ligand seems to be more appropriate than the conventional value of +1. In other words, the ligand requires three electrons from the metal centre in the formation of the M-(η-C_7H_7) covalent bond.

1.7 Summary

The chemistry of η-cycloheptatrienyl-transition metal complexes has been outlined in this chapter. In general, there are three main routes to η-cycloheptatrienyl-molybdenum and -tungsten compounds. The first one employs metal carbonyls as starting materials, *via* the synthetically useful complexes $[M(\eta\text{-}C_7H_7)(CO)_3]^+$ (M = Mo or W), $[M(\eta\text{-}C_7H_7)(CO)_2X]$ (M = Mo or W, X = halogen) and $[Mo(\eta\text{-}C_7H_7)(\eta\text{-}C_6H_5R)]^+$ (R = H or Me). This route is well-developed and most of the known $Mo(\eta\text{-}C_7H_7)$ and $W(\eta\text{-}C_7H_7)$ compounds have been derived from these compounds. However, removal of all the carbonyl ligands in $[M(\eta\text{-}C_7H_7)(CO)_2X]$ is uncommon and the products derived from these compounds usually contain at least one carbonyl ligand. The cations $[Mo(\eta\text{-}C_7H_7)(\eta\text{-}C_6H_5R)]^+$ can be used to prepare carbonyl free η-cycloheptatrienyl-molybdenum complexes, but it requires several steps to prepare. The tungsten analogues of $[Mo(\eta\text{-}C_7H_7)(\eta\text{-}C_6H_5R)]^+$ are unknown.

The second method involves the versatile metal vapour synthesis technique. The compounds $[M(\eta\text{-}C_7H_7)(\eta^5\text{-}C_7H_9)]$ (M = Mo or W) can be prepared by co-condensation of molybdenum or tungsten atoms with cycloheptatriene. The synthetic utility of $[Mo(\eta\text{-}C_7H_7)(\eta^5\text{-}C_7H_9)]$ has been briefly explored. Although this method can prepare useful compounds in one-step, it is restrictive because the apparatus required is not available in most laboratories.

The last method is the conventional reductive method. Compounds $[Mo(\eta\text{-}C_7H_7)(\eta\text{-}C_5H_5)]$ (M = Mo or W) can be prepared from the corresponding metal halides in a one-pot reaction. However, the extremely low yield of these reactions limits further investigation of the chemistry. The following two chapters describe the preparation of $[M(\eta\text{-}C_7H_7)(\eta^5\text{-}C_7H_9)]$ (M = Mo or W) by a reductive method and the derivation of other η-cycloheptatrienyl-molybdenum and -tungsten compounds from these complexes.

1.8 References

1 J. P. Collman, L. S. Hegedus, J. R. Norton and R. G. Finke, *Principles and Applications of Organotransition Metal Chemistry*, University Science, California, 1987.

2 *Inorganic Materials*, eds. D. W. Bruce and D. O'Hare, Wiley, Chichester, 1992.

3 A. Yamamoto, *Organotransition Metal Chemistry*, Wiley, New York, 1986, pp.412-419.

4 G. Marr and B. W. Rockett, in *The Chemistry of the Metal-Carbon Bond*, eds. F. R. Hartley and S. Patai, Wiley, New York, 1982, vol. 1, ch. 10.

5 H. Zeiss, P. J. Wheatley and H. J. S. Winkler, *Benzenoid-Metal Complexes*, Ronald Press, New York, 1966.

6 W. E. Silverthorn, *Adv. Organometal. Chem.*, 1975, **13**, 47.

7 E. O. Fischer and W. Hafner, *Z. Naturforsch*, 1955, **10B**, 655.

8 (a) F. W. S. Benfield, M. L. H. Green, J. S. Ogden and D. Young, *J. Chem. Soc., Chem. Commun.*, 1973, 866; (b) P. S. Skell, D. L. Williams-Smith and M. J. McGlinchey, *J. Am. Chem. Soc.*, 1973, **95**, 3337; (c) M. P. Silvon, E. M. Van Dam and P. S. Skell, *J. Am. Chem. Soc.*, 1974, **96** , 1945; (d) M. T. Anthony, M. L. H. Green and D. Young, *J. Chem. Soc., Dalton Trans.*, 1975, 1412; (e) F. G. N. Cloke, M. L. H. Green and D. H. Price, *J. Chem. Soc., Chem. Commun.*, 1978, 431; (f) F. G. N. Cloke, M. F. Lappert, G. A. Lawless and A. C. Swain, *J. Chem. Soc., Chem. Commun.*, 1987, 1667.

9 H. J. Dauben and L. R. Honnen, *J. Am. Chem. Soc.*, 1958, **80**, 5570.

10 G. Deganello, *Transition Metal Complexes of Cyclic polyolefins*, Academic Press, London, 1979, ch.1.

11 (a) H. O. Van Oven and H. J. de Liefde Meijer, *J. Organomet. Chem.*, 1970, **23**, 159; (b) B. Demerseman, G. Bouquet and M. Bigorgne, *J. Organomet. Chem.*, 1975, **101**, C24; (c) J. D. Zeinstra and J. L. De Boer, *J. Organomet. Chem.*, 1973, **54**, 207.

12 L. B. Kool, M. D. Rausch and R. D. Rogers, *J. Organomet. Chem.*, 1985, **297**, 289.

13 H. O. Van Oven, C. J. Groenenboom and H. J. de Liefde Meijer, *J. Organomet. Chem.*, 1974, **81**, 379.

14 (a) J. Blenkers, P. Bruin and J. H. Teuben, *J. Organomet. Chem.*, 1985, **297**, 61; (b) R. D. Rogers and J. H. Teuben, *J. Organomet. Chem.*, 1988, **354**, 169.

15 C. E. Davies, I. M. Gardiner, J. C. Green, M. L. H. Green, N. J. Hazel, P. D. Grebenik, V. S. B. Mtetwa and K. Prout, *J. Chem. Soc., Dalton Trans.*, 1985, 669.

16 (a) H. O. Van Oven and H. J. de Liefde Meijer, *J. Organomet. Chem.*, 1971, **31**, 71; (b) J. Müller and B. Mertschenk, *Chem. Ber.*, 1972, **105**, 3346; (c) P. L. Timms and T. W. Turney, *J. Chem. Soc., Dalton Trans.*, 1976, 2021.

17 J. C. Green, M. L. H. Green and N. M. Walker, *J. Chem. Soc., Dalton Trans.*, 1991, 173.

18 F. G. N. Cloke, M. L. H. Green and P. J. Lennon, *J. Organomet. Chem.*, 1980, **188**, C25.

19 H. T. Verkouw, M. E. E. Veldman, C. J. Groenenboom, H. O. Van Oven and H. J. de Liefde Meijer, *J. Organomet. Chem.*, 1975, **102**, 49.

20 G. M. Diamond, M. L. H. Green, P. Mountford, N. M. Walker and J. A. K. Howard, *J. Chem. Soc., Dalton Trans.*, 1992, 417.

21 M. L. H. Green, P. Mountford and N. M. Walker, *J. Chem. Soc., Chem. Commun.*, 1989, 908.

22 J. Müller and B. Mertschenk, *J. Organomet. Chem.*, 1972, **34**, C41.

23 (a) R. P. M. Werner and S. A. Manastyrskyj, *J. Am. Chem. Soc.*, 1961, **83**, 2023; (b) F. Calderazzo and P. L. Calvi, *Chim. Ind. (Milan)*, 1962, **44**, 1217.

24 M. L. H. Green, D. O'Hare and J. G. Watkin, *J. Chem. Soc., Chem. Commun.*, 1989, 698.

25 M. L. H. Green, A. K. Hughes, P. C. McGowan, P. Mountford, P. Scott and S. J. Simpson, *J. Chem. Soc., Dalton Trans.*, 1992, 1591.

26 (a) R. B. King and F. G. A. Stone, *J. Am. Chem. Soc.*, 1959, **81** , 5263; (b) R. B. King, *Organometal. Syn.*, 1965, **1**, 140; (c) J. Müller and W. Goll, *J. Organomet. Chem.*, 1974, **71**, 257.

27 J. C. Green, M. L. H. Green, N. Kaltsoyannis, P. Mountford, P. Scott and S. J. Simpson, *Organometallics*, 1992, **11**, 3353.

28 J. Müller, P. Göser and P. Laubereau, *J. Organomet. Chem.*, 1968, **14**, P7.

29 J. Müller and B. Mertschenk, *J. Organomet. Chem.*, 1972, **34**, 165.

30 E. W. Abel, M. A. Bennett, R. Burton and G. Wilkinson, *J. Chem. Soc.*, 1958, 4559.

31 (a) M. A. Bennett, L. Pratt and G. Wilkinson, *J. Chem. Soc.* , 1961, 2037; (b) W. Strohmeier, *Chem. Ber.*, 1961, **94**, 2490; (c) F. A. Cotton, J. A. McCleverty and J. E. White, *Inorg. Synth.*, 1967, **9**, 121.

32 R. B. King and A. Fronzaglia, *Inorg. Chem.*, 1966, **5**, 1837.

33 J. D. Dunitz and P. Pauling, *Helv. Chim. Acta*, 1960, **43**, 2188.

34 C. G. Kreiter, M. Lang and H. Strack, *Chem. Ber.*, 1975, **108**, 1502.

35 (a) W. R. Roth and W. Grimme, *Tetrahedron Lett.*, 1966, 2347; (b) M. I. Foreman, G. R. Knox, P. L. Pauson, K. H. Todd and W. E. Watts, *J. Chem. Soc., Chem. Commun.*, 1970, 843; (c) M. I. Foreman, G. R. Knox, P. L. Pauson, K. H. Todd and W. E. Watts, *J. Chem. Soc., Perkin Trans. 2*, 1972, 1141.

36 K. W. Egger, *J. Am. Chem. Soc.*, 1967, **89**, 3688.

37 (a) E. W. Abel, M. A. Bennett and G. Wilkinson, *J. Chem. Soc.*, 1959, 2323; (b) R. Schmutzler, *Chem. Ber.*, 1963, **96**, 2435; (c) L. Chandrasegaran and G. A. Rodley, *Inorg. Chem.*, 1965, **4**, 1360; (d) A. Pidcock and B. W. Taylor, *J. Chem. Soc. (A)*, 1967, 877; (e) H. Werner, K. Deckekmann and U. Schönenberger, *Helv. Chim. Acta.*, 1970, **53**, 2002; (f) M. Gower and L. A. P. Kane-Maguire, *Inorg. Chim. Acta*, 1979, **37**, 79.

38 W. Strohmeier and D. von Hobe, *Z. Naturforsch*, 1963, **18b**, 981.

39 D. L. S. Brown, J. A. Connor, C. P. Demain, M. L. Leung, J. A. Martinho-Simoes, H. A. Skinner and M. T. Zafarani-Moattar, *J. Organomet. Chem.*, 1977, **142**, 321.

40 K. M. Al-Kathumi and L. A. P. Kane-Maguire, *J. Chem. Soc., Dalton Trans.*, 1974, 428.

41 (a) R. B. King and K. H. Pannell, *Inorg. Chem.*, 1968, **7**, 273; (b) W. P. Anderson, W. G. Blenderman and K. A. Drews, *J. Organomet. Chem.*, 1972, **42**, 139; (c) M. Djazayeri, C. G. Kreiter, H. M. Kurz, M. Lang and S. Ozkar, *Z. Naturforsch*, 1976, **31B**, 1238.

42 (a) A. Salzer and H. Werner, *J. Organomet. Chem.*, 1975, **87**, 101; (b) A. Salzer and H. Werner, *Z. Anorg. Allg. Chem.*, 1975, **418**, 88.

43 J. D. Munro and P. L. Pauson, *J. Chem. Soc.*, 1961, 3475.

44 (a) G. R. Clark and G. J. Palenik, *J. Chem. Soc., Chem. Commun.* , 1969, 667; (b) G. R. Clark and G. J. Palenik, *J. Organomet. Chem.*, 1973, **50**, 185.

45 P. D. Harvey, I. S. Butler and D. F. R. Gilson, *Inorg. Chem.*, 1987, **26**, 32.

46 G. Hoch, R. Panter and M. L. Ziegler, *Z. Naturforsch*, 1976, **31B**, 294.

47 (a) G. Deganello, T. Boschi, L. Toniolo and G. Albertin, *Inorg. Chim. Acta*, 1974, **10**, L3; (b) E. E. Isaacs and W. A. G. Graham, *J. Organomet. Chem.* , 1975, **90**, 319; (c) Von. R. Panter and M. L. Ziegler, *Z. Anorg. Allg. Chem.*, 1979, **453**, 14.

48 (a) M. Bochmann, M. Cooke, M. Green, H. P. Kirsch, F. G. A. Stone and A. J. Welch, *J. Chem. Soc., Chem. Commun.*, 1976, 381; (b) M. Bochmann, M. Green, H. P. Kirsch and F. G. A. Stone, *J. Chem. Soc., Dalton Trans.*, 1977, 714.

49 N. W. Alcock, *Acta Crystallogr., Sect. B*, 1977, **33**, 2943.

50 (a) M. Green, H. P. Kirsch, F. G. A. Stone and A. J. Welch, *J. Chem. Soc., Dalton Trans.*, 1977, 1755; (b) M. Green, H. P. Kirsch, F. G. A. Stone and A. J. Welch, *Inorg. Chim. Acta*, 1978, **29**, 101.

51 (a) P. Hackett and G. Jaouen, *Inorg. Chim. Acta*, 1975, **12**, L19; (b) A. Salzer, *Inorg. Chim. Acta*, 1976, **17**, 221; (c) D. A. Sweigart, M. Gower and L. A. P. Kane-Maguire, *J. Organomet. Chem.*, 1976, **108**, C15.

52 (a) P. L. Pauson, G. H. Smith and J. H. Valentine, *J. Chem. Soc. (C)*, 1967, 1057; (b) K. M. Al-Kathumi and L. A. P. Kane-Maguire, *J. Organomet. Chem.*, 1975, **102**, C4; (c) P. O. Tremmel, K. Weidenhammer, H. Wienand and M. L. Ziegler, *Z. Naturforsch*, 1975, **30B**, 699; (d) G. Deganello and T. Boschi, *Chim. Ind. (Milan)*, 1976, **58**, 654; (e) D. A. Brown, N. J. Fitzpatrick, W. K. Glass and T. H. Taylor, *Organometallics*, 1986, **5**, 158.

53 J. D. Munro and P. L. Pauson, *J. Chem. Soc.*, 1961, 3479.

54 K. M. Al-Kathumi and L. A. P. Kane-Maguire, *J. Chem. Soc., Dalton Trans.*, 1973, 1683.

55 M. L. Ziegler, H. E. Sasse and B. Nuber, *Z. Naturforsch*, 1975, **30B**, 26.

56 (a) R. B. King, *Inorg. Chem.* , 1963, **2**, 936; (b) T. W. Beall and L. W. Houk, *Inorg. Chem.*, 1972, **11**, 915; (c) C. Bitcon, R. Breeze, P. F. Miller and M. W. Whiteley, *J. Organomet. Chem.*, 1989, **364**, 181.

57 T. W. Beall and L. W. Houk, *Inorg. Chem.*, 1973, **12**, 1979.

58 (a) M. D. Rausch, A. K. Ignatowicz, M. R. Churchill and T. A. O'Brien, *J. Am. Chem. Soc.*, 1968, **90**, 3242; (b) M. R. Churchill and T. A. O'Brien, *J. Chem. Soc. (A)*, 1969, 1110.

59 R. B. King and M. B. Bisnette, *Inorg. Chem.*, 1964, **3**, 785.

60 (a) E. E. Isaacs and W. A. G. Graham, *Can. J. Chem.*, 1975, **53**, 975; (b) H. E.

Sasse, G. Hoch and M. L. Ziegler, *Z. Anorg. Allg. Chem.*, 1974, **406**, 263; (c) M. L. Ziegler, H. E. Sasse and B. Nuber, *Z. Naturforsch*, 1975, **30B**, 22.

61 D. Mohr, H. Wienand and M. L. Ziegler, *Z. Naturforsch*, 1976, **31B**, 66.

62 D. Mohr, H. Wienand and M. L. Ziegler, *J. Organomet. Chem.*, 1977, **134**, 281.

63 I. B. Benson, S. A. R. Knox, P. J. Naish and A. J. Welch, *J. Chem. Soc., Chem. Commun.*, 1978, 878.

64 R. B. King and M. B. Bisnette, *Tetrahedron Lett.*, 1963, 1137.

65 (a) R. B. King and A. Fronzaglia , *J. Am. Chem. Soc.*, 1966, 88, 709; (b) R. B. King, *J. Organomet. Chem.*, 1967, **8**, 129; (c) M. A. Bennett, R. Bramley and R. Watt, *J. Am. Chem. Soc.*, 1969, **91**, 3089; (d) J. W. Faller, *Inorg. Chem.*, 1969, **8**, 767.

66 (a) R. Breeze, S. Endud and M. W. Whiteley, *J. Organomet. Chem.*, 1986, **302**, 371; (b) R. A. Brown, S. Endud, J. Friend, J. M. Hill and M. W. Whiteley, *J. Organomet. Chem.*, 1988, **339**, 283.

67 (a) R. Breeze, A. Ricalton and M. W. Whiteley, *J. Organomet. Chem.*, 1987, **327**, C29; (b) R. Breeze, M. S. Plant, A. Ricalton, D. J. Sutton and M. W. Whiteley, *J. Organomet. Chem.*, 1988, **356**, 343.

68 A. Ricalton and M. W. Whiteley, *J. Organomet. Chem.*, 1989, **361**, 101.

69 R. L. Beddoes, A. Ricalton and M. W. Whiteley, *Acta Crystallogr., Sect. C,* 1988, **44**, 2025.

70 D. L. Reger, D. J. Fauth and M. D. Dukes, *J. Organomet. Chem.*, 1979, **170**, 217.

71 M. L. H. Green and J. Knight, *J. Chem. Soc., Dalton Trans.*, 1976, 213.

72 M. B. Hossain and V. van der Helm, *Inorg. Chem.*, 1978, **17**, 2893.

73 E. F. Ashworth, J. C. Green, M. L. H. Green, J. Knight, R. B. A. Pardy and N. J. Wainwright, *J. Chem. Soc., Dalton Trans.*, 1977, 1693.

74 M. L. H. Green and R. B. A. Pardy, *Polyhedron*, 1985, **4**, 1035.

75 J. S. Adams, C. Bitcon, J. R. Brown, D. Collison, M. Cunningham and M. W. Whiteley, *J. Chem. Soc., Dalton Trans.*, 1987, 3049.

76 R. L. Beddoes, C. Bitcon, A. Ricalton and M. W. Whiteley, *J. Organomet. Chem.*, 1989, **367**, C21.

77 S. G. Davies, M. L. H. Green and D. M. P. Mingos, *Tetrahedron*, 1978, **34**, 3047.

78 E. M. van Dam, W. N. Brent, M. P. Silvon and P. S. Skell, *J. Am. Chem. Soc.*, 1975, **97**, 465.

79 J. R. Blackborrow, C. R. Eady, E. A. Koerner von Gustorf, A. Scrivanti and O. Wolfbeis, *J. Organomet. Chem.*, 1976, **108**, C32.

80 R. C. Tovey, D. Phil. Thesis, University of Oxford, 1986.

81 (a) M. L. H. Green and P. A. Newman, *J. Chem. Soc., Chem. Commun.*, 1984, 816; (b) M. L. H. Green and P. A. Newman, *J. Chem. Soc., Dalton Trans.*, 1989, 331.

82 A. Gourdon and K. Prout, *Acta Crystallogr., Sect. B,* 1982, **38**, 1596.

83 (a) E. O. Fisher and J. Müller, *Z. Naturforsch*, 1963, **18B**, 1137; (b) H. W. Wehner, E. O. Fisher and J. Müller, *Chem. Ber.*, 1970, **103**, 2258.

84 H. O. van Oven, C. J. Groenenboom and H. J. de Liefde Meijer, *J. Organomet. Chem.*, 1974, **81**, 379.

85 J. Müller and W. Holzinger, *Z. Naturforsch*, 1978, **33B**, 1309.

86 E. O. Fischer, F. Scherer and H. O. Stahl, *Chem. Ber.*, 1960, **93**, 2065.

87 M. L. H. Green and W. E. Silverthorn, *J. Chem. Soc., Dalton Trans.*, 1973, 301.

88 (a) E. O. Fisher and S. Breitschaft, *Angew. Chem., Int. Ed. Engl.*, 1963, **2**, 44; (b) E. O. Fisher and S. Breitschaft, *Angew. Chem., Int. Ed. Engl.*, 1963, **2**, 100; (c) E. O. Fisher and S. Breitschaft, *Chem. Ber.*, 1966, **99**, 2213.

89 M. L. H. Green, D. K. Siriwardene, D. O'Hare and L. -L. Wong, *J. Chem. Soc., Dalton Trans.*, 1988, 2851.

90 E. O. Fisher and S. Breitschaft, *Angew. Chem.*, 1963, **75**, 167.

91 P. L. Pauson and J. A. Segal, *J. Chem. Soc., Dalton Trans.*, 1975, 2387.

92 (a) T. H. Whitesides and R. A. Budnik, *J. Chem. Soc., Chem. Commun.*, 1971, 1514; (b) T. H. Whitesides and R. A. Budnik, *Inorg. Chem.*, 1976, **15**, 874.

93 J. E. Mahler, D. A. K. Jones and R. Pettit, *J. Am. Chem. Soc.*, 1964, **86**, 3589.

94 D. Ciappenelli and M. Rosenblum, *J. Am. Chem. Soc.*, 1969, **91**, 6876.

95 (a) H. Maltz and B. A. Kelly, *J. Chem. Soc., Chem. Commun.*, 1971, 1390; (b) M. Moll, H. Behrens, R. Kellner, H. Knöchel and P. Würstl, *Z. Naturforsch*, 1976, **31B**, 1019.

96 M. J. Bennett, J. L. Pratt, K. A. Simpson, L. K. K. Li Shing Man and J. Takats, *J. Am. Chem. Soc.*, 1976, **98**, 4810.

97 (a) J. R. Blackborow, K. Hildenbrand, E. Koerner von Gustorf, A. Scrivanti, C. R. Eady, D. Ehntolt and C. Krüger, *J. Chem. Soc., Chem. Commun.*, 1976, 16; (b) J. Müller, C. G. Kreiter, B. Mertschenk and S. Schmitt, *Chem. Ber.*, 1975,

108, 273.

98 S. A. R. Knox, R. P. Phillips and F. G. A. Stone, *J. Chem. Soc., Dalton Trans.*, 1976, 552.

99 M. A. Bennett, R. Bramley and R. Watt, *J. Am. Chem. Soc.*, 1969, **91**, 3089.

100 M. Green, D. M. Grove, J. L. Spencer and F. G. A. Stone, *J. Chem. Soc., Dalton Trans.*, 1977, 2228.

101 C. J. Groenenboom, G. Sawatzky, H. J. de Liefde Meijer and F. Jellinek, *J. Organomet. Chem.*, 1974, **76**, C4.

102 C. J. Groenenboom, H. J. de Liefde Meijer and F. Jellinek, *J. Organomet. Chem.*, 1974, **69**, 235.

103 C. J. Groenenboom and F. Jellinek, *J. Organomet. Chem.*, 1974, **80**, 229.

104 S. Evans, J. C. Green, S. E. Jackson and B. Higginson, *J. Chem. Soc., Dalton Trans.*, 1974, 304.

105 N. Kaltsoyannis, D. Phil. Thesis, University of Oxford, 1992.

106 D. W. Clack and K. D. Warren, *Inorg. Chim. Acta*, 1978, **30**, 251.

CHAPTER TWO

η-Cycloheptatrienyl-Molybdenum Chemistry

2.1 Introduction

As mentioned in the previous chapter, the compound [Mo(η-C_7H_7)(η^5-C_7H_9)] is a potentially useful precursor to other η-cycloheptatrienyl-molybdenum compounds.[1] However, the synthesis involves metal vapour synthesis for which the apparatus is not available in most laboratories.[2] Hence, the search for an alternative pathway to this compound is desirable.

The related chromium complexes have been prepared by a conventional reductive method. For example, reduction of [$CrCl_3(thf)_3$] with isopropylmagnesium bromide in the presence of cycloheptatriene gives [Cr(η-C_7H_7)(η^4-C_7H_{10})] in 6 % yield. The reaction of $CrCl_3$ with isopropylmagnesium bromide produces $CrPr^i_4$, which reacts with cycloheptatriene to afford a mixture of product, namely [Cr(η-C_7H_7)(η^4-C_7H_{10})] (42 %) and [Cr(η-C_7H_7)(η^5-C_7H_9)] (22 %).[3] However, no reduction of molybdenum or tungsten halides in the presence of cycloheptatriene as the sole olefin has so far been reported. This chapter describes the preparation of [Mo(η-C_7H_7)(η^5-C_7H_9)] from $MoCl_5$ and the exploration of η-cycloheptatrienyl-molybdenum chemistry based on this compound.

2.2 Preparation of [Mo(η-C_7H_7)(η^5-C_7H_9)]

A suspension of $MoCl_5$ in thf was treated with an excess of cycloheptatriene at -80^{0}C giving a greenish-yellow suspension. Five equivalents of sodium amalgam was then added with stirring and the mixture was allowed to warm to room temperature. During the course of the reaction, the colour of the mixture changed gradually from greenish yellow to brown, and then to deep green. After removing the volatiles and then extracting the residue with light petroleum (b.p. 40-60^{0}C), a deep green solution was obtained from which green microcrystals were separated. The ^{1}H NMR spectrum of these microcrystals showed that they were a mixture of [Mo(η^6-C_7H_8)$_2$] **4** and [Mo(η-C_7H_7)(η^5-C_7H_9)] **5** in 1.7 : 1 ratio (Scheme 2.1). Previously, these compounds were available only by a metal vapour synthesis route.[2]

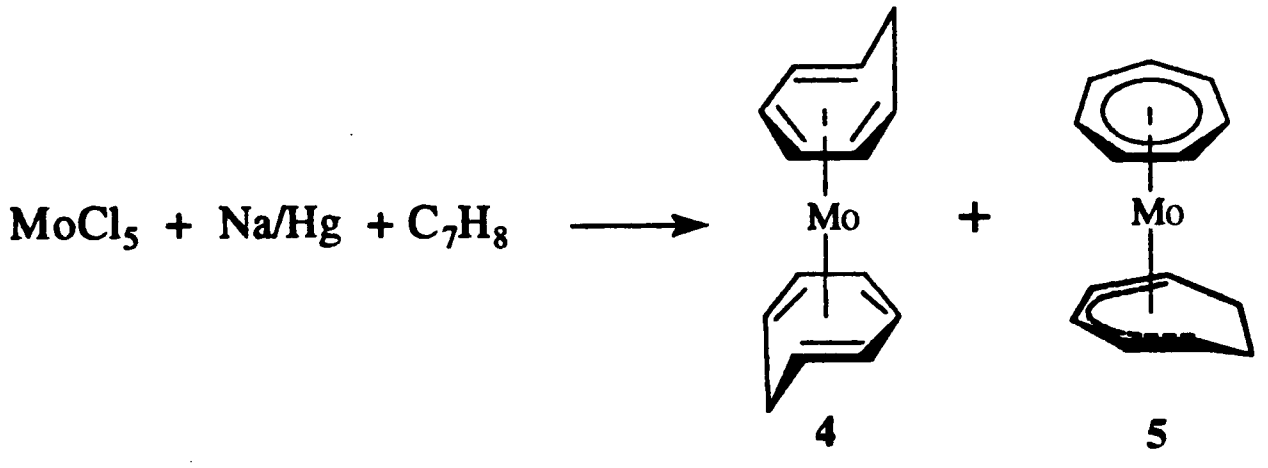

Scheme 2.1

It has been reported that the compound $[Mo(\eta^6\text{-}C_7H_8)_2]$ **4** is thermally unstable and isomerises quantitatively on heating to give the compound $[Mo(\eta\text{-}C_7H_7)(\eta^5\text{-}C_7H_9)]$ **5**.[2b] Thus it is reasonable to suggest that compound **4** is initially formed in the above reaction, but a portion of it isomerises to **5**. In fact, heating the green microcrystalline product at 70°C for 2 h gave pure **5** as dark red microcrystals. The above reduction reaction can be performed in a large scale. Typically, 10.0 g of $MoCl_5$ gave 4.0 g of $[Mo(\eta\text{-}C_7H_7)(\eta^5\text{-}C_7H_9)]$ **5** (39 % yield).

We note that $MoCl_5$ reacts with thf therefore the cold thf (-20°C) was added to $MoCl_5$ which was cooled by liquid nitrogen. Then this was warmed to -80°C before addition of cycloheptatriene and sodium amalgam as described in the Experimental section. These precautions can be neglected by using the Mo(IV) compound $[MoCl_4(thf)_2]$ as the starting material. This compound was prepared from $MoCl_5$ in two steps as shown in Scheme 2.2.[4] Reduction of $[MoCl_4(thf)_2]$ in thf with four equivalents of sodium amalgam in the presence of cycloheptatriene produced a mixture of $[Mo(\eta^6\text{-}C_7H_8)_2]$ **4** and $[Mo(\eta\text{-}C_7H_7)(\eta^5\text{-}C_7H_9)]$ **5** in 3 : 2 ratio in 46 % yield.

Scheme 2.2

2.3 Preparation and Characterisation of $[Mo(\eta\text{-}C_7H_7)(MeCN)I_2]$

Tovey reported that the oxidation of $[Mo(\eta\text{-}C_7H_7)(\eta^5\text{-}C_7H_9)]$ with one equivalent of iodine in thf gave a mixture of products $[Mo(\eta\text{-}C_7H_7)(thf)I_2]$ and $[Mo(\eta\text{-}C_7H_7)(\eta^5\text{-}C_7H_9)I][I]$ and both of these complexes reacted with acetonitrile to give $[Mo(\eta\text{-}C_7H_7)(MeCN)I_2]$.[1] It is logical to perform the oxidation in acetonitrile with a view to preparing $[Mo(\eta\text{-}C_7H_7)(MeCN)I_2]$ in one step. As expected, oxidation of $[Mo(\eta\text{-}C_7H_7)(\eta^5\text{-}C_7H_9)]$ with one equivalent of iodine in acetonitrile afforded the compound $[Mo(\eta\text{-}C_7H_7)(MeCN)I_2]$ **6** in good yield (Scheme 2.3). The compound **6** is more thermally robust than $[Mo(\eta\text{-}C_7H_7)(thf)I_2]$ and is stable indefinitely at 50°C and is air and water stable in solid and solution.

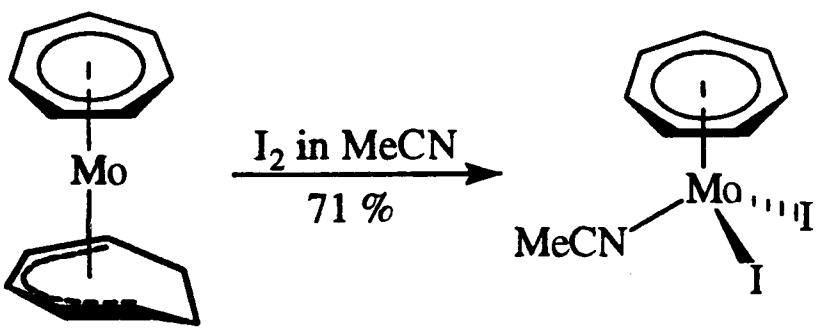

5 **6**

Scheme 2.3

The compound **6** was characterised by microanalysis, IR and EPR spectroscopy and the data were reported previously.[1] Unambiguous characterisation by X-ray structure determination has been performed in this study. Single crystals of **6** suitable for an X-ray structure analysis were grown by cooling a concentrated acetonitrile solution. An X-ray diffraction study was performed by Dr. Philip Mountford of this laboratory. The molecular structure of **6** is shown in Fig. 2.1. It has a typical three-legged piano stool structure with the $\eta\text{-}C_7H_7$ ligand bonded symmetrically to the metal. The acetonitrile ligand is N-bonded to the Mo centre. A complete listing of bond lengths and angles, atomic coordinates and thermal parameters is given in Appendix B1. Selected bond lengths and angles appear in Table 2.1. These data are unexceptional.

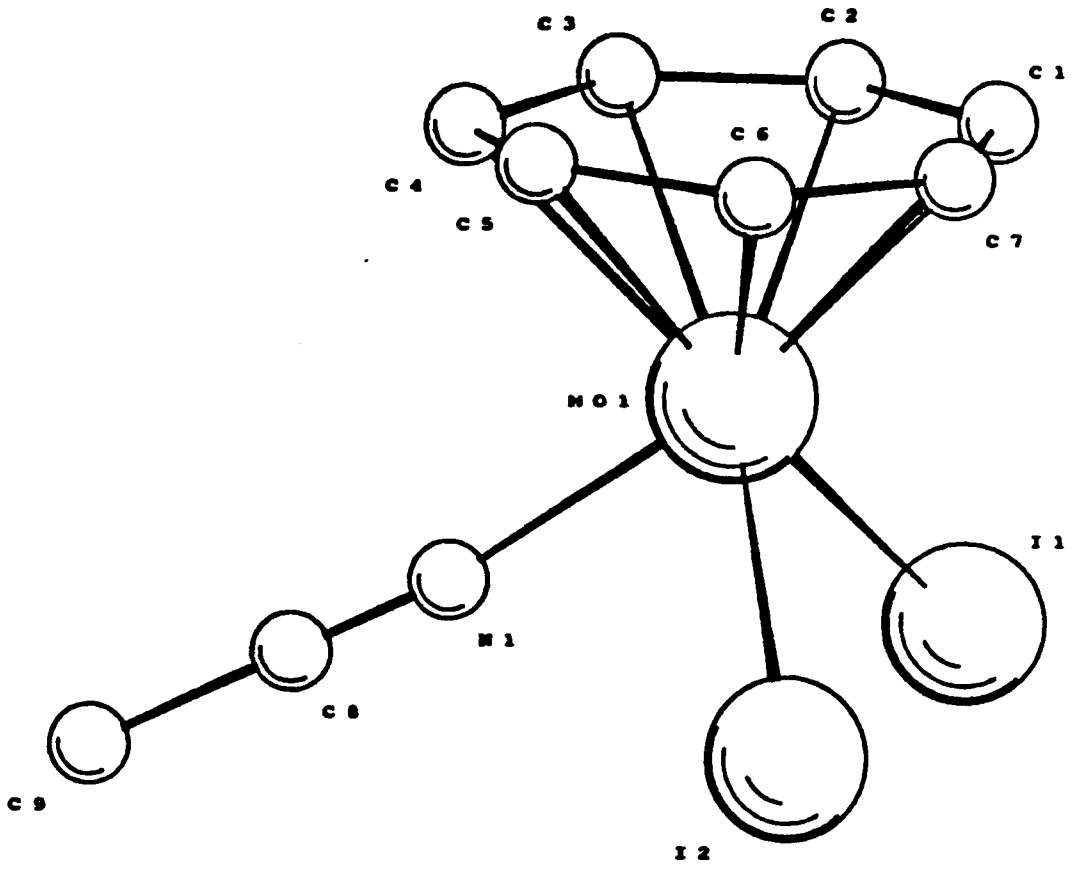

Fig. 2.1 Molecular structure of $[Mo(\eta\text{-}C_7H_7)(MeCN)I_2]$ **6**

Table 2.1 : Selected bond length (Å) and angles (0) for $[Mo(\eta\text{-}C_7H_7)(MeCN)I_2]$ **6**

Mo(1) - I(1)	2.8210(4)	C(1) - C(2)	1.389(8)
Mo(1) - I(2)	2.8003(4)	C(2) - C(3)	1.409(8)
Mo(1) - N(1)	2.166(3)	C(3) - C(4)	1.392(9)
Mo(1) - C(1)	2.264(4)	C(4) - C(5)	1.41(1)
Mo(1) - C(2)	2.271(5)	C(5) - C(6)	1.42(1)
Mo(1) - C(3)	2.272(5)	C(6) - C(7)	1.404(9)
Mo(1) - C(4)	2.258(5)	C(1) - C(7)	1.389(9)
Mo(1) - C(5)	2.280(5)	N(1) - C(8)	1.135(6)
Mo(1) - C(6)	2.260(5)	C(8) - C(9)	1.450(6)
Mo(1) - C(7)	2.270(5)	Mo(1) - C_7(centroid)	1.592

N(1) - Mo(1) - I(1)	84.1(1)	I(2) - Mo(1) - I(1)	87.47(1)
N(1) - Mo(1) - I(2)	84.6(1)	C(8) - N(1) - Mo(1)	173.8(4)

The 17-electron compound $[Mo(\eta\text{-}C_7H_7)(MeCN)I_2]$ **6** behaves as a one-dimensional antiferromagnet which was suggested by magnetic model fittings and its crystal structure. The details will be described in chapter four.

2.4 Reactivity Studies of $[Mo(\eta\text{-}C_7H_7)(MeCN)I_2]$

The compound $[Mo(\eta\text{-}C_7H_7)(MeCN)I_2]$ is an excellent precursor to other η-cycloheptatrienyl-molybdenum derivatives. The reactivity studies of this compound will be the focus of this section.

2.4.1 Reaction with PMe_3

The MeCN ligand in **6** is rather labile and, for example, can be displaced by PPh_3 under forcing conditions.[1] However, treatment of $[Mo(\eta\text{-}C_7H_7)(MeCN)I_2]$ **6** with one equivalent of PMe_3 in thf at room temperature gave a red-green dichroic solution from which dark red crystals of $[Mo(\eta\text{-}C_7H_7)(PMe_3)I_2]$ **7** were isolated in good yield (Scheme 2.4). Previously, this air-stable compound together with $[Mo(\eta\text{-}C_7H_7)(PMe_3)_2I][I]$ were obtained in a reaction of $[Mo(\eta\text{-}C_7H_7)(thf)I_2]$ and an excess of PMe_3.[1] The yields of these compounds were not mentioned.

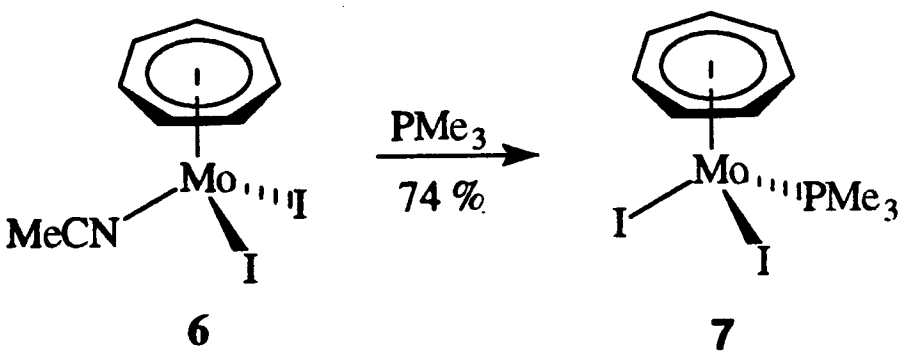

6 **7**

Scheme 2.4

2.4.2 Reaction with Na/Hg and PMe_3

Reduction of $[Mo(\eta\text{-}C_7H_7)(MeCN)I_2]$ **6** with one equivalent of sodium amalgam in the presence of two equivalents of PMe_3 in toluene gave the air-sensitive product $[Mo(\eta\text{-}C_7H_7)(PMe_3)_2I]$ **8** in excellent yield (Scheme 2.5). This diamagnetic compound was prepared previously by treating $[Mo(\eta\text{-}C_7H_7)(PMe_3)I_2]$ **7** with $LiAlH_4$ in 30 % yield.[1]

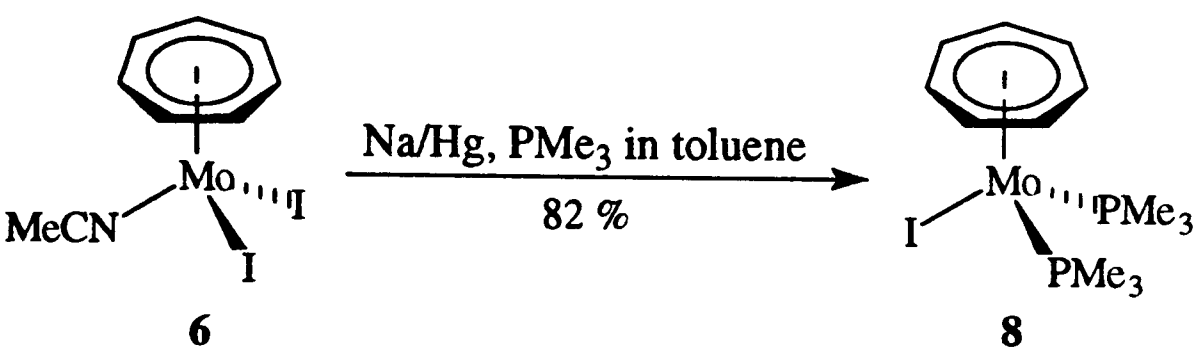

6 **8**

Scheme 2.5

The ^1H NMR spectrum of **8** in $[^2H_6]$-benzene showed a triplet at δ 4.74 (J = 2.2 Hz) and a virtual triplet at δ 1.05 (J = 3.3 Hz) in *ca.* 7 : 18 ratio. The former triplet was assigned to the $\eta\text{-}C_7H_7$ group while the latter triplet was assigned to the PMe_3 ligands. These data indicate the presence of two equivalent PMe_3 molecules bound to the molybdenum. The $^{13}C\{^1H\}$ NMR spectrum displayed a singlet at δ 86.6 assignable to the $\eta\text{-}C_7H_7$ ring carbons and a virtual triplet at δ 20.8 assignable to the PMe_3 carbons. The $^{31}P\{^1H\}$ NMR spectrum of **8** showed a signal at δ -24.5 which is due to the coordinated PMe_3 ligands.

2.4.3 Reaction with Na/Hg and dmpe

Treatment of [Mo(η-C_7H_7)(MeCN)I_2] **6** with one equivalent of sodium amalgam in the presence of one equivalent of dmpe gave diamagnetic [Mo(η-C_7H_7)(dmpe)I] **9** as a green solid (Scheme 2.6). This air-sensitive compound could be purified by sublimation.

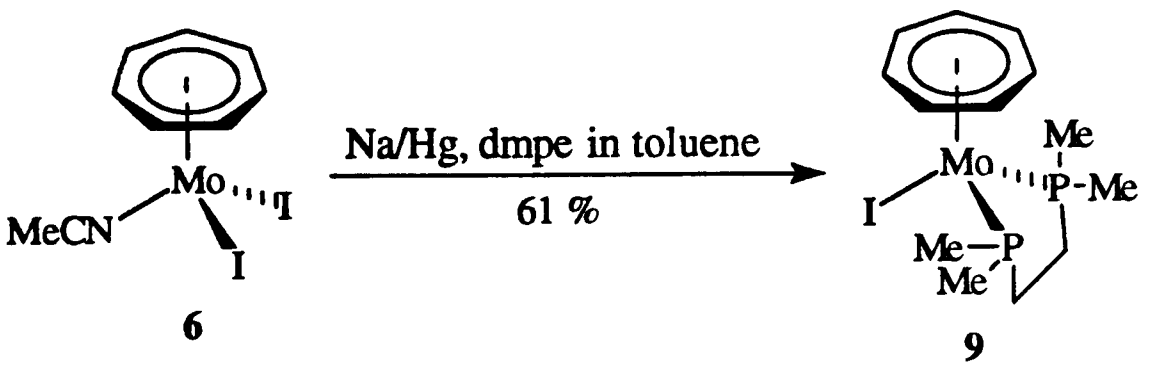

Scheme 2.6

Microanalytical data (C, H and I) are consistent with the proposed formulation. The mass spectrum (EI) showed the molecular ion M+ at m/e 466 and other peak at m/z 339 assignable to the fragment [Mo(η-C_7H_7)(dmpe)]+.

The ^{1}H NMR spectrum of **9** (Fig. 2.2) showed a triplet at δ 4.81 with coupling constant ^3J (H-P) 2.2 Hz assignable to the η-C_7H_7 protons, two doublets at δ 1.61 and δ 0.78 assignable to two sets of methyl groups, 'up' and 'down', and two multiplets at δ 1.19-1.34 and δ 0.53-0.75 assignable to two sets of methylene protons. These data are markedly different from those of the complexes [M(η-C_7H_7)(dmpe)Cl] (M = Ti[5] or Zr[6]). Firstly, the coupling between the ring protons and the diphosphine was not observed for M = Zr, and only barely resolved for M = Ti. Secondly, for both of these compounds, the ^{1}H NMR signals for the dmpe ligand were very broad at room temperature. This was explained by a reversible dissociation of a M-P bond (Scheme 2.7).[5,6b] The well-resolved triplet for the ring protons and well-separated doublets for the methyl groups in the spectrum of **9** clearly indicate that a dissociative process is less significant in this complex. This may suggest that the Mo-P bond in **9** is stronger than the Ti-P and Zr-P bonds in related complexes.

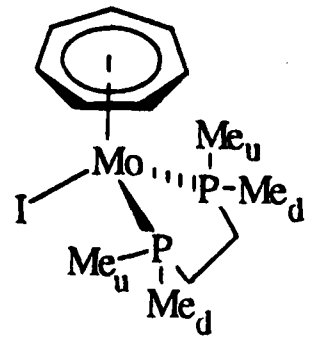

Fig. 2.2 ^{1}H NMR spectrum of [Mo(η-C_7H_7)(dmpe)I] **9** in [$^{2}H_6$]-benzene : *indicates solvent

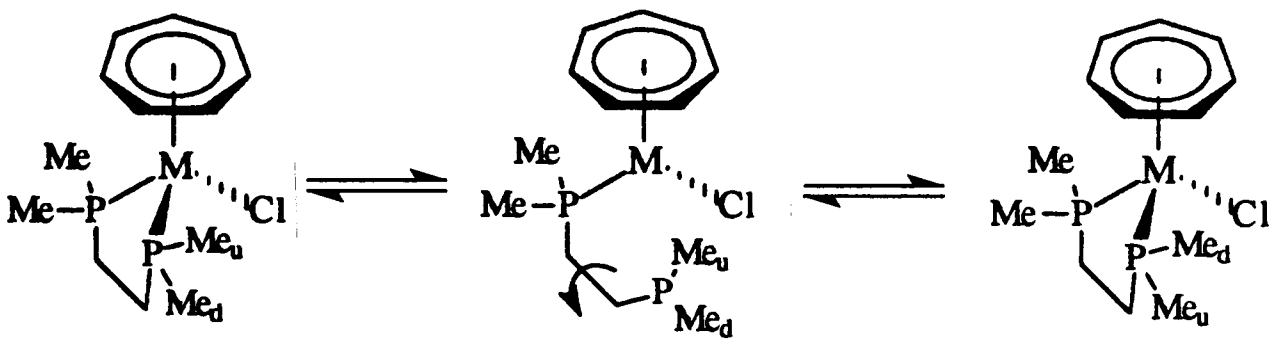

Scheme 2.7

The DEPT ($\theta = 3\pi/4$) $^{13}C\{^1H\}$ NMR spectrum of **9** showed a singlet with positive intensity at δ 86.0 (η-C_7H_7), a virtual triplet with negative intensity at δ 28.4 (PCH_2) and two virtual triplets with positive intensity at δ 21.7 and δ 15.6 (PMe). The $^{31}P\{^1H\}$ NMR spectrum exhibited a singlet at δ 19.9 assignable to the dmpe ligand.

2.4.4 Reaction with Na/Hg and dppe

Similarly, reduction of [Mo(η-C_7H_7)(MeCN)I_2] **6** with one equivalent of sodium amalgam in the presence of one equivalent of dppe gave the previously described[7] diamagnetic [Mo(η-C_7H_7)(dppe)I] **10** in 65 % yield (Scheme 2.8). The ^1H NMR spectrum of **10** showed a well-resolved triplet at δ 4.91 with coupling constant ^3J (H-P) 1.9 Hz which was attributed to the η-C_7H_7 ligand. This signal was not observed in the spectrum reported previously.[7b] The ^{13}C and ^{31}P NMR spectra are consistent with the proposed structure.

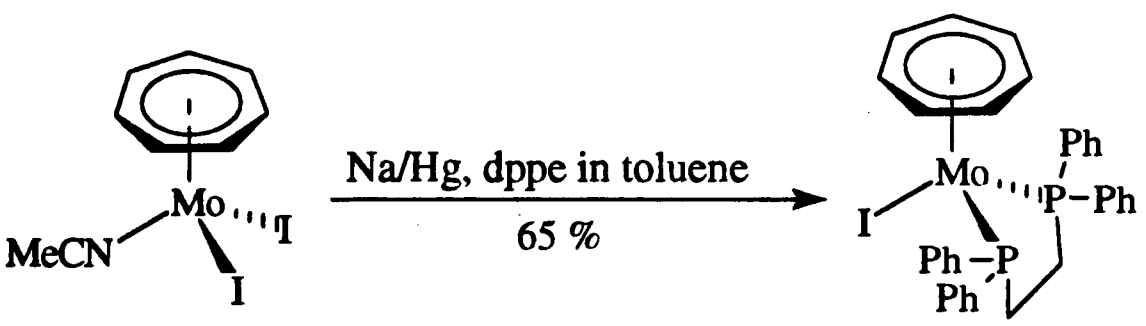

Scheme 2.8

2.4.5 Reaction with [NBu$_4$][I]

The MeCN ligand in [Mo(η-C_7H_7)(MeCN)I_2] **6** can also be displaced by weak anionic nucleophiles, such as iodide ion. Thus treatment of the compound **6** with one equivalent of tetrabutylammonium iodide in acetone at room temperature gave a purple solid which was soluble in thf. Slow diffusion of diethyl ether into the thf solution gave large purple crystals of [NBu_4][Mo(η-C_7H_7)I_3] **11** (Scheme 2.9).

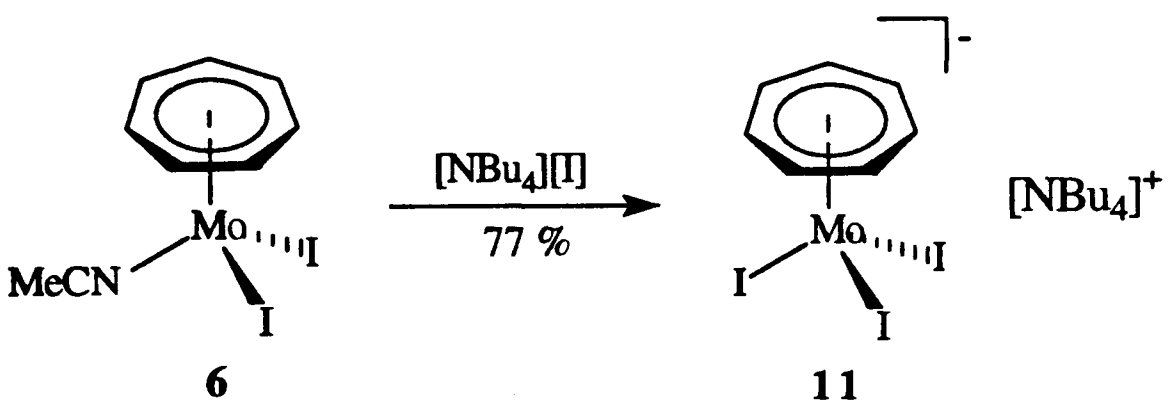

Scheme 2.9

These crystals were suitable for structure determination by X-ray diffraction. Diffraction analysis performed by Dr. Alex Chernega revealed that crystals of **11** consist of discrete cations and anions; there is no significant intermolecular non-bonded contacts. Perspective views of the anion [Mo(η-C_7H_7)I_3]$^-$ with atom numbering scheme are shown in Fig. 2.3, selected bond lengths and angles are given in Table 2.2. The crystallographic details are given in Appendix B2.

The anion [Mo(η-C_7H_7)I_3]$^-$ has a typical three-legged piano stool structure with the η-C_7H_7 ligand bonded symmetrically to the metal. The Mo-C distances range from 2.21 (1) - 2.236 (8) Å (mean 2.222 Å), which are comparable with those in the 17-electron compounds [Mo(η-C_7H_7)(thf)I_2] [2.23 (2) - 2.29 (2) Å, mean 2.25 Å],[8] [Mo(η-C_7H_7)(MeCN)I_2] [2.258 (5) - 2.280 (5), mean 2.268 Å] and [Mo(η-C_7H_7)(acac)(H_2O)]$^+$ [2.248 (6) - 2.291 (8), mean 2.265 Å][9] and they are, on average, shorter than the corresponding values observed in the 18-electron compounds [Mo(η-C_7H_7)$(CO)_2$X] (X = Cl, mean 2.307 Å; X = Br, mean 2.321 Å)[10] and [Mo(η-C_7H_7)$(CO)_2$(σ-C_6F_5)] (mean

2.318 Å).[11] However, the Mo-I bond lengths of 2.8386 (9) Å and 2.8394 (7) Å are significantly longer than those in [Mo(η-C_7H_7)(thf)I_2] [2.800(2) - 2.829 (2) Å][8] and [Mo(η-C_7H_7)(MeCN)I_2] [2.8003(4) and 2.8210 (4) Å].

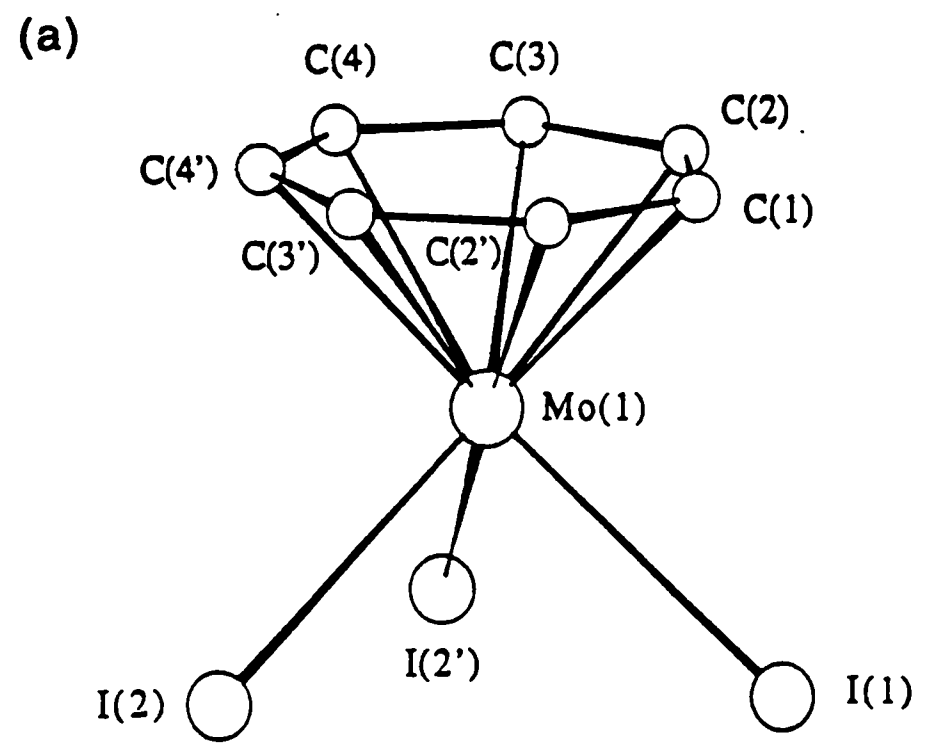

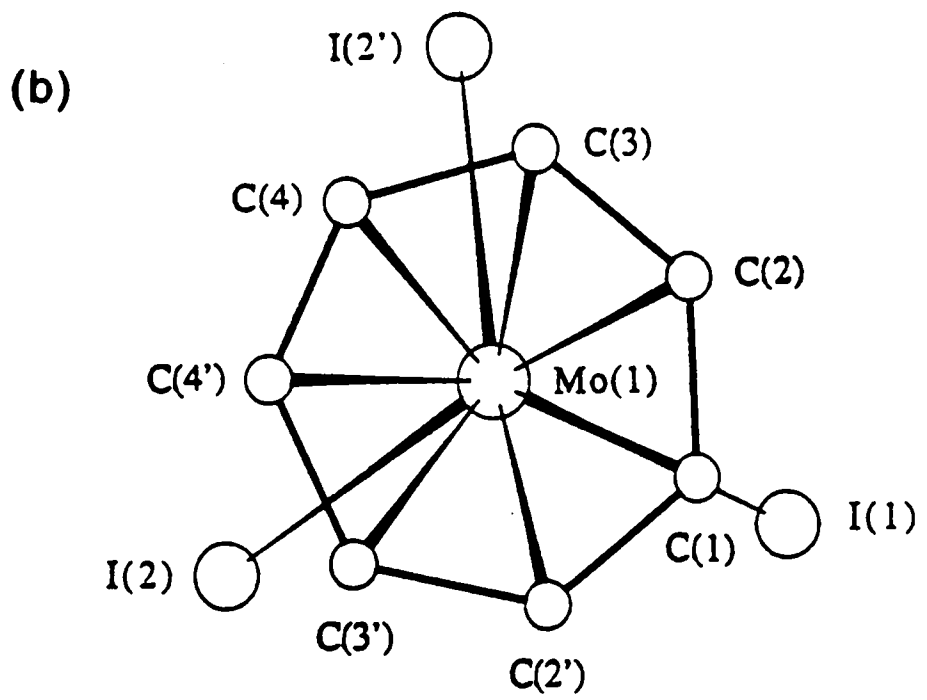

Fig. 2.3 The structure and labelling scheme for the [Mo(η-C_7H_7)I_3]- anion (the primed atoms are generated from the asymmetric unit using the mirror plane). (a) A general view (b) A projection on the plane C_7-ring

Table 2.2 : Selected bond length (Å) and angles (°) for $[Mo(\eta\text{-}C_7H_7)I_3]^-$

Mo (1) - I (1)	2.8386 (9)	C (1) - C (2)	1.36 (2)
Mo (1) - I (2)	2.8394 (7)	C (2) - C (3)	1.34 (2)
Mo (1) - C (1)	2.22 (1)	C (3) - C (4)	1.34 (2)
Mo (1) - C (2)	2.21 (1)	C (4) - C (4')	1.32 (2)
Mo (1) - C (3)	2.22 (1)	Mo(1) - C_7(centroid)	1.598
Mo (1) - C (4)	2.236 (8)	Mo(1) - C_7(plane)	1.597

I(1) - Mo(1) - I(2)	87.47 (2)
I(2) - Mo(1) - I(2')	86.33 (3)
C_7(centroid) - Mo(1) - I(1)	127.9
C_7(centroid) - Mo(1) - I(2)	127.0

The paramagnetic nature of compound **11** was determined by EPR spectroscopy and magnetic susceptibility measurements. The solution EPR spectrum of **11** in thf showed a main signal centred at g = 2.04 with a line width of 22 G. It also exhibited molybdenum hyperfine splitting (^{95}Mo and ^{97}Mo have spin = 5/2) with A_{iso} = 46 G. The magnetic susceptibility data were collected in the temperature range 6-180 K at 1 T and 3 T. Both sets of data could be fitted with the Curie-Weiss expression [$\chi_M = C/(T-\theta)$] with a Curie constant C = 0.31 emu-K mol^{-1} and a Weiss constant θ = -1.2 K. The effective magnetic moment of 1.57 μ_B corresponds to one unpair electron per formula unit (Fig. 2.4).

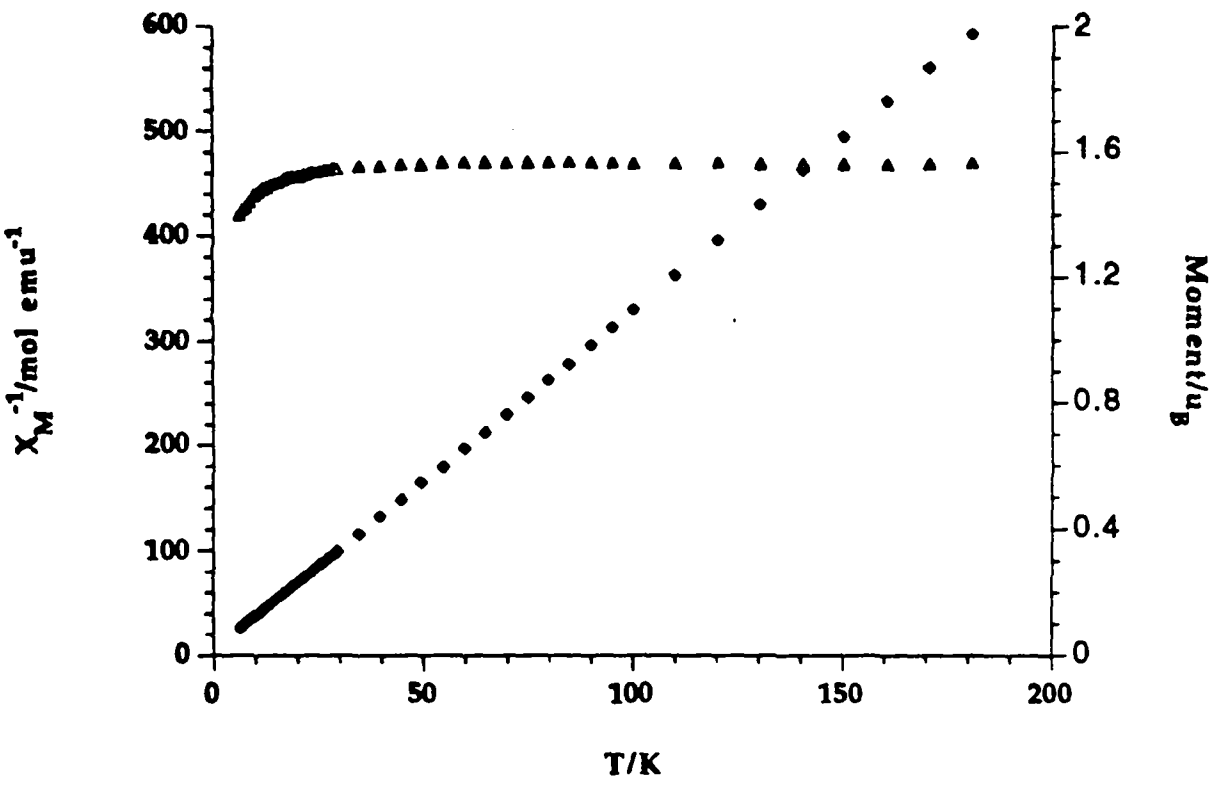

Fig. 2.4 Inverse molar magnetic susceptibility (◆) and effective moment (Δ) as a function of temperature for $[NBu_4][Mo(\eta\text{-}C_7H_7)I_3]$ **11** at 1 T

2.4.6 Reaction with NaC_5H_5

Treatment of compound $[Mo(\eta\text{-}C_7H_7)(MeCN)I_2]$ **6** with an excess of sodium cyclopentadienide in thf gave the mixed sandwich compound $[Mo(\eta\text{-}C_7H_7)(\eta\text{-}C_5H_5)]$ **12** in 65 % yield (Scheme 2.10). This compound was prepared previously from $MoCl_5$[12] or $[MoCl_3(thf)_3]$[13] in 1.8 or 15 % yield, respectively.

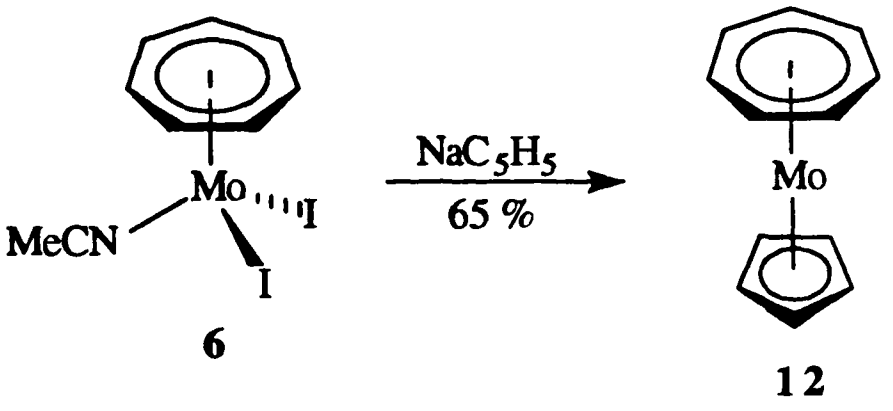

Scheme 2.10

Sandwich compounds almost invariably undergo electron-transfer reactions,[14] hence it is not unexpected that compound **12** was found to be redox active. Cyclic voltammetric studies showed that **12** undergoes one fully reversible oxidation at $E_{1/2}$ = -0.60 V *vs*. SCE. A typical voltammogram is shown in Fig. 2.5. Chemical oxidation of **12** with iodine to give the corresponding cation $[Mo(\eta\text{-}C_7H_7)(\eta\text{-}C_5H_5)]^+$ was reported previously.[12]

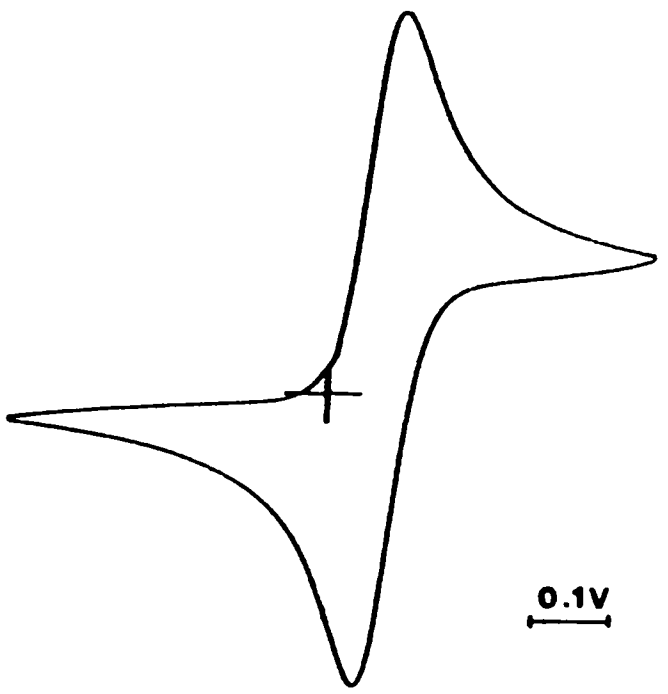

Fig. 2.5 Cyclic voltammogram of $[Mo(\eta\text{-}C_7H_7)(\eta\text{-}C_5H_5)]$ **12** recorded in acetonitrile at a scan rate of 50 mV s^{-1} with $[NBu_4][PF_6]$ as electrolyte

2.4.7 Reaction with NaC_5H_4Me

Similarly, treatment of $[Mo(\eta\text{-}C_7H_7)(MeCN)I_2]$ **6** with an excess of sodium methylcyclopentadienide in thf gave good yield (85 %) of the new compound $[Mo(\eta\text{-}C_7H_7)(\eta\text{-}C_5H_4Me)]$ **13**. This compound is extremely air-sensitive and as a result, satisfactory microanalytical data could not be obtained. It has been characterised, however, by various spectroscopic methods and X-ray structure determination.

The mass spectrum (EI) of **13** showed the presence of the parent cation M+, which occurred as the base peak. The spectrum also showed band at m/e 189 assignable to the fragment $[Mo(C_7H_7)]^+$.

The ^1H NMR spectrum of **13** in $[^2H_6]$-benzene is shown in Fig. 2.6, which comprises a singlet at δ 4.90 assignable to the η-C_7H_7 group, a singlet at δ 1.75 and two triplets at δ 4.66 and δ 4.80 assignable to the η-C_5H_4Me group. The ^{13}C NMR data is consistent with the proposed structure.

Single crystals of [Mo(η-C_7H_7)(η-C_5H_4Me)] **13** were grown by cooling of a saturated light petroleum (b.p. 40-60°C) solution at -20°C. The molecular structure and atom labelling scheme for **13** are shown in Fig. 2.7, selected bond lengths and angles are given in Table 2.3. The crystallographic details, including a complete listing of bond lengths and angles, atomic coordinates and thermal parameters are given in Appendix B3.

The molybdenum is sandwiched between the five- and seven-membered rings, which are both planar within the experimental error. The carbon C(6) bends out of the best C_5 plane by 4.01° away from the Mo atom. The two rings are essentially parallel and the angle subtended at molybdenum by the two ring centroids is 179.72°. As shown in Fig. 2.7(b), the arrangement of the two rings of **13** deviates from the ideally eclipsed conformation which is found for [M(η-C_7H_7)(η-C_5H_5)] (M = Ti[15] or V[16]).

Compound **13** undergoes one fully reversible oxidation at $E_{1/2}$ = -0.63 V *vs.* SCE as shown by cyclic voltammetry. The introduction of a methyl group in the C_5 ring only slightly decreases the $E_{1/2}$ value.

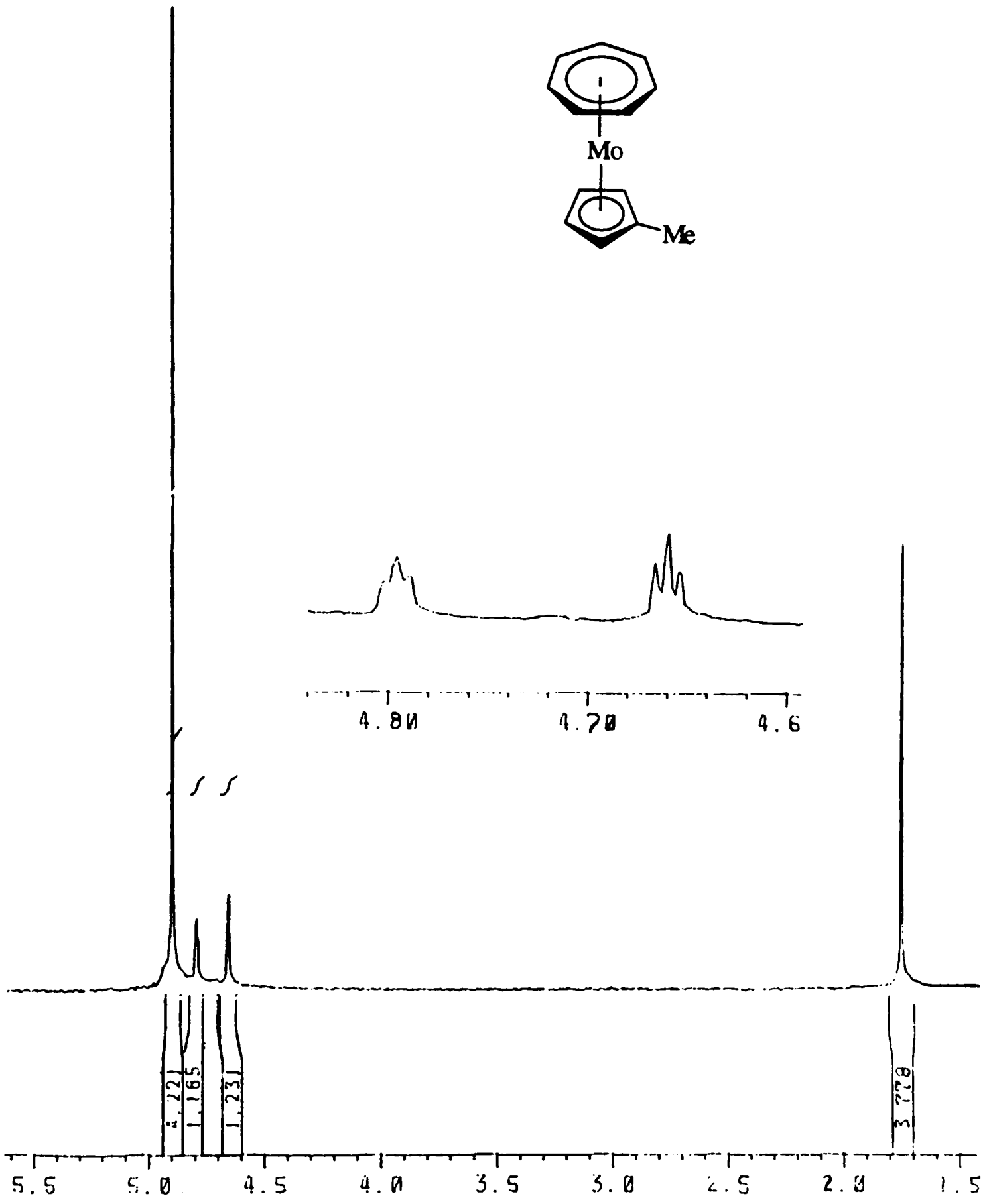

Fig. 2.6 ^{1}H NMR spectrum of [Mo(η-C_7H_7)(η-C_5H_4Me)] **13** in [$^{2}H_6$]-benzene

(a)

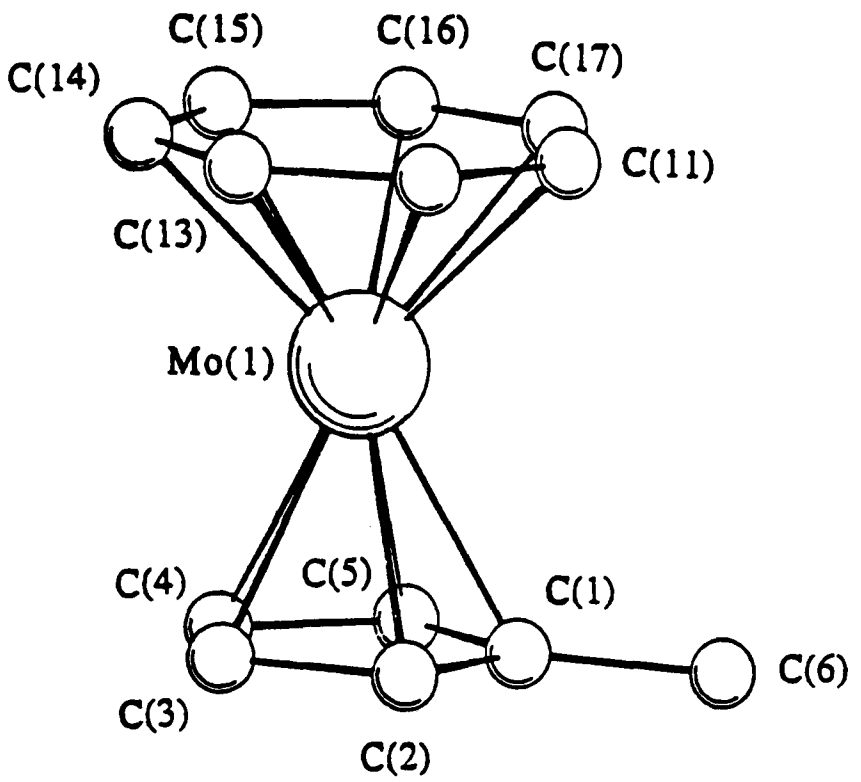

(b)

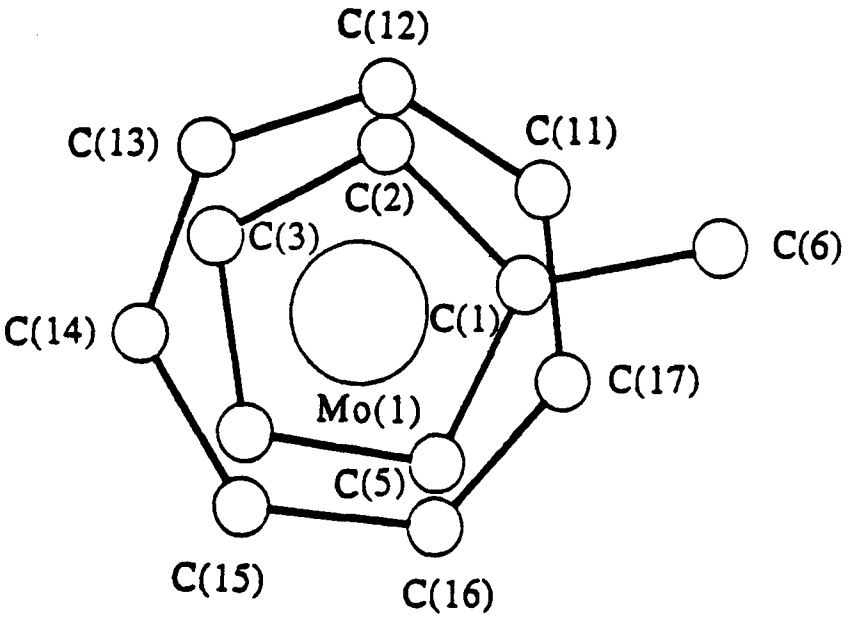

Fig. 2.7 Molecular structure of [Mo(η-C_7H_7)(η-C_5H_4Me)] **13**. (a) A general view (b) A projection of molecule perpendicular to the molecular axis

Table 2.3 : Selected bond length (Å) and angles (0)

for [Mo(η-C_7H_7)(η-C_5H_4Me)] **13**

Mo (1) - C (1)	2.334 (4)	C (1) - C (2)	1.417 (7)
Mo (1) - C (2)	2.312 (5)	C (1) - C (5)	1.409 (7)
Mo (1) - C (3)	2.306 (5)	C (1) - C (6)	1.497 (7)
Mo (1) - C (4)	2.304 (5)	C (2) - C (3)	1.393 (8)
Mo (1) - C (5)	2.317 (5)	C (3) - C (4)	1.393 (8)
Mo (1) - C (11)	2.255 (5)	C (4) - C (5)	1.417 (7)
Mo (1) - C (12)	2.246 (5)	C (11) - C (12)	1.357 (9)
Mo (1) - C (13)	2.269 (5)	C (11) - C (17)	1.36 (1)
Mo (1) - C (14)	2.247 (5)	C (12) - C (13)	1.381 (9)
Mo (1) - C (15)	2.247 (5)	C (13) - C (14)	1.391 (9)
Mo (1) - C (16)	2.243 (6)	C (14) - C (15)	1.42 (1)
Mo (1) - C (17)	2.241 (6)	C (15) - C (16)	1.42 (1)
Mo (1) - C_5 (centroid)	1.982	C (16) - C (17)	1.39 (1)
Mo (1) - C_7 (centroid)	1.583		

C_5 (centroid) - Mo (1) - C_7 (centroid)	179.72
C_5 (centroid) - C (1) - C (6)	85.99

2.4.8 Reaction with LiC_9H_7

The reaction between compound $[Mo(\eta\text{-}C_7H_7)(MeCN)I_2]$ **6** and an excess of lithium indenide in thf resulted in the formation of a purple suspension from which purple crystals of $[Mo(\eta\text{-}C_7H_7)(\eta^5\text{-}C_9H_7)]$ **14** were isolated (Scheme 2.11). The stoichiometry of **14** was confirmed by microanalysis and the mass spectrum (EI) showed the base peak at m/e 304 attributable to the parent cation.

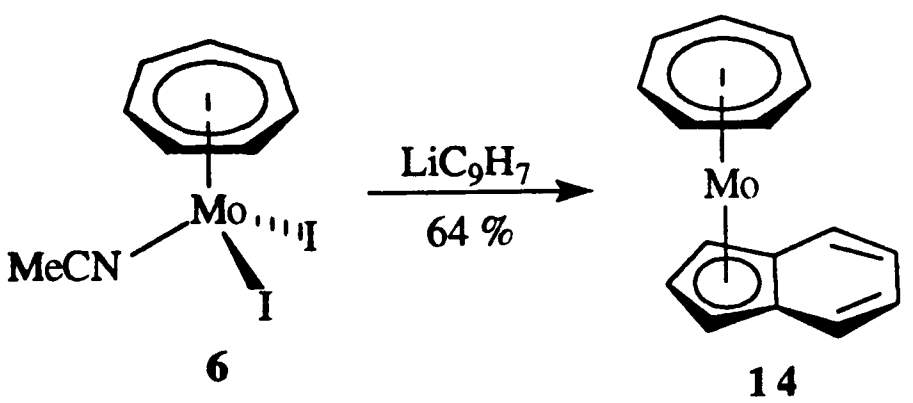

6 **14**

Scheme 2.11

The ^1H NMR spectrum of the purple crystals in $[^2H_6]$-benzene (Fig. 2.8a) showed two virtual doublet of doublets at δ 7.26 and 6.74 assignable to H_o and H_m and a very broad signal at *ca.* δ 5 for the C_5 and C_7 ring protons. The poor resolution may due to the presence of paramagnetic impurities. Purification of the crude product by sublimation gave a spectrum with improved resolution (Fig. 2.8b). Changing the solvent from $[^2H_6]$-benzene to $[^2H_6]$-acetone also slightly improved the resolution. Recrystallisation of the crude product twice from light petroleum (b.p. 40-60°C) eventually gave a well resolved ^1H NMR spectrum in $[^2H_6]$-acetone (Fig. 2.8c). The spectrum showed a sharp singlet at δ 4.75 assignable to the $\eta\text{-}C_7H_7$ ring, a triplet at δ 5.38 and a doublet at δ 5.50 assignable to protons H_b and H_a on the C_5 ring, respectively. The ^{13}C NMR spectrum of the purified product supported the ^1H NMR assignments.

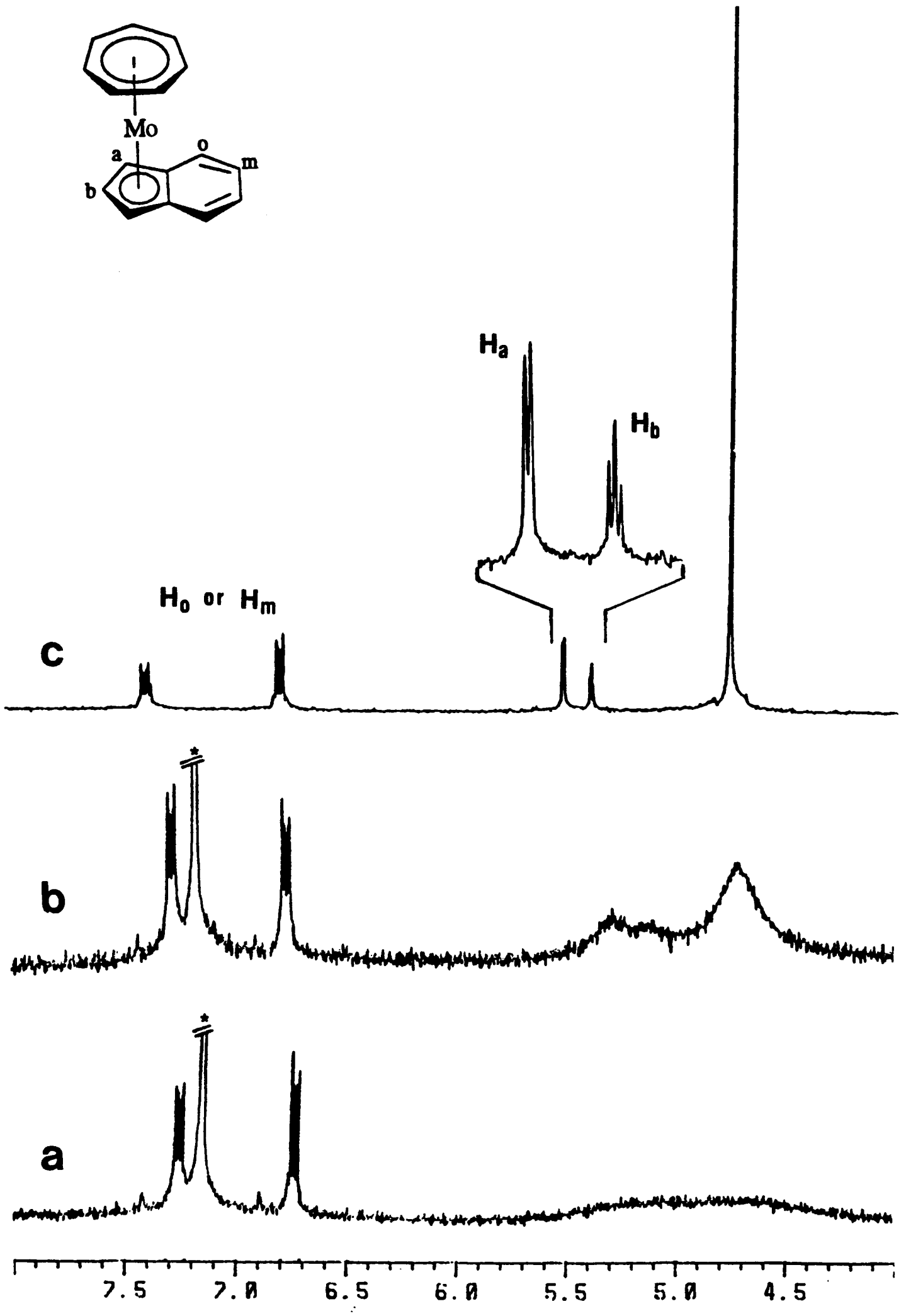

Fig. 2.8 ^1H NMR spectra of [Mo(η-C_7H_7)(η^5-C_9H_7)] **14**. (a) Crude product in [$^2H_6$]-benzene (b) Purified product from sublimation in [$^2H_6$]-benzene (c) Purified product from recrystallisation in [$^2H_6$]-acetone : *indicates solvent

The electrochemistry of compound **14** was studied by cyclic voltammetry. A fully reversible wave at $E_{1/2}$ = -0.48 V *vs*. SCE was observed in its voltammogram. The electrochemical data of **12-14** are listed in Table 2.4 which also includes the half-wave potentials of related sandwich compounds for comparison.

Table 2.4 : Electrochemical potentials of selected sandwich compounds *vs.* SCE

Compound	$E_{1/2}$ / V	Reference
$[Mo(\eta\text{-}C_7H_7)(\eta\text{-}C_5H_5)]$ **12** $^{+/0}$	-0.60	This work
$[Mo(\eta\text{-}C_7H_7)(\eta\text{-}C_5H_4Me)]$ **13** $^{+/0}$	-0.63	This work
$[Mo(\eta\text{-}C_7H_7)(\eta^5\text{-}C_9H_7)]$ **14** $^{+/0}$	-0.48	This work
$[Mo(\eta\text{-}C_7H_7)(\eta^5\text{-}C_7H_9)]$ **5** $^{+/0}$	+0.17	2b
$[Mo(\eta^6\text{-}C_7H_8)_2]$ **4** $^{+/0}$	-0.08	2b
$[Mo(\eta\text{-}C_6H_6)_2]$ $^{+/0}$	-0.71	17
$[Cr(\eta\text{-}C_5H_5)_2]$ $^{+/0}$	-0.67	18
$[Co(\eta\text{-}C_5H_5)_2]$ $^{+/0}$	-0.94	19

2.4.9 Polymerisation of norbornene

Metal-carbene complexes play an important role in ring-opening metathesis polymerisation (ROMP).[20] Grubbs and co-workers have demonstrated that norbornene can be polymerised by a titanacyclobutane/titanium carbene complex.[21] Several well-characterised tungsten (VI) alkylidene complexes are also known to be good catalysts in ROMP.[22] It has been reported that some trimethylsilylmethyl derivatives of tungsten may undergo α-elimination forming tungsten-carbene species (Scheme 2.12) which are active catalysts in the polymerisation of cyclic olefins.[23] Based on these observations, the catalytic property of $[Mo(\eta\text{-}C_7H_7)(MeCN)I_2]$ / Me_3SiCH_2MgCl system in ROMP was investigated.

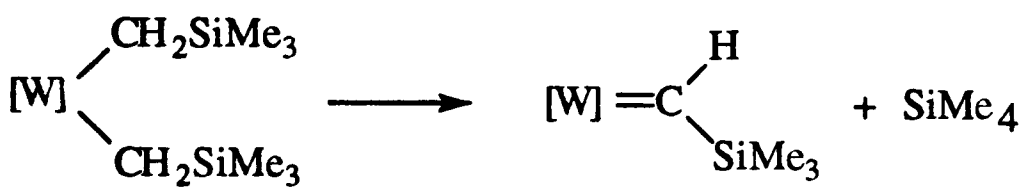

Scheme 2.12

In a preliminary study, a suspension of $[Mo(\eta\text{-}C_7H_7)(MeCN)I_2]$ **6** (35 mg) in toluene (50 cm^3) was treated with 300 equivalents of norbornene (2 g). There was no observable change. However, when a few drops of Me_3SiCH_2MgCl solution in diethyl ether was added, precipitation occurred almost immediately and the viscosity of the mixture increased. The mixture was stirred at room temperature for 17 h to give a yellow brown viscous solution. Subsequent work-up gave 0.2 g of white fibrous poly(1,3-cyclopentylenevinylene) (Scheme 2.13). In another run, the compound **6** (25 mg) activated with Me_3SiCH_2MgCl was treated with 200 equivalents of norbornene (1 g) in toluene (30 cm^3) at 60 °C for 1 h. After the usual work-up procedure, 0.15 g of white polymer was obtained.

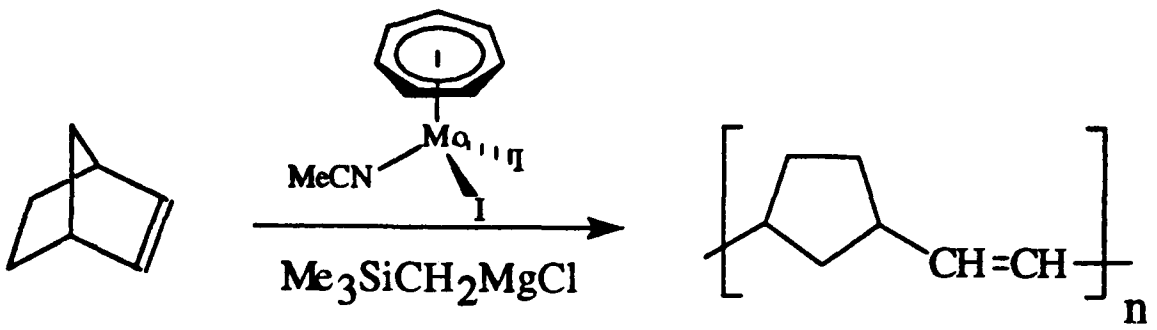

Scheme 2.13

It is well-documented that ^{13}C NMR spectroscopy can provide a good deal of information about the microstructure of polymer. Fig. 2. 9 shows the DEPT ($\theta = 3\pi/4$) $^{13}C\{^1H\}$ NMR spectrum of the polymer in [$^2H_1$]-chloroform. The simplicity of the spectrum clearly indicates a high stereoregularity in the polymer. By comparing with the data in literature,[24] it was found that essentially all of the double bonds in the polymer are in the *trans*-configuration. It is noted that $MoCl_5$ in CCl_4 at 50 ^{0}C also catalyses the polymerisation of norbornene giving a polymer which has 80-95 % *trans*-content as indicated by IR spectroscopy.[25]

The ring-opening polymerisation of norbornene with [Mo(η-C_7H_7)(MeCN)I_2] / Me_3SiCH_2MgCl system represents the first example of the use of a η-cycloheptatrienyl-transition metal complex as a homogeneous catalyst. Unfortunately, attempts to polymerise cyclopentene with this catalyst system were unsuccessful. Due to the limited of time, this catalyst system has only been briefly examined. Thus further investigation, such as finding an optimum condition, characterisation of the polymer and isolation of the active species, is worthy of study.

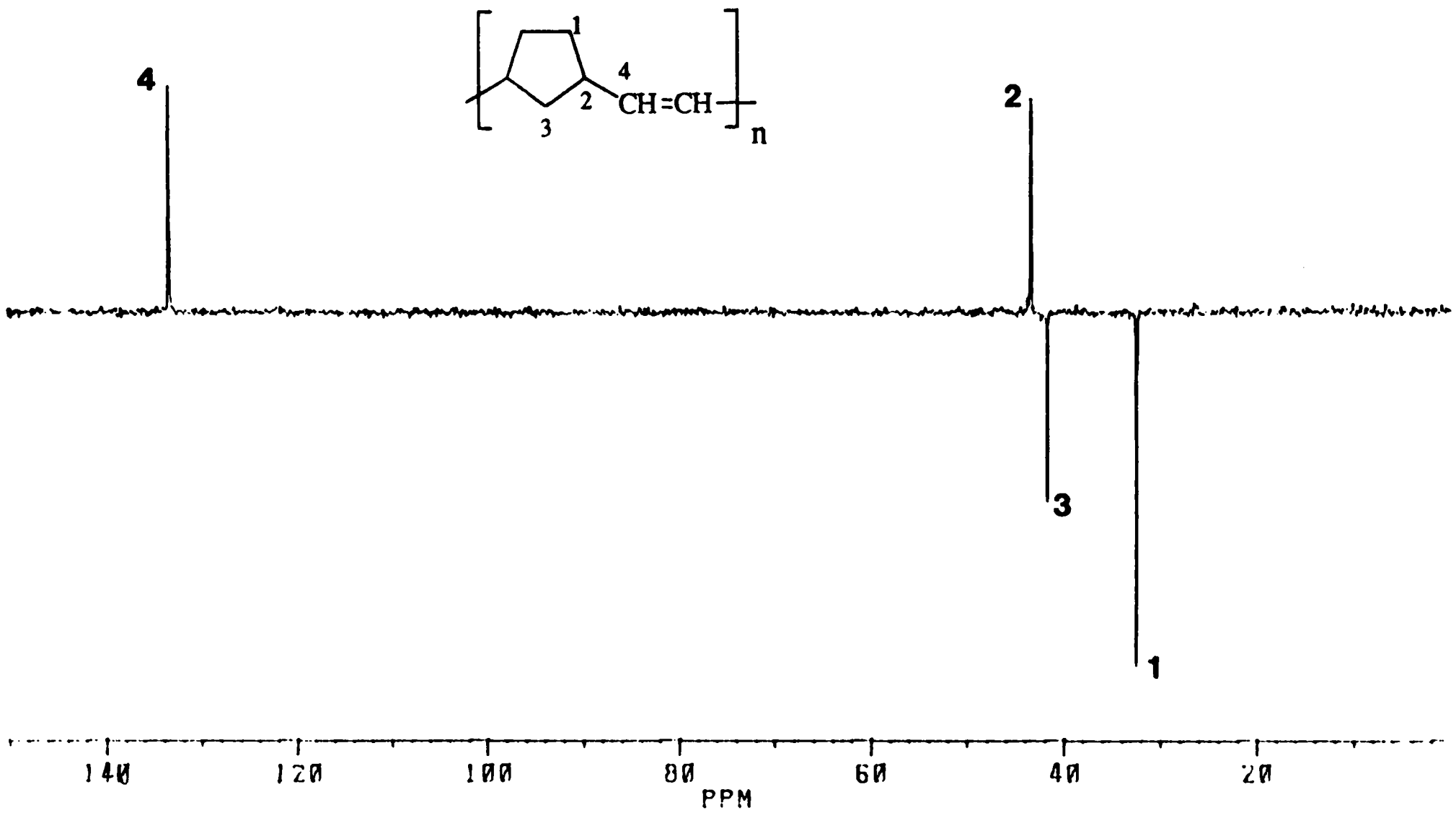

Fig. 2.9 DEPT ($\theta = 3\pi/4$) $^{13}C\{^1H\}$ NMR spectrum of all-*trans* poly(1,3-cyclopentylenevinylene) in [$^2H_1$]-chloroform

2.5 Preparation and Characterisation of $[Mo(\eta\text{-}C_7H_7)(MeCN)Cl_2]$

The dichloro analogue of **6**, namely $[Mo(\eta\text{-}C_7H_7)(MeCN)Cl_2]$ **15**, was prepared by treating $[Mo(\eta\text{-}C_7H_7)(\eta^5\text{-}C_7H_9)]$ **5** with an excess of $PhICl_2$ in toluene; the resulting brown precipitate was recrystallised from acetonitrile giving orange crystals of **15** in 54 % yield (Scheme 2.14).

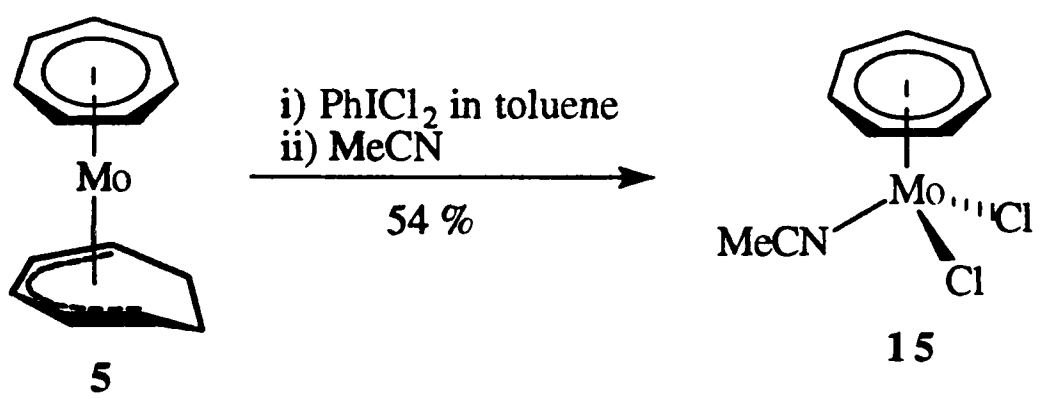

5 15

Scheme 2.14

Microanalytical data for **15** were in accord with the proposed stoichiometry. The IR spectrum was very similar to that of $[Mo(\eta\text{-}C_7H_7)(MeCN)I_2]$ **6** and showed a strong band at 2287 cm^{-1} assignable to the coordinated acetonitrile.

The solid state EPR spectrum of **15** at ambient temperature gave a broad signal at g = 1.99 (line width = 100 G) without hyperfine splitting due to molybdenum. Lowering the temperature to 4 K caused only a slight sharpening of the signal (line width = 70 G). However, the EPR spectrum of a solution of **15** in $[^2H_3]$-acetonitrile displayed a main signal at g = 1.97 with a line width of 14 G together with molybdenum hyperfine splitting (A^{Mo} = 45 G) (Fig 2.10).

The magnetic susceptibility of compound **15** was measured in the temperature range 6-290 K at 1 T using a superconducting quantum interference device (SQUID) magnetometer. The data are displayed in Fig. 2.11. It can be seen that the susceptibility rises with decreasing temperature and the data can be fitted by the Curie-Weiss expression [$\chi_M = C/(T-\theta)$] with a Curie constant C = 0.30 emu-K mol^{-1} and a Weiss constant θ = -0.5 K, yielding an effective moment (μ_{eff} = 1.55 μ_B) which is consistent with the existence of one S = 1/2 spin. The effective moment is lower than the value of 1.71 μ_B calculated on the basis of the spin-only formula : $\mu_{eff}^2 = g^2[S\ (S+1)]$ where g is taken from the EPR data.

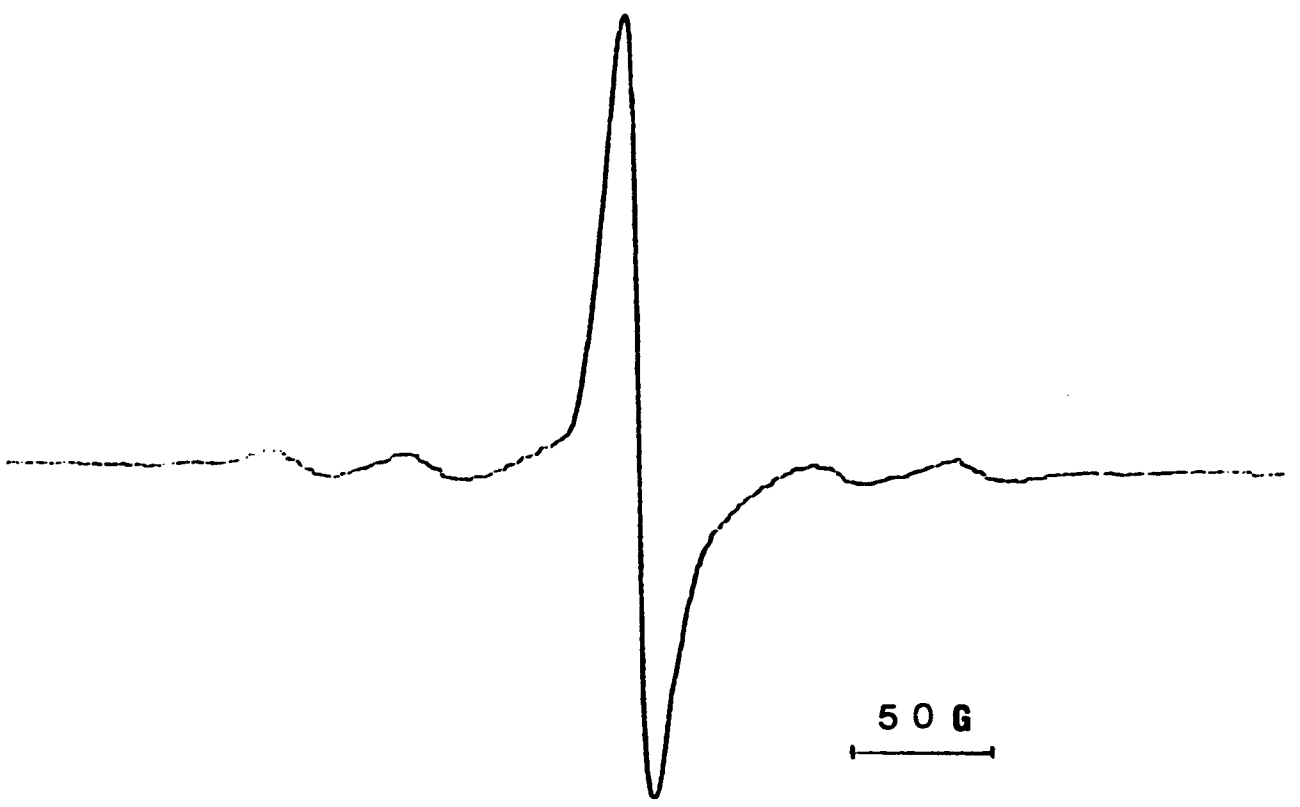

Fig. 2.10 EPR spectrum of [Mo(η-C_7H_7)(MeCN)Cl_2] **15** in [$^2H_3$]-acetonitrile

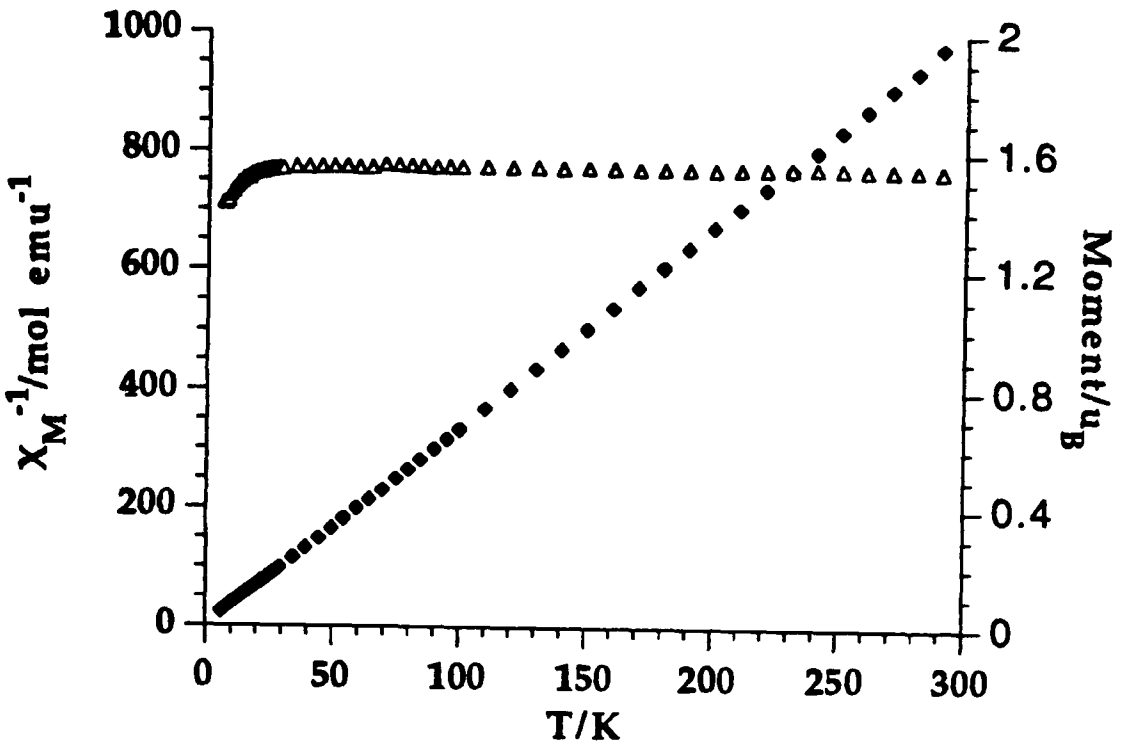

Fig. 2.11 Inverse molar magnetic susceptibility (◆) and effective moment (Δ) as a function of temperature for [Mo(η-C_7H_7)(MeCN)Cl_2] **15** at 1 T

The reaction between [Mo(η-C_7H_7)(η^5-C_7H_9)] **5** and one equivalent of $PhICl_2$ in toluene, however, resulted in the formation of a deep brown solution and a green solid. The deep brown solution reacted with an excess of $PhICl_2$ giving a brown solid which on recrystallisation from acetonitrile gave compound **15**. The green solid was recrystallised from dichloromethane giving green plates. The IR spectrum of these green plates displayed strong band at 802 cm^{-1} which is characteristic of η-C_7H_7 group.[12] The ^1H NMR spectrum of a solution in [$^2H_2$]-dichloromethane showed only a peak due to residual protio solvent. The EPR spectrum of a solution in dichloromethane exhibited a rather broad signal at g = 1.99 (line width = 40 G). No hyperfine splitting was observed. These results suggested that the green product is a paramagnetic species. Microanalysis gave the ratio of C : H : Cl = 6.1 : 6.6 : 1.0. Unfortunately, the mass spectrum (EI) did not give any conclusive result. Therefore, the structure of the green crystals remains elusive.

Treatment of the green crystals with $PhICl_2$ in toluene or dichlomethane followed by recrystallisation of the crude product from acetonitrile also resulted in the isolation of $[Mo(\eta\text{-}C_7H_7)(MeCN)Cl_2]$ **15**. This indicated that the green substance is an intermediate in the reaction between $[Mo(\eta\text{-}C_7H_7)(\eta^5\text{-}C_7H_9)]$ **5** and $PhICl_2$.

It is worth mentioning that the breaking of the robust Mo-C_7H_7 bond was observed in these reactions. The ^1H NMR spectra of the crude products isolated from the above reactions all showed a singlet at δ 9.2. This downfield signal may be assigned to the tropylium cation $[C_7H_7]^+$. This was the only occasion that the breaking of Mo-C_7H_7 bond was observed during the work described in this thesis.

2.6 Reactivity Studies of $[Mo(\eta\text{-}C_7H_7)(\eta\text{-}C_5H_4R)]$ (R = H or Me)

Sandwich compounds are an important class of organometallic compounds. The facile electron transfer in these species leads to the formation of some interesting and potentially useful materials. For example, the electron-transfer complexes $[Fe(\eta\text{-}C_5Me_5)_2][tcne]$[26] and $[Mn(\eta\text{-}C_5Me_5)_2][tcne]$[27] (tcne = tetracyanoethene) show three-dimensional ferromagnetic groud states with Curie temperatures (T_c) of 4.8 and 8.8 K respectively; whilst $[Fe(\eta\text{-}C_5H_5)(\eta\text{-}C_6Me_6)][tcnq]$ (tcnq = 7,7,8,8-tetrancyanoquino-dimethane) shows semiconductor behaviour with σ(300 K) in the range 5.8-7.4 $\Omega^{-1}cm^{-1}$.[28] The intercalation of $[Co(\eta\text{-}C_5H_5)_2]$ into $SnSe_2$ converts the host lattice into a type II superconductor with T_c = 6.1 K.[29]

Most of the sandwich compounds reported in the formation of these materials contain η-cyclopentadienyl and/or η-arene rings. Due to the lack of synthetic route to sandwich compounds containing η-cycloheptatrienyl ring, the use of them as electron donor in the preparation of these materials is virtually unknown.[30a]

As described in the previous section, the sandwich compounds $[Mo(\eta\text{-}C_7H_7)(\eta\text{-}C_5H_4R)]$ (R = H or Me) can be prepared readily and are electron-rich. Thus we have explored their corresponding electron-transfer complexes and intercalation compound. The details are described in this section.

2.6.1 Reaction with tcne

Reaction of [Mo(η-C_7H_7)(η-C_5H_4Me)] **13** with a stoichiometric amount of tcne in thf resulted in a spontaneous precipitation. The mixture was layered with diethyl ether giving a black solid which was recrystallised from dichloromethane. Purple crystals were obtained by cooling a saturated dichloromethane solution. Microanalysis correspond to the 1 : 1 electron-transfer complex [Mo(η-C_7H_7)(η-C_5H_4Me)][tcne] **16** (Scheme 2.15).

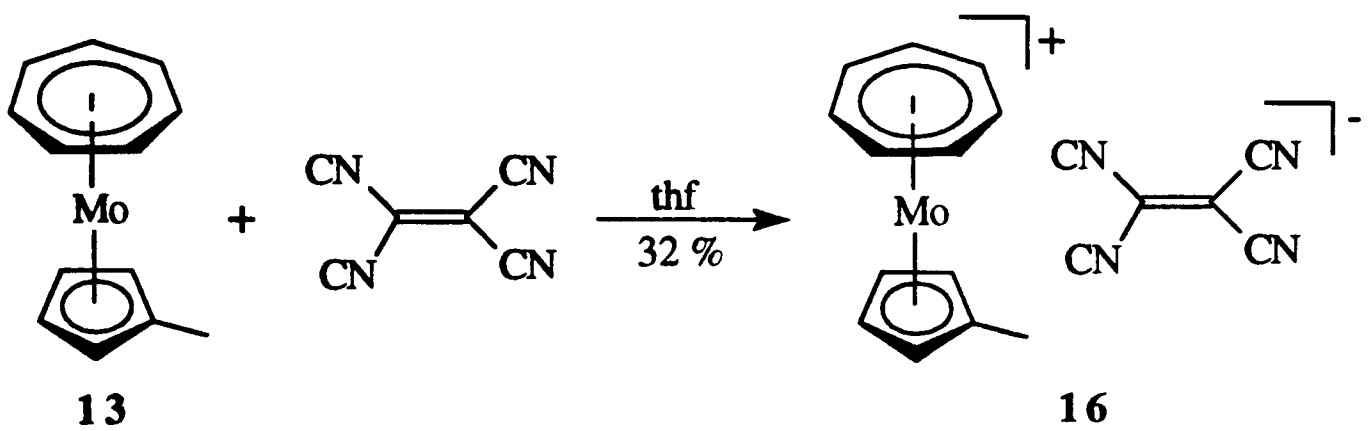

13 **16**

Scheme 2.15

IR spectroscopy is an useful technique in characterising electron-transfer complexes with polycyano acceptor. By considering the stretching frequencies of ν (C≡N), it is possible to determine the nature of the acceptor (Table 2.5).[31] The IR spectrum of **16** showed three bands assignable to C≡N stretching vibrations at 2160 (s), 2171 (s) and 2192 (m) cm^{-1} (Fig. 2.12). These are characteristic for the dimeric dianions $[tcne]_2^{2-}$.[31b] A related electron-transfer complex [Cr(η-$C_6H_6)_2$][tcne], has a structure which consists of linear chains of ···D$^+$$A_2^{2-}$D+D$^+$$A_2^{2-}D^+$··· (D = donor, A = acceptor), has been reported.[31b]

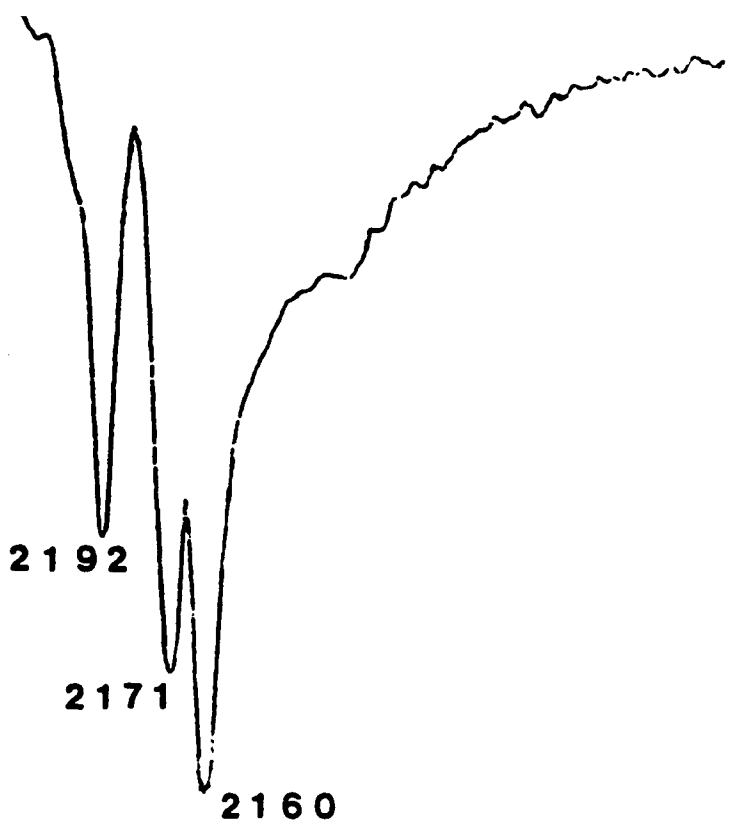

Fig. 2.12 IR spectrum of [Mo(η-C_7H_7)(η-C_5H_4Me)][tcne] **16**

Table 2.5 : Infrared vibrational transitions for acceptor complexes

	tcne	tcnq
Neutral	2221 (m), 2259 (s)	2222 (m), 2226 (m)
Monoanion	2144 (s), 2183 (s)	2153 (m), 2179 (s)
Dianion	2069 (s), 2104 (s)	2105 (s), 2150 (s)
Dimeric Dianion	2159 (s), 2170 (s), 2189 (m)	2182 (s), 2175 (s), 2156 (m)

Since the dimeric dianion $[tcne]_2^{2-}$ is diamagnetic, only one signal due to the cation should be observed in the solid state EPR spectrum of **16**. As expected, the spectrum showed an isotropic signal with g = 1.995 and line width = 50 G. No hyperfine splitting was observed. This g value is in good agreement with the value of 1.997 found for [Mo(η-C_7H_7)(η-C_5H_4Me)][PF_6].[32]

It has been reported that the solution EPR spectrum of $[Cr(\eta\text{-}C_6H_6)_2][tcne]$ gives two isotropic signals at g= 2.001 and 1.896 characteristic of $[tcne]^-$ and $[Cr(\eta\text{-}C_6H_6)_2]^+$; thus, $[tcne]^-$ and not $[tcne]_2^{2-}$ is present in solution.[31b] The EPR spectrum of **16** in dichloromethane also revealed the presence of $[Mo(\eta\text{-}C_7H_7)(\eta\text{-}C_5H_4Me)]^+$ (g = 1.995) and $[tcne]^-$ (g = 2.000). However, the g values of these ions are so close to each other that the two signals overlap, as shown in Fig. 2.13.

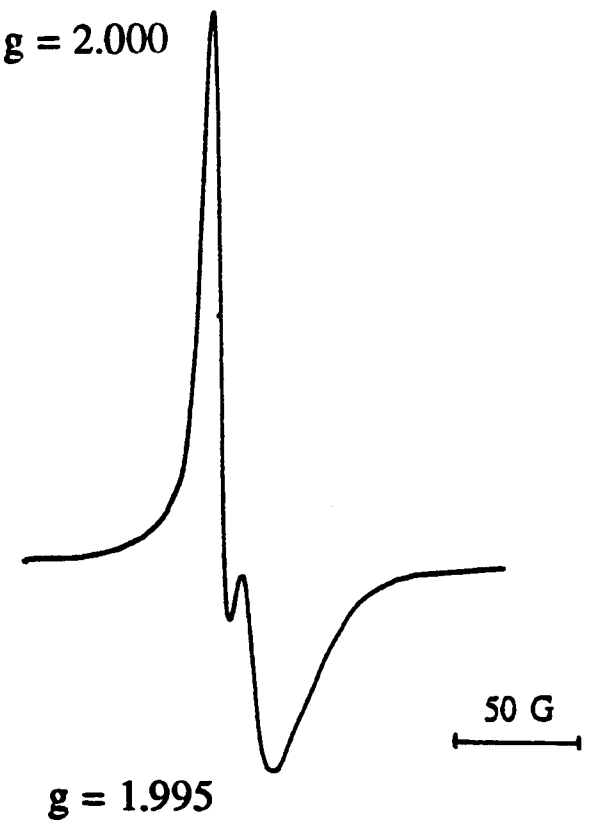

Fig. 2.13 EPR spectrum of $[Mo(\eta\text{-}C_7H_7)(\eta\text{-}C_5H_4Me)][tcne]$ **16** in dichloromethane

The molar magnetic susceptibility of **16** was measured in the temperature range 6-300 K at 0.2 T using a SQUID magnetometer. As shown in Fig. 2.14, the compound obeys the Curie-Weiss law [$\chi_M = C / (T - \theta)$] with C = 0.35 emu-K/mol and θ = -3.1 K, yielding an effective moment μ_{eff} = 1.67 μ_B. The value of μ_{eff} indicates that only one S = 1/2 radical per formula unit is contributing to the susceptibility. This is consistent with the structure possessing S = 0 $[tcne]_2^{2-}$ and S = 1/2 $[Mo(\eta\text{-}C_7H_7)(\eta\text{-}C_5H_4Me)]^+$. The effective moment is close to the value of 1.73 μ_B calculated on the basis of the spin-only formula.

Based on these results, it is likely that solid state structure of **16** also consists of linear chains of ···D+A_2^{2-}D+D+A_2^{2-}D+···. Unfortunately, attempts to grow single crystals of compound **16** were unsuccessful.

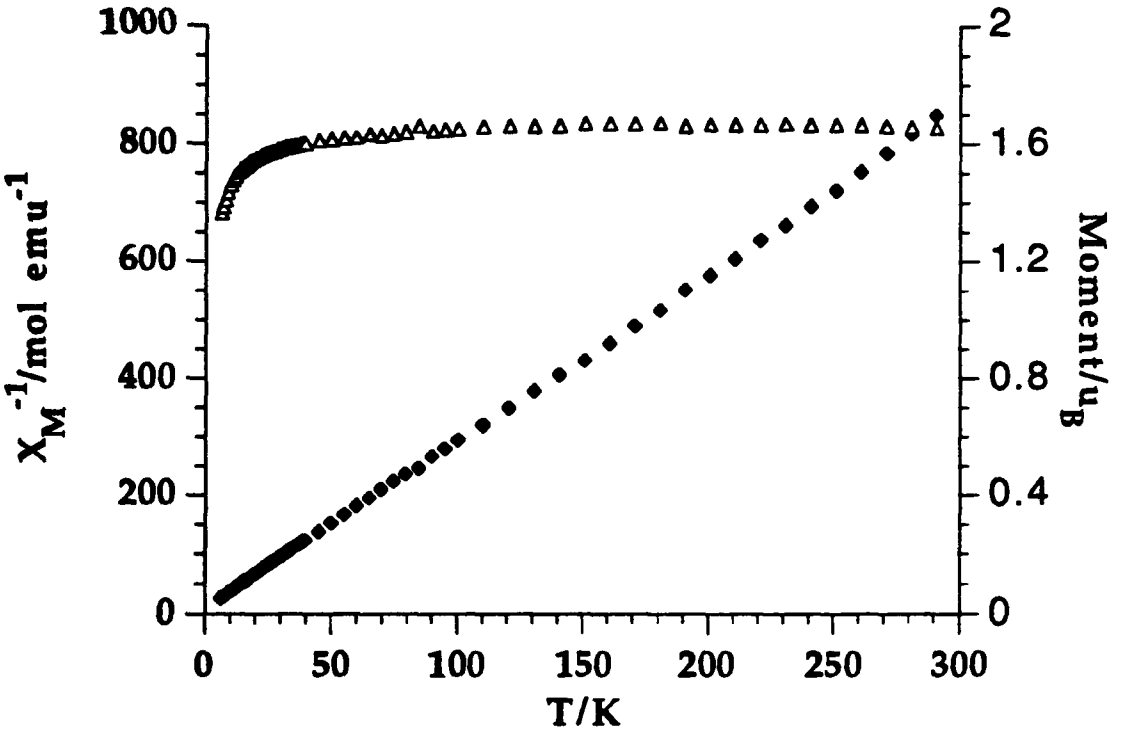

Fig. 2.14 Inverse molar magnetic susceptibility (◆) and effective moment (Δ) as a function of temperature for $[Mo(\eta\text{-}C_7H_7)(\eta\text{-}C_5H_4Me)][tcne]$ **16** at 0.2 T

2.6.2 Reaction with tcnq

A stirred suspension of tcnq in acetonitrile was treated with one molar equivalent of [Mo(η-C_7H_7)(η-C_5H_5)] **12** in dichloromethane, giving a green solution and a small amount of precipitate. Filtration followed by layering with diethyl ether led to the isolation of dark green solid. The IR spectrum displayed strong absorptions at 2104 and 2150 cm^{-1} which suggested the presence of dianion $[tcnq]^{2-}$ (Table 2.5).[31a] Microanalysis for nitrogen and hydrogen were consistent with the values calculated for the 2 : 1 electron-transfer complex {[Mo(η-C_7H_7)(η-C_5H_5)]$_2$[tcnq]} **17**, but the carbon content was 3.7 % lower than expected. Attempts to purify **17** by recrystallisation from dichloromethane or acetonitrile, by layering with diethyl ether onto a dichloromethane solution or by diffusion of diethyl ether into a dichloromethane solution were unsuccessful. Thus no satisfactory magnetic data could be obtained. However, the ambient temperture solid state EPR spectrum of **17** exhibited an absorption centred at g = 1.982 with line width = 36 G. This was assigned to the cation [Mo(η-C_7H_7)(η-C_5H_5)]$^+$ whilst the dianion $[tcnq]^{2-}$ has S = 0. In solution, the signal sharpened slightly (line width = 25 G). No hyperfine splitting was observed in either spectrum.

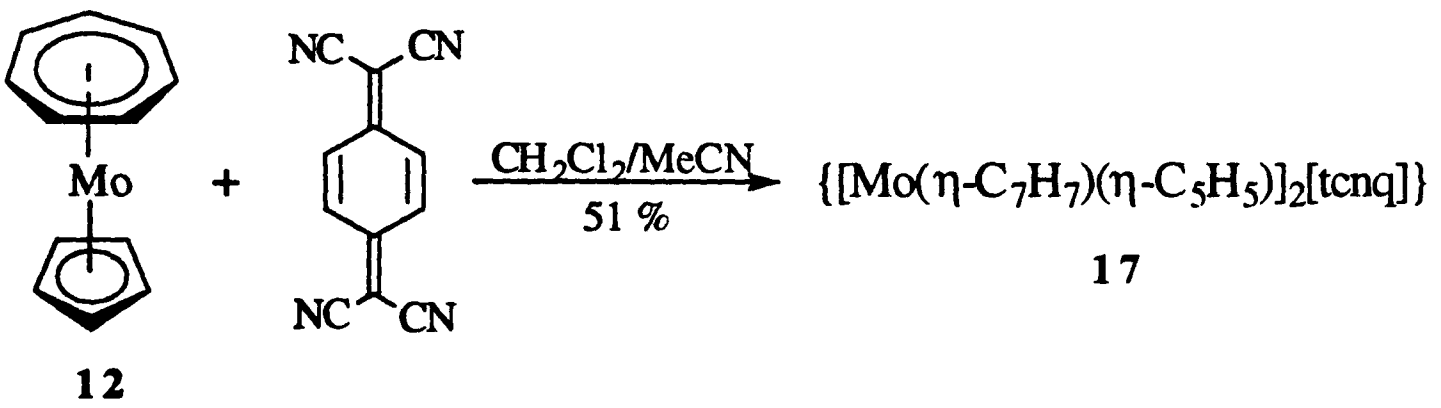

Scheme 2.16

2.6.3 Intercalation into ZrS_2

It has been shown that neutral electron-rich organometallic sandwich compounds which form stable cations can intercalate into layered transition-metal dichalcogenides.[30] The electrochemical data (Table 2.4) shows the compounds [Mo(η-C_7H_7)(η-C_5H_4R)] (R = H or Me) may be classed as electron-rich and that they form cations stable to isolation. The intercalation of [Cr(η-C_7H_7)(η-C_5H_5)] into ZrS_2 has been reported and the resulting intercalate {ZrS_2[Cr(η-C_7H_7)(η-C_5H_5)]$_{0.25}$} has a lattice expansion of 6.17 Å.[30a] Therefore we were interested to study the intercalation of [Mo(η-C_7H_7)(η-C_5H_4Me)] into ZrS_2.

Treatment of zirconium disulfide powder with an excess of [Mo(η-C_7H_7)(η-C_5H_4Me)] **13** in toluene at 120°C resulted in intercalation of the sandwich compound; thorough washing of the resulting solid with toluene gave a brown compound of stoichiometry {ZrS_2[Mo(η-C_7H_7)(η-C_5H_4Me)]$_{0.22}$} **18**. The intercalation reaction was assumed complete when no lines due to starting material were observed in the X-ray powder diffraction pattern. The stoichiometry of the intercalate was determined by microanalysis which also confirmed that the C : H ratio remains unchanged upon intercalation.

Fig. 2.15 shows the X-ray diffraction patterns of ZrS_2 and the intercalates **18**. Because of disorder in the ab plane characteristic of such intercalation compounds,[33] only 00l lines could be indexed. From the measured c axis of the intercalate and the c axis of the host lattice (5.83 Å for ZrS_2),[30b] the lattice expansion (Δc) which occurs on intercalation of **13** into the van der Waals gap of the host lattice was obtained. The indexing as well as observed and calculated *d* spacings are given in Appendix C. The cell parameter c for **18** was found to be 11.93 (1) Å, hence (Δc) was calculated to be 6.10 (1) Å.

The EPR spectrum of a solid sample of **18** showed a signal at g = 1.98 (line width = 60 G) at room temperature. No hyperfine splitting due to molybdenum or hydrogen was observed.

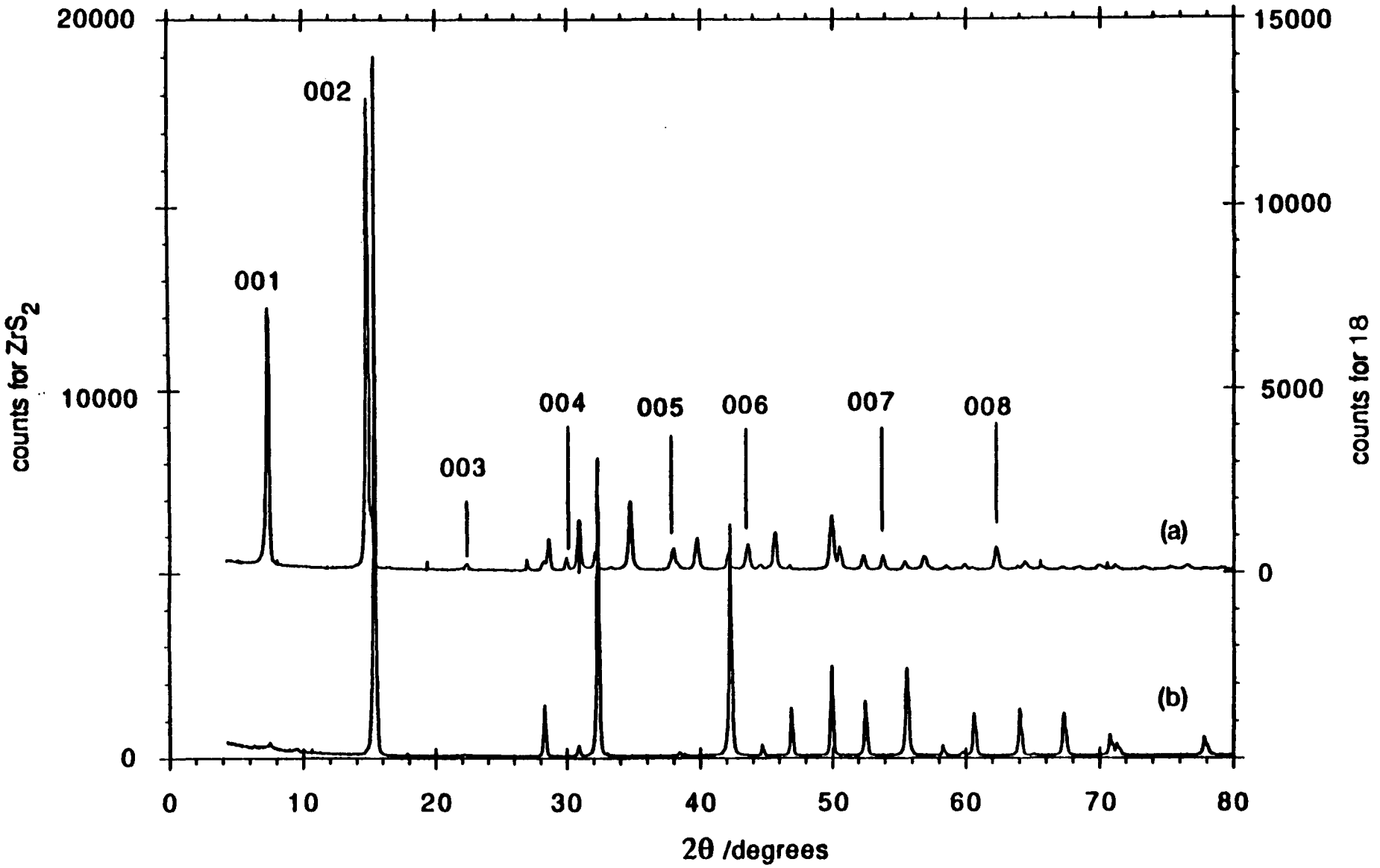

Fig. 2.15 X-ray powder diffraction patterns of (a) $\{ZrS_2[Mo(\eta\text{-}C_7H_7)(\eta\text{-}C_5H_4Me)]_{0.22}\}$ **18** and (b) ZrS_2

The magnetic susceptibility of the intercalate **18** was measured in the temperature range 6-125 K at 2 and 3 T using a SQUID magnetometer. The data were field independent. As shown in Fig 2.16, the magnetic susceptibility of **18** can be fitted by the Curie-Weiss expression, $\chi_M = C / (T - \theta)$ with C = 0.043 emu-K/mol and θ = -2.4 K, yielding an effective moment μ_{eff} = 0.58 μ_B. If we assume that all of the sandwich compound **13** converts to the corresponding cation in the formation of the intercalate **18** and only the guest is contributing to the susceptibility, then by using the spin-only formula and the observed stoichiometry, the expected value of μ_{eff} should be 0.80 μ_B. On this basis, we estimate the percentage of ionisation of **13** in the formation of **18** to be 53 %.

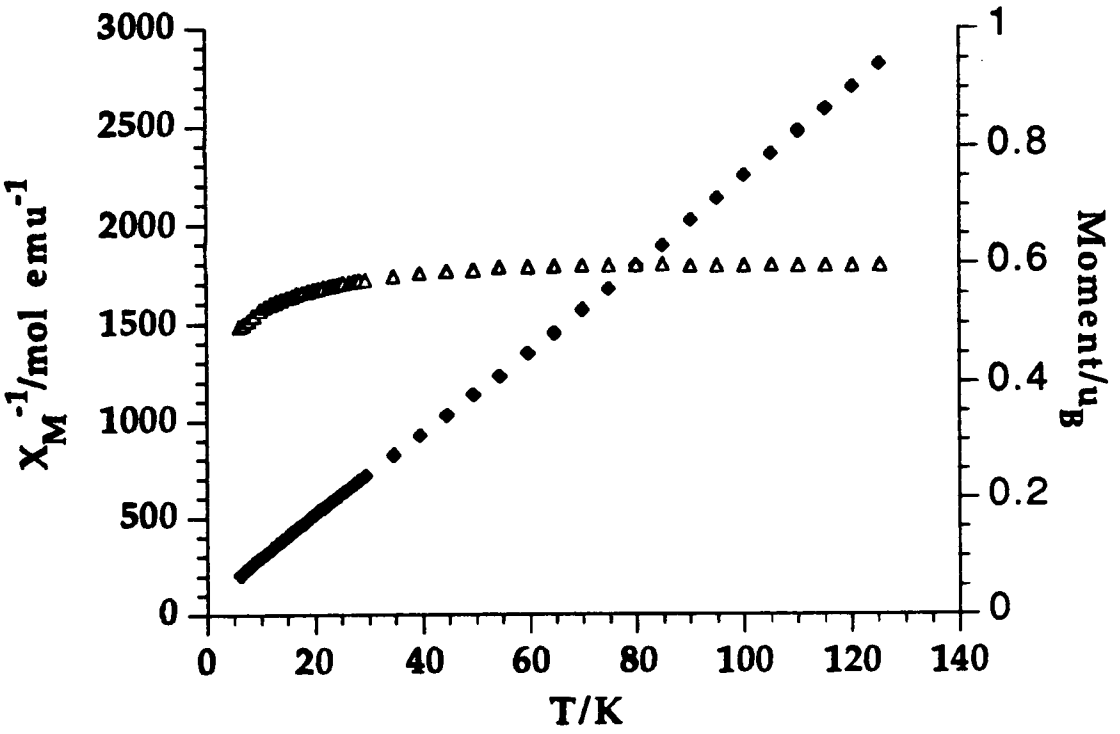

Fig. 2.16 Inverse molar magnetic susceptibility (◆) and effective moment (Δ) as a function of temperature for $\{ZrS_2[Mo(\eta\text{-}C_7H_7)(\eta\text{-}C_5H_4Me)]_{0.22}\}$ **18** at 2 T

2.7 Summary

A substantially improved synthetic pathway to [Mo(η-C_7H_7)(η^5-C_7H_9)] has been described in this chapter. This compound can be converted to [Mo(η-C_7H_7)(MeCN)I_2], which is an excellent precursor to other η-cycloheptatrienyl-molybdenum derivatives. Compound [Mo(η-C_7H_7)(MeCN)I_2], activated with Me_3SiCH_2MgCl, is a catalyst for ring-opening polymerisation of norbornene giving polymer has *trans*-content exclusively. The sandwich compounds [Mo(η-C_7H_7)(η-C_5H_4R)] (R = H or Me) have been used as electron donors in the formation of electron-transfer complexes and intercalation compound. The new chemistry described in this chapter is summarised in Scheme 2.17.

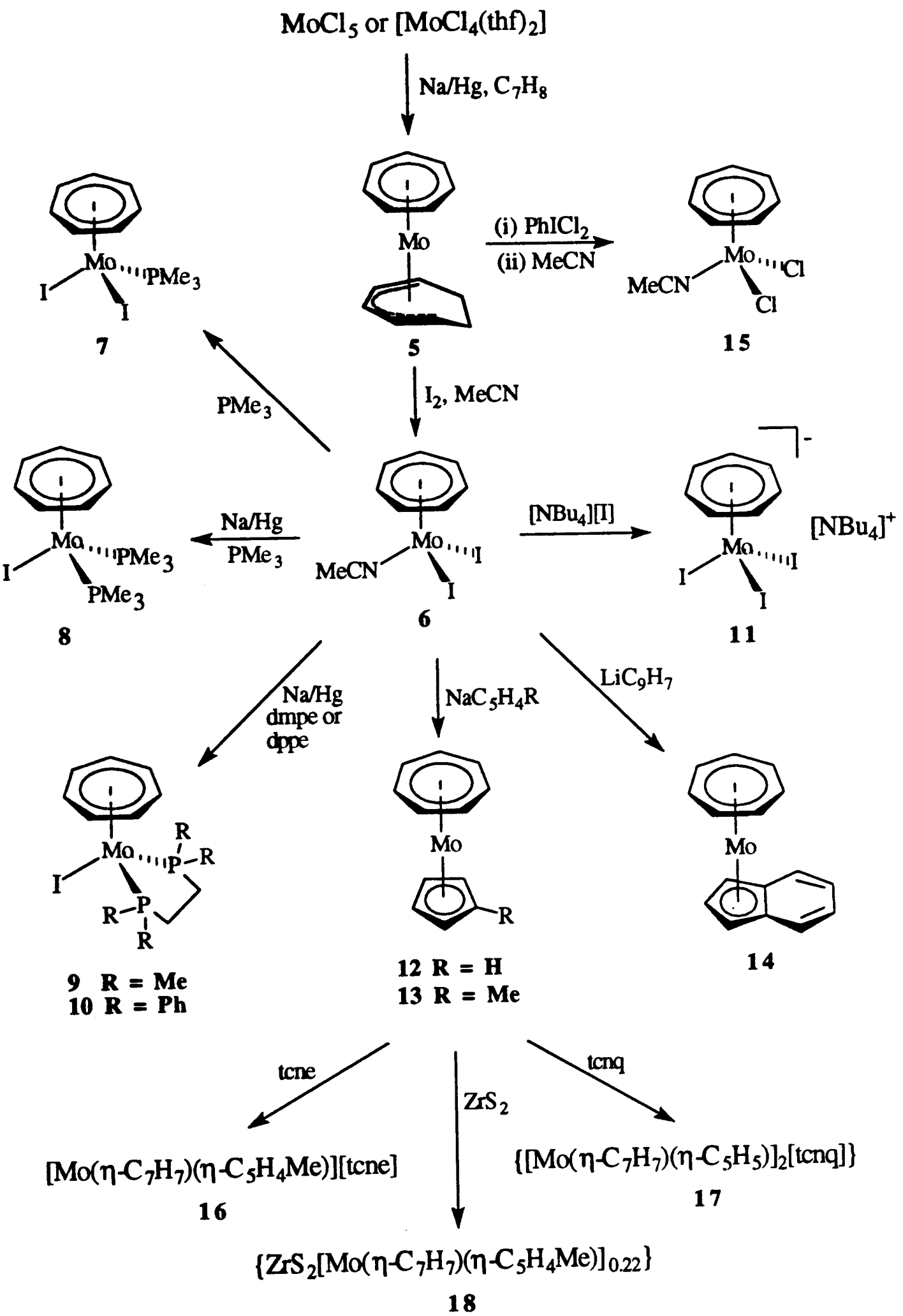
MoCl5 or [MoCl4(thf)2]
Na/Hg, C7H8
Mo
(i) PhICl2
(ii) MeCN
MeCN
Cl
Cl
15
Mo
PMe3
I
I
7
5
I2, MeCN
PMe3
Na/Hg
PMe3
Mo
PMe3
I
PMe3
8
MeCN
I
I
6
[NBu4][I]
[NBu4]+
11
Na/Hg
dmpe or
dppe
NaC5H4R
LiC9H7
Mo
I
P
R
R
R
R
9 R = Me
10 R = Ph
Mo
R
12 R = H
13 R = Me
Mo
14
tcne
ZrS2
tcnq
[Mo(η-C7H7)(η-C5H4Me)][tcne]
16
{[Mo(η-C7H7)(η-C5H5)]2[tcnq]}
17
{ZrS2[Mo(η-C7H7)(η-C5H4Me)]0.22}
18

Scheme 2.17

2.8 References

1 R. C. Tovey, D. Phil. Thesis, University of Oxford, 1986.

2 (a) E. M. van Dam, W. N. Brent, M. P. Silvon and P. S. Skell, *J. Am. Chem. Soc.*, 1975, **97**, 465; (b) M. L. H. Green and P. A. Newman, *J. Chem. Soc., Dalton Trans.*, 1989, 331.

3 J. Müller and W. Holzinger, *Z. Naturforsch*, 1978, **33B**, 1309.

4 J. R. Dilworth and R. L. Richards, *Inorg. Synth.*, 1980, **20**, 119.

5 C. E. Davies, I. M. Gardiner, J. C. Green, M. L. H. Green, N. J. Hazel, P. D. Grebenik, V. S. B. Mtetwa and K. Prout, *J. Chem. Soc., Dalton Trans.*, 1985, 669.

6 (a) J. C. Green, M. L. H. Green and N. M. Walker, *J. Chem. Soc., Dalton Trans.*, 1991, 173; (b) N. M. Walker, D. Phil. Thesis, University of Oxford, 1989.

7 (a) T. W. Beall and L. W. Houk, *Inorg. Chem.*, 1973, **12**, 1979; (b) M. L. H. Green and R. B. A. Pardy, *Polyhedron*, 1985, **4**, 1035.

8 A. Gourdon and K. Prout, *Acta Crystallogr., Sect. B,* 1982, **38**, 1596.

9 M. Green, H. P. Kirsch, F. G. A. Stone and A. J. Welch, *J. Chem. Soc., Dalton Trans.*, 1977, 1755.

10 M. L. Ziegler, H. E. Sasse and B. Nuber, *Z. Naturforsch*, 1975, **30B**, 26.

11 M. D. Rausch, A. K. Ignatowicz, M. R. Churchill and T. A. O'Brien, *J. Am. Chem. Soc.*, 1968, **90**, 3242.

12 H. W. Wehner, E. O. Fisher and J. Müller, *Chem. Ber.*, 1970, **103**, 2258.

13 H. O. van Oven, C. J. Groenenboom and H. J. de Liefde Meijer, *J. Organomet. Chem.*, 1974, **81**, 379.

14 N. G. Connelly and W. E. Geiger, *Adv. Organomet. Chem.*, 1984, **23**, 1.

15 J. D. Zeinstra and J. L. de Boer, *J. Organomet. Chem.*, 1973, **54**, 207.

16 G. Engebretson and R. E. Rundle, *J. Am. Chem. Soc.*, 1963, **85**, 481.

17 C. Furlani and G. Sartori, *Ric. Sci. Riv.*, 1958, **28**, 973. (*Chem. Abstr.*, 1958, **52**, 19606)

18 J. D. L. Holloway and W. E. Geiger, Jr., *J. Am. Chem. Soc.*, 1979, **101**, 2038.

19 W. E. Geiger, Jr., *J. Am. Chem. Soc.*, 1974, **96**, 2632.

20 (a) R. H. Grubbs, in *Comprehensive Organometallic Chemistry*, eds. G. Wilkinson, F. G. A. Stone and E. W. Abel, Pergamon, New York, 1982, vol. 8, ch. 54; (b) K. J. Ivin, *Olefin Metathesis*, Academic Press, London, 1983; (c) V. Dragutan, A. T. Balaban and M. Dimonie, *Olefins Metathesis and Ring Opening Polymerization of*

Cycloolefins, Wiley, New York, 1986.

21 L. R. Gilliom and R. H. Grubbs, *J. Am. Chem. Soc.*, 1986, **108**, 733.

22 (a) J. Feldman and R. R. Schrock, *Prog. Inorg. Chem.*, 1991, **39**,1; (b) R. R. Schrock, *Acc. Chem. Res.*, 1990, **23**, 158.

23 (a) B. A. Dolgoplosk, I. A. Oreshkin, K. L. Makovetsky, E. I. Tinyakova, I. Ya. Ostrovskaya, I. L. Kershenbaum and G. M. Chernenko, *J. Organomet. Chem.*, 1977, **128**, 339; (b) P. A. van der Schaaf, W. J. J. Smeets, A. L. Spek and G. van Koten, *J. Chem. Soc., Chem. Commun.*, 1992, 717; (c) P. A. van der Schaaf, R. A. T. M. Abbenhuis, D. M. Grove, W. J. J. Smeets, A. L. Spek and G. van Koten, *J. Chem. Soc., Chem. Commun.*, 1993, 504.

24 K. J. Ivin, D. T. Laverty and J. J. Rooney, *Makromol. Chem.*, 1977, **178**, 1545.

25 T. Oshika and H. Tabuchi, *Bull. Chem. Soc. Jpn.*, 1968, **41**, 211.

26 J. S. Miller, J. C. Calabrese, H. Rommelmann, S. R. Chittipeddi, J. H. Zhang, W. M. Reiff and A. J. Epstein, *J. Am. Chem. Soc.*, 1987, **109**, 769.

27 G. T. Lee, J. M. Manriquez, D. A. Dixon, R. S. McLean, D. M. Groski, R. B. Flippen, K. S. Narayan, A. J. Epstein and J. S. Miller, *Adv. Mater.*, 1991, **3**, 309.

28 W. Pukacki, M. Pawlak, A. Graja, M. Lequan and R. M. Lequan, *Inorg. Chem.*, 1987, **26**, 1328.

29 C. A. Formstone, E. F. Fitzgerald, D. O'Hare, P. A. Cox, M. Kurmoo, J. W. Hodby, D. Lillcrap, M. Goss-Custard, *J. Chem. Soc., Chem. Commun.*, 1990, 501.

30 (a) W. B. Davies, M. L. H. Green and A. J. Jacobson, *J. Chem. Soc., Chem. Commun.*, 1976, 781; (b) R. P. Clement, W. B. Davies, K. A. Ford, M. L. H. Green and A. J. Jacobson, *Inorg. Chem.*, 1978, **17**, 2754.

31 (a) J. S. Miller and D. A. Dixon, *Science*, 1987, **235**, 871; (b) J. S. Miller, D. M. O'Hare, A. Chakraborty and A. J. Epstein, *J. Am. Chem. Soc.*, 1989, **111**, 7853; (c) D. M. O'Hare, M. D. Ward and J. S. Miller, *Chem. Mater.*, 1990, **2(6)**, 758.

32 F. Arnold and M. L. H. Green, unpublished results.

33 D. O'Hare, J. S. O. Evans, P. J. Wiseman and C. K. Prout, *Angew. Chem., Int. Ed. Engl.*, 1991, **30**, 1156.

CHAPTER THREE

η-Cycloheptatrienyl-Tungsten Chemistry

3.1 Introduction

The chemistry of η-cycloheptatrienyl-tungsten compounds has been relatively little studied compared with that of η-cycloheptatrienyl-molybdenum compounds. As described in chapter one, most of the known η-cycloheptatrienyl derivatives of tungsten are derived from $[W(\eta\text{-}C_7H_7)(CO)_2I]$, which requires several steps to synthesise from the commercially available starting materials.[1] Another drawback of this route is the difficulty in removing the carbonyl ligands of $[W(\eta\text{-}C_7H_7)(CO)_2I]$ and the products derived from this compound usually contain at least one carbonyl ligand. The codeposition of tungsten atoms with cycloheptatriene gives $[W(\eta\text{-}C_7H_7)(\eta^5\text{-}C_7H_9)]$ but no further chemistry was reported.[2] This route is restrictive because it requires the apparatus for metal vapour synthesis, which is not available in most laboratories. The compound $[W(\eta\text{-}C_7H_7)(\eta\text{-}C_5H_5)]$ has been prepared from WCl_6 in a one-pot reaction by a reductive method.[3] However, the extremely low yield (1.4 %) of this reaction limits further investigation of the chemistry. In the preceding chapter, we have described a one-pot gram-scale preparation of $[Mo(\eta\text{-}C_7H_7)(\eta^5\text{-}C_7H_9)]$ by reducing $MoCl_5$ with sodium amalgam in the presence of cycloheptatriene and demonstrated the synthetic utilities of this compound. Here we report the extension of these synthetic pathways to tungsten.

3.2 Preparation of $[W(\eta\text{-}C_7H_7)(\eta^5\text{-}C_7H_9)]$

The compound $[W(\eta\text{-}C_7H_7)(\eta^5\text{-}C_7H_9)]$ **19** can be prepared by reduction of WCl_6 in thf with sodium amalgam in the presence of an excess of cycloheptatriene (Scheme 3.1). Large scale preparations using 12 g of WCl_6 gave 3 g of the product **1** (27 % yield).

The formation of $[W(\eta\text{-}C_7H_7)(\eta^5\text{-}C_7H_9)]$ **19** may proceed through intermediate $[W(\eta^6\text{-}C_7H_8)_2]$. However, in contrast to the corresponding molybdenum chemistry, this compound could not be detected. Possibly, the intramolecular hydrogen migration for $[W(\eta^6\text{-}C_7H_8)_2]$ is faster than that for $[Mo(\eta^6\text{-}C_7H_8)_2]$.[4]

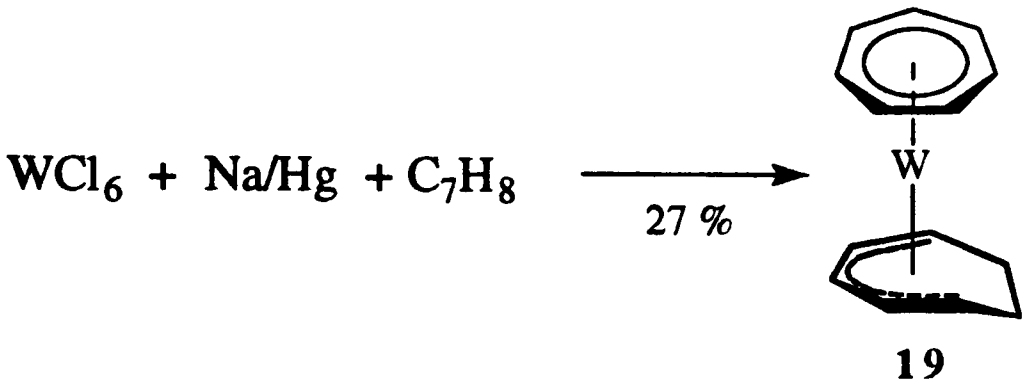

19

Scheme 3.1

3.3 Preparation and Characterisation of [W(η-C_7H_7)(MeCN)I_2]

When the reddish brown suspension of [W(η-C_7H_7)(η^5-C_7H_9)] **19** in acetonitrile was treated with one equivalent of iodine the colour darkened gradually. Heating this mixture to 80 °C for 3 h gave a bright red solution from which air-stable dark red crystals of [W(η-C_7H_7)(MeCN)I_2] **20** were obtained in 86 % yield (Scheme 3.2).

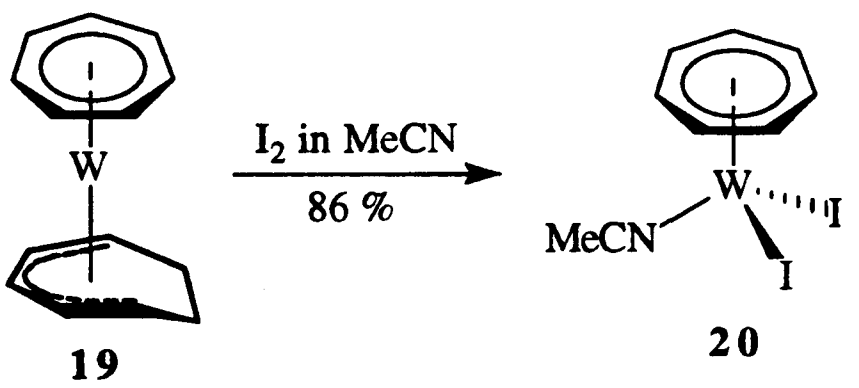

19 20

Scheme 3.2

The microanalytical data for compound **20** is consistent with the proposed stoichiometry. The mass spectrum (FAB) of **20** showed the presence of the parent cation M+. The IR spectrum exhibited bands at 2280 (m) and 2310 (m) cm^{-1} assignable to the coordinated MeCN ligand, and 813 (vs) cm^{-1} which is characteristic of the η-C_7H_7 group.[3] The structure for **20** is proposed by analogy with the molecular structure of the molybdenum congener [Mo(η-C_7H_7)(MeCN)I_2], which has been described in the preceding chapter.

The solution EPR spectrum of compound **20** is consistent with the presence of one unpaired electron and shows a rather broad signal at g = 1.941 with line width = 56 G without hyperfine splitting due to tungsten.

3.4 Preparation and Characterisation of $[W(\eta\text{-}C_7H_7)(MeCN)Br_2]$

Treatment of $[W(\eta\text{-}C_7H_7)(\eta^5\text{-}C_7H_9)]$ **19** with one equivalent of bromine in acetonitrile gave a mixture of products from which a small amount of $[W(\eta\text{-}C_7H_7)(MeCN)Br_2]$ **21** could be isolated as green microcrystals. The IR spectrum of compound **21** showed bands characteristic of the $\eta\text{-}C_7H_7$ ring (818 cm^{-1}) and MeCN ligand (2279 and 2308 cm^{-1}). The room temperature solid state EPR spectrum of **21** exhibited a very broad signal at g = 1.927. Due to the limited amount of sample, this compound was not further characterised.

3.5 Preparation and Characterisation of $[W(\eta\text{-}C_7H_7)(PMe_3)Br_2]$

Treatment of **19** with one equivalent of bromine in thf followed by addition of one equivalent of PMe_3 led to the isolation of orange brown crystals of $[W(\eta\text{-}C_7H_7)(PMe_3)Br_2]$ **22** in 44 % yield (Scheme 3.3). The stoichiometry of **22** was confirmed by microanalysis and the mass spectrum (FAB) showed bands at m/e 509 (M^+) and 430 (M - Br). Bands at 816 (vs), 946 (vs) and 962 (vs) cm^{-1} in the IR spectrum of **22** were consistent with the presence of $\eta\text{-}C_7H_7$ and PMe_3 ligands, respectively. The solution EPR spectrum of complex **22** in thf at 153 K also displayed a rather broad signal at g = 1.943 with line width = 57 G. No hyperfine splitting was observed.

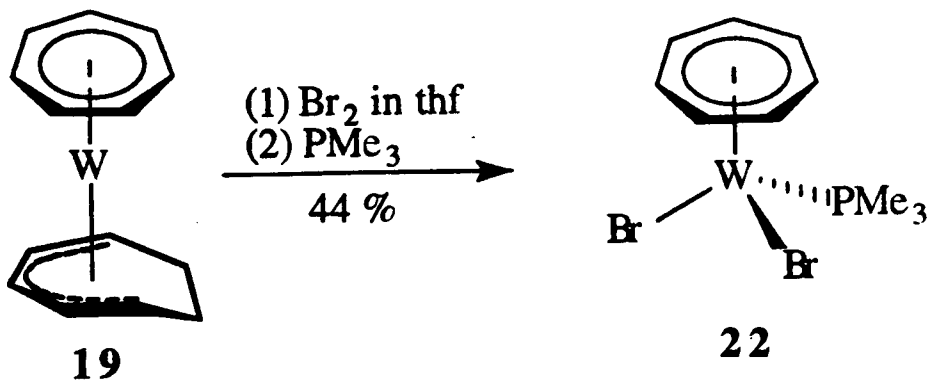

19 **22**

Scheme 3.3

3.6 Reactivity Studies of $[W(\eta\text{-}C_7H_7)(MeCN)I_2]$

The tungsten complex $[W(\eta\text{-}C_7H_7)(MeCN)I_2]$ **20** is similar to compound $[Mo(\eta\text{-}C_7H_7)(MeCN)I_2]$ **6**; it is highly reactive and is a precursor to other η-cycloheptatrienyl-tungsten derivatives. This section describes the reactivity studies of this compound.

3.6.1 Reaction with PMe_3

As expected, the MeCN ligand in $[W(\eta\text{-}C_7H_7)(MeCN)I_2]$ **20** is labile and can be displaced, for example, by PMe_3 giving red crystals of $[W(\eta\text{-}C_7H_7)(PMe_3)I_2]$ **23** in 70 % yield (Scheme 3.4). This compound is stable in air and was characterised by microanalysis and IR spectroscopy. The IR spectrum of **23** is very similar to that of $[W(\eta\text{-}C_7H_7)(PMe_3)Br_2]$ **22**.

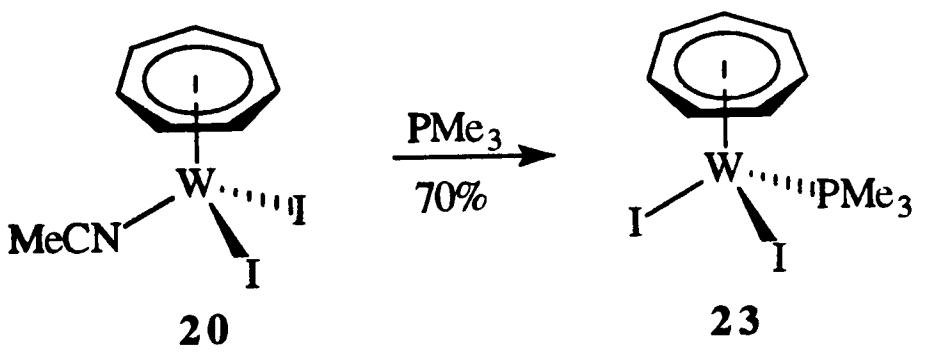

Scheme 3.4

The room temperature EPR spectrum of compound **23** in thf exhibited a rather broad absorption centred at g = 1.988 with line width = 60 G but no hyperfine coupling to ^{183}W and ^{31}P was observed; lowering the temperature to 153 K only caused slight sharpening of the signal (line width = 53 G).

The 17-electron compounds **20**-**23** are all air-stable in solid state, but solutions in air decompose gradually.

Compounds **20**, **22** and **23** show interesting antiferromagnetic coupling. The details will be described in chapter 4.

3.6.2 Reaction with Na/Hg and dmpe

Reduction of [W(η-C_7H_7)(MeCN)I_2] **20** with one equivalent of sodium amalgam in the presence of one equivalent of dmpe in thf led to the formation of diamagnetic [W(η-C_7H_7)(dmpe)I] **24** as a green solid (Scheme 3.5). This compound is air-sensitive both in solid state and in solution.

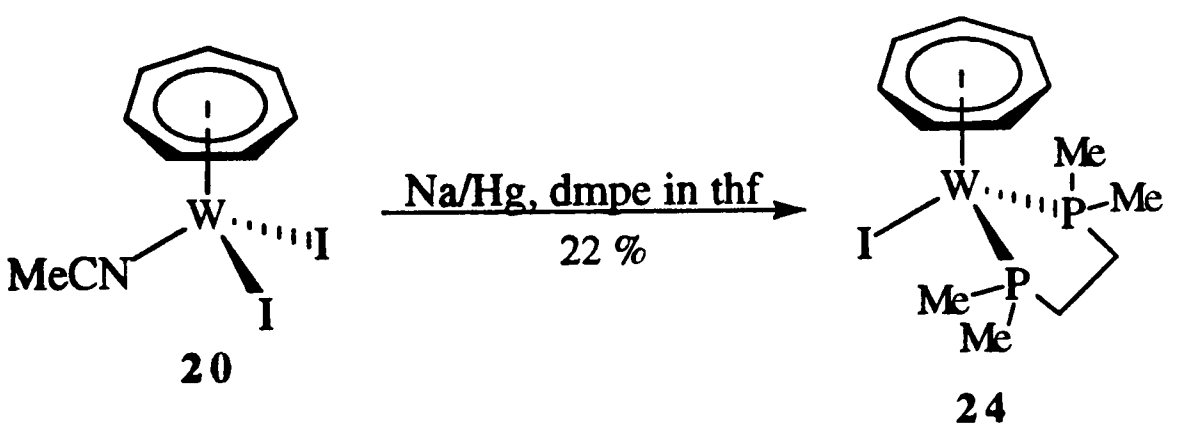

20 **24**

Scheme 3.5

The stoichiometry of **24** was confirmed by microanalysis. The mass spectrum (EI) showed the presence of the parent cation M^+ with predicted isotope pattern, together with peaks at m/e 402 and 91 due to the fragments $(M\text{-dmpe})^+$ and $C_7H_7^+$ respectively. The IR spectrum of **24** showed strong bands at 811 cm^{-1} assignable to the η-C_7H_7 group and 941 cm^{-1} assignable to P-Me stretch.

The NMR data of compound **24** are similar to those of [Mo(η-C_7H_7)(dmpe)I] **9**. Fig. 3.1 shows the ^1H NMR spectrum of **24**, which comprises a well-resolved triplet at δ 4.99 assignable to the η-C_7H_7 ligand, two well-separated doublets at δ 1.61 and δ 0.88 due to two sets of methyl groups, 'up' and 'down', and two multiplets, one of them is obscured by the doublet at δ 0.88, due to two sets of methylene protons. The DEPT (θ = 3π/4) $^{13}C\{^1H\}$ NMR spectrum of **24** is consistent with this interpretation. The $^{31}P\{^1H\}$ NMR spectrum showed a singlet resonance at δ -7.9 flanked by ^{183}W satellites from which ^1J (P-W) = 346.0 Hz could be obtained.

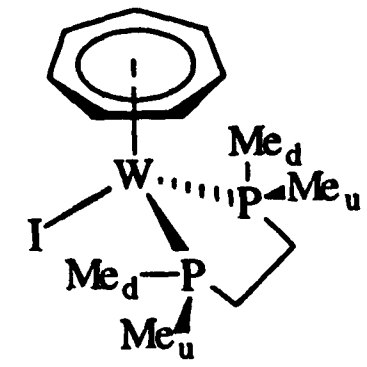

Fig. 3.1 ^1H NMR spectrum of [W(η-C_7H_7)(dmpe)I] **24** in [$^2H_8$]-toluene:*indicates solvent

3.6.3 Reaction with NaC_5H_5

The reaction between $[W(\eta\text{-}C_7H_7)(MeCN)I_2]$ **20** and an excess of NaC_5H_5 in thf afforded dark brown crystals of $[W(\eta\text{-}C_7H_7)(\eta\text{-}C_5H_5)]$ **25** in 40 % yield. Alternatively, the compound **25** could be prepared by treating $[W(\eta\text{-}C_7H_7)(\eta^5\text{-}C_7H_9)]$ **19** with one equivalent of iodine in thf, followed by the treatment of an excess of NaC_5H_5. The isolated yield of this reaction was 14 % (Scheme 3.6). It was reported that the reaction between **19** and NaC_5H_5 did not lead to the isolation of pure **25**; only mass spectral evidence could be obtained for its presence.[2] Hence, oxidation with iodine is crucial in the displacement of $\eta^5\text{-}C_7H_9$ ring in **19**. The compound **25** was prepared previously from WCl_6 but this synthesis gave an extremely low yield (1.4 %).[3]

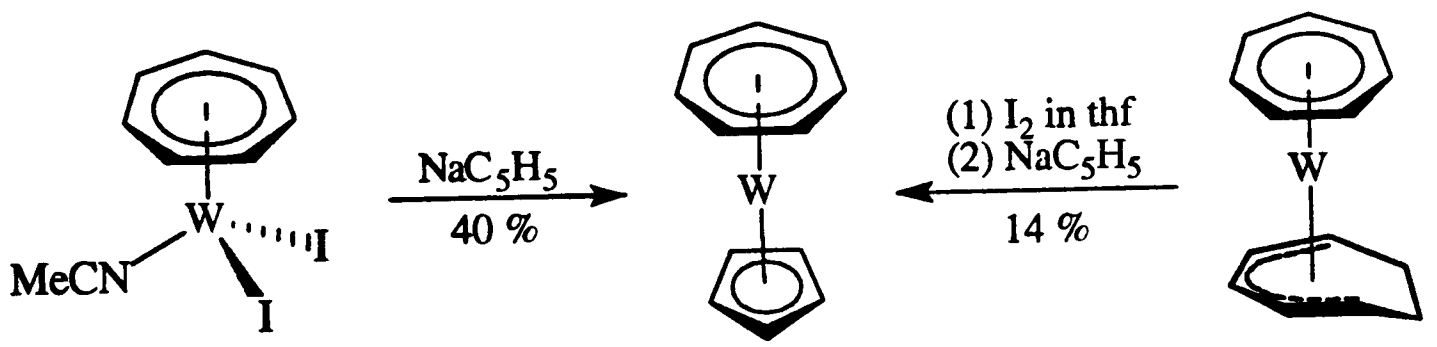

20 **25** **19**

Scheme 3.6

It was claimed that **25** did not dissolve in common organic solvents, thus no NMR data could be obtained.[3] However, we found that **25** is soluble in the solvents light petroleum (b.p. 40-60^{0}C), benzene and dichloromethane, and the ^1H and ^{13}C NMR spectra give bands unambiguously assignable to $\eta\text{-}C_7H_7$ and $\eta\text{-}C_5H_5$ ligands.

It is well documented that ^{13}C NMR chemical shifts of cyclic olefins strongly depend on the charge on the carbon atoms of the compounds; an increase in the negative charge gives rise to an upfield shift of the ^{13}C resonance, indicating an increase in the shielding of the carbon atoms.[5] Table 3.1 summarises the ^{13}C NMR data of the compounds $[M(\eta\text{-}C_7H_7)(\eta\text{-}C_5H_5)]$ (M = Cr, Mo or W). It can be seen that for the chromium compound the signal at higher field is due to the C_5 ring, while for the

molybdenum and tungsten compounds it is due to the C_7 ring. This may suggest that in the chromium compound the electron density of the carbon atoms of the C_5 ring is larger than that of the C_7 ring which is in accord with the X-ray photoelectron spectroscopy studies,[6] while the reverse is true for the molybdenum and tungsten compounds. A similar trend is not observed in the ^1H NMR data. This may due to the fact that the interpretation of ^1H NMR spectrum is complicated by local magnetic anisotropies and shieldings which are of less importance in ^{13}C NMR.[7]

Table 3.1 : ^{13}C NMR data for $[M(\eta\text{-}C_7H_7)(\eta\text{-}C_5H_5)]$

Compound	$\delta C(C_5H_5)$	$\delta C(C_7H_7)$	Solvent	Reference
M = Cr	75.4	86.9	CS_2	8
M = Mo	83.8	80.0	C_6D_6	8
M = W	82.5	73.8	C_6D_6	This work

The electrochemistry of $[W(\eta\text{-}C_7H_7)(\eta\text{-}C_5H_5)]$ **25** was studied by cyclic voltammetry. Fig. 3.2 shows a typical cyclic voltammogram of **25** with ferrocene as internal standard. It was found that **25** undergoes one fully reversible oxidation at $E_{1/2}$ = -0.77 V *vs.* SCE. This value is smaller than the corresponding value (-0.60 V) of $[Mo(\eta\text{-}C_7H_7)(\eta\text{-}C_5H_5)]$ **12**, indicating that the tungsten compound is more reducing than the molybdenum congener. Chemical oxidation of **25** with iodine to the corresponding monocation $[W(\eta\text{-}C_7H_7)(\eta\text{-}C_5H_5)]^+$ has been reported previously.[3]

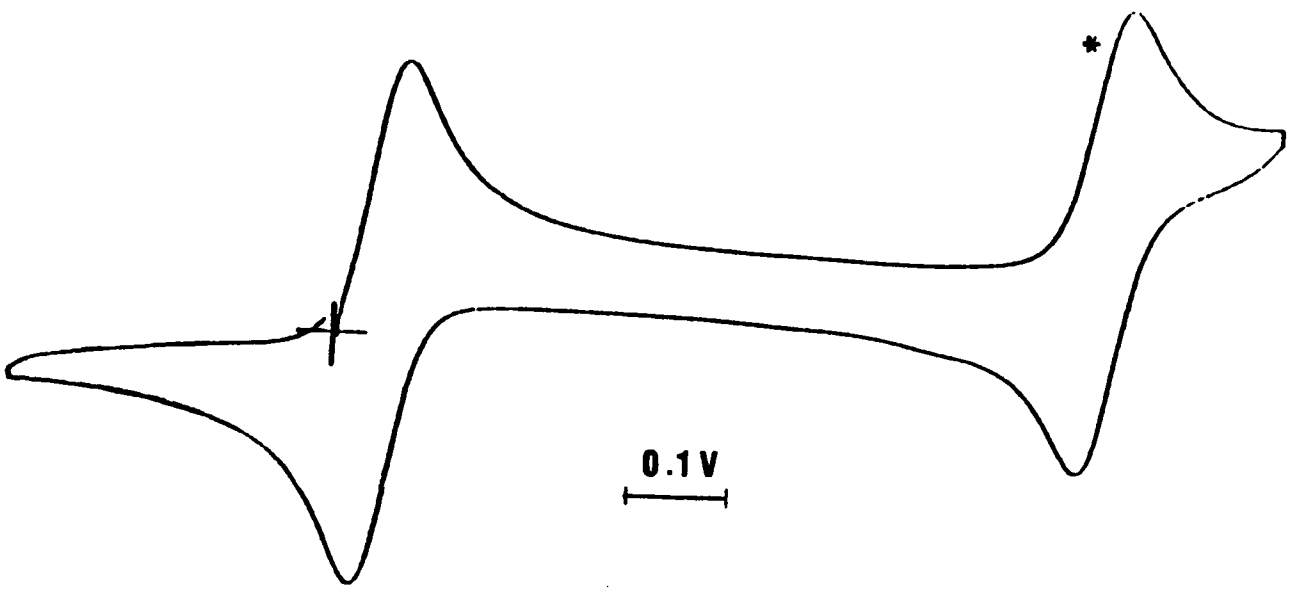

Fig. 3.2 Cyclic voltammogram of [W(η-C_7H_7)(η-C_5H_5)] **25** recorded in acetonitrile at a scan rate of 50 mV S^{-1} with [NBu_4][PF_6] as electrolyte and ferrocene as internal standard: * indicates peak due to ferrocene/ferrocium couple

3.6.4 Reaction with NaC_5H_4Me

Treatment of [W(η-C_7H_7)(MeCN)I_2] **20** with an excess of NaC_5H_4Me in thf gave dark brown crystals of [W(η-C_7H_7)(η-C_5H_4Me)] **26** in 80 % yield. The dibromo compound [W(η-C_7H_7)(PMe_3)Br_2] **22** could also be used instead of **20** to prepare compound **26** in 60 % yield. As an alternative pathway to prepare **26**, the compound [W(η-C_7H_7)(η^5-C_7H_9)] **19** was treated with one equivalent of iodine in thf, then the resulting mixture was reacted with an excess of NaC_5H_4Me to give the compound **26** in 50 % yield. The product was characterised by microanalysis and NMR spectroscopy.

The ^1H NMR spectrum of **26** in [$^2H_6$]-benzene (Fig. 3.3) showed a singlet at δ 5.21 assignable to the η-C_7H_7 ligand, two broad bands at δ 5.28 and δ 5.16, and a singlet at δ 1.76 which were attributed to the η-C_5H_4Me ligand. The ^{13}C NMR spectrum of **26** is consistent with the proposed sandwich structure.

Cyclic voltammetric studies showed that **26** is reducing and undergoes one reversible oxidation at $E_{1/2}$ = -0.79 V *vs.* SCE.

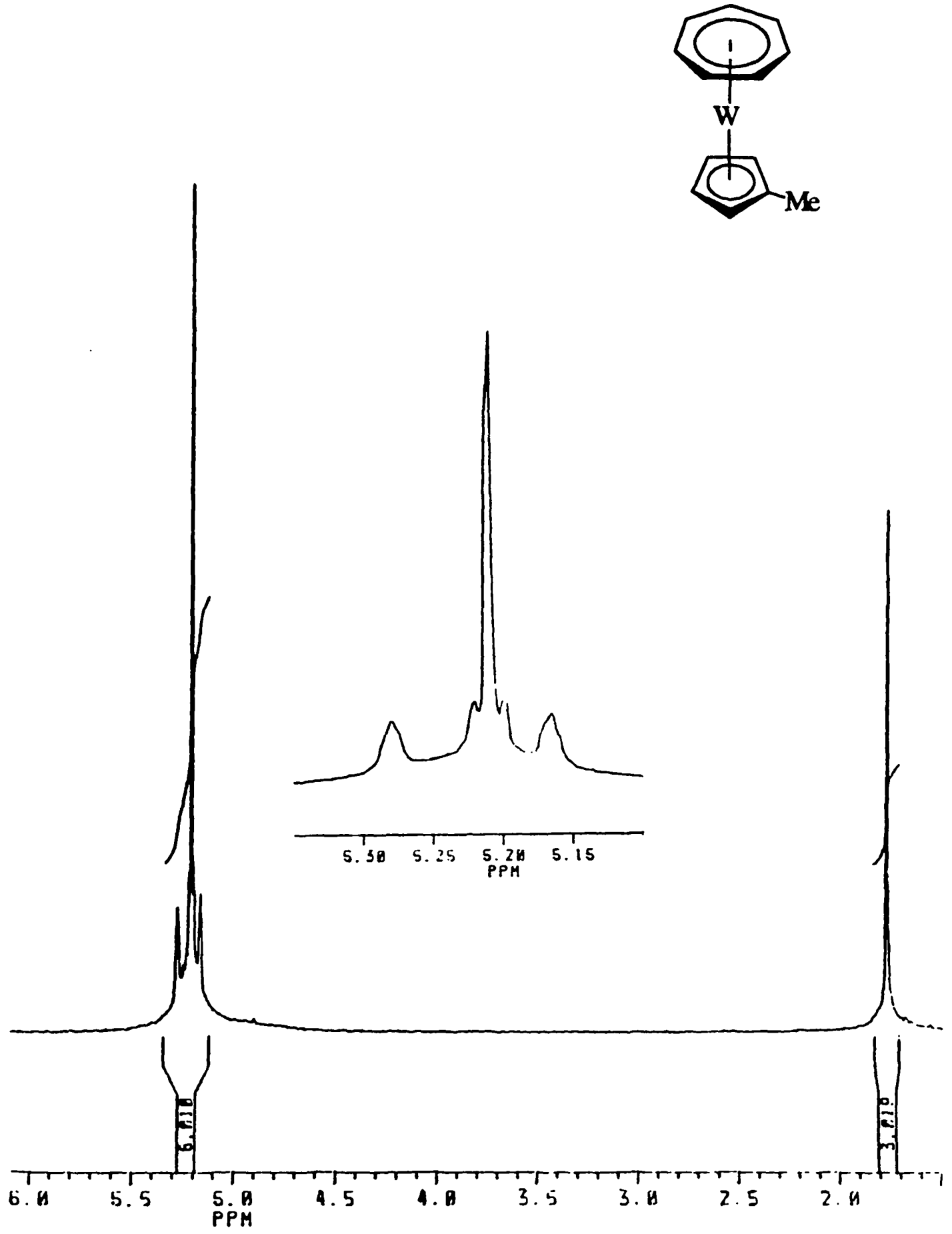

Fig. 3.3 ^{1}H NMR spectrum of $[W(\eta\text{-}C_7H_7)(\eta\text{-}C_5H_4Me)]$ **26** in $[^{2}H_6]$-benzene

3.6.5 Reaction with LiC_9H_7

Treatment of $[W(\eta\text{-}C_7H_7)(MeCN)I_2]$ **20** with an excess of lithium indenide in thf gave a dark brown solution from which purple crystals of $[W(\eta\text{-}C_7H_7)(\eta^5\text{-}C_9H_7)]$ **27** were isolated in 25 % yield (Scheme 3.7). The ^1H NMR spectrum of the purple crystals in $[^2H_6]$-benzene showed broad bands assignable to the ring protons which may due to the presence of paramagnetic impurities. Recrystallisation of the crude product from light petroleum (b.p. 40-60^{0}C) and using $[^2H_6]$-acetone as solvent produced a well-resolved spectrum as shown in Fig. 3.4. The ^{13}C NMR data of **27** are consistent with the proposed structure.

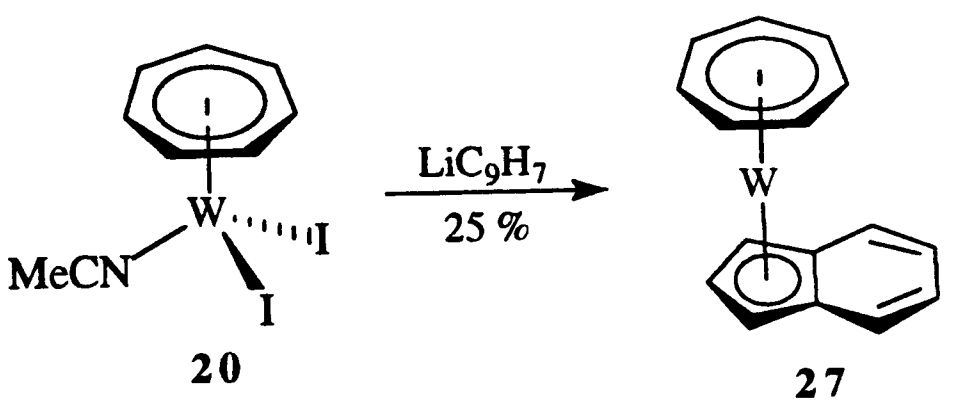

20 **27**

Scheme 3.7

The electrochemistry of compound **27** was studied by cyclic voltammetry. The voltammogram of **27** exhibited one reversible wave at $E_{1/2}$ = -0.66 V *vs.* SCE. The electrochemical data of **25-27** are listed in Table 3.2, which also includes the half-wave potentials of the molybdenum analogues for comparison. It can be seen that the tungsten complexes are more reducing than their molybdenum congeners and that on changing the pentahapto-ring from η-cyclopentadienyl to η-indenyl ligand the compounds become less reducing.

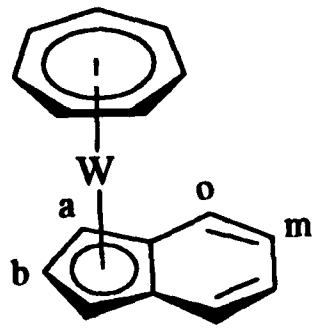

Fig. 3.4 ^1H NMR spectrum of $[W(\eta\text{-}C_7H_7)(\eta^5\text{-}C_9H_7)]$ **27** in $[^2H_6]$-acetone: *indicates solvent

Table 3.2 : Half-wave potentials (V) of $[M(\eta\text{-}C_7H_7)(\eta\text{-}C_5H_4R)]$ and $[M(\eta\text{-}C_7H_7)(\eta^5\text{-}C_9H_7)]$ *vs.* SCE

	M = Mo	M = W
$[M(\eta\text{-}C_7H_7)(\eta\text{-}C_5H_5)]^{+/0}$	-0.60	-0.77
$[M(\eta\text{-}C_7H_7)(\eta\text{-}C_5H_4Me)]^{+/0}$	-0.63	-0.79
$[M(\eta\text{-}C_7H_7)(\eta^5\text{-}C_9H_7)]^{+/0}$	-0.48	-0.66

3.6.6 Polymerisation of norbornene

It is well-documented that $[Zr(\eta\text{-}C_5H_5)_2Cl_2]$ and related group 4 bent metallocene complexes activated with aluminoxane are Ziegler type catalysts for olefin polymerisation.[9] Thus we were interested in studying the catalytic property of $[W(\eta\text{-}C_7H_7)(MeCN)I_2]$ **20** in this aspect. When a solution of aluminoxane (1 g) in toluene was added to a red suspension of **20** (10 mg) in toluene, the colour changed to orange-brown immediately. Then styrene (36 g) was added and the mixture was heated at 50^{0}C overnight. Unfortunately, no polymer could be isolated when the mixture was poured into methanol.

Although compound **20**/aluminoxane does not catalyse the polymerisation of styrene, the compound $[W(\eta\text{-}C_7H_7)(MeCN)I_2]$ **20** activated with Me_3SiCH_2MgCl was found to be an active catalyst for ring-opening polymerisation of norbornene (Scheme 3.8). In a preliminary study, a suspension of **20** (20 mg) in toluene (30 cm^3) was treated with 300 equivalents of norbornene (1 g). The mixture was stirred at room temperature for 15 minutes without any observable change. However, when a few drops of Me_3SiCH_2MgCl solution in diethyl ether was added, precipitation occurred and the viscosity of the mixture increased. The mixture was stirred at room temperature for 24 h to give a very viscous green solution from which 0.53 g of polymer was isolated as white fibrous material.

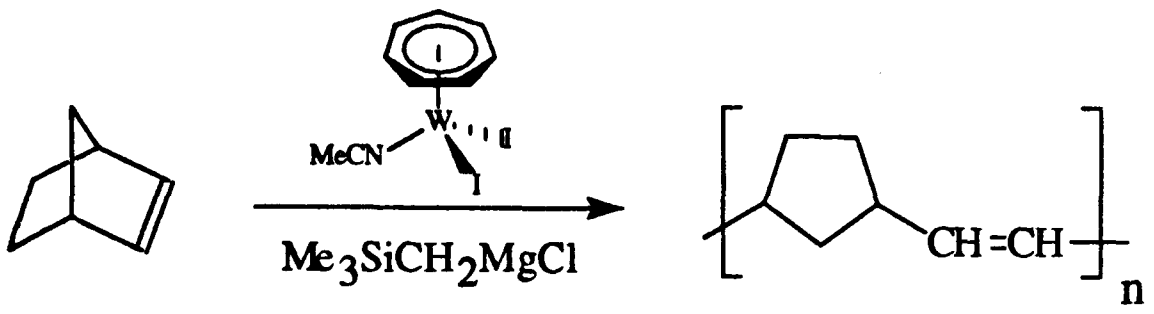

Scheme 3.8

Fig. 3.5 shows the DEPT ($\theta = 3\pi/4$) $^{13}C\{^1H\}$ NMR spectrum of the product in [$^2H_1$]-chloroform. The assignments based on the literature values[10] are shown in the figure, in which the first letter denotes the *cis* or *trans* structure at the nearest double bond; the second letter, at the next nearest double bond. The data show that **20** yields ring-opened polynorbornene with a *trans* : *cis* ratio of 2.2 to 1. Further analysis of the ^{13}C NMR spectrum indicates a tendency towards a blocky distribution.[11] This preliminary experiment shows that the catalytic activity of compound **20** in polymerisation of norbornene is less selective but much higher than that of the molybdenum congener [Mo(η-C_7H_7)(MeCN)I_2] **6**.

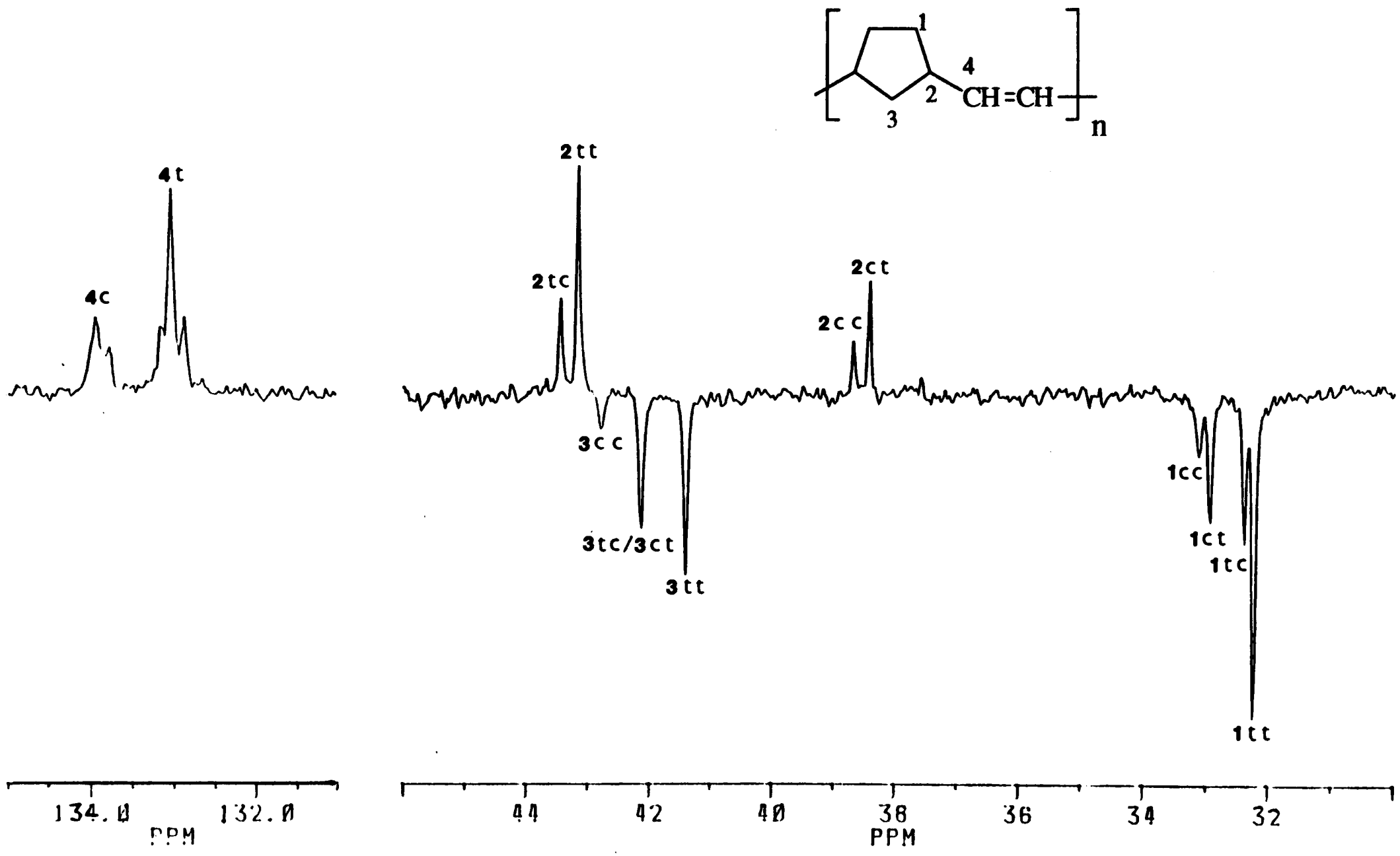

Fig. 3.5 DEPT ($\theta = 3\pi/4$) $^{13}C\{^1H\}$ NMR spectrum of poly(1,3-cyclopentylene-vinylene) in [$^2H_1$]-chloroform

3.7 PES studies of [W(η-C_7H_7)(η-C_5H_4R)] (R = H or Me)

The electronic structure of [W(η-C_7H_7)(η-C_5H_4R)] (R = H **25** or Me **26**) has been examined by photoelectron spectroscopy (PES). The previously described X-ray crystal structures of [M(η-C_7H_7)(η-C_5H_5)] (M = Ti,[12] V[13] or Cr[14]) and [Mo(η-C_7H_7)(η-C_5H_4Me)] show that the two hydrocarbon rings are planar and parallel, and it may be reasonably assumed that the analogous **25** and **26** have similar structures. The qualitative molecular orbital diagram shown in Fig. 1.1 (p. 40) is thus applied and the electronic configuration of these 18-electron molecules is $(1e_1)^4(2e_1)^4(1e_2)^4(1a_1)^2$.

The He I and He II PE spectra of **25** and **26** recorded by Christian Whitaker are shown in Fig. 3.6 and 3.7 respectively. Vertical ionisation energy (IE) data and assignments are given in Table 3.3, which also includes the corresponding data for [M(η-C_7H_7)(η-C_5H_5)] (M = Cr[15] or Mo[16]) for comparison.

The assignments put forward in Table 3.3 are as given by previous workers.[15,16] The first band in Fig. 3.6(a) and 3.7(a) arises from the ionisation of helium atoms by He II radiation. Band A is sharp and is due to ionisation from the $1a_1$ orbital, which is mainly metal d_{z^2} in character. Band B is assigned to ionisation from the $1e_2$ orbitals, the splitting of which may arise from the $^2E_{5/2}$ and $^2E_{3/2}$ molecular ion states or a Jahn-Teller distortion. The spin-orbit coupling constant of tungsten may be sufficiently large for these spin-orbit states to be resolved. In free W^+, the splitting of the $5d_{3/2}$ and $5d_{5/2}$ levels is predicted as $2\zeta = 0.64$ eV.[17] The lower value found in **25** and **26** (0.33 eV) suggests that the $1e_2$ electrons are delocalised onto the ligands. Band C is characteristic in position and shape of ionisation from the $2e_1$ orbitals (mainly cyclopentadienyl); the asymmetry is probably due to a Jahn-Teller distortion localised on the cyclopentadienyl ring. Band D is assigned to ionisation from the $1e_1$ orbitals (mainly cycloheptatrienyl).

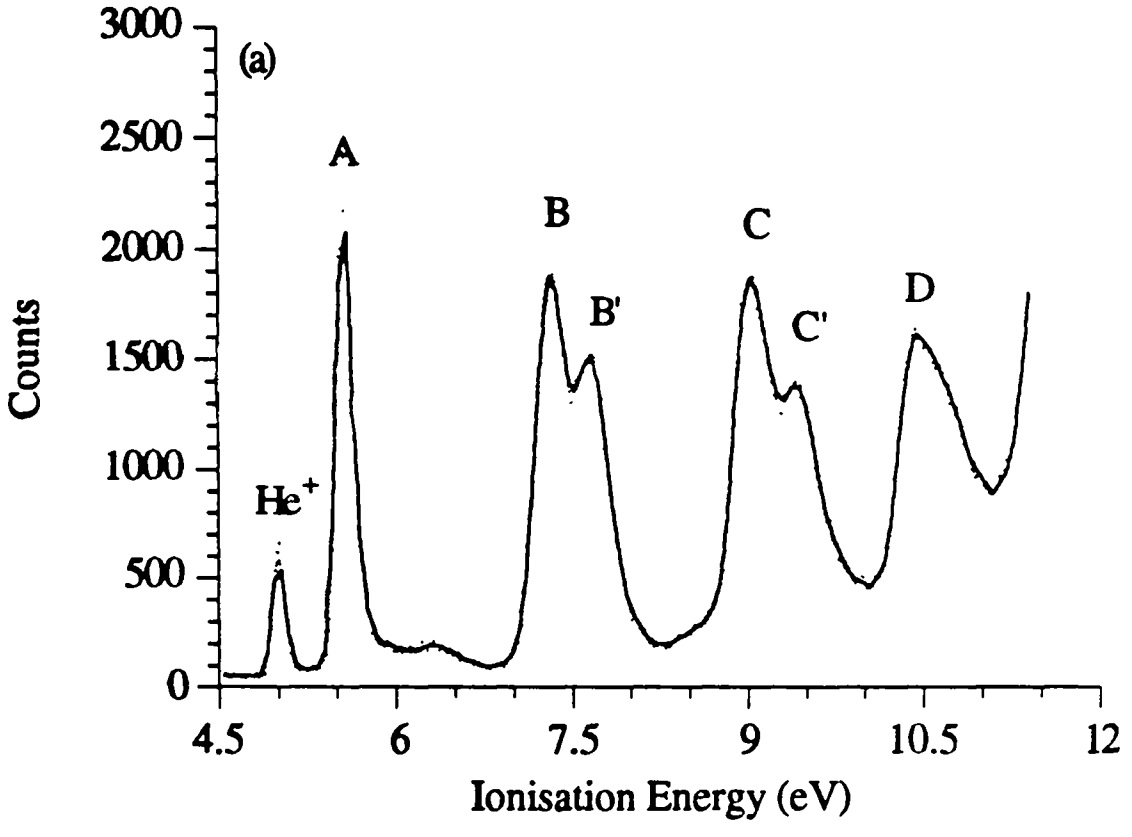

Fig. 3.6 (a) He I and (b) He II photoelectron spectra of [W(η-C_7H_7)(η-C_5H_5)] **25**

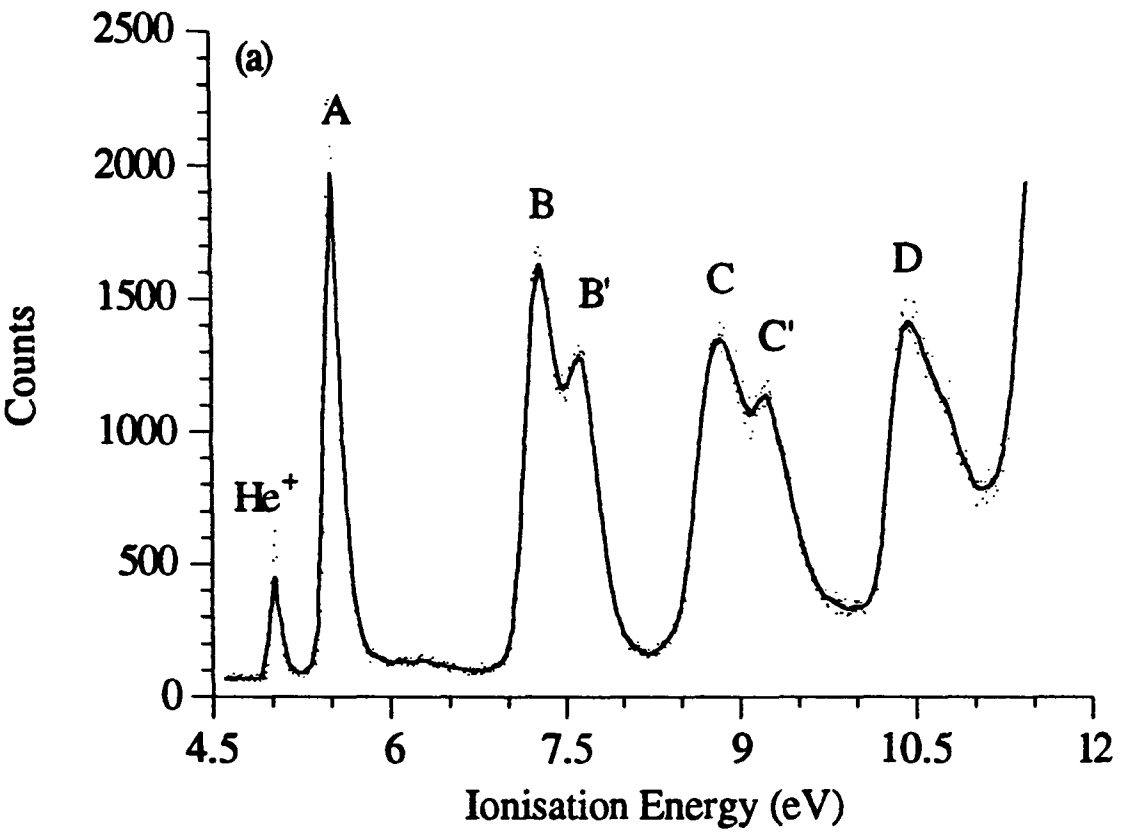

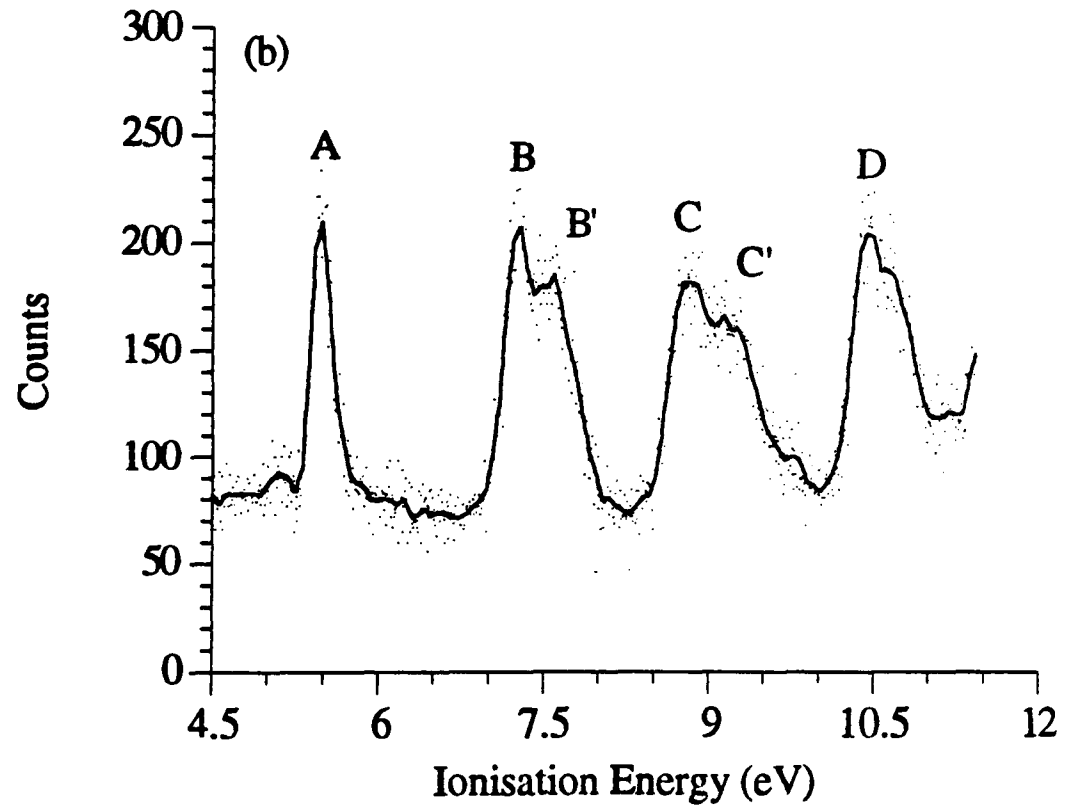

Fig. 3.7 (a) He I and (b) He II photoelectron spectra of [W(η-C_7H_7)(η-C_5H_4Me)] **26**

Table 3.3 : Vertical ionisation energies and assignments of $[M(\eta\text{-}C_7H_7)(\eta\text{-}C_5H_4R)]$

Compound	Band	IE/eV	Assignment
$[W(\eta\text{-}C_7H_7)(\eta\text{-}C_5H_4Me)]$ **26**	A	5.50	$^2A_1\ (1a_1)$
	B	7.27	$^2E_{5/2}\ (1e_2)$
	B'	7.60	$^2E_{3/2}\ (1e_2)$
	C	8.81	$2e_1$
	C'	9.21	$2e_1$
	D	10.42	$1e_1$
$[W(\eta\text{-}C_7H_7)(\eta\text{-}C_5H_5)]$ **25**	A	5.58	$^2A_1\ (1a_1)$
	B	7.31	$^2E_{5/2}\ (1e_2)$
	B'	7.64	$^2E_{3/2}\ (1e_2)$
	C	9.01	$2e_1$
	C'	9.41	$2e_1$
	D	10.42	$1e_1$
$[Mo(\eta\text{-}C_7H_7)(\eta\text{-}C_5H_5)]$[16a(16b)]	A	5.70 (5.87)	$^2A_1\ (1a_1)$
	B	7.38 (7.55)	$^2E_2\ (1e_2)$
	C	8.86 (8.93)	$2e_1$
	C'	9.25 (9.28)	$2e_1$
	D	10.38 (10.4)	$1e_1$
$[Cr(\eta\text{-}C_7H_7)(\eta\text{-}C_5H_5)]$[15]	A	5.59	$^2A_1\ (1a_1)$
	B	7.19	$^2E_2\ (1e_2)$
	C	8.69	$2e_1$
	C'	9.00	$2e_1$
	D	10.4	$1e_1$

In Table 3.3, it can be seen that methyl substitution in the C_5 ring decreases the ionisation energies of $1a_1$, $1e_2$ and $2e_1$ orbitals. The effect is greatest for ionisation from the $2e_1$ orbitals where decreases of 0.2 eV in corresponding bands is observed. This confirms that this ionisation arises from orbitals mainly localised on the cyclopentadienyl ring. As the $1a_1$ orbital is mainly non-bonding in character this decrease appears to be a result of increased electron-electron repulsion.

Fig. 3.8 shows the variation in ionisation energies in [M(η-C_7H_7)(η-C_5H_5)] (M = Cr, Mo or W). It is interesting to note that the $1a_1$ orbital ionisation energies for the Cr and W compounds are close to each other whereas the corresponding ionisation energy for the Mo compound is slightly higher (*ca.* 0.2 eV). A similar trend has been found for the series of isoelectronic molecules [M(η-C_6H_6)$_2$] [M = Cr (5.4 eV),[15] Mo (5.52 eV)[15] or W (5.40 eV)[18]]. The ionisation energy of $2e_1$ orbitals increases across the series which may reflect that the electron density in the C_5 ring in [M(η-C_7H_7)(η-C_5H_5)] follows the order Cr > Mo > W. In contrast, the $1e_1$ (mainly cycloheptatrienyl) orbital energies are insensitive to changes of the metal and of the methyl substitution in the C_5 ring.

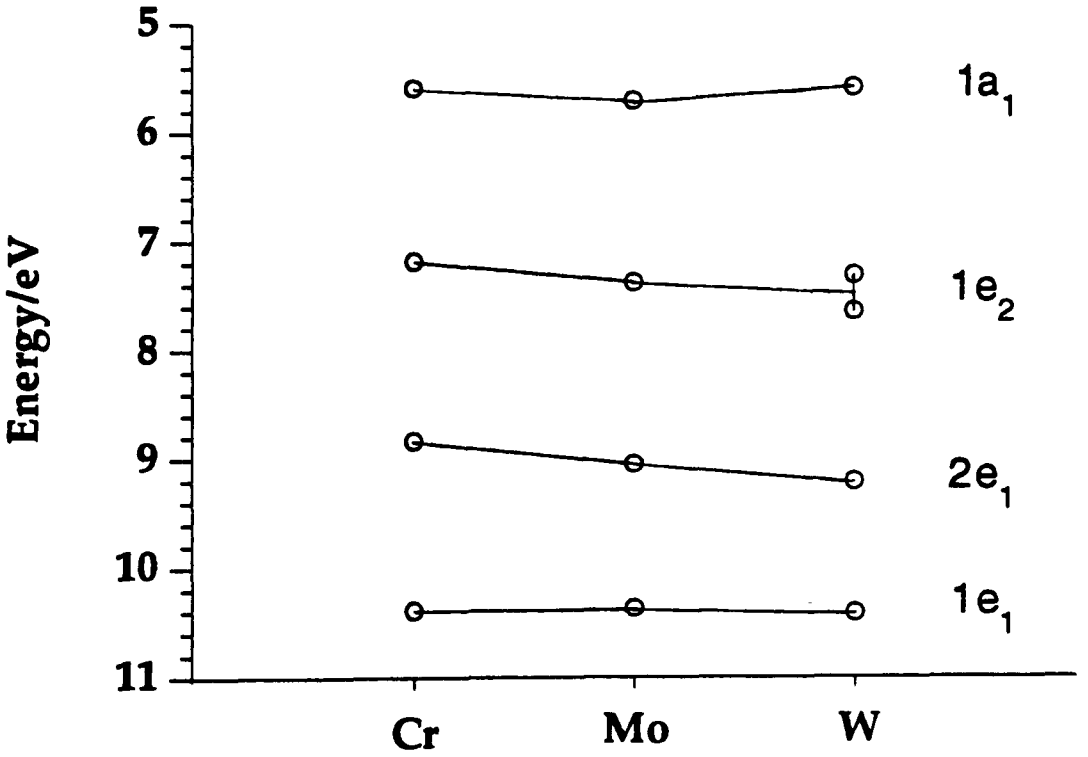

Fig. 3.8 Vertical ionisation energies of [M(η-C_7H_7)(η-C_5H_5)]

3.8 Reactivity Studies of [W(η-C_7H_7)(η-C_5H_4Me)]

As shown by the electrochemical measurements and PES studies, the sandwich compounds [W(η-C_7H_7)(η-C_5H_4R)] (R = H **25** or Me **26**) are electron-rich and they form cations stable to isolation. Therefore it is expected that these compounds react with appropriate electron acceptors. This section describes the reactions between **26** and the planar polycyano acceptors (tcnq and tcne), and the intercalation of **26** into layered ZrS_2.

3.8.1 Reactions with tcnq and tcne

Compound [W(η-C_7H_7)(η-C_5H_4Me)] **26** was treated with a stoichiometric amount of tcnq in dichloromethane causing an immediate precipitation. The resulting dark purple solid was collected by filtration and was tried to purify by recrystallisation. However it was only very sparingly soluble in dichloromethane, acetonitrile and thf. Microanalysis of the crude product showed that the C, H and N contents are close to the calculated values for 1 : 1 electron-transfer complex [W(η-C_7H_7)(η-C_5H_4Me)][tcnq] [C 51.0 (53.8), H 3.3 (3.3) N 10.8 (10.0)]. But the IR spectrum exhibited two bands at 2190 (s) and 2104 (vs) cm^{-1} which are not consistent with the ν (C≡N) of tcnq- [2179 (s) and 2153 (m) cm^{-1}] (see Table 2.5). The solid state EPR spectrum of the crude product showed a broad signal at g = 1.97 (line width = 96 G) which is probably due to the cation [W(η-C_7H_7)(η-C_5H_4Me)]+. The low solubility of this compound in common organic solvents precludes the purification by recrystallisation. Thus this compound was not further characterised.

The reaction between **26** and a stoichiometric amount of tcne in thf also led to immediate precipitation. After filtration, a dark red solution was obtained which was layered with diethyl ether giving a dark purple solid. The IR spectrum of the crude product showed two strong bands at 2187 and 2125 cm^{-1} which are close to the expected values for tcne- [2183 (s) and 2144 (s) cm^{-1}] (see Table 2.5). However, the microanalytical data did not correspond to the 1 : 1 electron-transfer complex. Attempts to purify the crude product by recrystallisation were unsuccessful.

3.8.2 Intercalation into ZrS_2

Treatment of zirconium disulfide powder with [W(η-C_7H_7)(η-C_5H_4Me)] **26** in toluene at 120°C for 5 days led to the formation of a dull black solid which was thoroughly washed with toluene and then dried *in vacuo*. Powder X-ray diffraction of this black solid showed that intercalation had occurred. Microanalysis gave the stoichiometry {ZrS_2[W(η-C_7H_7)(η-C_5H_4Me)]$_{0.20}$} **28** and confirmed the expected C : H ratio.

Fig. 3.9 shows the X-ray diffraction pattern of the intercalate **28**. The indexing as well as observed and calculated *d* spacings are given in Appendix C. The cell parameters for **28** together with those for the chromium and molybdenum analogues are listed in Table 3.4. It is interesting that both the stoichiometry (x) and the lattice expansion (Δc) decrease down the group.

The room temperature solid state EPR spectrum of the intercalate **28** showed no signal, however, on cooling to 26 K, a broad signal at g = 1.95 (line width = 210 G) appeared.

Table 3.4 : Cell parameters of {ZrS_2[M(η-C_7H_7)(η-C_5H_4R)]$_x$}

Guest	x	c / Å	Δc / Å	reference
[Cr(η-C_7H_7)(η-C_5H_5)]	0.25	36.0 (2)[a]	6.17 (7)	19
[Mo(η-C_7H_7)(η-C_5H_4Me)]	0.22	11.93 (1)	6.10 (1)	This work
[W(η-C_7H_7)(η-C_5H_4Me)]	0.20	11.85 (2)	6.02 (2)	This work

[a] the c-axis was tripled

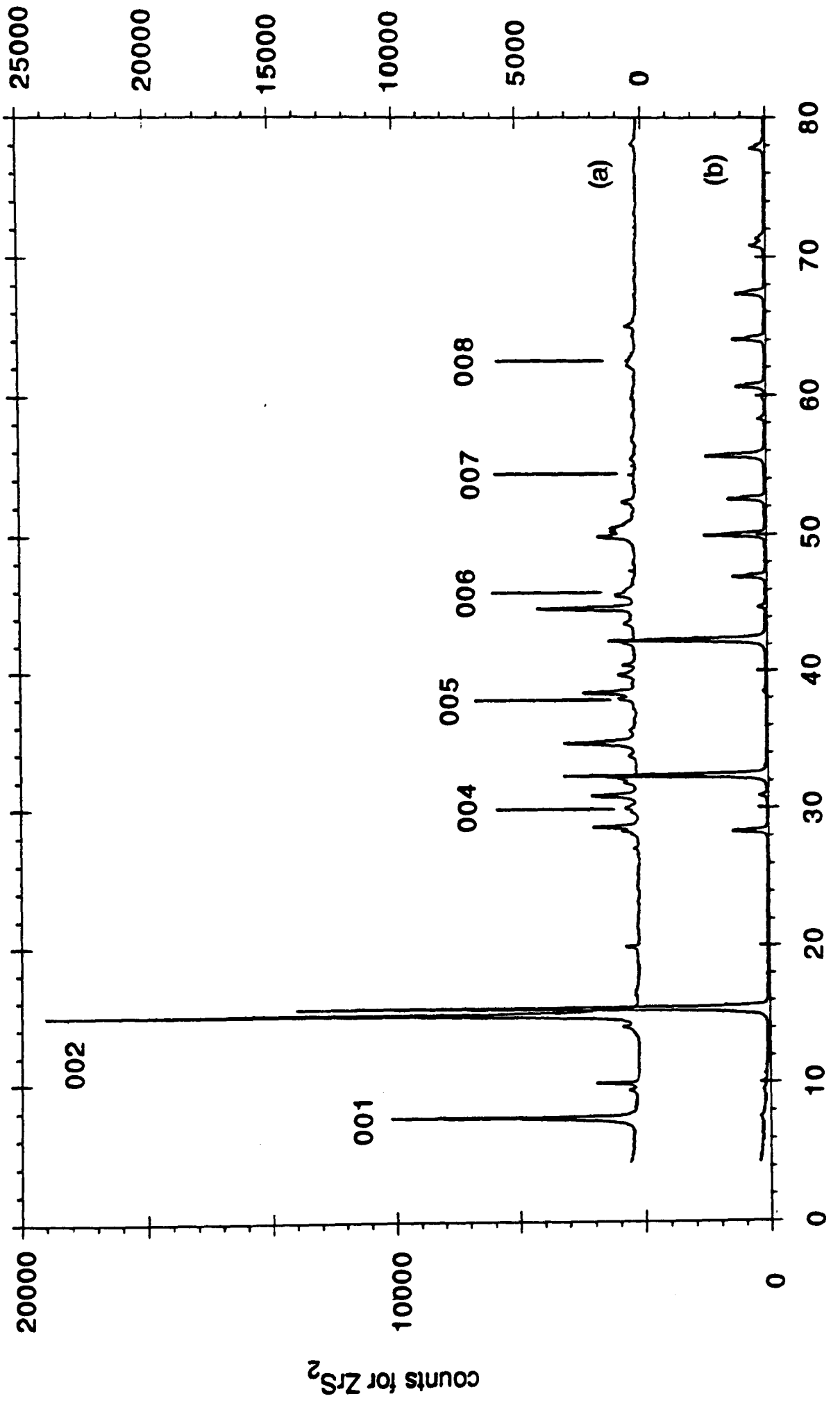

Fig. 3.9 X-ray powder diffraction patterns of (a) $\{ZrS_2[W(\eta\text{-}C_7H_7)(\eta\text{-}C_5H_4Me)]_{0.20}\}$ **28** and (b) ZrS_2

The magnetic property of **28** was studied in the temperature range 6-180 K at 1T, 2 T and 3 T. The data were field-independent and could be fitted with the Curie-Weiss expression [$\chi_M = C / (T - \theta)$] with C = 0.049 emu-K/mol and θ = -5.2 K. As shown in Fig. 3.10, the effective moment has a steady value of 0.61 μ_B at higher temperatures. The percentage of ionisation of **26** in the formation of intercalate **28** was thus estimated to be 65 %. This value is higher than that of the molybdenum analogue (52 %), which suggests that the least tightly bound electron in [W(η-C_7H_7)(η-C_5H_4Me)] can be removed more readily than in [Mo(η-C_7H_7)(η-C_5H_4Me)]. This result is consistent with the electrochemical measurements and PES studies.

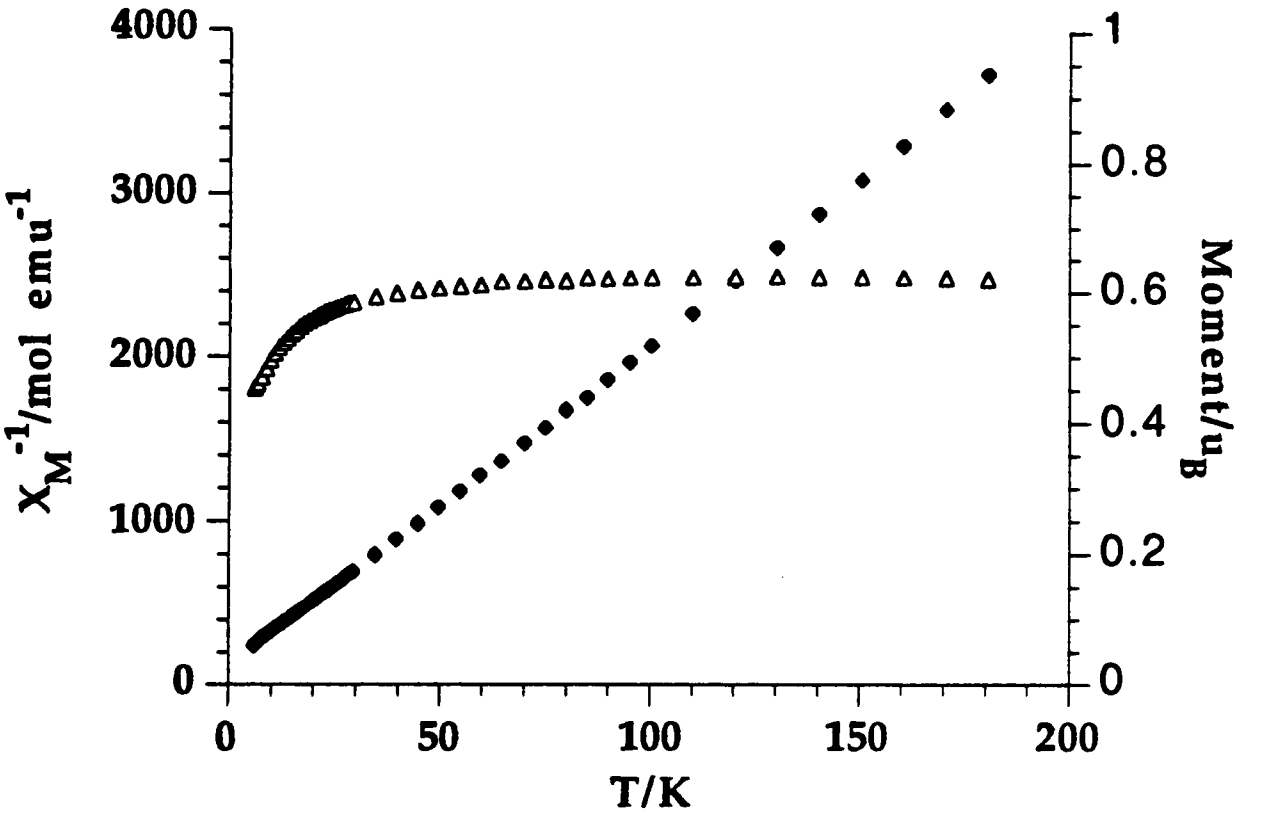

Fig. 3.10 Inverse molar magnetic susceptibility (◆) and effective moment (Δ) as a function of temperature for {ZrS_2[W(η-C_7H_7)(η-C_5H_4Me)]$_{0.20}$} **28** at 1 T

3.9 Summary

This chapter has demonstrated new synthetic pathways in η-cycloheptatrienyl-tungsten chemistry. The one-pot synthesis of $[W(\eta\text{-}C_7H_7)(\eta^5\text{-}C_7H_9)]$ provides an effective route to other η-cycloheptatrienyl-tungsten derivatives. The new chemistry is summarised in Scheme 3.9. The catalytic properties of $[W(\eta\text{-}C_7H_7)(MeCN)I_2]$ / Me_3SiCH_2MgCl system in ring-opening polymerisation of norbornene and the electronic structure of $[W(\eta\text{-}C_7H_7)(\eta\text{-}C_5H_4R)]$ (R = H or Me) have also been discussed in this chapter.

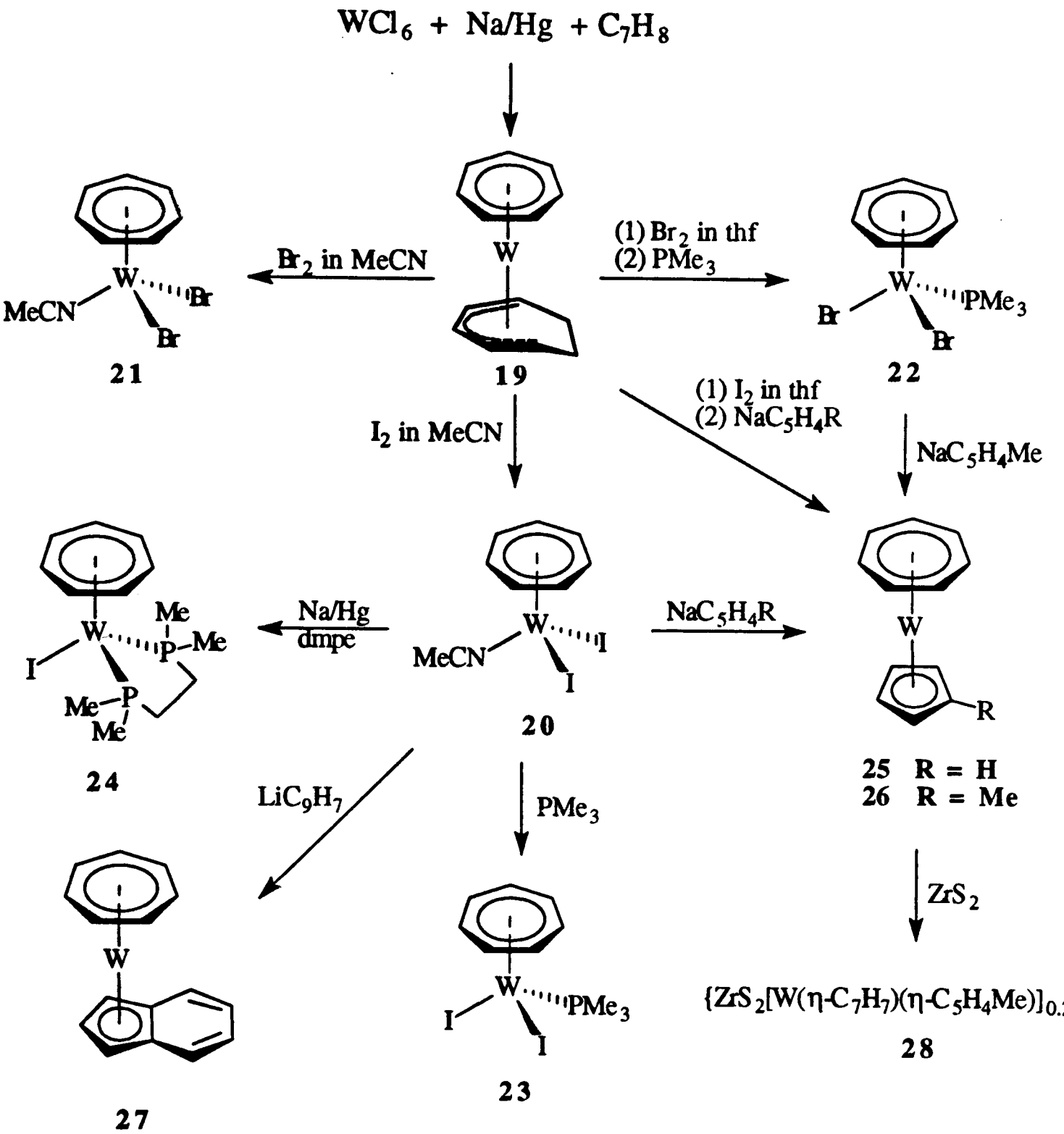

21 19 22

20

24 23 27

28

Scheme 3.9

3.10 References

1 R. B. king and A. Fronzaglia, *Inorg. Chem.*, 1966, **5**, 1837.

2 E. M. van Dam, W. N. Brend, M. P. Silvon and P. S. Skell, *J. Am. Chem. Soc.*, 1975, **97**, 465.

3 H. W. Wehner, E. O. Fisher and J. Müller, *Chem. Ber.*, 1970, **103**, 2258.

4 M. L. H. Green, P. A. Newman and J. A. Bandy, *J. Chem. Soc., Dalton Trans.*, 1989, 331.

5 H. Spiesecke and W. G. Schneider, *Tetrahedron Lett.*, 1961, 468.

6 C. J. Groenenboom, G. Sawatzky, H. J. de Liefde Meijer and F. Jellinek, *J. Organomet. Chem.*, 1974, **76**, C4.

7 J. M. Sichel and M. A. Whitehead, *Theor. Chim. Acta (Berlin)*, 1966, **5**, 35.

8 C. J. Groenenboom and F. Jellinek, *J. Organomet. Chem.*, 1974, **80**, 229.

9 G. Erker, R. Nolte, R. Aul, S. Wilker, C. Krüger and R. Noe, *J. Am. Chem. Soc.*, 1991, **113**, 7594 and references therein.

10 K. J. Ivin, D. T. Laverty and J. J. Rooney, *Makromol. Chem.*, 1977, **178**, 1545.

11 (a) K. J. Ivin, D. T. Laverty and J. J. Rooney, *Makromol. Chem.*, 1978, **179**, 253; (b) K. J. Ivin, *Olefin Metathesis*, Academic Press, London, 1983, ch. 11.

12 J. D. Zeinstra and J. L. de Boer, *J. Organomet. Chem.*, 1973, **54**, 207.

13 G. Engebretson and R. E. Rundle, *J. Am. Chem. Soc.*, 1963, **85**, 481.

14 Cited in : C. J. Groenenboom, H. J. de Liefde Meijer and F. Jellinek, *J. Organomet. Chem.*, 1974, **69**, 235.

15 S. Evans, J. C. Green, S. E. Jackson and B. Higginson, *J. Chem. Soc., Dalton Trans.*, 1974, 304.

16 (a) N. Kaltsoyannis, D. Phil. Thesis, University of Oxford, 1992; (b) C. J. Groenenboom, H. J. de Liefde Meijer, F. Jellinek and A. Oskam, *J. Organomet. Chem.*, 1975, **97**, 73.

17 J. S. Griffith, *The Theory of Transition-Metal Ions*, Cambridge University Press, Cambridge, 1961.

18 F. G. N. Cloke, A. N. Dix, J. C. Green, R. N. Perutz and E. A. Seddon, *Organometallics*, 1983, **2**, 1150.

19 W. B. Davies, M. L. H. Green and A. J. Jacobson, *J. Chem. Soc., Chem. Commun.*, 1976, 781.

CHAPTER FOUR

One Dimensional Antiferromagnetic Cycloheptatrienyl-Molybdenum and -Tungsten Compounds

4.1 Introduction

One-dimensional magnetic systems continue to excite the interest of experimentalists and theorists. This is partly due to the fact that they provide simple models for more complex magnetic materials, and partly because certain physical phenomena are unique to low-dimensional magnets. Although classical inorganic co-ordination compounds with a linear chain structure have been known and studied extensively,[1] organometallic compounds, in particular of the early transition metals have received much less attention.[2] During the course of exploration of η-cycloheptatrienyl-molybdenum and -tungsten chemistry, it was found that the 17-electron compounds [M(η-C_7H_7)LX_2] (M = Mo, L = MeCN, X = I, **6**; M = Mo, L = PMe_3, X = I, **7**; M = W, L = MeCN, X = I, **20**; M = W, L = PMe_3, X = I, **23**; M = W, L = PMe_3, X = Br, **22**) behaved as one-dimensional antiferromagnets. This chapter describes the magnetic studies on these compounds.

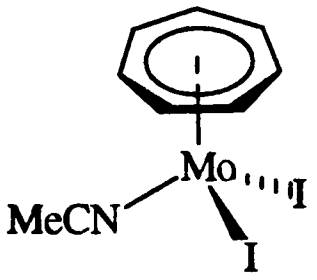

6

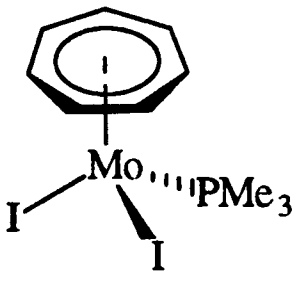

7

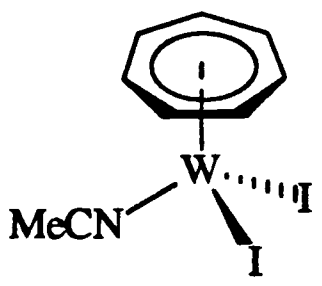

20

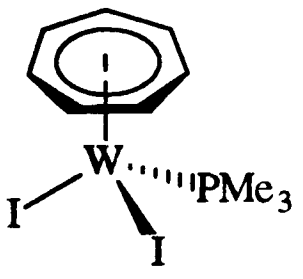

23

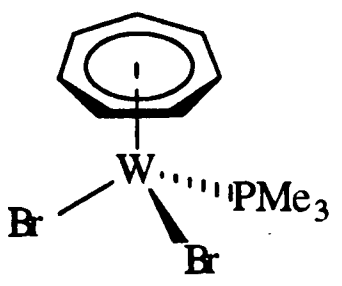

22

4.2 Magnetic Properties of $[Mo(\eta\text{-}C_7H_7)(MeCN)I_2]$

The molar magnetic susceptibility of $[Mo(\eta\text{-}C_7H_7)(MeCN)I_2]$ **6** has been measured in the temperature range 2-300 K using a SQUID magnetometer. The data collected at 1.0 T are displayed in Fig. 4.1. The maximum at 16 K in the χ_M *vs.* T plot provides strong evidence for antiferromagnetic exchange interactions. The susceptibility falls to 0.15 χ_{max} at 3 K. On further cooling below 3 K the susceptibility rises which may be due to the presence of traces of paramagnetic impurities or to parasitic ferromagnetism. As shown in the $1/\chi_M$ *vs.* T plot, the compound **6** obeys the Curie-Weiss law [$\chi_M = C/(T-\theta)$] with a Curie constant C = 0.29 emu-K mol^{-1} and a Weiss constant θ = -5.2 K at higher temperatures (50-300 K). The negative Weiss constant suggests the presence of significant antiferromagnetic interactions. The effective magnetic moment μ_{eff} was calculated with the formula : $\chi = N\mu_{eff}^2/3kT$ and the temperature dependence is shown in Fig. 4.2. At higher temperatures, μ_{eff} has a steady value of *ca.* 1.53 μ_B which is lower than the value of 1.75 calculated on the basis of the spin-only formula : $\mu_{eff}^2 = g^2[S(S+1)]$ where g is taken from the EPR data. Changing the magnetic field from 1.0 T to 0.2 T does not produce a significant change in the magnetic susceptibility data.

The crystal structure of compound **6** has been determined which provides insight into the exchange mechanism. The molecular structure of **6** has been reported in chapter two. This compound crystallises in the triclinic crystal system with space group $P\bar{1}$. As shown in Fig. 4.3 the crystal structure consists of chains of molecules. The shortest inter-molecular distance within a chain is 3.670 Å and occurs between I_1 and C_5 of the $\eta\text{-}C_7H_7$ ring. This distance is shorter than the sum of van der Waals radii of carbon and iodine (4.00 Å). The neighbouring chains are arranged antiparallel to each other as shown in Fig. 4.3(a) and 4.3(d). The distance between the centroids of cycloheptatrienyl rings of adjacent molecules is 3.710 Å, which is close to the inter-layer distance of graphite (3.35 Å). In short, the structure may be described as a chain of dimers incorporated in a ladder-like structure while the pairs of molecules called "dimer" are depicted in Fig. 4.3(a) as A_2-B_1, A_3-B_2 etc..

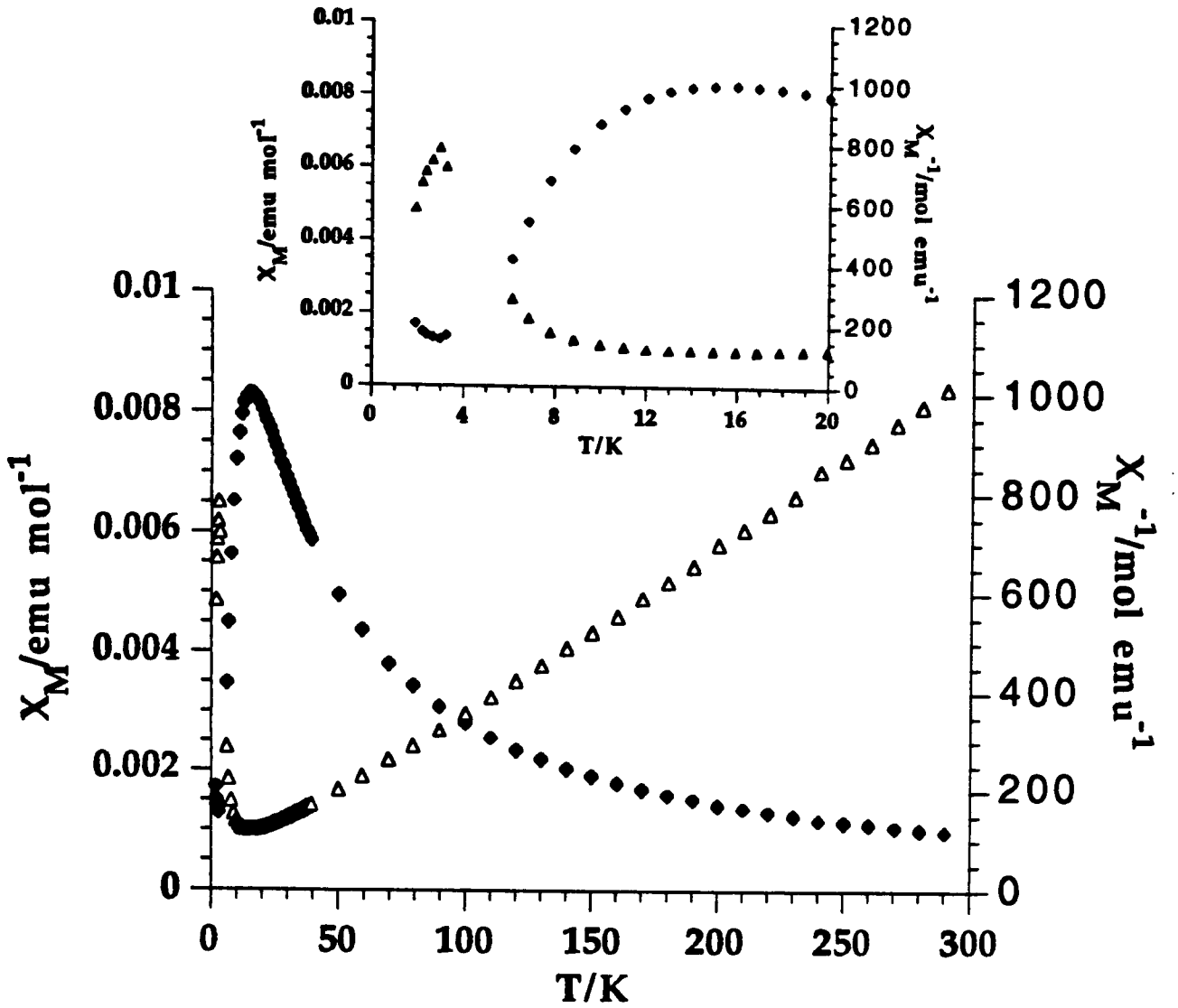

Fig. 4.1 Plots of χ_M (◆) and $1/\chi_M$ (Δ) *vs.* T for [Mo(η-C_7H_7)(MeCN)I_2] **6**. The inset shows the expansion at low-temperature region

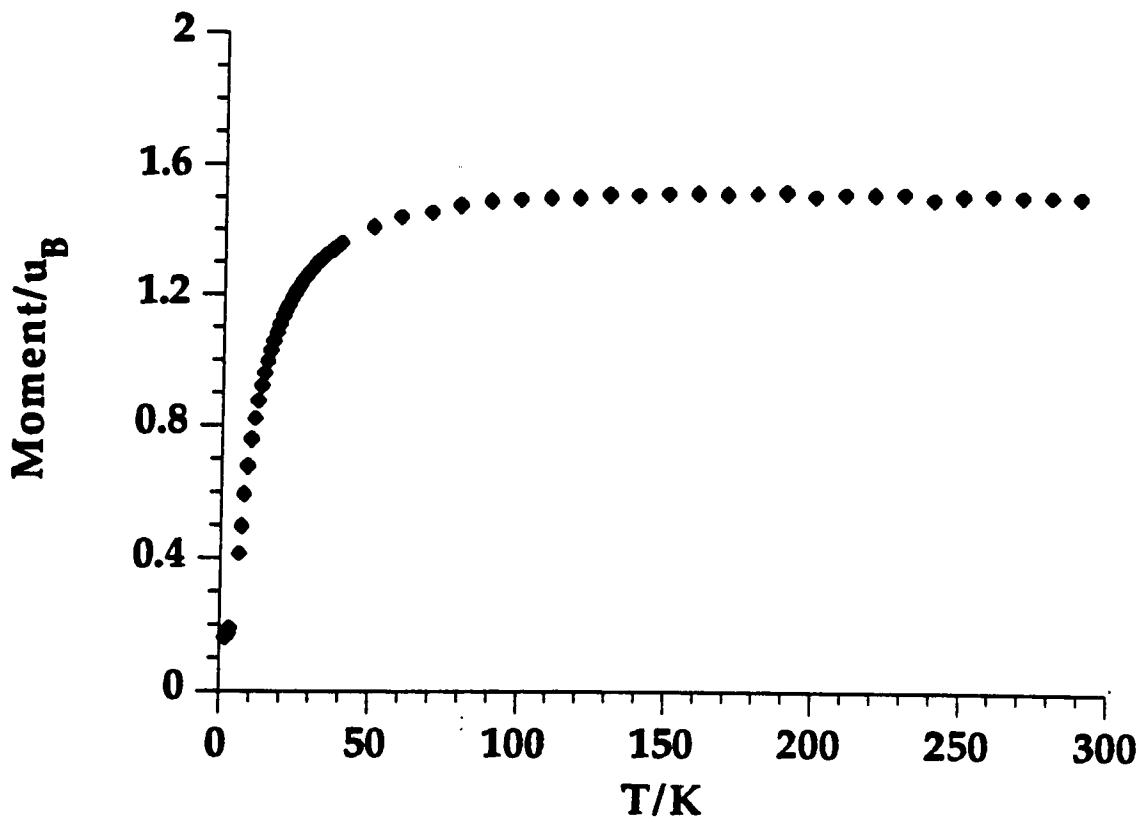

Fig. 4.2 Plot of μ_{eff} *vs.* T for [Mo(η-C_7H_7)(MeCN)I_2] **6**

Fig. 4.3(a)

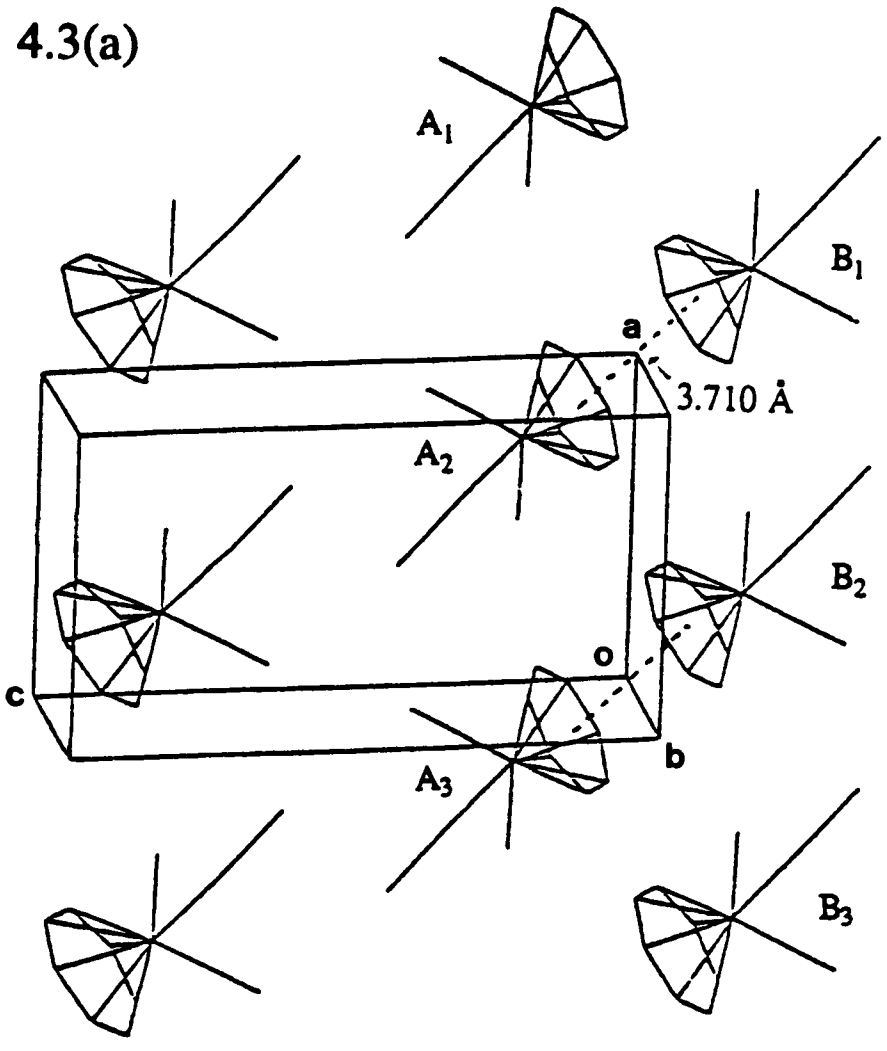

Fig. 4.3(d)

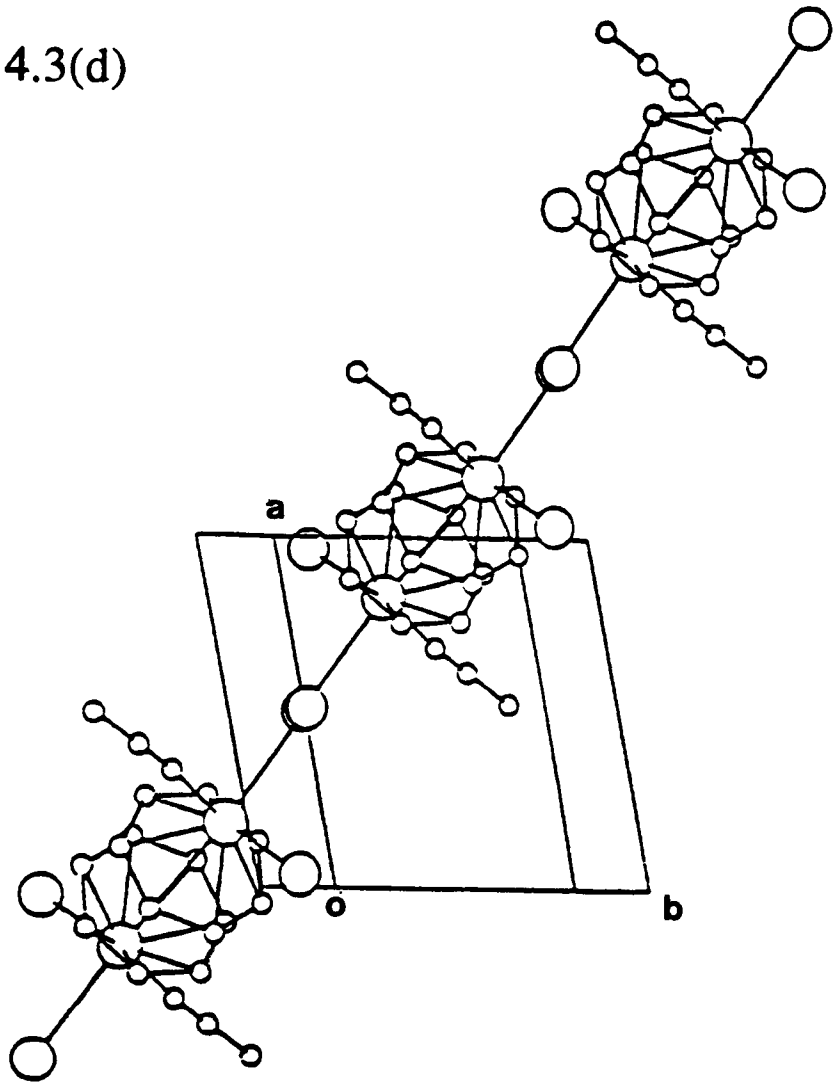

Fig. 4.3(b)

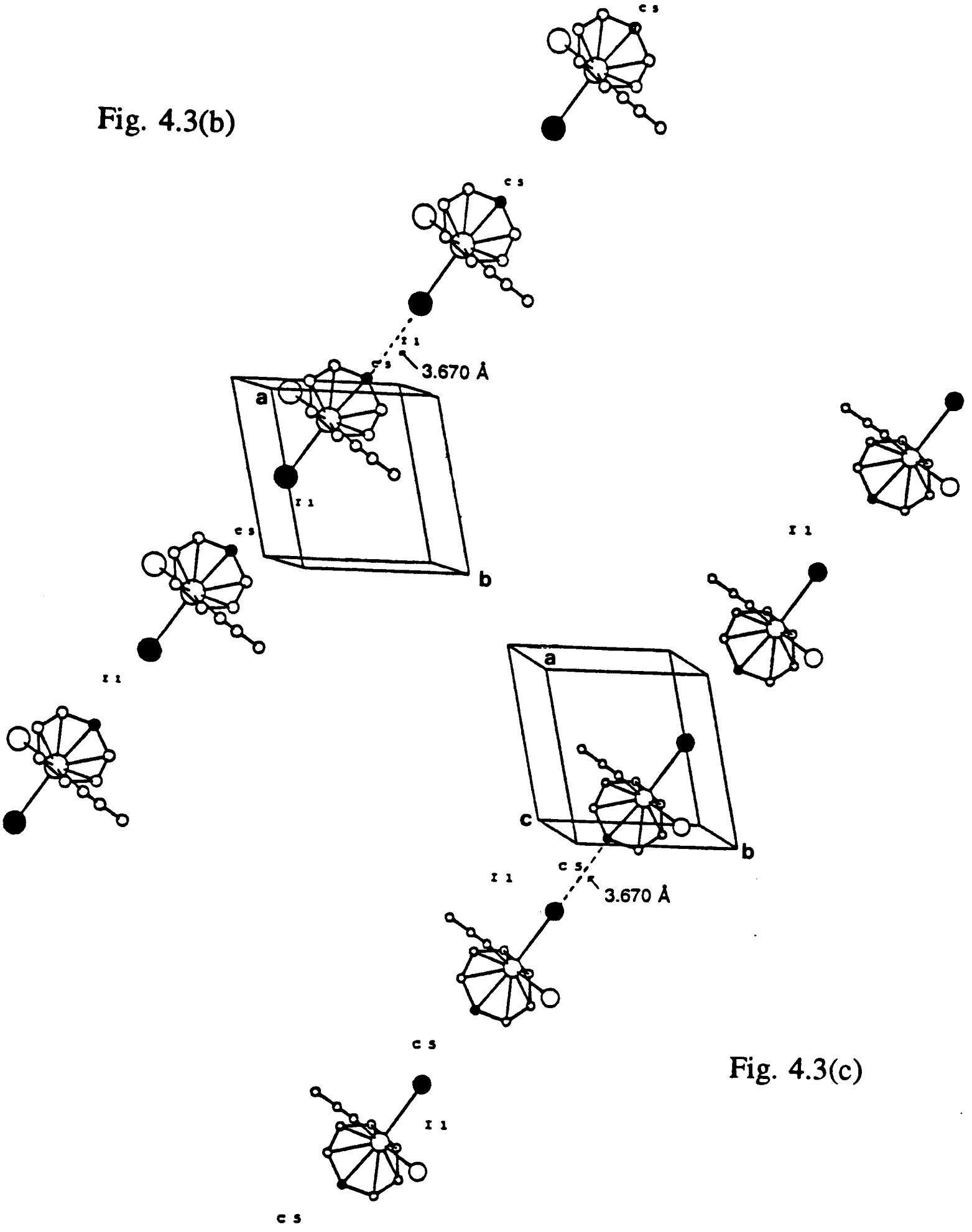

Fig. 4.3(c)

Fig. 4.3 Crystal structure of [Mo(η-C_7H_7)(MeCN)I_2] **6**. (a) View along the *b* axis (b) View of molecules A_x along the *c* axis (c) View of molecules B_x along the *c* axis (d) View along the *c* axis

In the light of the structure of [Mo(η-C_7H_7)(MeCN)I_2] **6**, it is envisaged that magnetic interactions may occur along the chains of iodine-bridged molybdenum centres through the super-exchange mechanism. Interactions within the dimers of molecules [Fig. 4.3(a)] through the η-cycloheptatrienyl rings which face each other may also be significant.

The magnetic data of compounds **6** has been analysed by curve-fitting using different magnetic models. Attempts to fit the data to the Bleaney-Bowers expression,[3] which assumes exchange to be significant only within dimers, were not successful. However, close fit was obtained for **6** by using the modified Bleaney-Bowers equation[3] for an exchange-coupled pair of S = 1/2 ions (eq. 1). The term θ in eq. 1 was included to account for interactions between the dimers. However, the best-fit of eq. 1 to the data yielded θ = -10.5 K and J = -8.9 K which was not acceptable since the correction term |θ| was greater than the primary interaction parameter |J|.

$$\chi_M = \left[\frac{Ng^2\mu_B^2}{3k(T-\theta)}\right]\left[1+\left(\frac{1}{3}\right)\exp\left(\frac{-2J}{kT}\right)\right]^{-1} \qquad \text{(eq. 1)}$$

It was found that the susceptibility data of compound **6** could be described by one-dimensional chain models. Thus good fit was obtained for **6** by using the Bonner-Fisher analysis for a uniformly spaced antiferromagnetic Heisenberg linear chain of S = 1/2 (eq. 2).[4] Fig. 4.4 shows the best-fit based on eq. 2. The values of g and J were calculated to be 1.84 and -8.9 K respectively from the least-squares fit.

$$\chi_M = \left(\frac{Ng^2\mu_B^2}{kT}\right)\left(\frac{0.25+0.14995\,x+0.030094\,x^2}{1.0+1.9862\,x+0.68854\,x^2+6.0626\,x^3}\right) \text{ where } x = \frac{|J|}{kT} \qquad \text{(eq. 2)}$$

In an attempt to account for the interchain interactions, a molecular field correction term was included in eq. 2 (eq. 3),[4b] where χ_{corr} is the corrected magnetic susceptibility, χ_{iso} is the susceptibility of an isolated Heisenberg chain of S = 1/2 ions, z is the number of nearest neighbours in adjacent chains, and J' is the interchain exchange parameter. Although excellent fit was obtained for compound **6** with this coupled-chain model, the fit was not acceptable since the correction term $|zJ'| = 12.0$ K was greater than the primary interaction term $|J| = 9.0$ K.

$$\chi_{corr} = \frac{\chi_{iso}}{\left[1 - \left(\frac{2zJ'\chi_{iso}}{Ng^2\mu_B^2}\right)\right]} \qquad \text{(eq. 3)}$$

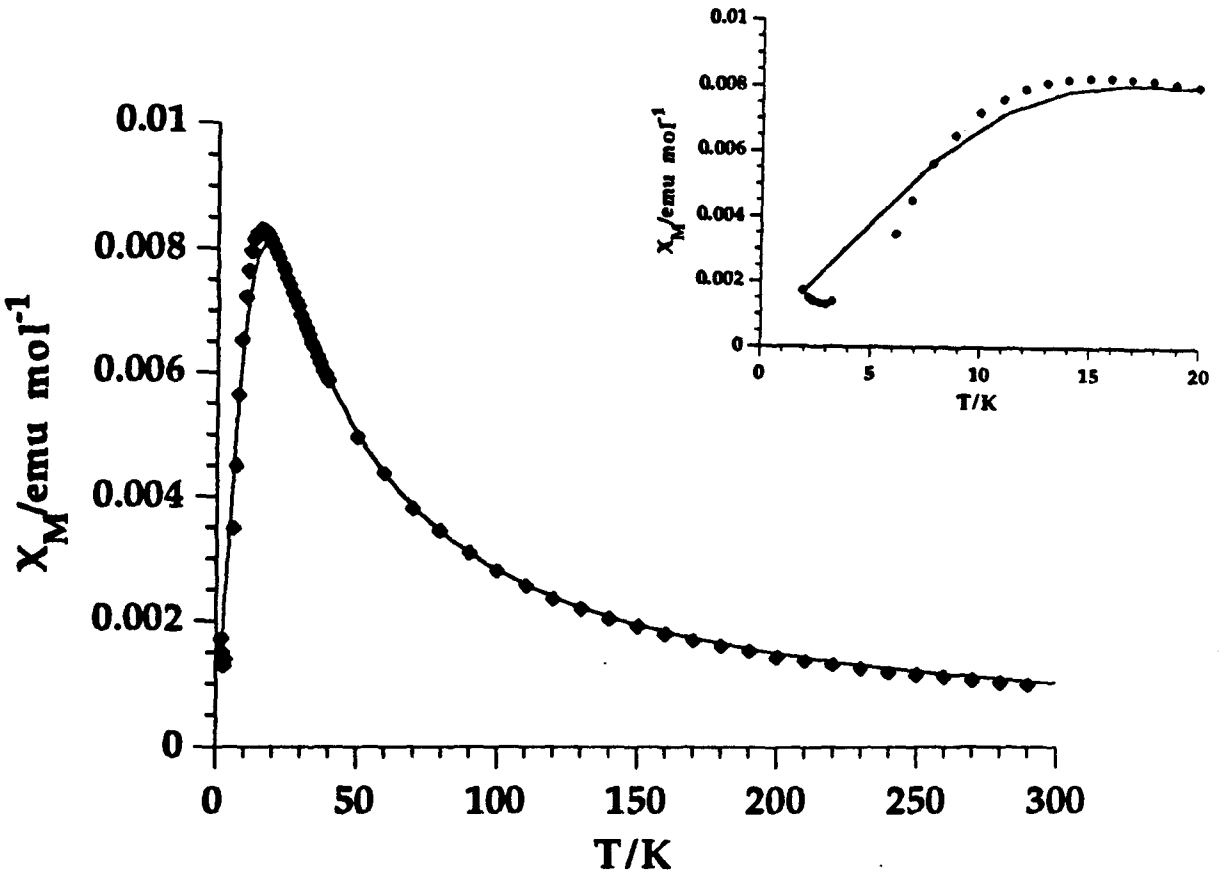

Fig. 4.4 Plot of χ_M *vs.* T for [Mo(η-C_7H_7)(MeCN)I_2] **6**. The solid line is the best-fit generated by eq. 2 for the 1D-Heisenberg model. The inset shows the expansion at low-temperature region

A one-dimensional Ising model can also be used to describe the magnetic behaviour of compound **6**. The corresponding expression for S = 1/2 is shown in eq. 4.[5] Fig. 4.5 shows the calculated curve closely corresponds to the experimental data. The best-fit gives the values of g = 1.92 and J = -15.6 K.

$$\chi_M = \frac{1}{3}\chi_{\parallel} + \frac{2}{3}\chi_{\perp}$$

where $$\chi_{\parallel} = \left(\frac{Ng_{\parallel}^2\mu_B^2}{4kT}\right)\exp\left(\frac{J}{kT}\right)$$

$$\chi_{\perp} = \left(\frac{Ng_{\perp}^2\mu_B^2}{4J}\right)\left[\tanh\left(\frac{J}{2kT}\right) + \left(\frac{J}{2kT}\right)\mathrm{sech}^2\left(\frac{J}{2kT}\right)\right] \qquad \text{(eq. 4)}$$

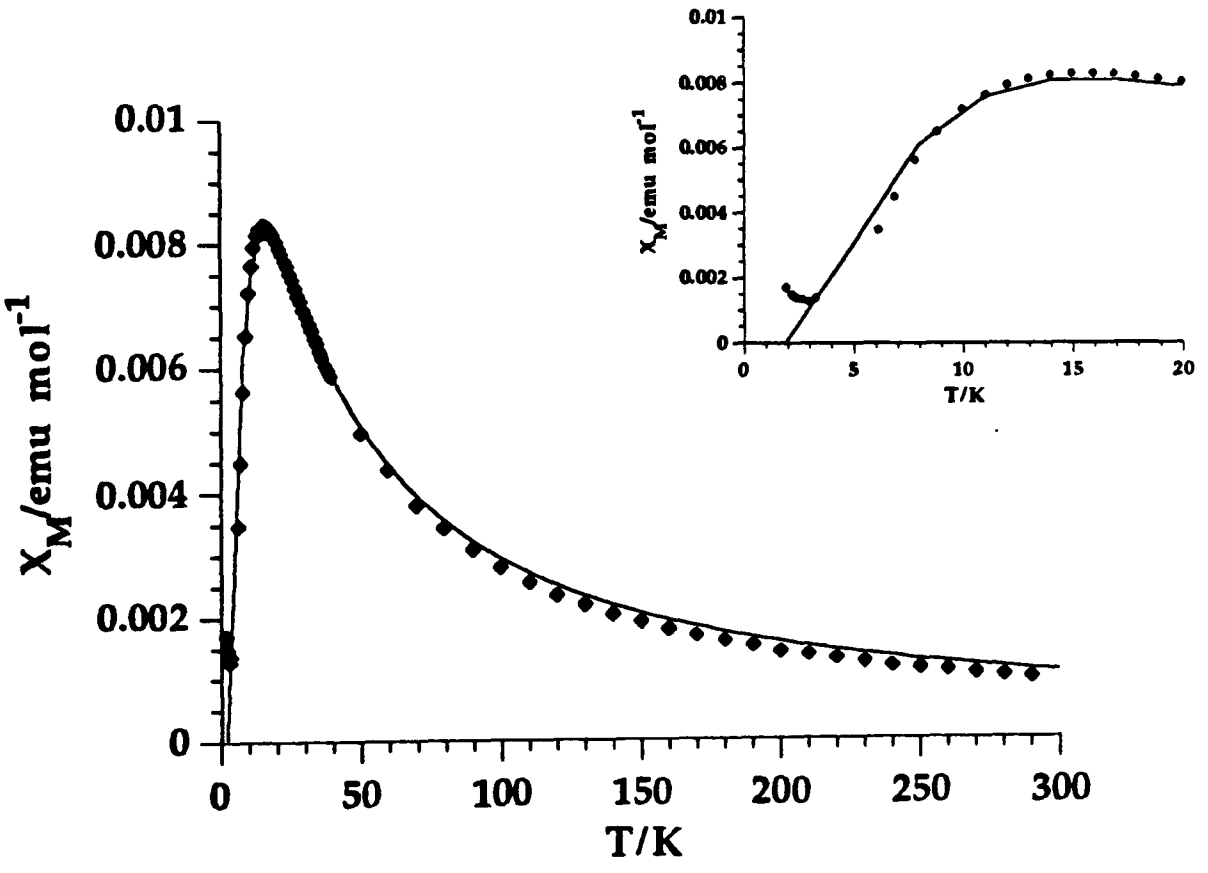

Fig. 4.5 Plot of χ_M *vs.* T for [Mo(η-C_7H_7)(MeCN)I_2] **6**. The solid line is the best-fit generated by eq. 4 for the 1D-Ising model. The inset shows the expansion at low-temperature region

4.3 Magnetic Properties of [Mo(η-C_7H_7)(PMe_3)I_2]

The magnetic susceptibility of [Mo(η-C_7H_7)(PMe_3)I_2] **7** has been measured in the temperature range 6-230 K at 0.2 T. The temperature dependences of the molar magnetic susceptibility χ_M and $1/\chi_M$ are shown in Fig. 4.6. The susceptibility rises to a maximum at 12 K indicating the presence of antiferromagnetic interactions. At higher temperatures (45-230 K) the compound **7** obeys the Curie-Weiss law [$\chi_M = C/(T-\theta)$] with a Curie constant C = 0.26 emu-K mol^{-1} and a Weiss constant θ = -2.6 K. The negative Weiss constant also provides evidence for antiferromagnetic coupling. The effective magnetic moment μ_{eff} is plotted as a function of temperature in Fig. 4.7. The μ_{eff} value of compound **7** at higher temperatures has a steady value of *ca.* 1.43 μ_B and decreases with decreasing temperature.

The magnetic analyses have been carried out using different magnetic models. Attempts to describe the susceptibility data of compound **7** using the Bleaney-Bowers equation[3] failed for any reasonable set of parameters. Although close fit was generated by using the modified Bleaney-Bowers expression for an exchange-coupled pair of S = 1/2 ions (eq. 1),[3] the result was not acceptable since the best-fit parameters |θ| (14.2 K) was greater then |J| (5.6 K), *i.e.* the correction term |θ| was greater than the primary interaction parameter |J|.

However, the susceptibility data can be fitted by one-dimensional models. As shown by the solid line in Fig. 4.8, the data can be well reproduced by the Bonner-Fisher results for a uniformly spaced antiferromagnetic Heisenberg linear chain of S = 1/2 ions (eq. 2)[4] using the magnetic parameters g = 1.67 and J = -6.9 K. Allowance for magnetic interchain interactions was made through the use of the molecular field correction given in eq. 3.[4b] In this case, good fit was obtained which yielded g = 1.80, J = -6.4 K and zJ' = -15.2 K. However, this fit was not acceptable since the correction term was again greater than the primary interaction parameter. Fig. 4.9 shows the calculated curve based on one-dimensional Ising model for S = 1/2 (eq. 4).[5] The best-fitting parameters g (1.75) and J (-12.2 K) were obtained from this simulation.

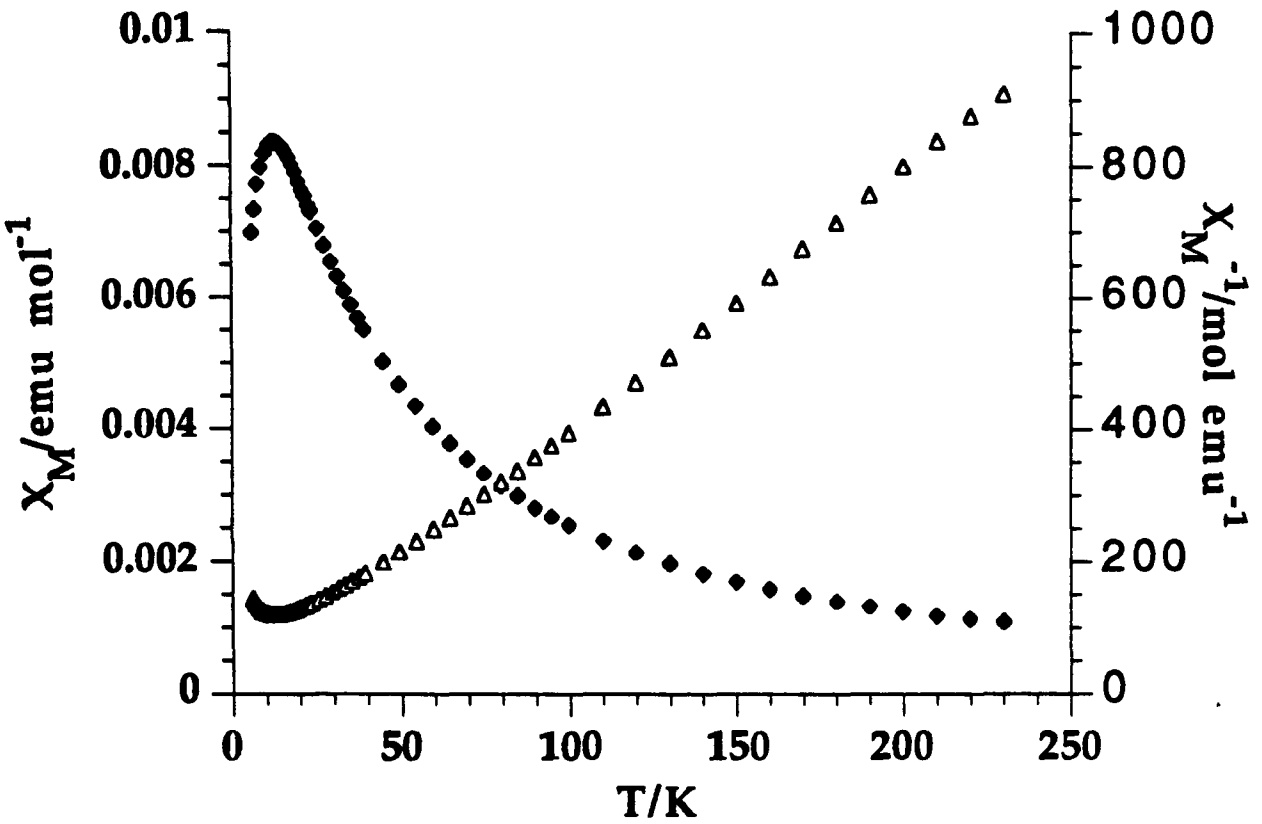

Fig. 4.6 Plots of χ_M (◆) and $1/\chi_M$ (Δ) *vs.* T for [Mo(η-C_7H_7)(PMe_3)I_2] **7**

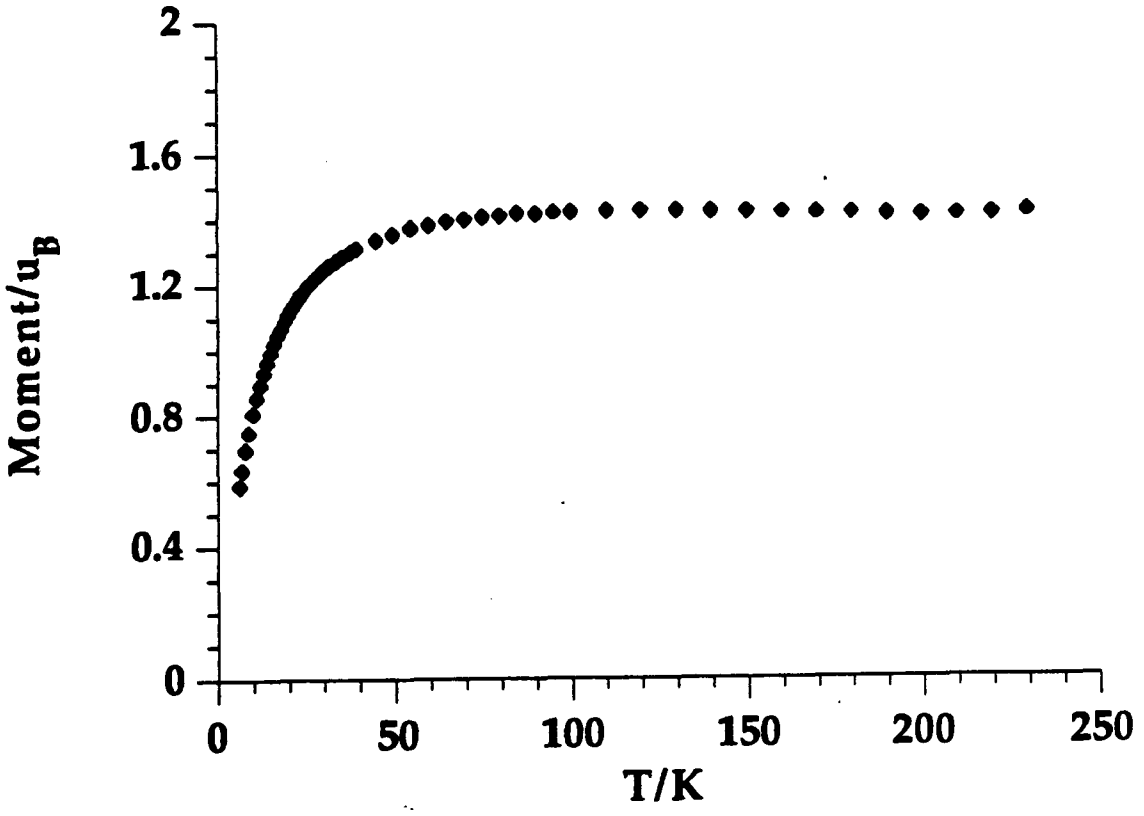

Fig. 4.7 Plot of μ_{eff} *vs.* T for [Mo(η-C_7H_7)(PMe_3)I_2] **7**

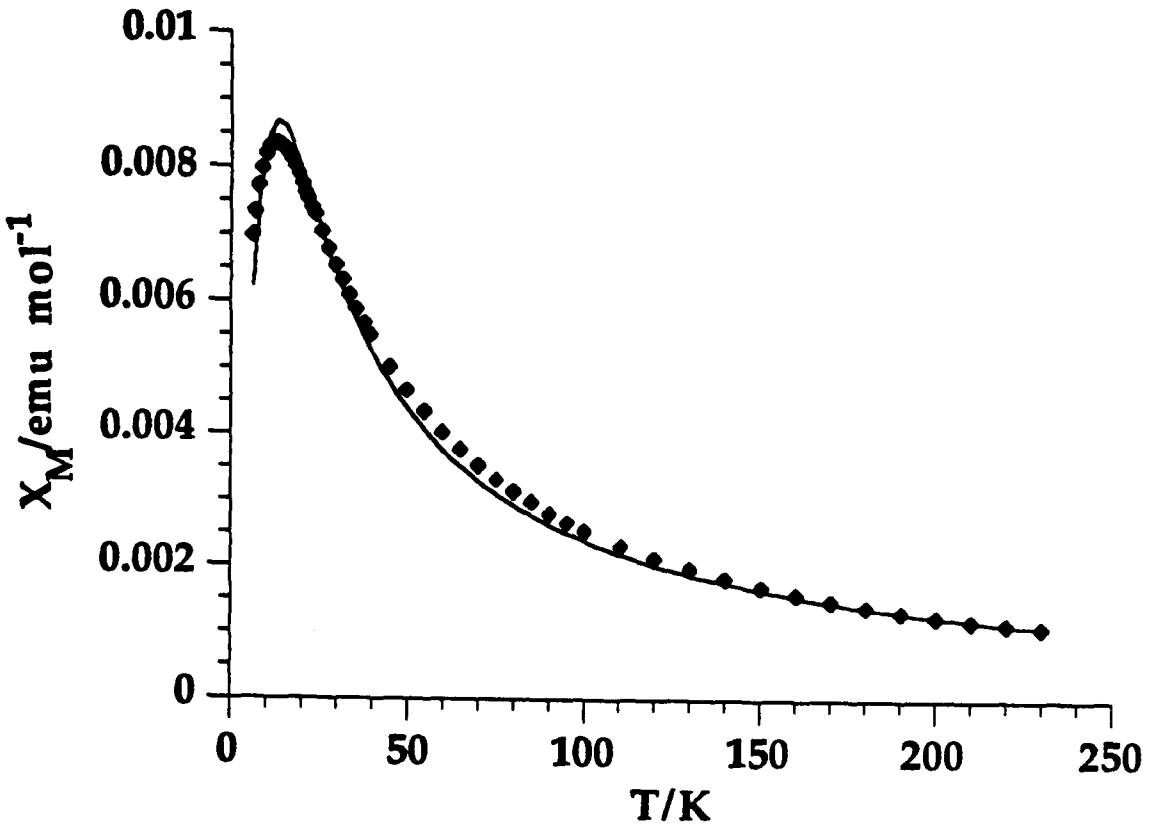

Fig. 4.8 Plot of χ_M *vs.* T for [Mo(η-C_7H_7)(PMe_3)I_2] **7**. The solid line is the best-fit generated by eq. 2 for the 1D-Heisenberg model

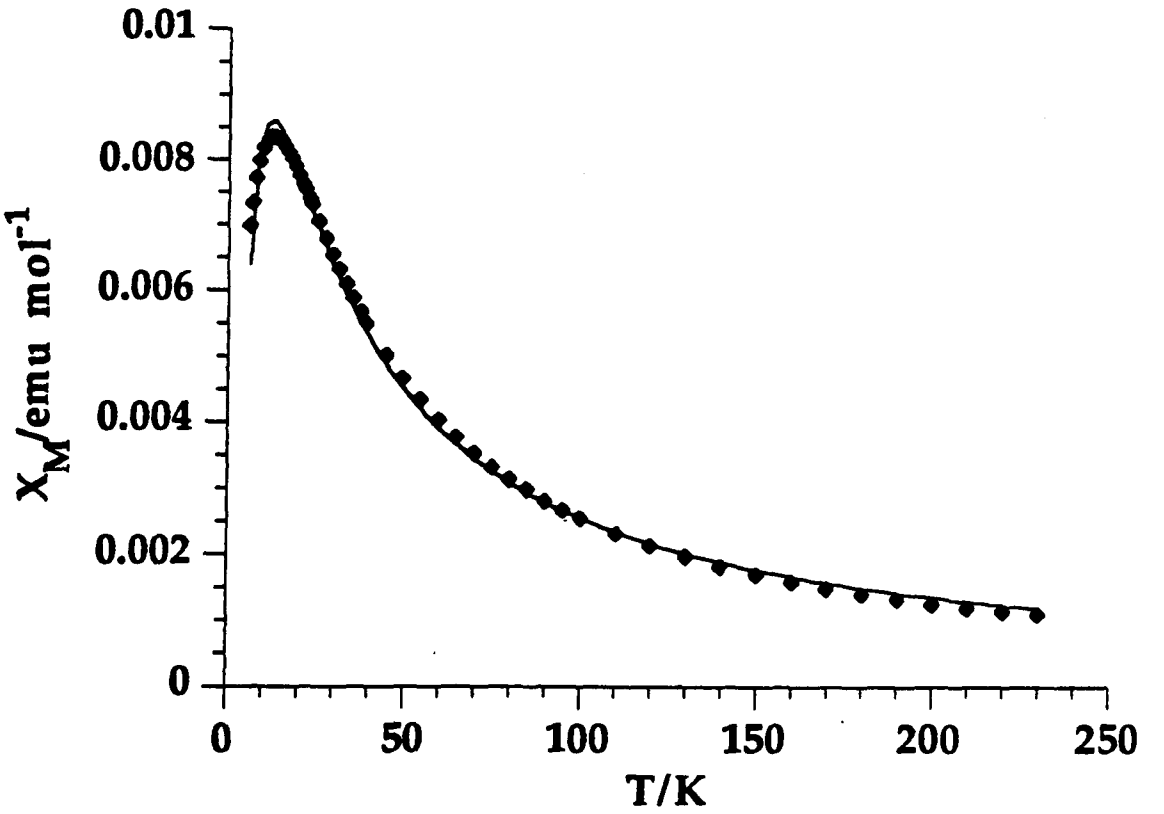

Fig. 4.9 Plot of χ_M *vs.* T for [Mo(η-C_7H_7)(PMe_3)I_2] **7**. The solid line is the best-fit generated by eq. 4 for the 1D-Ising model

4.4 Magnetic Properties of $[W(\eta\text{-}C_7H_7)(MeCN)I_2]$

The magnetic susceptibility data of compound $[W(\eta\text{-}C_7H_7)(MeCN)I_2]$ **20** displayed in Fig. 4.10 have been collected in the temperature range 6-296 K at 0.2 T. It can be seen that the magnetic susceptibility data exhibit a maximum at 17 K that is indicative of antiferromagnetic interactions. As shown in Fig. 4.10, the $1/\chi_M$ *vs.* T plot gives concave curve with small curvature at *ca.* 40-296 K. It is not possible to find a satisfactory least-squares fit of the data using the Curie-Weiss expression. The effective magnetic moment μ_{eff} rises with increasing temperature and reaches a steady value of *ca.* 1.44 μ_B at room temperature (Fig. 4.11).

Attempts to fit the magnetic data by the isolated Heisenberg dimer model failed,[3] but excellent fit was obtained for the coupled dimer model described by eq. 1 with g = 1.84, θ = -22.7 K and J = -7.3 K.[3] However, the value of $|\theta|$ was greater than the value of |J| which led to the rejection of this fit. The magnetic data for compound **20** were analysed in terms of the one-dimensional Heisenberg model by using the numerical results of Hatfield and co-workers (eq. 2)[4b] with the parameters g = 1.72 and J = -10.5 K (Fig. 4.12). The inclusion of a molecular field correction term as shown in eq. 3,[4b] which accounts for the interchain interactions, also produced an excellent fit. However, the correction term |zJ'| (15.9 K) was again greater than the primary interaction term |J| (9.9 K). A one-dimensional Ising model[5] can also be used to described the magnetic behaviour of **20**. Fig. 4.13 shows the simulated curve based on eq. 4 closely corresponds to the experimental data. The least-squares fit parameters g and J were calculated to be 1.76 and -17.5 K respectively.

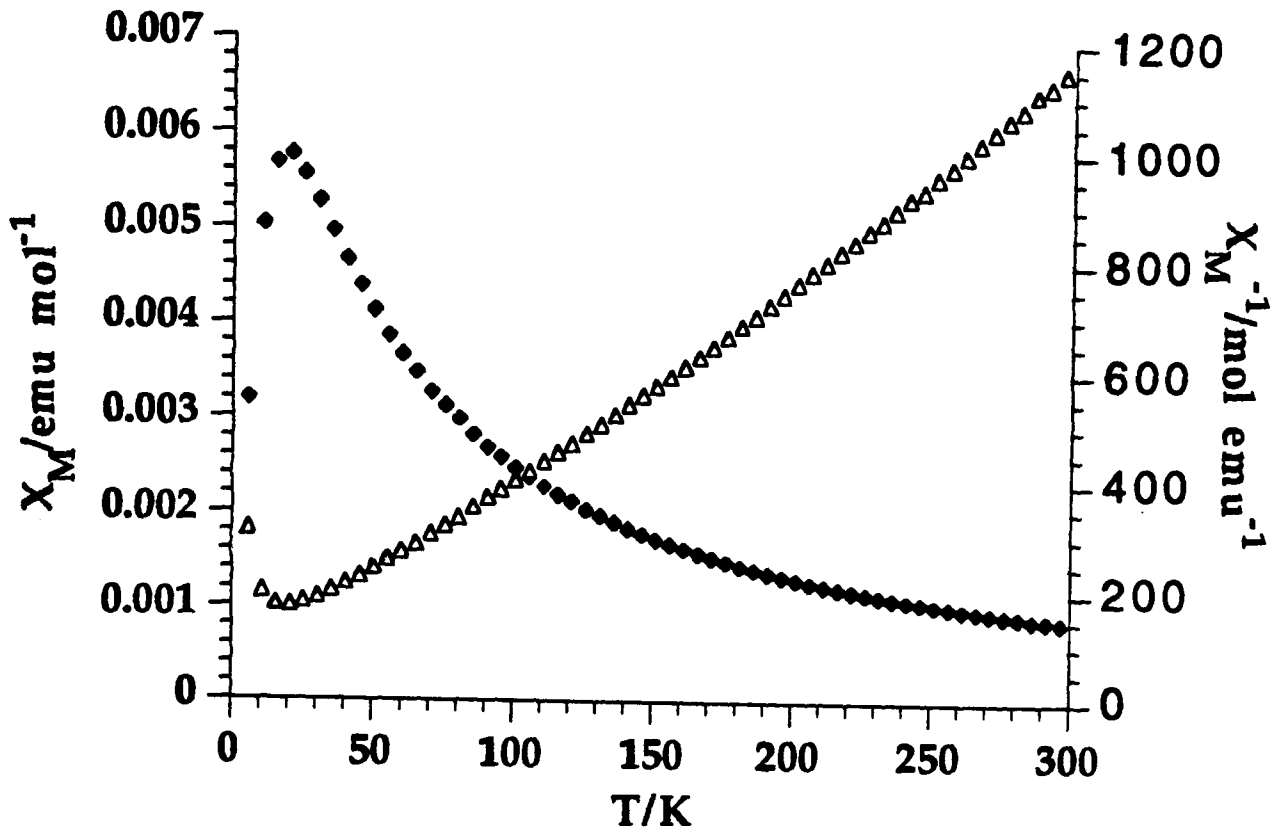

Fig. 4.10 Plots of χ_M (◆) and $1/\chi_M$ (Δ) *vs.* T for $[W(\eta\text{-}C_7H_7)(MeCN)I_2]$ **20**

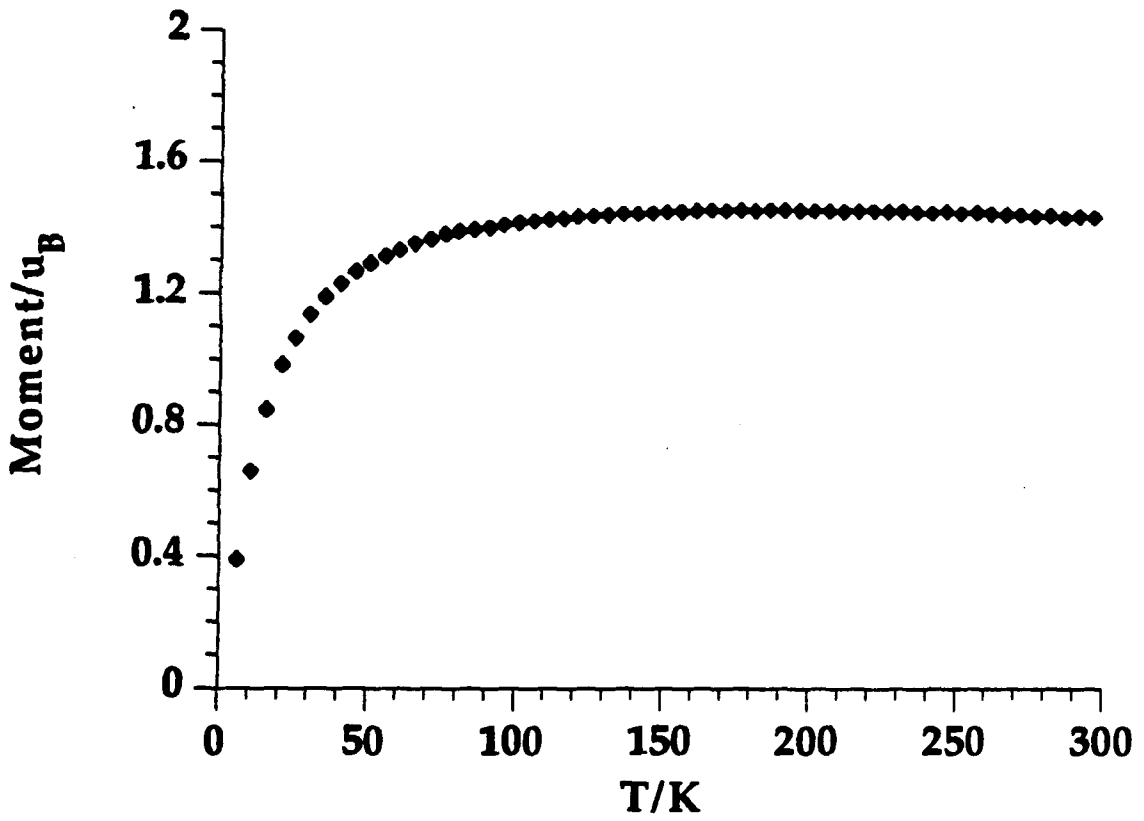

Fig. 4.11 Plot of μ_{eff} *vs.* T for $[W(\eta\text{-}C_7H_7)(MeCN)I_2]$ **20**

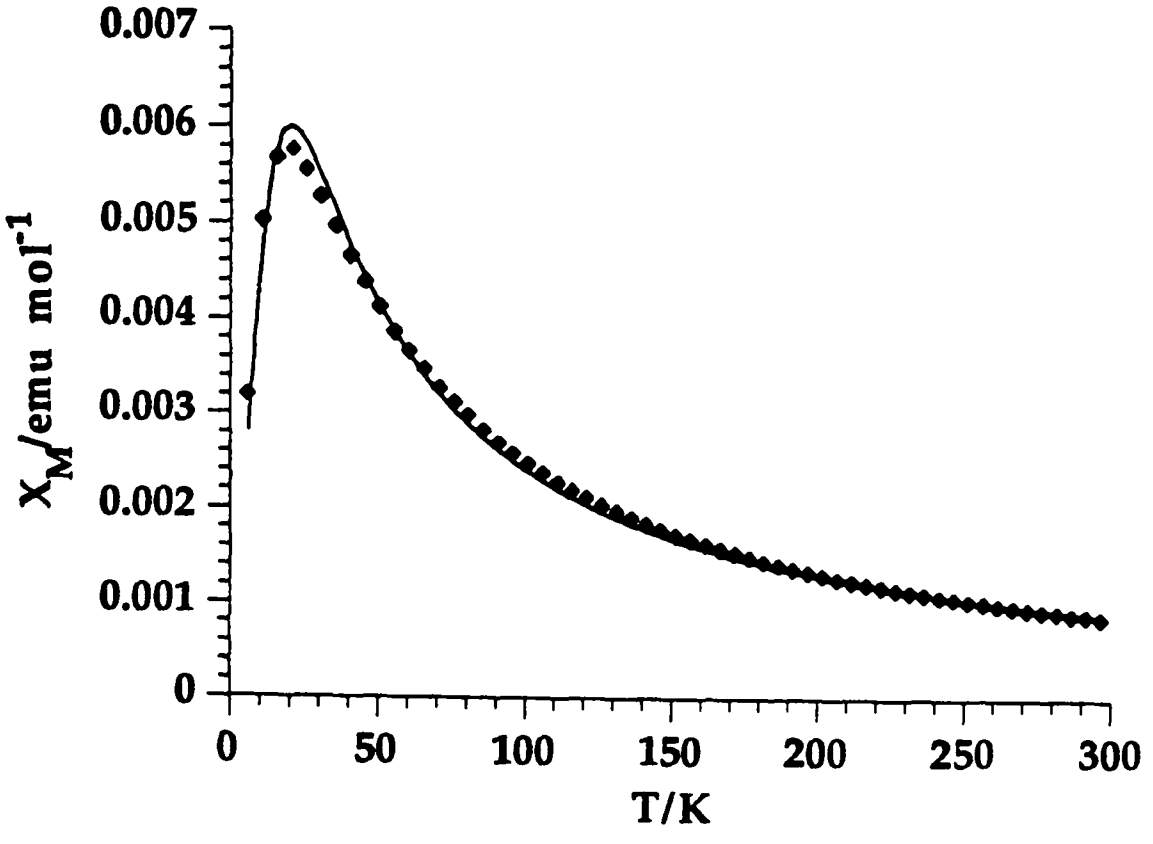

Fig. 4.12 Plot of χ_M *vs.* T for [W(η-C_7H_7)(MeCN)I_2] **20**. The solid line is the best-fit generated by eq. 2 for the 1D-Heisenberg model

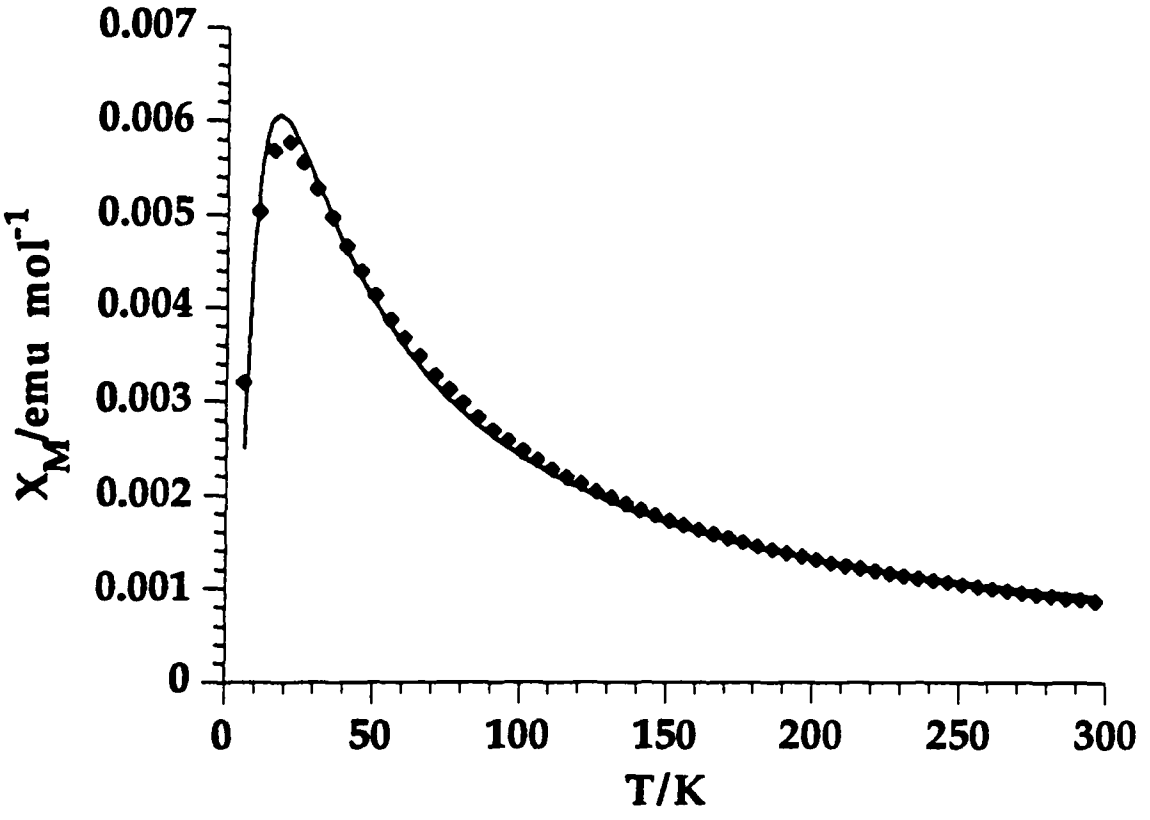

Fig. 4.13 Plot of χ_M *vs.* T for [W(η-C_7H_7)(MeCN)I_2] **20**. The solid line is the best-fit generated by eq. 4 for the 1D-Ising model

4.5 Magnetic Properties of $[W(\eta\text{-}C_7H_7)(PMe_3)I_2]$

The magnetic susceptibility of compound $[W(\eta\text{-}C_7H_7)(PMe_3)I_2]$ **23** has been measured in the temperature range 6-296 K at 0.2 T and is displayed in Fig. 4.14. The maximum at 13 K in the susceptibility curve provides evidence for antiferromagnetic interactions. The $1/\chi_M$ *vs.* T plot gives a concave curve with small curvature at *ca.* 40-296 K. It is not possible to find a satisfactory least-squares fit of the data using the Curie-Weiss expression. The effective magnetic moment μ_{eff} is plotted as a function of temperature in Fig. 4.15. The steady value of 1.50 μ_B at higher temperatures is lower than the value of 1.72 μ_B calculated on the basis of the spin-only formula.

Attempts to fit the data to the Bleaney-Bowers expression[3] were not successful. An excellent fit was obtained for **23** by using the modified Bleaney-Bowers equation[3] (eq. 1). However, the least-squares fit of eq. 1 to the data also yielded values of $|\theta| > |J|$ which were not acceptable.

It was found that the susceptibility data of **23** can be described by one-dimensional chain models. In Fig. 4.16, the curve through the data is based on the Bonner-Fisher result for a spin 1/2 Heisenberg linear chain (eq. 2).[4] The fit yields g =1.73 and J = -8.1 K. In an attempt to account for the interchain interactions, a molecular field correction term was included in eq. 2 (eq. 3).[4b] Although an excellent fit was obtained for compounds **23** with this coupled-chain model, the fit was not acceptable since the correction term $|zJ'|$ (21.8 K) was greater than the primary interaction term $|J|$ (7.2 K). The magnetic data for **23** was also analysed in terms of the one-dimensional Ising model (eq. 4)[5] (Fig. 4.17). The best-fit gives g = 1.78 and J = -13.8 K.

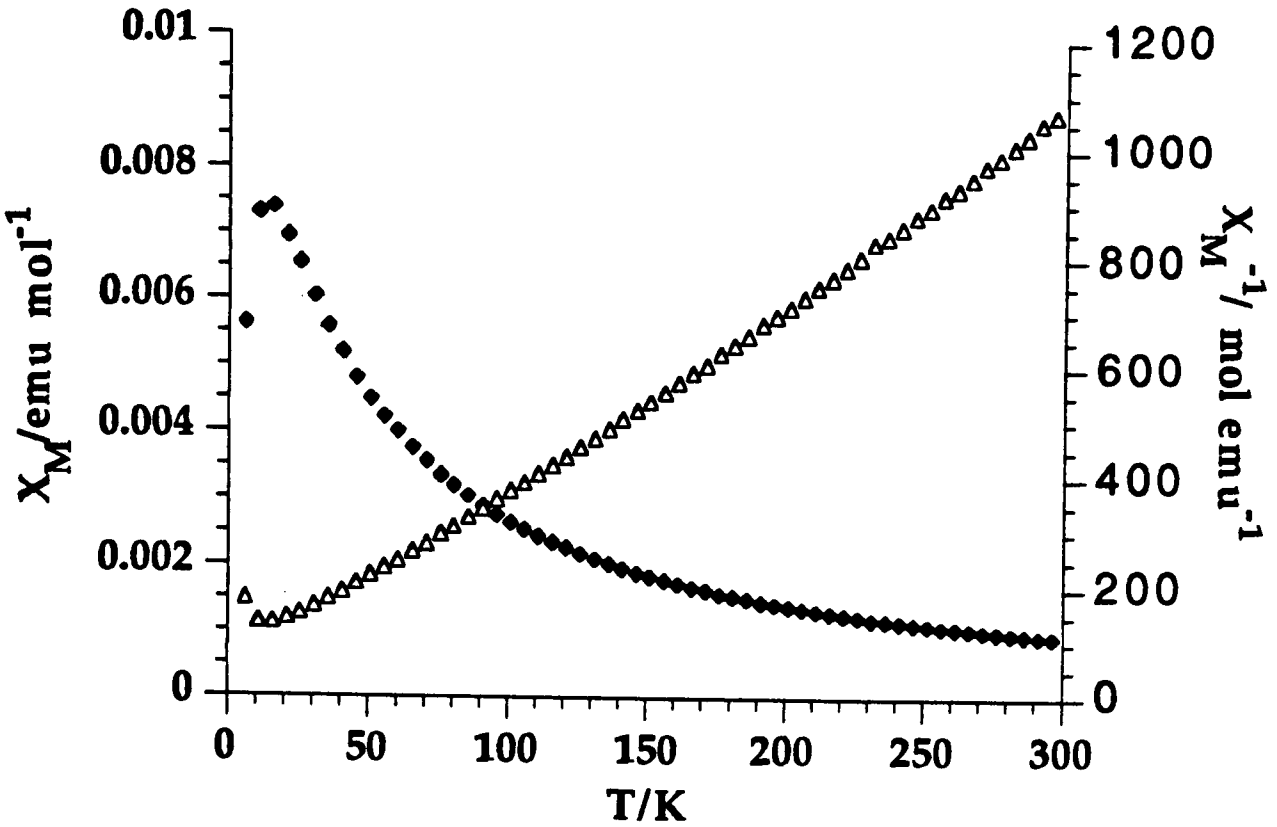

Fig. 4.14 Plots of χ_M (◆) and $1/\chi_M$ (Δ) *vs.* T for [W(η-C_7H_7)(PMe_3)I_2] **23**

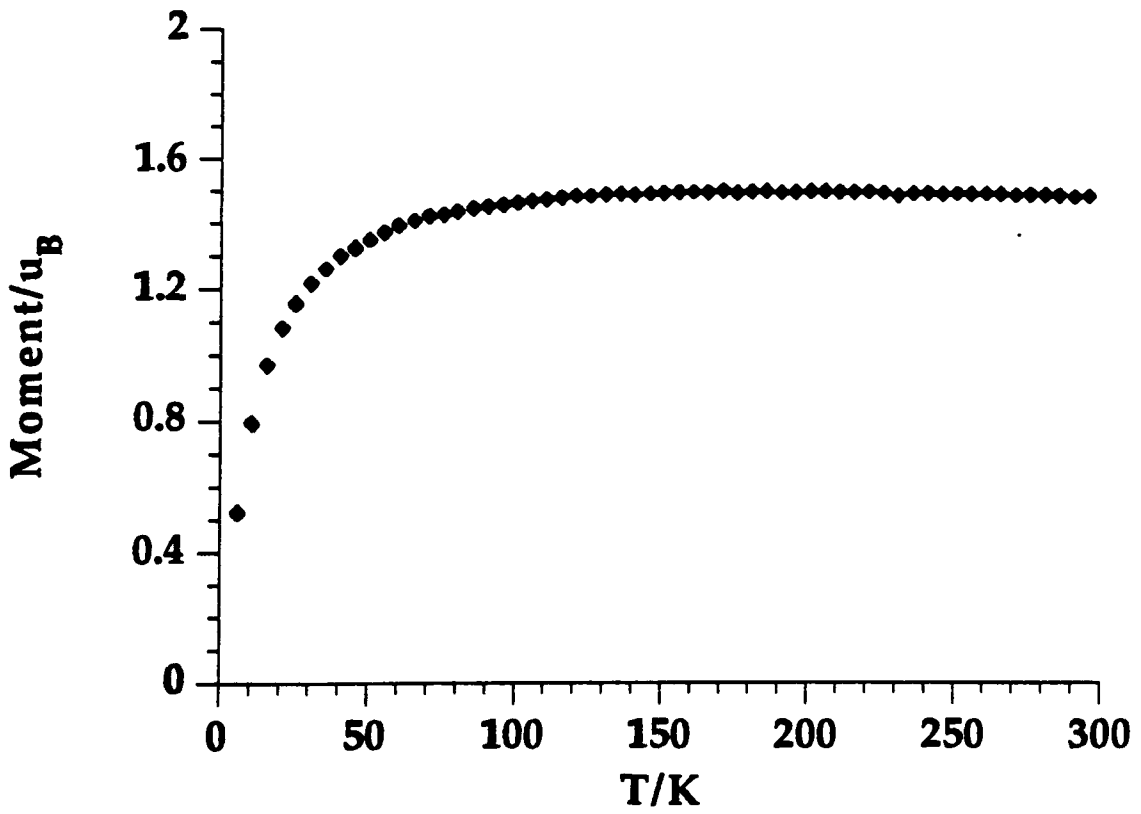

Fig. 4.15 Plot of μ_{eff} *vs.* T for [W(η-C_7H_7)(PMe_3)I_2] **23**

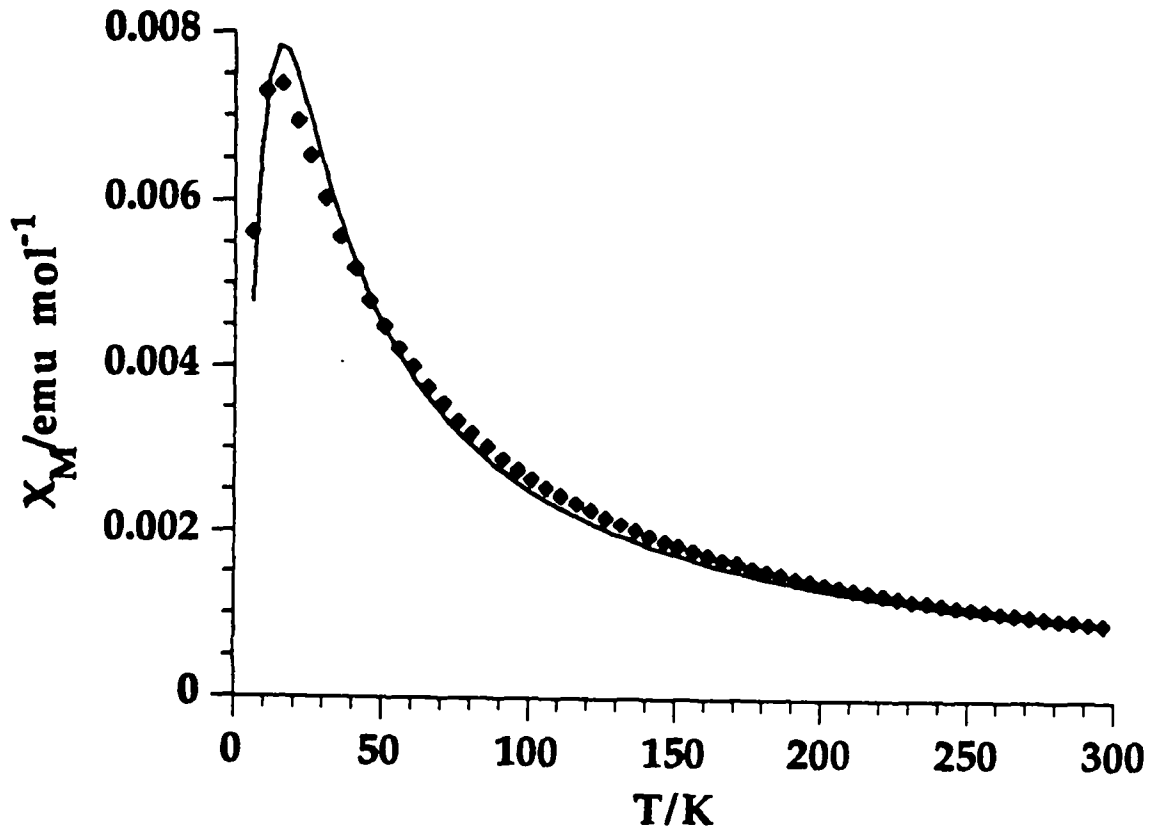

Fig. 4.16 Plot of χ_M *vs.* T for [W(η-C_7H_7)(PMe_3)I_2] **23**. The solid line is the best-fit generated by eq. 2 for the 1D-Heisenberg model

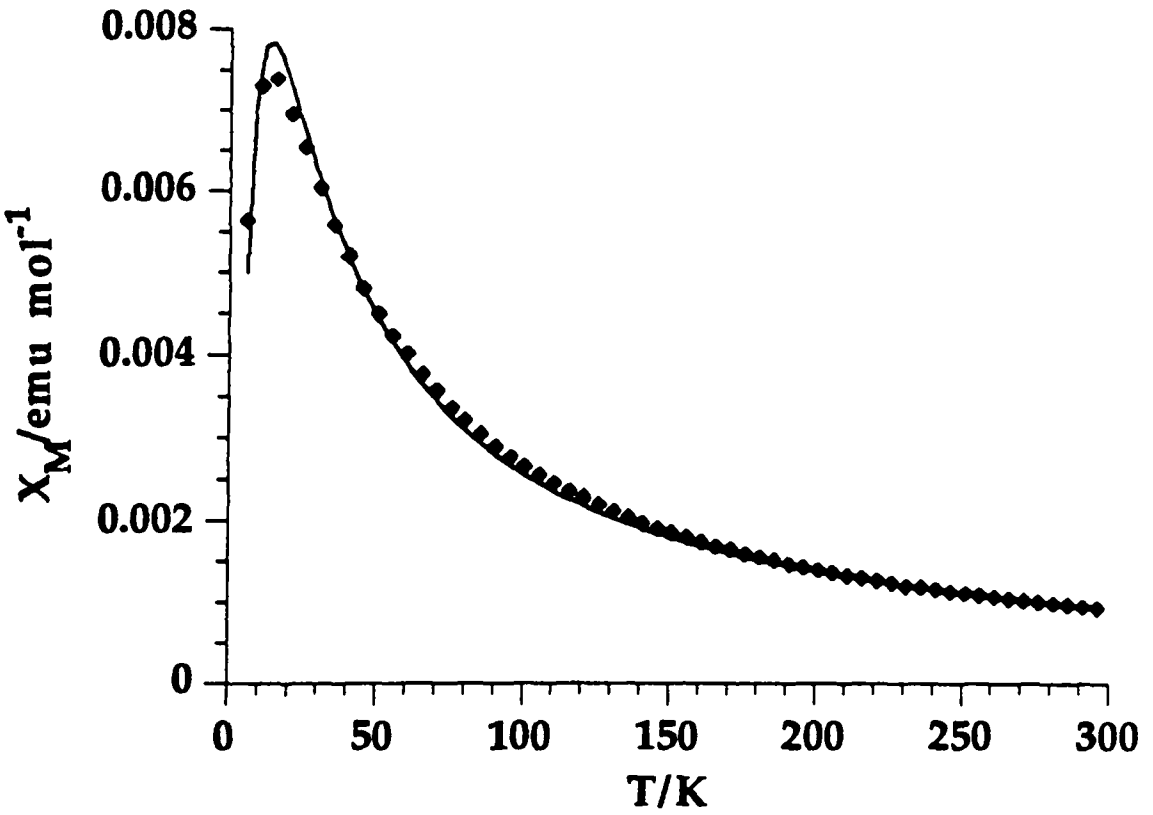

Fig. 4.17 Plot of χ_M *vs.* T for [W(η-C_7H_7)(PMe_3)I_2] **23**. The solid line is the best-fit generated by eq. 4 for the 1D-Ising model

4.6 Magnetic Properties of $[W(\eta\text{-}C_7H_7)(PMe_3)Br_2]$

The magnetic susceptibility of compound $[W(\eta\text{-}C_7H_7)(PMe_3)Br_2]$ **22** has been measured in the temperature range 6-296 K. However, at higher temperature (> 140 K at 0.2 T or > 95 K at 1 T), due to the limited amount of sample, the diamagnetic contribution arising from the bucket overcomes the paramagnetic contribution arising from the sample. Thus only the low-temperature data were used. Fig. 4.18 shows the χ_M *vs.* T and $1/\chi_M$ *vs.* T plots for **22** at 0.2 T. It can be seen that the magnetic susceptibility data display a maximum at 13 K which is indicative of antiferromagnetic interactions. The data above 45 K may be fitted by the Curie-Weiss law with a Curie constant C = 0.20 emu-K mol^{-1} and a Weiss constant θ = -3.6 K. The negative Weiss constant also suggests the presence of significant antiferromagnetic interactions. The temperature dependence of effective magnetic moment μ_{eff} of **22** is shown in Fig. 4.19. At higher temperatures, μ_{eff} has a steady value of *ca.* 1.27 μ_B which is lower than the value of 1.68 μ_B calculated on the basis of the spin-only formula.

The magnetic data has been analysed by curve-fitting using the dimer model and the couple dimer model as described previously.[3] The former model does not work for any reasonable set of parameters while the latter model works well with g = 1.60, θ = -10.0 K and J = -7.5 K. However, this fit is not acceptable since the correction term is greater than the primary interaction term.

An excellent fit was obtained by using the one-dimensional Heisenberg model (eq. 2)[4] with g = 1.53 and J = -7.4 K (Fig. 4.20). In an attempt to account for the interchain interactions, eq. 3[4b] was used and it was found that the magnetic data can be described by the curve with parameter g = 1.54, J = -7.4 K and zJ' = -1.3 K (Fig. 4.21). The data can also be fitted by using a one-dimensional Ising model.[5] Fig. 4.22 shows the best-fit generated with g = 1.61 and J = -13.4 K.

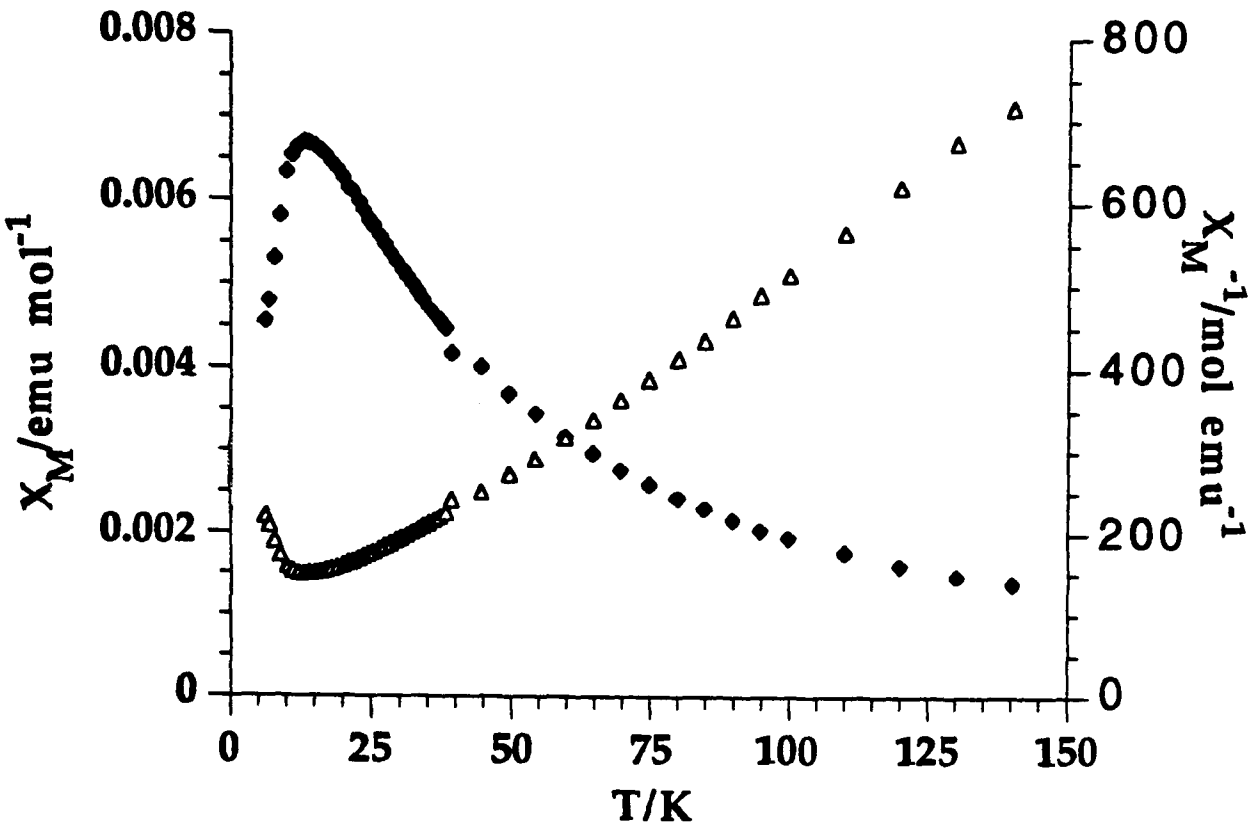

Fig. 4.18 Plots of χ_M (◆) and $1/\chi_M$ (Δ) *vs.* T for [W(η-C_7H_7)(PMe_3)Br_2] **22**

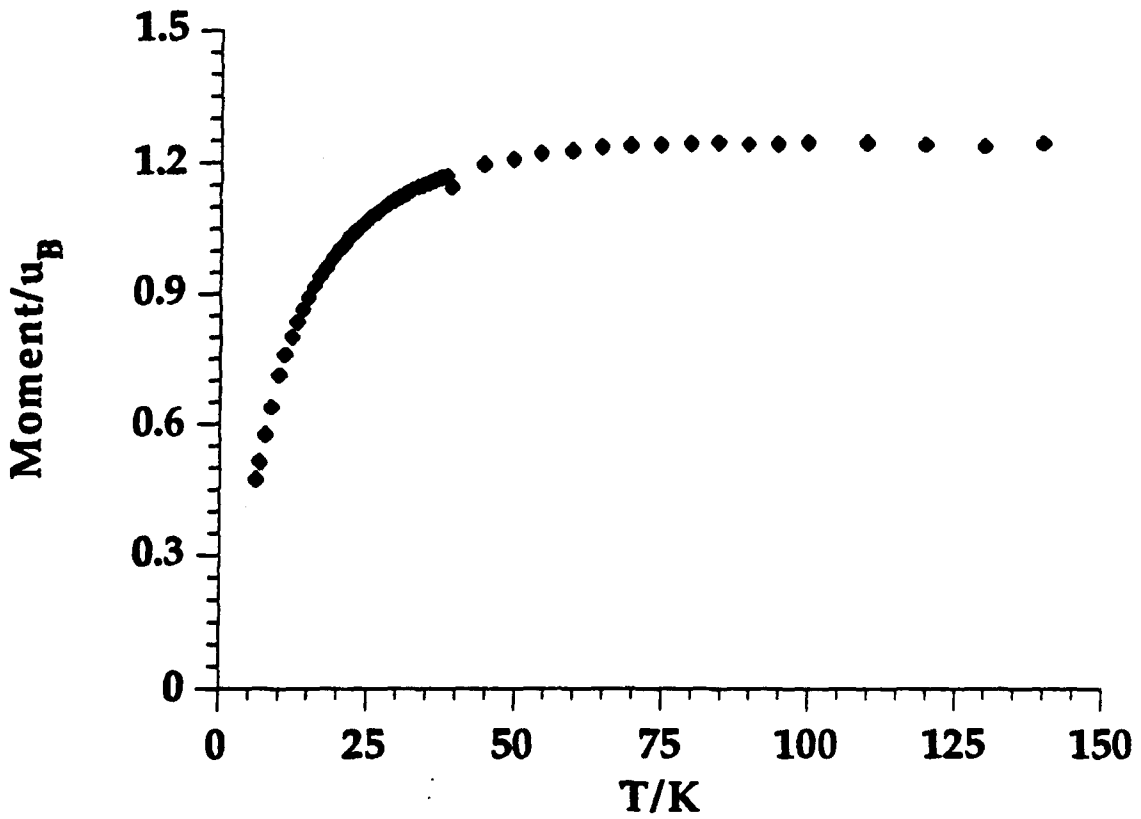

Fig. 4.19 Plot of μ_{eff} *vs.* T for [W(η-C_7H_7)(PMe_3)Br_2] **22**

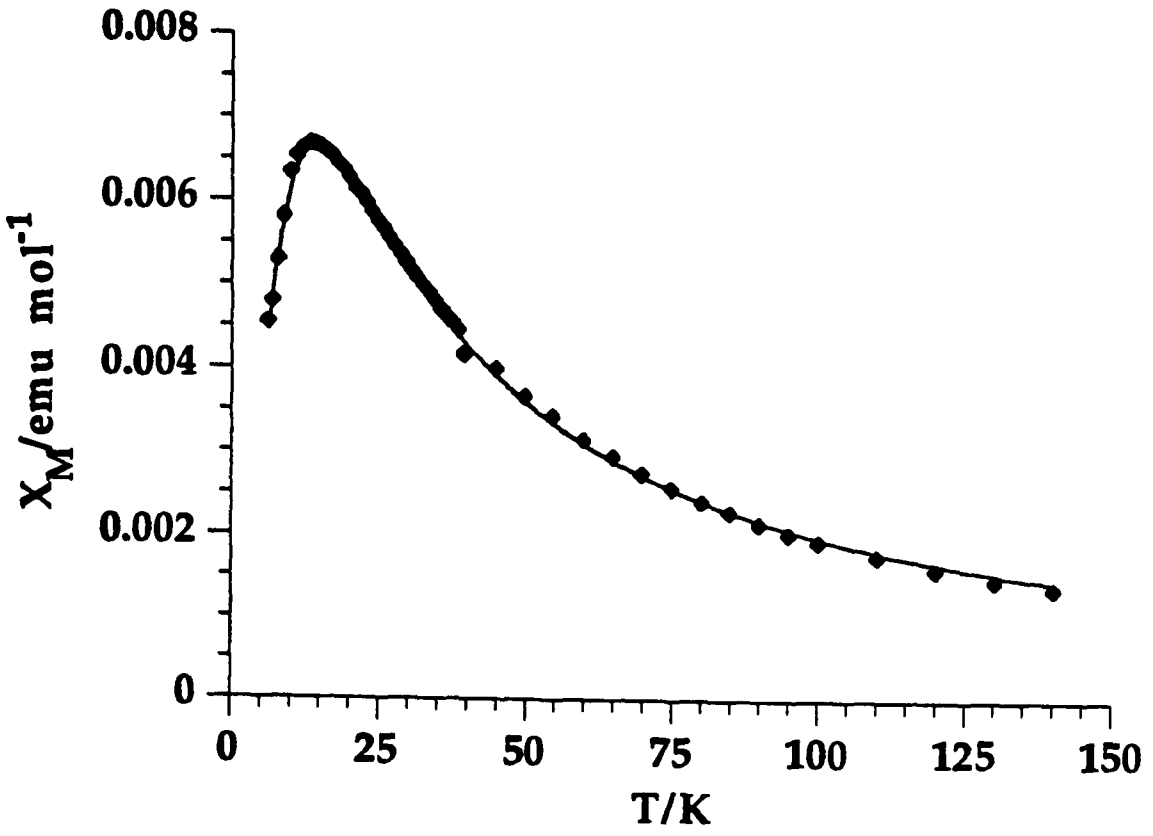

Fig. 4.20 Plot of χ_M *vs.* T for [W(η-C_7H_7)(PMe_3)Br_2] **22**. The solid line is the best-fit generated by eq. 2 for the 1D-Heisenberg model

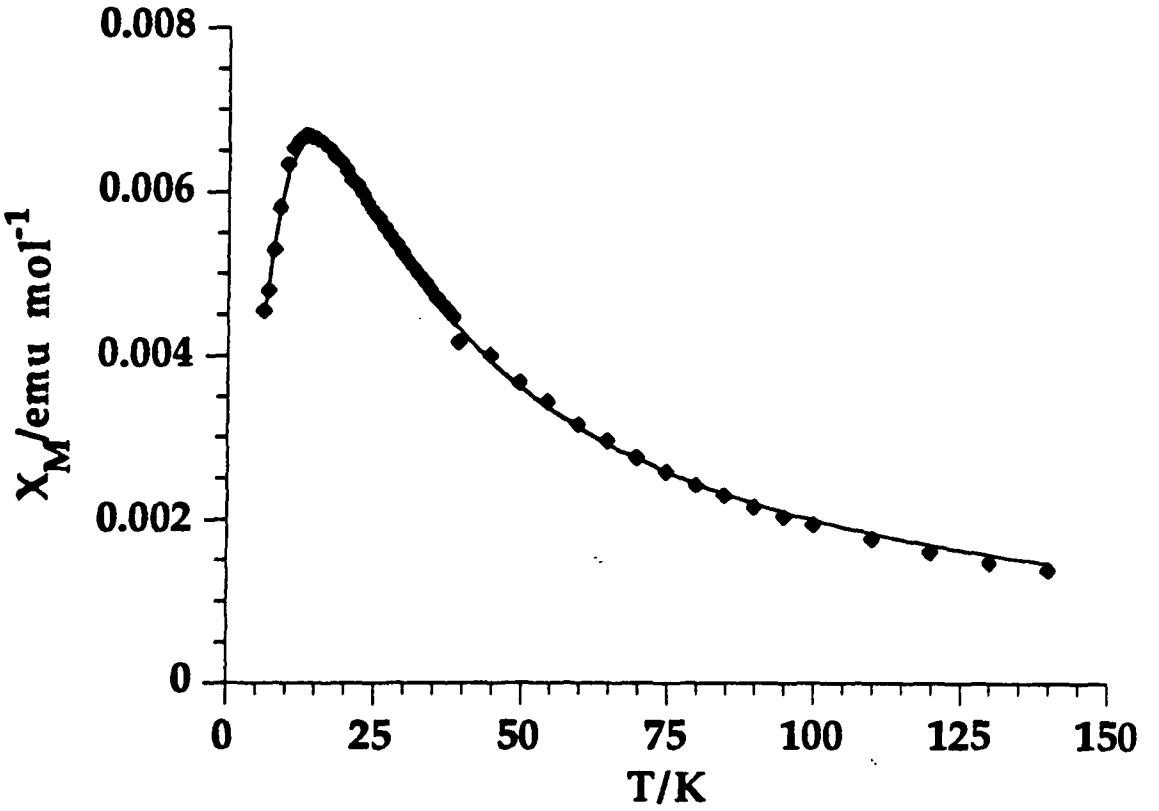

Fig. 4.21 Plot of χ_M *vs.* T for [W(η-C_7H_7)(PMe_3)Br_2] **22**. The solid line is the best-fit generated by eq. 3 for the coupled-chain model

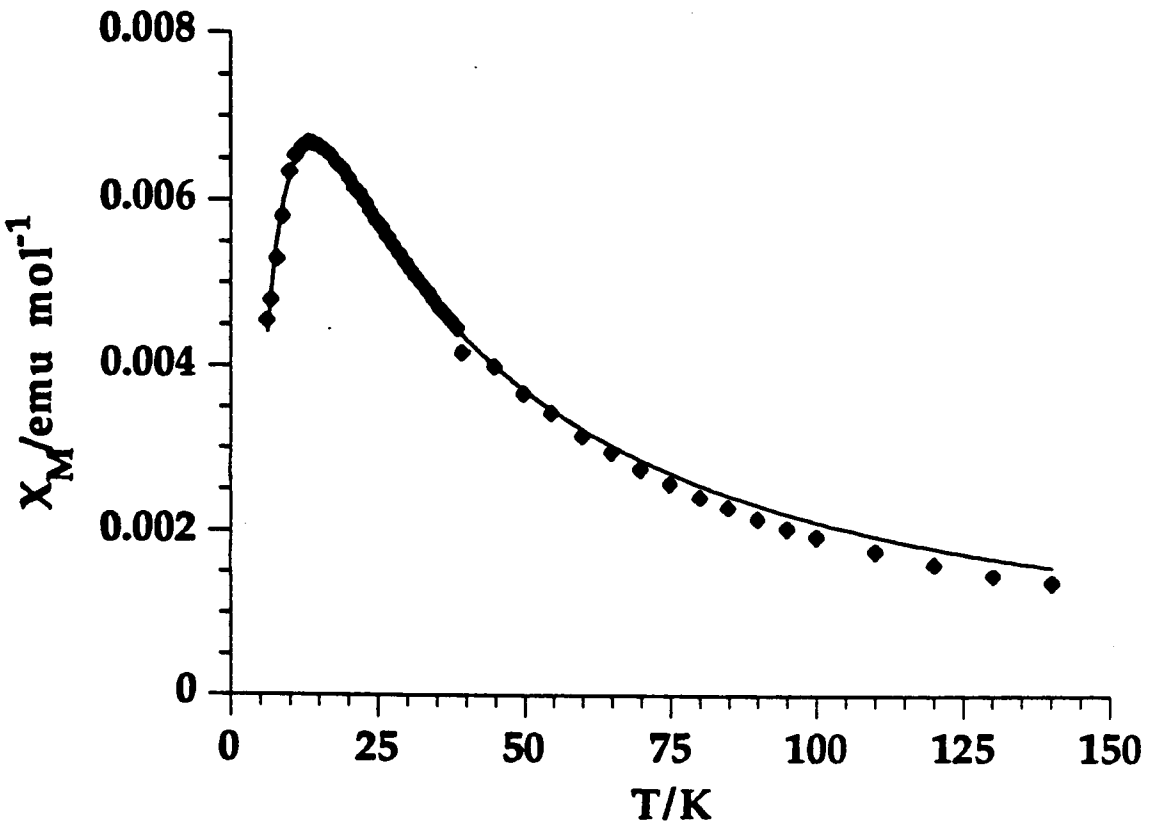

Fig. 4.22 Plots of χ_M *vs.* T for [W(η-C_7H_7)(PMe_3)Br_2] **22**. The solid line is the best-fit generated by eq. 4 for the 1D-Ising model

4.7 Summary

The magnetic data of the 17-electron compounds **6, 7, 20, 22, 23** described in this chapter are compiled in Table 4.1. For each of the compounds, the moments were measured from 0 to 3 Tesla at 6 K. The plot of moment against field gave a straight line which indicates that the magnetic data are field independent. For example, as shown in Table 4.1, changing the magnetic field from 0.2 T to 1 T does not produce a significant change in the magnetic susceptibility data. It is also worth noting that the steady values of effective moment found at high temperatures are significantly lower than would be expected for a spin-only ion with S = 1/2. The deviation from the predictions for spin-only ions are shown in Table 4.1 in the form of values of g calculated using the spin-only formula and S = 1/2. An analysis of the values of g for both EPR and susceptibility data requires knowledge of the strength and symmetry of the ligand field and exchange interactions as well as an estimate of the covalency of the bonds between metal and its ligands. In the absence of reliable estimates of all these quantities it is pointless to take the analysis further.

Table 4.1 : Magnetic susceptibility data for $[M(\eta\text{-}C_7H_7)LX_2]$

Compound	Fieid/T	R_A/K[a]	R_B/K[b]	C/emu-K mol^{-1}	θ/K	μ_{eff}/μ_B	T(χ_{max})/K[c]	g[d]
6	0.2	2-300	50-300	0.29	-4.6	1.54	16	1.77 (2.03)
	1.0	2-300	50-300	0.29	-5.2	1.53	16	1.77 (2.03)
7	0.2	6-230	45-230	0.26	-2.6	1.43	12	1.65 (2.06)
	1.0	6-200	45-200	0.26	-4.5	1.43	12	1.65 (2.06)
20	0.2	6-296	----------	-------	-------	1.44	17	1.66 (1.94)
23	0.2	6-296	----------	-------	-------	1.50	13	1.73 (1.99)
	1.0	6-296	----------	-------	-------	1.46	13	1.69 (1.99)
22	0.2	6-140	45-140	0.20	-3.6	1.27	13	1.46 (1.94)
	1.0	6-95	45-95	0.19	-4.2	1.23	13	1.42 (1.94)

[a] R_A = temperature range within which the data were collected; [b] R_B = temperature range within which the compound obeys the Curie-Weiss law
[c] T(χ_{max}) = temperature at χ_{max}; [d] calculated from μ_{eff} by the spin-only formula; experimental values (from EPR) given in parenthesis

The magnetic behaviour of compounds **6, 7, 20, 22, 23** can be described by one-dimensional Heisenberg or Ising model which is supported by the crystal structure of [Mo(η-C_7H_7)(MeCN)I_2] **6**. The least-squares fit parameters for these compounds are given in Table 4.2. As shown in the table, both models give best-fit g values which agree well with the experimental values obtained from susceptibility measurements.

Some general trends can also be observed in Table 4.2. Firstly, changing the metal centre from molybdenum to tungsten increases the exchange constant by 1.2-1.9 K. Since the d-electrons in tungsten are more diffuse than that in molybdenum, it is expected that the interaction along the chain between the W-W would be stronger than for Mo-Mo. Secondly, changing the ligand from MeCN to PMe_3 decreases the J value by 2.0-3.7 K. It is likely that the more bulky PMe_3 ligand would lengthen the metal-metal separation in the chain resulting in smaller values for J. Finally, changing the halogen from iodine to bromine also decreases the value of J by 0.4-0.7 K. It is worth noting that the compound [Mo(η-C_7H_7)(MeCN)Cl_2] **15** does not show antiferromagnetic coupling. These may suggest that the efficiency of super-exchange pathway *via* M-I-M > M-Br-M > M-Cl-M. In the above discussion, it has been assumed that the compounds **7, 15, 20, 22, 23** are essentially isostructural with **6**. Attempts to grow single crystals of these compounds suitable for X-ray analysis were unsuccessful.

Table 4.2 : Best-fit parameters for compounds [M(η-C_7H_7)LX_2]

Compound	**1D-Heisenberg model**		**1D-Ising model**	
	g	**J/K**	**g**	**J/K**
[Mo(η-C_7H_7)(MeCN)I_2] **6**	1.84	-8.9	1.92	-15.6
[Mo(η-C_7H_7)(PMe_3)I_2] **7**	1.67	-6.9	1.75	-12.2
[W(η-C_7H_7)(MeCN)I_2] **20**	1.72	-10.5	1.76	-17.5
[W(η-C_7H_7)(PMe_3)I_2] **23**	1.73	-8.1	1.78	-13.8
[W(η-C_7H_7)(PMe_3)Br_2] **22**	1.53	-7.4	1.61	-13.4

4.8 References

1 (a) L. J. de Jough and A. R. Miedema, *Adv. Phys.*, 1974, **23**, 1; (b) *Extended Linear Chain Complexes*, ed. J. S. Miller, Plenum, New York, 1981-1983, vol 1-3; (c) *Magneto-Structural Correlations in Exchange Coupled Systems*, eds. R. D. Willett, D. Gatteschi and O. Kahn, Reidel, Dordrecht, 1985.

2 W. Bünder and E. Weiss, *Z. Naturforsch*, 1978, **33B**, 1235.

3 R. L. Carlin, *Magnetochemistry*, Springer-Verlag, Berlin, 1986, ch. 5.

4 (a) J. C. Bonner and M. E. Fisher, *Phys. Rev., Sect. A*, 1964, **135**, 640; (b) W. E. Hatfield, R. R. Weller and J. W. Hall, *Inorg. Chem.*, 1980, **19**, 3825.

5 (a) M. E. Fisher, *J. Math. Phys.*, 1963, **4**, 124; (b) A. Pires and D. Hone, *J. Phys. Soc. Jap.* 1978, **44**, 43.

CHAPTER FIVE

Thiolato- and Imido-bridged η-Cycloheptatrienyl-Molybdenum Complexes

5.1 Thiolato-bridged η-Cycloheptatrienyl-Molybdenum Complexes

5.1.1 Introduction

There is an extensive chemistry of molybdenum compounds with sulfur ligands. Apart from their intrinsic interest, the chemistry has been developed with a view to providing insight into the mechanism of the important industrial process of hydrodesulfurisation[1] and the active site of molybdenum nitrogenase which catalyses the reduction of dinitrogen to ammonia.[2]

Although many thiolato-bridged complexes with a variety of co-ligands have been reported, the use of the cycloheptatrienyl moiety as a supporting ligand remains relatively unexploited.[3] The relative paucity of these compounds is due primarily to the lack of synthetic routes to suitable starting materials. As discussed in chapter one, the compounds $[Mo(\eta\text{-}C_7H_7)(\eta\text{-}C_6H_5R)][PF_6]$ (R = H or Me) and $[Mo(\eta\text{-}C_7H_7)(\eta^5\text{-}C_7H_9)]$ are excellent precursors to half-sandwich derivatives of the $Mo(\eta\text{-}C_7H_7)$ moiety.[4,5] This section describes the use of these compounds to prepare a new series of binuclear thiolato-bridged molybdenum compounds with cycloheptatrienyl rings.

5.1.2 Synthetic Studies

5.1.2.1 $[(\eta\text{-}C_7H_7)Mo(\mu\text{-}SBu)_3Mo(\eta\text{-}C_7H_7)][BF_4]$

When compound $[Mo(\eta\text{-}C_7H_7)(\eta\text{-}C_6H_5Me)][BF_4]$ **29** was treated with butane-1-thiol at 80°C, the reaction mixture changed from light- to dark-green over a period of 4 h. Removal of the volatiles *in vacuo* followed by recrystallisation from a diethyl ether/thf mixture gave a dark green crystalline $[(\eta\text{-}C_7H_7)Mo(\mu\text{-}SBu)_3Mo(\eta\text{-}C_7H_7)][BF_4]$ **30** in 70% yield (Scheme 5.1). The reaction was clean giving only a small amount of side-products as monitored by ^1H NMR spectroscopy. Being an ionic species with long aliphatic chains, **30** is, as expected, slightly soluble in toluene and diethyl ether, but very soluble in thf, acetone, dichloromethane and chloroform. Compound **30** is apparently stable in air.

Microanalysis for **30** was consistent with the proposed stoichiometry and the mass spectrum (FAB) showed the presence of $[(\eta\text{-}C_7H_7)Mo(\mu\text{-}SBu)_3Mo(\eta\text{-}C_7H_7)]^+$ as the base peak. The room temperature ^1H NMR spectrum of **30** showed a singlet at δ 5.53

assignable to the η-C_7H_7 protons and a triplet at δ 1.00 assignable to the methyl protons in the butyl groups. The spectrum also comprised three broad signals at δ 2.58, 1.68 and 1.50 which may be attributed to the methylene protons in the butyl groups. The occurrence of broad bands suggested that this compound is fluxional and variable-temperature NMR studies were performed, the details of which are given in Section 5.1.3.

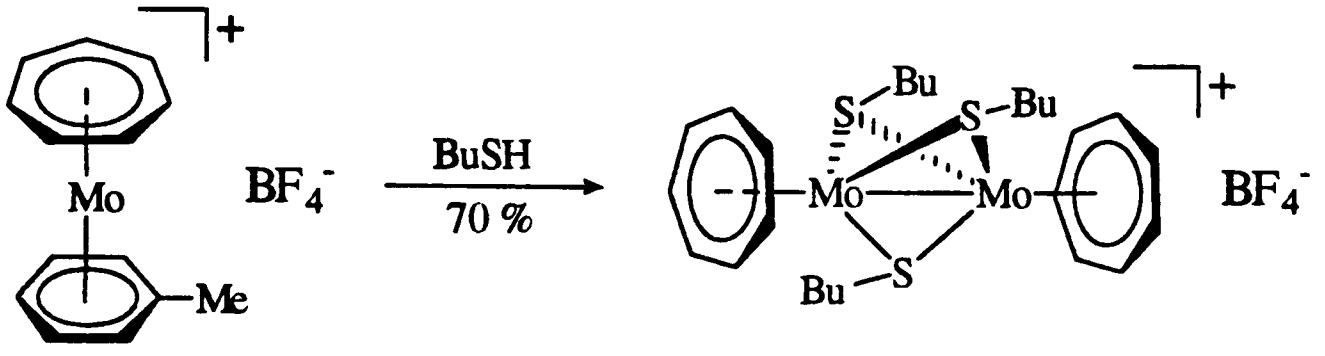

29 **30**

Scheme 5.1

5.1.2.2 [(η-C_7H_7)Mo(μ-SPr)$_3$Mo(η-C_7H_7)][BF_4]

The complex [(η-C_7H_7)Mo(μ-SPr)$_3$Mo(η-C_7H_7)][BF_4] **31** was prepared similarly by treating **29** with propane-1-thiol. However, this reaction took longer (20 h) to consume all of the starting compound **29** and significant amounts of unidentified side-products were also formed. Compound **31** was also characterised by microanalysis and NMR spectroscopy.

The ^{1}H NMR spectrum of **31** is similar to that of **30**. It showed a singlet at δ 5.53 assignable to the η-C_7H_7 protons and a poorly resolved triplet at δ 1.10 assignable to the methyl groups together with two broad signals at δ 2.56 and 1.72 which were due to the methylene protons in the propyl groups.

5.1.2.3 [(η-C_7H_7)Mo(μ-SPh)$_3$Mo(η-C_7H_7)][BF_4]

When compound **29** was treated with benzenethiol, a dark green suspension was obtained. The mixture was heated at 100°C for 6 h, then light petroleum (b.p. 40-60°C) was added to precipitate the product [(η-C_7H_7)Mo(μ-SPh)$_3$Mo(η-C_7H_7)][BF_4] **32** as a green solid. After washing thoroughly with light petroleum (b.p. 40-60°C), the product was dried *in vacuo* and it was essentially pure as shown by ^{1}H NMR spectroscopy. An analytically pure sample was obtained by recrystallisation from an acetone/thf mixture at -20°C.

An alternative route to this binuclear compound was through the paramagnetic salt [Mo(η-C_7H_7)(η^5-C_7H_9)][BF_4] which was prepared by treating [Mo(η-C_7H_7)(η^5-C_7H_9)] **5** with $HBF_4.Et_2O$ in diethyl ether.[5] Treatment of [Mo(η-C_7H_7)(η^5-C_7H_9)][BF_4] with benzenethiol at 80°C for 3 h gave compound **32** in 71 % yield based on **5** (Scheme 5.2).

The microanalytical data for **32** are consistent with the proposed stoichiometry. The mass spectrum (FAB) showed the base peak at m/e 705, which was due to the cation [(η-C_7H_7)Mo(μ-SPh)$_3$Mo(η-C_7H_7)]$^+$. The ^{1}H NMR spectrum of **32** (Fig. 5.1) showed a singlet at δ 5.54 for the η-C_7H_7 ligand and two multiplets at δ 7.41-7.49 and 7.55-7.59 for the phenyl protons. The ^{13}C{^{1}H} NMR spectrum showed a band at δ 96.6 assignable to the η-C_7H_7 group and four bands at δ 129.3, 130.5, 131.9 and 143.2 assignable to the phenyl groups.

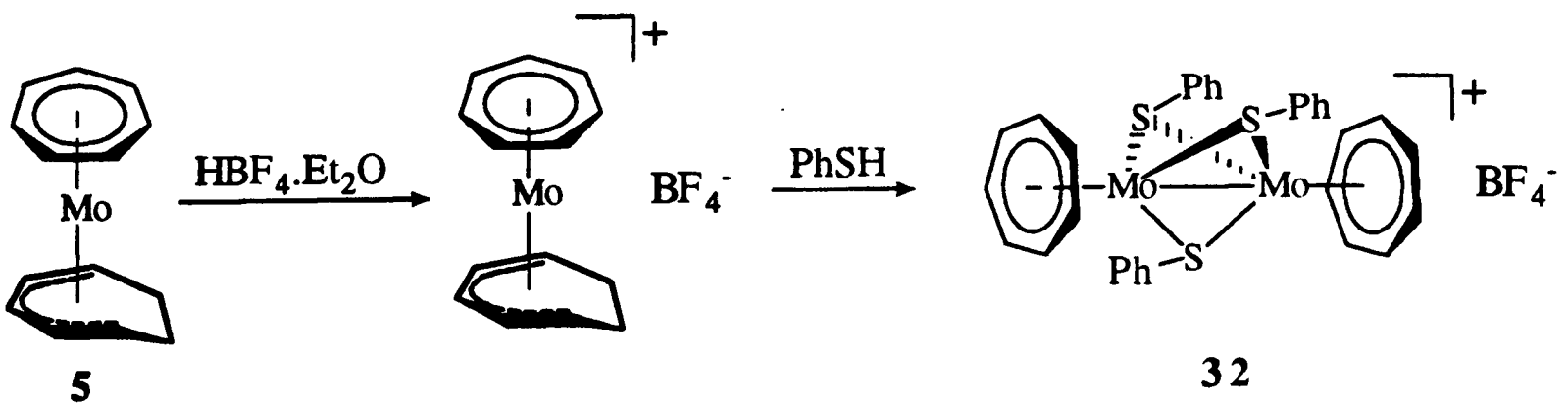

5 **32**

Scheme 5.2

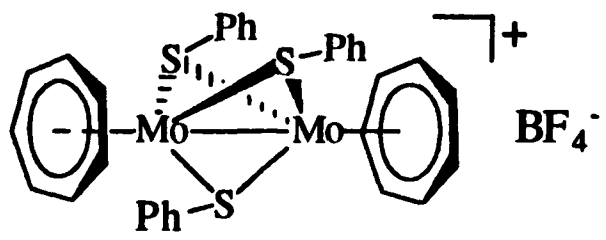

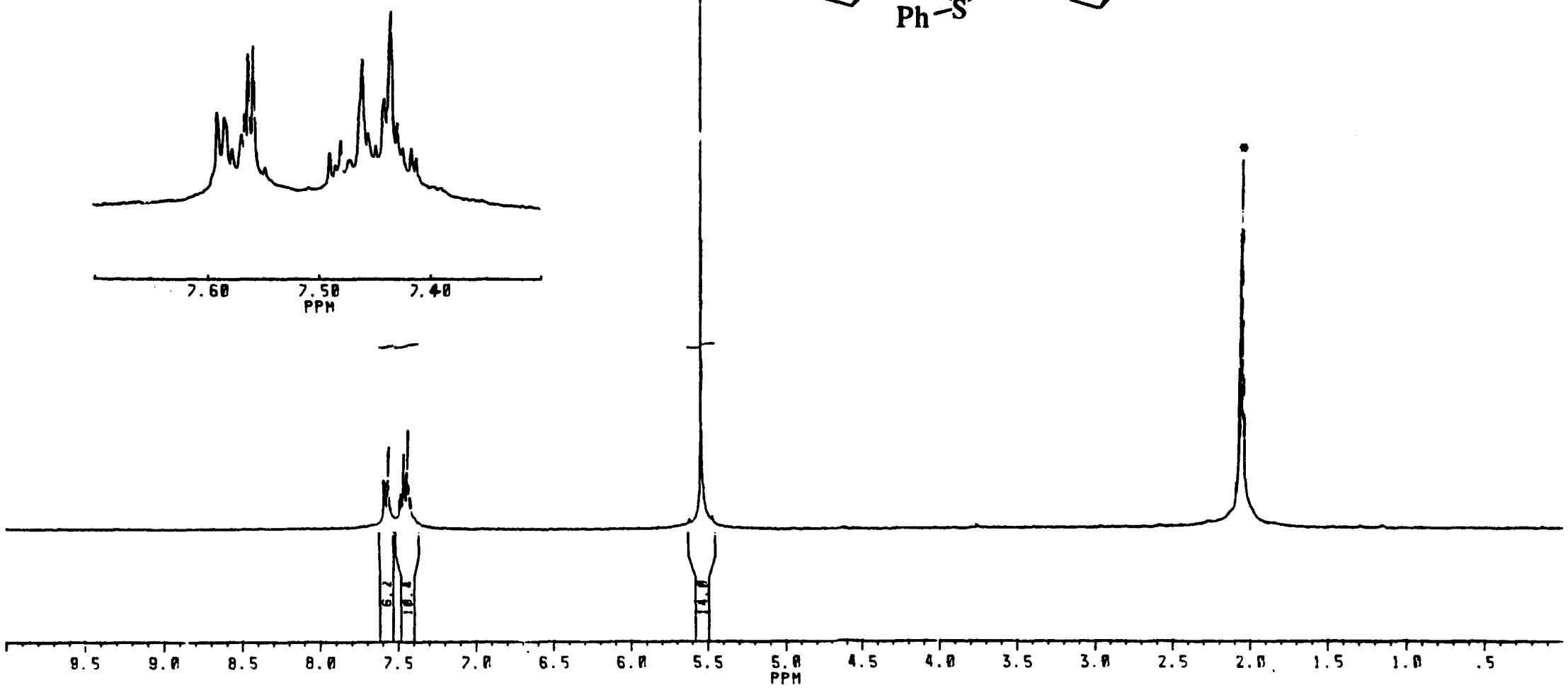

Fig. 5.1 ^{1}H NMR spectrum of $[(\eta\text{-}C_7H_7)Mo(\mu\text{-}SPh)_3Mo(\eta\text{-}C_7H_7)][BF_4]$ **32** in $[^{2}H_6]$-acetone : *indicates solvent

5.1.2.4 [(η-C_7H_7)Mo(μ-SCH_2Ph)$_3$Mo(η-C_7H_7)][BF_4]

Compound **29** was treated with phenylmethanethiol giving a dark green suspension. Upon addition of light petroleum (b.p. 40-60°C), a greenish-brown precipitate appeared which was washed with light petroleum (b.p. 40-60°C) and then recrystallised from an acetone/thf mixture at -20°C. Brown [(η-C_7H_7)Mo(μ-SCH_2Ph)$_3$Mo(η-C_7H_7)][BF_4] **33** was isolated in 88 % yield. Alternatively, compound **33** could also be obtained by treating [Mo(η-C_7H_7)(η^5-C_7H_9)][BF_4] with phenylmethanethiol.

The stoichiometry of **33** was confirmed by microanalysis and the mass spectrum (FAB) showed the base peak at m/e 747 (M - BF_4). The room temperature ^{1}H NMR spectrum displayed a multiplet at δ 7.40-7.57 (phenyl), a singlet at δ 5.55 (η-C_7H_7) and a broad signal at δ 3.98 (SCH_2) whilst the ^{13}C NMR spectrum showed bands which were consistent with the proposed structure.

5.1.2.5 [(η-C_7H_7)Mo(μ-SEt)$_3$Mo(η-C_7H_7)][BF_4]

It was anticipated that the complex **29**, upon treatment with thiolate ions (SR^-), might give the neutral complexes [(η-C_7H_7)Mo(μ-SR)$_3$Mo(η-C_7H_7)]. However the reaction between **29** and 1.5 equivalents of lithium thioethoxide in thf gave a mixture of products from which only the salt [(η-C_7H_7)Mo(μ-SEt)$_3$Mo(η-C_7H_7)][BF_4] **34** was isolated, in low yield.

Microanalytical data (C, H and S) for **34** were consistent with the proposed formulation. The mass spectrum (FAB) showed the base peak at m/e 561 which was due to the [(η-C_7H_7)Mo(μ-SEt)$_3$Mo(η-C_7H_7)]$^+$ cation. The room temperature ^{1}H NMR spectrum of **34** showed a singlet at δ 5.79 and two broad signals at δ 2.76 and δ 1.35 which were assigned to the η-C_7H_7, SCH_2 and CH_3 group, respectively. The ^{13}C NMR spectrum displayed bands at δ 94.1 (η-C_7H_7), 41.0 (SCH_2) and 17.9 (CH_3), which were consistent with the proposed structure.

5.1.2.6 [(η-$C_7H_3Me_4$-1,2,4,6)Mo(μ-SPh)$_3$Mo(η-$C_7H_3Me_4$-1,2,4,6)][BF_4]

The mixed sandwich compound [Mo(η-$C_7H_3Me_4$-1,2,4,6)(η-C_6H_5Me)][BF_4] was prepared during the course of exploration of η-1,2,4,6-tetramethylcycloheptatrienyl molybdenum chemistry which will be described in next chapter. Treatment of this compound with benzenethiol at 100^{0}C for 5 h afforded [(η - $C_7H_3Me_4$-1,2,4,6)Mo(μ-SPh)$_3$Mo(η-$C_7H_3Me_4$-1,2,4,6)][BF_4] **35** as green crystals in excellent yield (Scheme 5.3). The compound was characterised by microanalysis and various spectroscopic methods.

Fig. 5.2 shows the ^{1}H NMR spectrum of **35** in [$^2H_6$]-acetone. It comprises a broad signal at δ 7.43 assignable to the phenyl groups, three singlets at δ 5.14, 4.85 and 4.73 assignable to the C_7 ring protons, and four singlets at δ 2.58, 2.40, 2.13 and 1.61 assignable to the methyl groups. The ^{13}C NMR spectrum exhibits seven peaks for the C_7 ring carbons and four peaks for the methyl carbons. These results clearly indicate that the two cycloheptatrienyl rings are symmetry related but there is no plane of symmetry through the Mo-Mo bond in the molecule. This result is consistent with the structure proposed in Scheme 5.3.

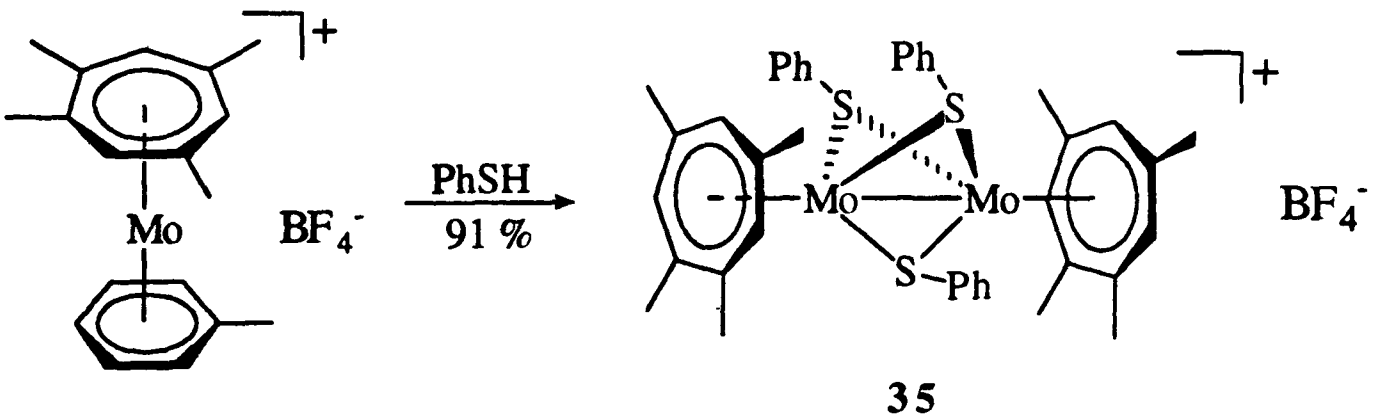

35

Scheme 5.3

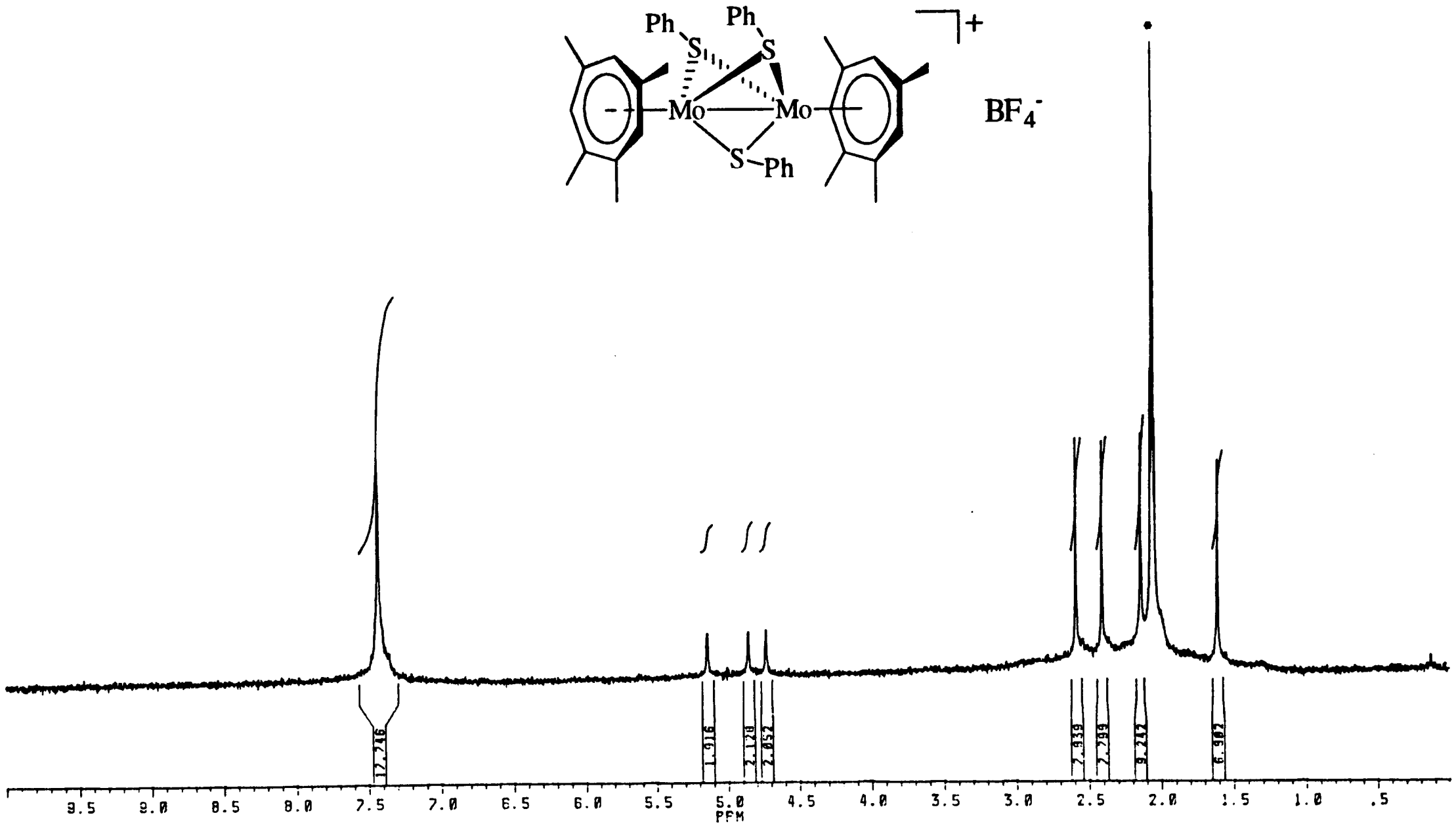

Fig. 5.2 ^{1}H NMR spectrum of $[(\eta\text{-}C_7H_3Me_4\text{-}1,2,4,6)Mo(\mu\text{-}SPh)_3Mo(\eta\text{-}C_7H_3Me_4\text{-}1,2,4,6)][BF_4]$ **35** in $[^{2}H_6]$-acetone : *indicates solvent

5.1.3 Variable-temperature NMR Studies

The room temperature ^1H NMR spectra of complexes **30**, **31**, **33** and **34** each show the band assignable to the SCH_2 protons is broad. For compounds **30** and **31**, the bands assigned to the other methylene protons also occur as broad signals. These observations suggested that the molecules are fluxional and variable-temperature NMR studies were performed. Fig. 5.3 shows the variable-temperature ^1H NMR spectrum of **34** in [$^2H_6$]-acetone. This shows a sharp singlet at δ 5.78 assignable to the η-C_7H_7 protons, a poorly resolved quartet at δ 2.78 assignable to the SCH_2 protons and a triplet at δ 1.38 assignable to the methyl groups at 318 K. On cooling to 283 K line broadening occurs to give two broad signals for the SCH_2 and CH_3 protons. Further lowering the temperature to 243 K sharpens these bands and gives the low-temperature limit spectrum. The spectrum shows that the triplet and quartet reappear but are shifted upfield while the η-C_7H_7 singlet exhibits a small downfield shift. The lower temperature spectra also develop new bands but in much lower intensity. These occur as a singlet at δ 5.80, two overlapping quartets at δ 2.96 and 2.91, a quartet at δ 2.38 and two overlapping triplets at δ 1.47 and 1.45. The *J* (H-H) coupling constants are 7.4 Hz for all of these triplets and quartets. These spectra of **34** are attributed to the presence of two isomers **A** and **B** of compound **34** which interconvert through inversion at the sulfur (Fig. 5.4).[6] At low temperature, the rate of interconversion is so slow that the lifetime of each isomer is long relative to the NMR time-scale. Thus ^1H NMR spectrum of **34** at 243 K exhibits resonances at δ 5.82 (η-C_7H_7), 2.71 (SCH_2) and 1.25 (CH_3) due to the isomer **A** (R = Et) and at δ 5.80 (η-C_7H_7), 2.96 and 2.91 (S_aCH_2 and S_cCH_2), 2.38 (S_bCH_2), and 1.47 and 1.45 ($S_aCH_2C\underline{H}_3$ and $S_cCH_2C\underline{H}_3$) due to the isomer **B** (R = Et). It is assumed that the absorption of the remaining $S_bCH_2C\underline{H}_3$ is obscured by the triplet at δ 1.25. Integrations of the two η-C_7H_7 signals show the ratio of the isomers **A** : **B** (R = Et) is *ca.* 3.5 : 1 at the slow-exchange limit. This observation is in contrast to the results reported by Knox and co-workers who found that for the compounds [$(CO)_3$ $Mo(\mu\text{-}SR)_3Mo(\eta\text{-}C_7H_7)$] (R = Me, Et, Pr^i or Bu^t), the isomer of type **B** was the major isomer.[3b]

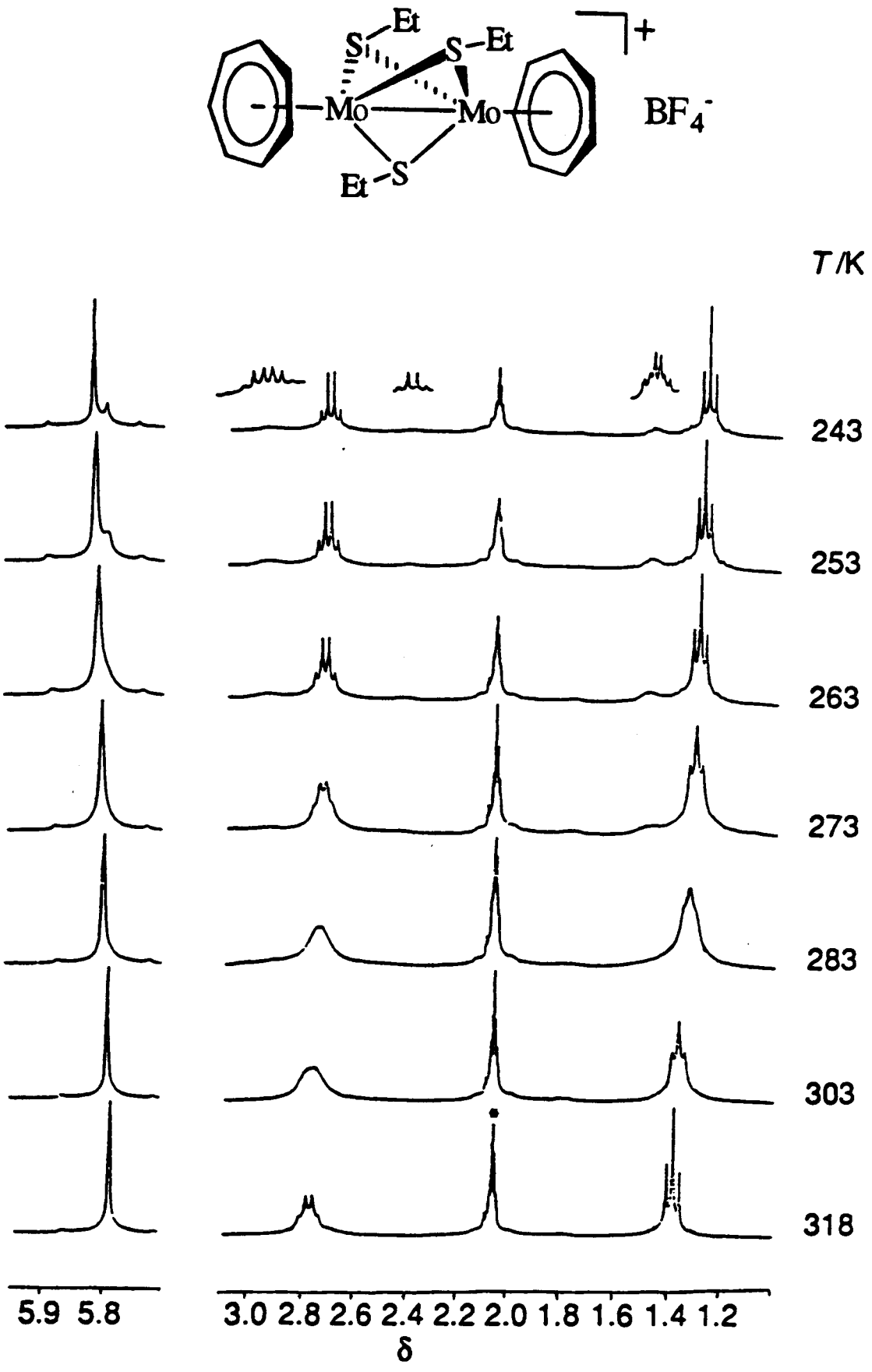

Fig. 5.3 Variable-temperature ^1H NMR spectra of $[(\eta\text{-}C_7H_7)Mo(\mu\text{-}SEt)_3Mo(\eta\text{-}C_7H_7)][BF_4]$ **34** in $[^2H_6]$-acetone : *indicates solvent

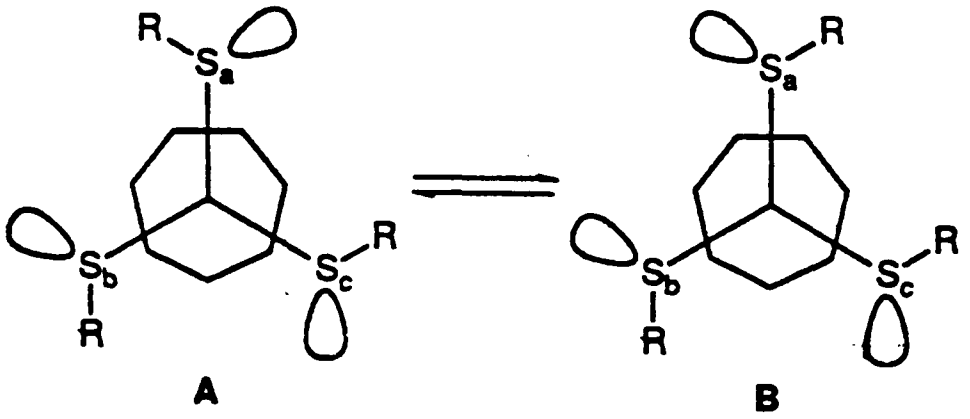

Fig. 5.4 View of the proposed molecular geometry of $[(\eta\text{-}C_7H_7)Mo(\mu\text{-}SR)_3Mo(\eta\text{-}C_7H_7)]^+$ down the Mo-Mo bond axis

The compound $[(\eta\text{-}C_7H_7)Mo(\mu\text{-}SPr)_3Mo(\eta\text{-}C_7H_7)][BF_4]$ **31** has similar temperature-dependent ^1H NMR spectra as shown in Fig. 5.5. At 293 K, the spectrum shows a poorly resolved triplet at δ 1.10 assignable to the methyl groups and two broad signals at δ 1.72 and 2.56 assignable to $SCH_2C\underline{H}_2$ and SCH_2 protons respectively. At higher temperature, these signals sharpen and eventually become a well-resolved triplet, a virtual sextet and a poorly resolved triplet, respectively at 323 K. This sharpening of signals is clearly due to the averging of signals arised from the fast interconversion between isomers **A** and **B** (R = Pr). On cooling to 273 K line broadening occurs to give three broad signals for the propyl groups. Further cooling to 243 K sharpens these bands and gives the low-temperature limit spectrum. This spectrum shows the presence of both isomer **A** and **B** (R = Pr), thus a singlet at δ 5.54 ($\eta\text{-}C_7H_7$), a triplet at δ 2.47 (SCH_2), a partially resolved sextet at δ 1.64 ($SCH_2C\underline{H}_2$) and a triplet at δ 1.05 (CH_3) due to the isomer **A** (R = Pr) are observed. In addition, a singlet at δ 5.51 ($\eta\text{-}C_7H_7$), two overlapping triplets at δ 2.78 and 2.81 (S_aCH_2 and S_cCH_2), a triplet at δ 2.16 (S_bCH_2), a broad signal at δ 1.85 ($SCH_2C\underline{H}_2$) and a triplet at δ 1.13 (CH_3) due to the isomer **B** (R = Pr) are developed but in much lower intensity. By integrating the two $\eta\text{-}C_7H_7$ signals, the ratio of the isomers **A** : **B** (R = Pr) was estimated to be 3.1 : 1 at the slow-exchange limit.

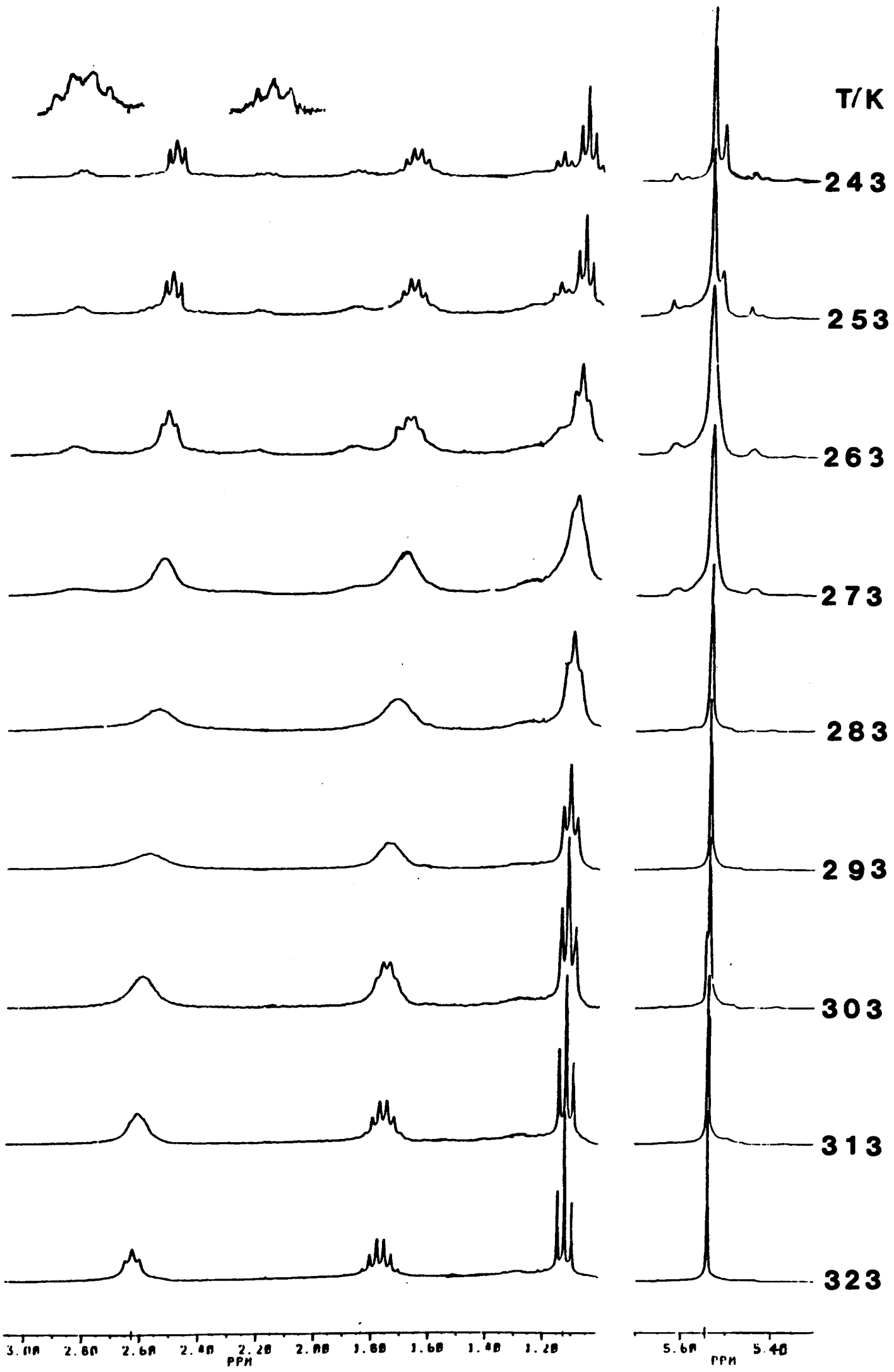

Fig. 5.5 Variable-temperature ^1H NMR spectra of $[(\eta\text{-}C_7H_7)Mo(\mu\text{-}SPr)_3Mo(\eta\text{-}C_7H_7)][BF_4]$ **31** in $[^2H_1]$-chloroform

The compound $[(\eta\text{-}C_7H_7)Mo(\mu\text{-}SBu)_3Mo(\eta\text{-}C_7H_7)][BF_4]$ **30** also undergoes sulfur inversion process as indicated by its variable-temperature ^1H NMR spectra (Fig. 5.6) . At 318 K, the spectrum gives a singlet at δ 5.54 ($\eta\text{-}C_7H_7$), a broad signal at δ 2.64 (SCH_2), a quintet at δ 1.72 ($SCH_2C\underline{H}_2$), a sextet at δ 1.53 ($SCH_2CH_2C\underline{H}_2$) and a triplet at δ 1.02 (CH_3). On cooling to 283 K line broadening occurs to give three broad signals for the methylene protons. Further lowering the temperature to 243 K sharpens these bands and gives the low-temperature limit spectrum. Due to the low abundance of the minor isomer **B** (R = Bu) and band overlap, unambiguous assignment could not be made. Nevertheless, a singlet at δ 5.51 ($\eta\text{-}C_7H_7$), two overlapping triplets at δ 2.83 and 2.85 (S_aCH_2 and S_cCH_2) and a triplet at δ 2.17 (S_bCH_2) are observed which are due to the isomer **B** (R = Bu). Based on the integrations of the two $\eta\text{-}C_7H_7$ signals, the ratio of isomers **A** : **B** is ca. 3.3 : 1 at the slow-exchange limit.

Fig 5.7 shows the variable-temperature ^1H NMR spectra of $[(\eta\text{-}C_7H_7)Mo(\mu\text{-}SCH_2Ph)_3Mo(\eta\text{-}C_7H_7)][BF_4]$ **33** in $[^2H_6]$-acetone. It can be observed that the singlet at δ 5.51 at 313 K splits into two bands with unequal intensity at lower temperature. These bands may be attributed to the $\eta\text{-}C_7H_7$ absorptions of the isomers **A** and **B** (R = CH_2Ph). In contrast to the above cases, the band due to the minor isomer **B** occurs at lower field than that due to the major isomer **A**. Moreover, the ratio of isomers **A** : **B** is higher for this compound (4.6 : 1). It is rather unexpected that the SCH_2 absorptions for the isomer **B** are not observed at low temperature.

A variable-temperature ^1H NMR study was also carried out on the compound $[(\eta\text{-}C_7H_7)Mo(\mu\text{-}SPh)_3Mo(\eta\text{-}C_7H_7)][BF_4]$ **32**. Although line broadening occurs for the phenyl absorptions at low temperature, the $\eta\text{-}C_7H_7$ absorption remains as a sharp singlet. It seems that inversion at the sulfur does not occur in this compound. Presumably, the bulkiness of the phenyl groups precludes the formation of the less symmetrical isomer **B**.

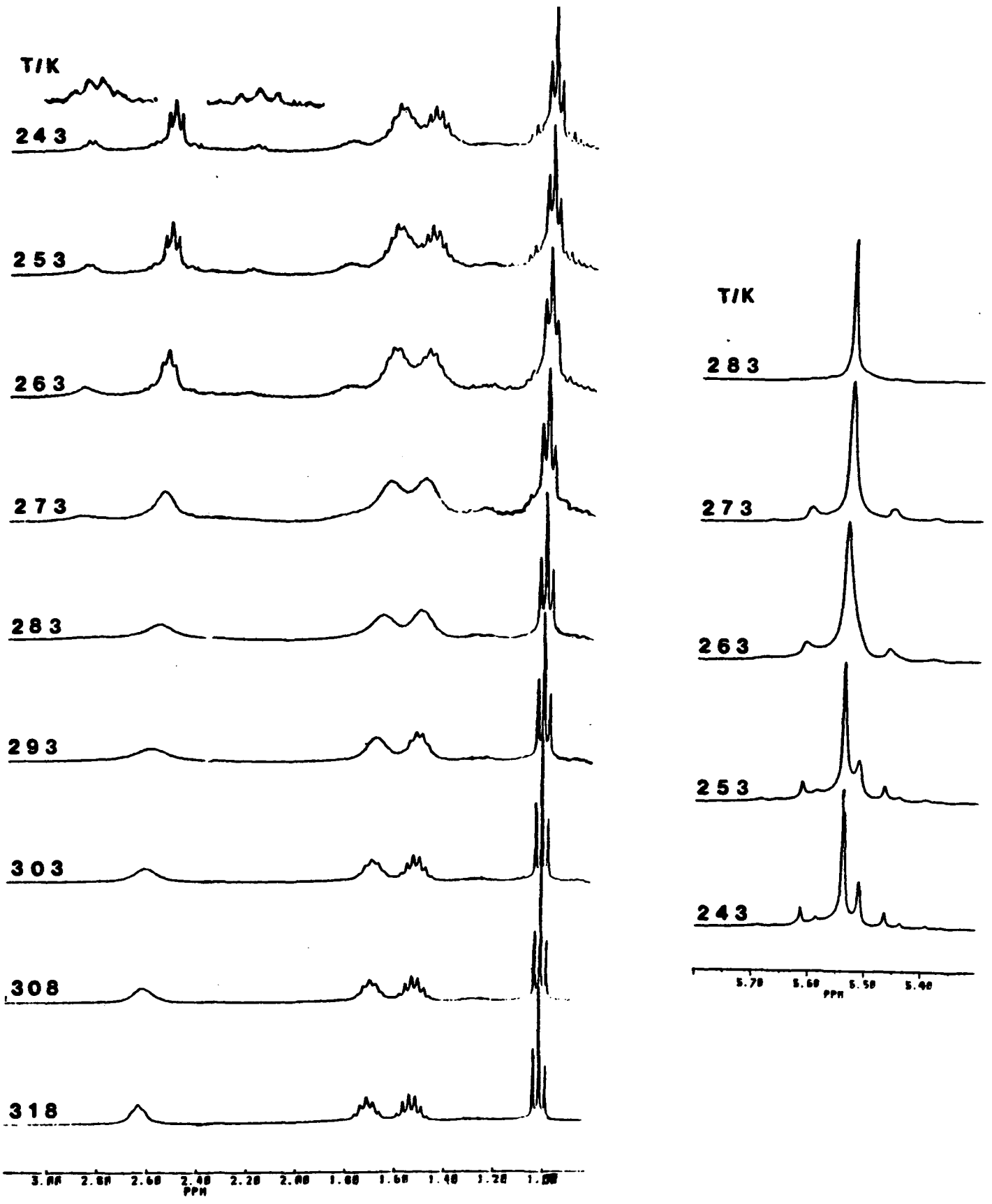

Fig. 5.6 Variable-temperature ^1H NMR spectra of $[(\eta\text{-}C_7H_7)Mo(\mu\text{-}SBu)_3Mo(\eta\text{-}C_7H_7)][BF_4]$ **30** in $[^2H_1]$-chloroform

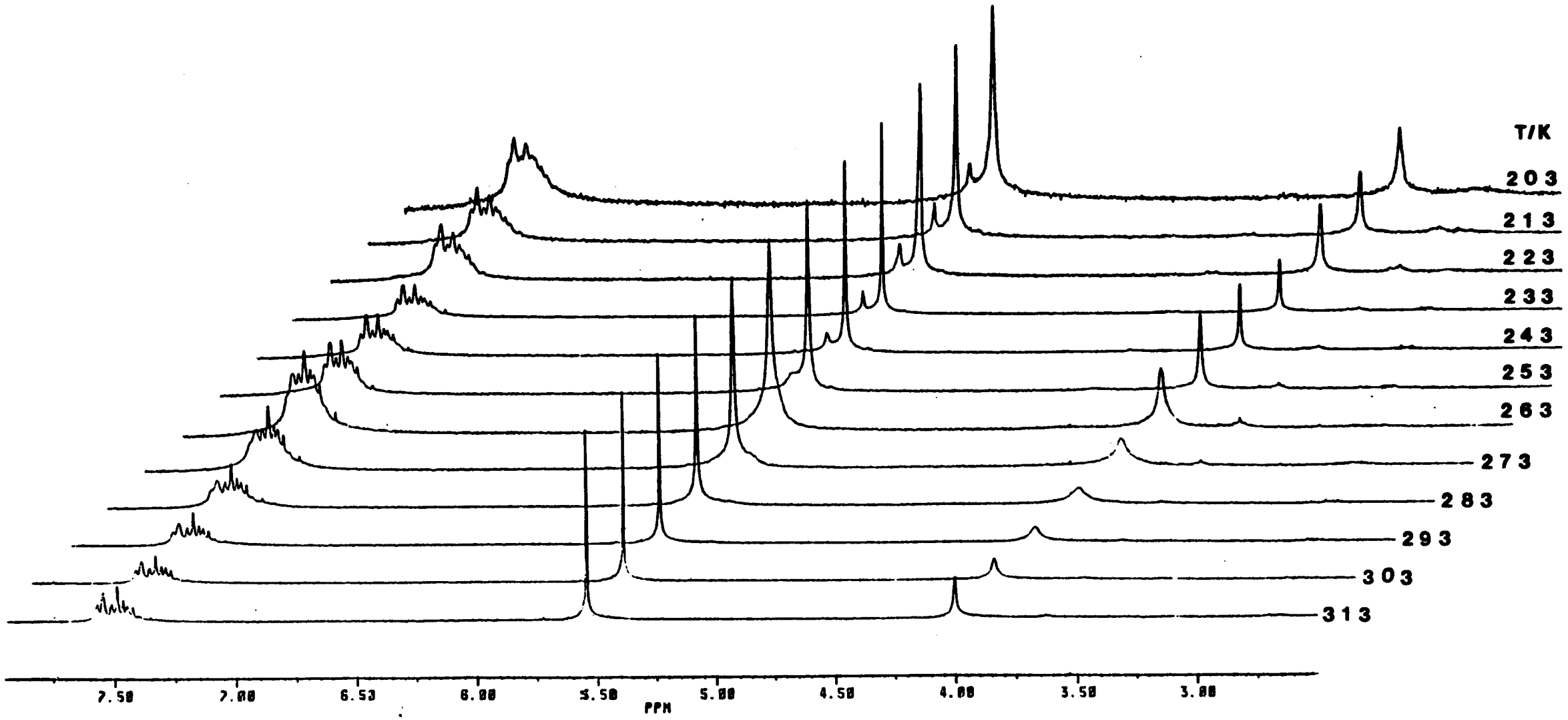

Fig. 5.7 Variable-temperature ^1H NMR spectra of $[(\eta\text{-}C_7H_7)Mo(\mu\text{-}SCH_2Ph)_3Mo(\eta\text{-}C_7H_7)][BF_4]$ **33** in $[^2H_6]$-acetone

The activation parameters for the dynamic processes were estimated by the coalescence temperature method described by Sandström.[7] By considering the two cycloheptatrienyl absorptions, the sulfur inversion process may be approximated to a two-site exchange process with unequal equilibrium site populations and no coupling between sites. The results are tabulated in Table 5.1 and the estimated $\Delta G^{\ddagger}$ values are in good agreement with the values reported for related compounds[3b,8] and occur in the order R = Et > Pr > Bu > CH_2Ph.

Table 5.1 : Data from NMR coalescence-temperature studies

Compound	ΔP^a	$\delta\nu^b$ / Hz	k^c / s^{-1}	T_c^d / K	$\Delta G^{\ddagger e}$/ kJ mol^{-1}	Reference
30	0.54	8.8	23.6	263 ± 5	57.2	This work
31	0.54	7.4	19.8	263 ± 5	57.6	This work
33	0.64	24.3	62.0	253 ± 5	53.0	This work
34	0.55	5.4	14.4	263 ± 5	58.3	This work
36 [L = $P(OMe)_3$, R = Bu^t]					58.8	3b
36 (L = PPh_2Me, R = Bu^t)					46.9	3b
36 (L = $PPhMe_2$, R = Bu^t)					47.7	3b
36 (L = PMe_3, R = Bu^t)					46.7	3b
37 (R = CH_2Ph)					58.7	8a
38 (L = PPh_3)					54.4	8b
38 [L = $As(CH_2SiMe_3)_3$]					54.6	8b

[a]Difference in fractional proportion of the sites. The total population is taken as unity.

[b] Difference in chemical shift of the sites. [c] Rate constant. [d] Coalescence temperature.

[e] Error = ± 1.0 kJ mol^{-1}.

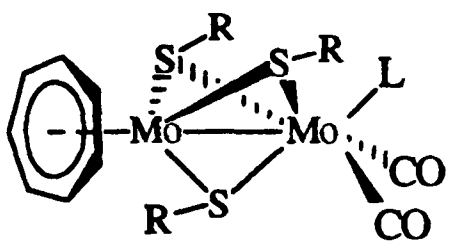

36

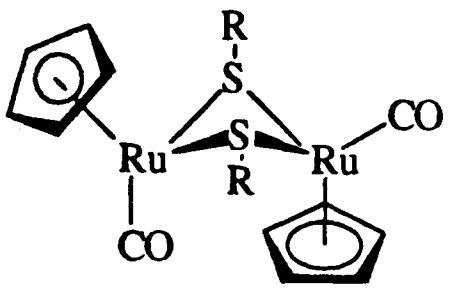

37

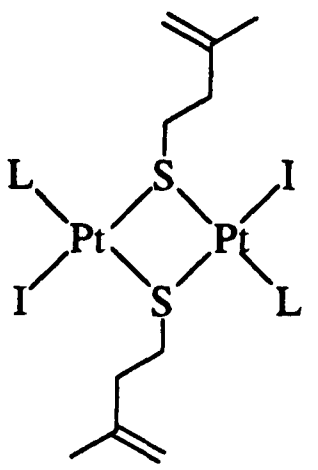

38

The $^{13}C\{^1H\}$ NMR spectra of **30** and **31** are also worth mentioning. At room temperature, the $^{13}C\{^1H\}$ NMR spectrum of **30** in $[^2H_6]$-acetone shows only three signals assignable to aliphatic carbons. Lowering the temperature to 243 K causes a small upshift shifts for the three signals and gives one more signal at δ 47.5 together with some weaker peaks (Fig. 5.8). It is obvious that the signals with higher intensity at δ 94.2, 47.5, 35.2, 22.8 and 14.4 at 243 K are due to the major isomer **A** (R = Bu), whilst the weaker peaks are due to the minor isomer **B** (R = Bu). Because of the low abundance and the inequivalence of the three bridges of the minor isomer not all of the signals appear in the spectrum. Nevertheless, the three weak peaks at δ 52.8, 51.2 and 46.6 may be assigned to the three carbons next to S_a, S_b and S_c. The absence of the SCH_2 signal at room temperature may result from the fast averaging sulfur inversion process which broadens the signal to the baseline. The room temperature $^{13}C\{^1H\}$ NMR spectrum of **31** in $[^2H_6]$-acetone exhibits a very small broad signal for the SCH_2 groups which sharpens at 243 K.

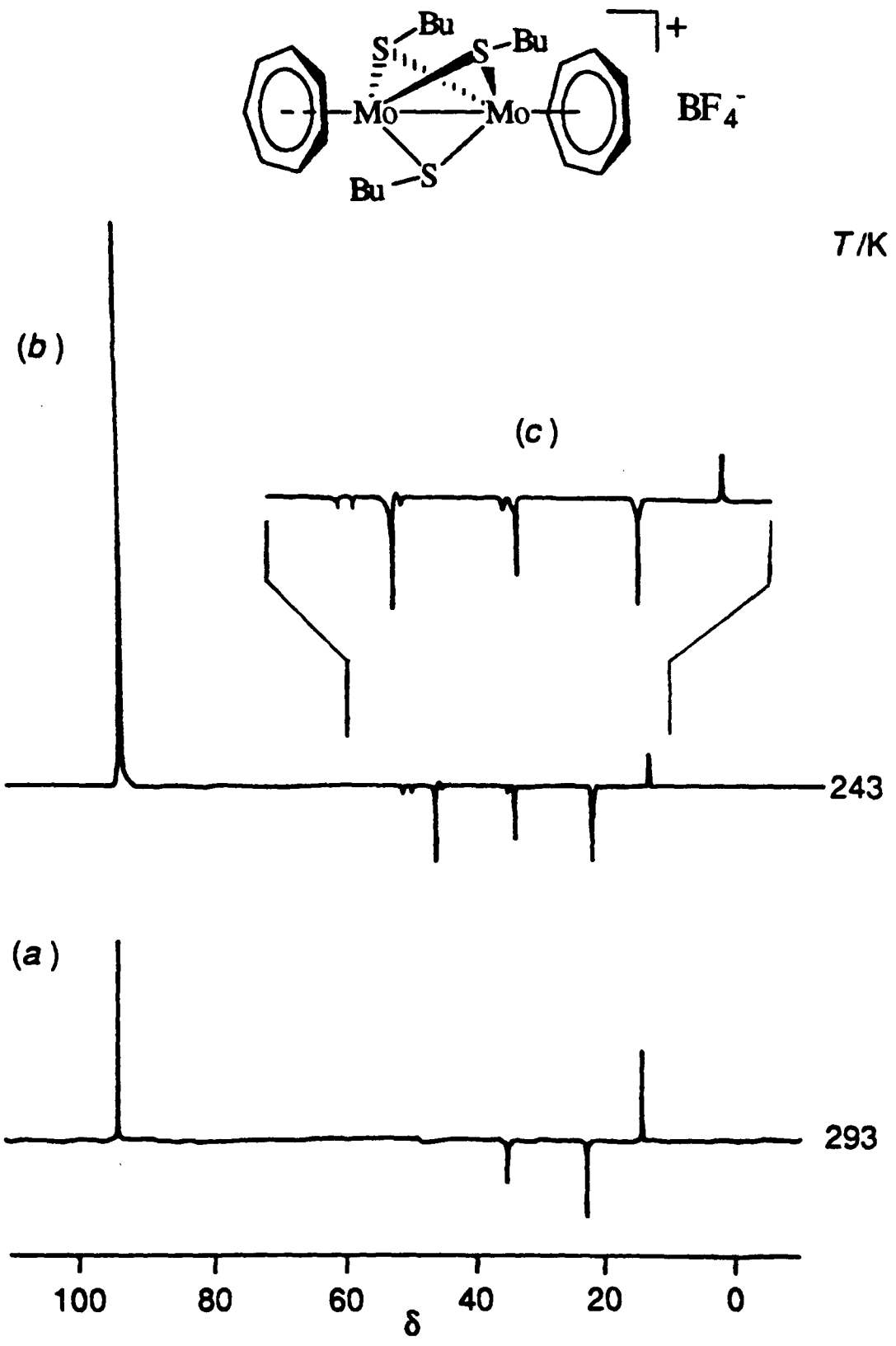

Fig. 5.8 DEPT ($\theta = 3\pi/4$) $^{13}C\{^{1}H\}$ NMR spectra of $[(\eta\text{-}C_7H_7)Mo(\mu\text{-}SBu)_3Mo(\eta\text{-}C_7H_7)][BF_4]$ **30** in $[^2H_6]$-acetone

5.1.4 Electrochemical Studies

The electrochemistry of this new series of complexes has been studied by cyclic voltammetry. All of these complexes exhibit two reversible reduction waves (Red.1 and Red.2). Fig. 5.9 shows the cyclic voltammogram for the compound **30** which is typical. The electrochemical data are summarised in Table 5.2. The reduction potentials ($E_{1/2}$) depend on the substituent on the sulfur atoms and increase in the order R = Pr < Bu < Et < CH_2Ph < Ph which reflects the electron donating nature of the alkyl group and the electron withdrawing property of the phenyl group. A similar trend was also observed for the complexes $[Mo(\eta\text{-}C_5H_5)(NO)(\mu\text{-}SR)]_2$,[9] $[NEt_4][(CO)_3Mn(\mu\text{-}SR)_3Mn(CO)_3]$[10] and $[(\eta\text{-}C_5H_4Pr^i)Mo(\mu\text{-}SR)_4Mo(\eta\text{-}C_5H_4Pr^i)]$.[11] The presence of four methyl groups of the cycloheptatrienyl rings in **35** lowers the $E_{1/2}$ values substantially as expected.

We propose that the two one-electron reductions are accompanied by cleavage of the Mo-Mo bond giving the anions $[(\eta\text{-}C_7H_3R^1{}_4)Mo(\mu\text{-}SR^2)_3Mo(\eta\text{-}C_7H_3R^1{}_4)]^-$ in which both molybdenum atoms retain 18 electrons. A similar proposal has been made for the two one-electron oxidations of the compound $[NEt_4][(CO)_3Mn(\mu\text{-}SR)_3Mn(CO)_3]$.[10] It was suggested that the oxidation is accompanied by an increase in bond order between the manganese atoms.

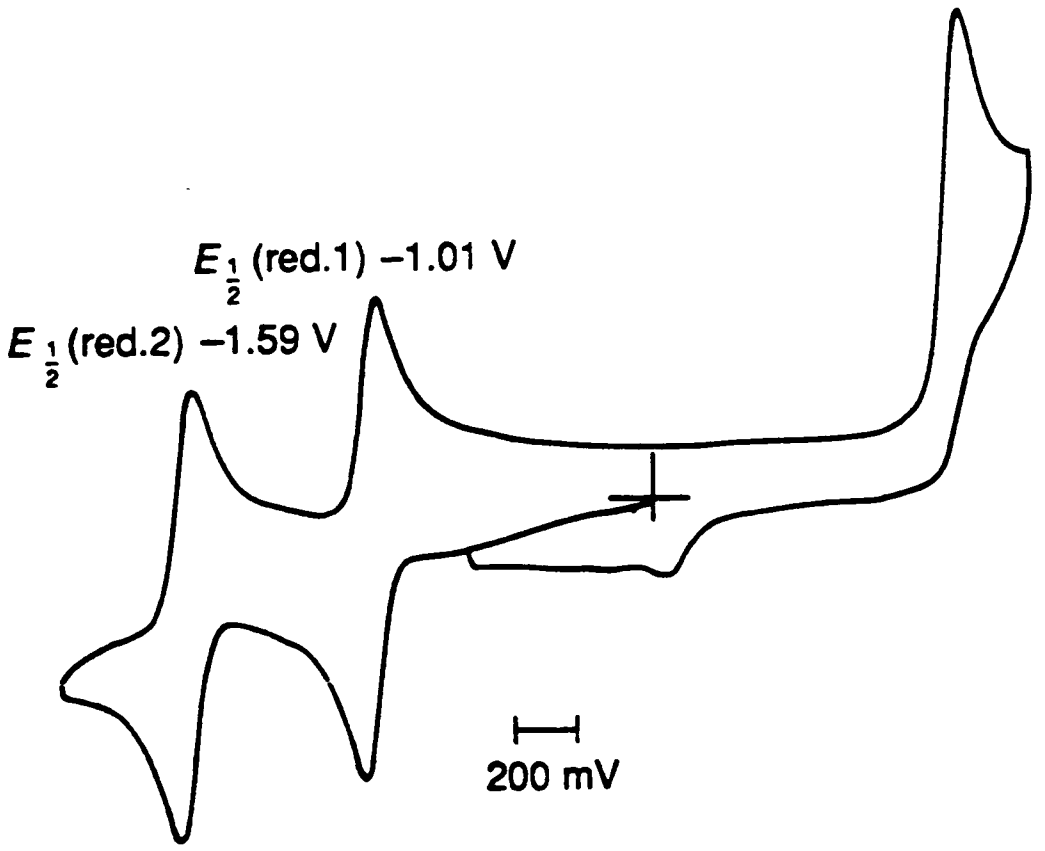

Fig. 5.9 Cyclic voltammogram of $[(\eta\text{-}C_7H_7)Mo(\mu\text{-}SBu)_3Mo(\eta\text{-}C_7H_7)][BF_4]$ **30** recorded in acetonitrile at a scan rate of 100 mV s^{-1} with $[NBu_4][PF_6]$ as electrolyte

Table 5.2 : Electrochemical data for

$[(\eta\text{-}C_7H_3R^1{}_4)Mo(\mu\text{-}SR^2)_3Mo(\eta\text{-}C_7H_3R^1{}_4)][BF_4]$ [a]

Compound	$E_{1/2}$ (red.1)[b]/V	$\Delta E_p(1)$[c]/mV	$E_{1/2}$ (red.2)[b]/V	$\Delta E_p(2)$[c]/mV
30	-1.01	55	-1.59	60
31	-1.02	60	-1.60	65
32	-0.79	60	-1.30	60
33	-0.95	60	-1.52	65
34	-0.98	50	-1.57	60
35	-0.99	50	-1.54	60

[a] Recorded with $[NBu_4][PF_6]$ as electrolyte in MeCN (0.1 mol dm^{-3}) at ambient temperature. Scan rate = 100 mV s^{-1}. [b] Relative to SCE. [c] Separation between the anodic and cathodic potentials.

5.1.5 Reactivity Studies

The thiolato-bridged complexes usually have high stability. For example, the polymeric compound $[Pd(SPh)Cl]_n$ **39** undergoes bridge-splitting reactions on the chlorine bridges, but the thiolate bridges remain intact when **39** is treated with C_6H_5N, PPh_3, $AsPh_3$, en or $[AsPh_4][Cl]$.[12] But an exception has been reported, that the thiolate bridges of complexes $[Rh_2(COD)_2(\mu\text{-}SR)_2]$ **40** (COD = cycloocta-1,5-diene) could be split by the treatment of PPh_3, giving rise to mononuclear species $[Rh(COD)(PPh_3)(SR)]$.[13]

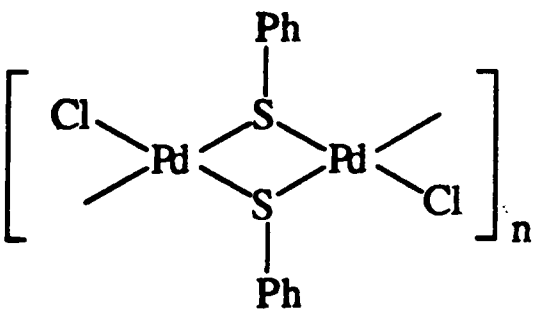

39

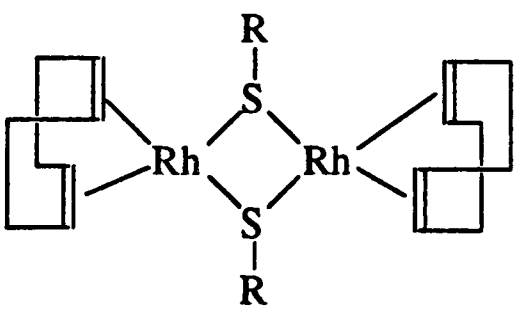

40

Both of the Mo centres in the complexes $[(\eta\text{-}C_7H_3R^1{}_4)Mo(\mu\text{-}SR^2)_3Mo(\eta\text{-}C_7H_3R^1{}_4)][BF_4]$ attain 18-electron configuration. It is expected that these complexes would be stable towards ligand displacement reactions. In fact, treatment of **32** with 3 equivalents of PPh_3 in refluxing thf for 12 h led to recovery of starting materials.

In an attempt to prepare the neutral complex $[(\eta\text{-}C_7H_7)Mo(\mu\text{-}SPh)_3Mo(\eta\text{-}C_7H_7)]$, compound **32** was treated with one equivalent of sodium amalgam in thf at room temperature. Subsequent work-up gave a green solid which is insoluble in light petroleum (b.p. 40-60°C) but soluble in toluene and dimethyl sulphoxide. Attempts to purify the crude product(s) by recrystallisation failed. The green solid did not sublimed even at 180°C (0.1 mmHg). Thus no further attempt was made to characterise the product(s).

5.1.6 Summary

A new series of binuclear thiolato-bridged molybdenum complexes $[(\eta\text{-}C_7H_3R^1{}_4)Mo(\mu\text{-}SR^2)_3Mo(\eta\text{-}C_7H_3R^1{}_4)][BF_4]$ have been described. The complexes exhibit inversion at the sulfur centre with low energy barriers and undergo two one-electron reversible reductions.

5.2 Imido-bridged η-Cycloheptatrienyl-Molybdenum Complex

5.2.1 Introduction

Transition-metal imido complexes are of much current interest not only because of their industrial[14] and biological[15] relevance but also because of their involvement in alkene metathesis[16] and carbon-hydrogen bond activation.[17] Although many organometallic imido complexes with a variety of co-ligands have been reported, those with the η-cycloheptatrienyl group as a supporting ligand are unknown. This section describes the preparation and characterisation of the first transition-metal imido complex with η-cycloheptatrienyl ligand, namely $[(\eta\text{-}C_7H_7)Mo(\mu\text{-}NAr)_2Mo(\eta\text{-}C_7H_7)]$ (Ar = 2,6-diisopropylphenyl) **41**.

5.2.2 Preparation and Characterisation of $[(\eta\text{-}C_7H_7)Mo(\mu\text{-}NAr)_2Mo(\eta\text{-}C_7H_7)]$ (Ar = 2,6-diisopropylphenyl)

The previously described dimer $[(\eta\text{-}C_7H_7)Mo(\mu\text{-}Cl)_3Mo(\eta\text{-}C_7H_7)]$ **42** [4a,18] was treated with $Bu^tNHSiMe_3$, but no reaction was observed even upon prolonged heating. Treatment of **42** with 3 equivalents of Bu^tNHLi in thf gave an intractable brown material. However, the reaction between **42** and 3 equivalents of ArNHLi (Ar = 2,6-diisopropylphenyl) in thf yielded a brown suspension from which dark red crystals of $[(\eta\text{-}C_7H_7)Mo(\mu\text{-}NAr)_2Mo(\eta\text{-}C_7H_7)]$ **41** were isolated in 56 % yield (Scheme 5.4).

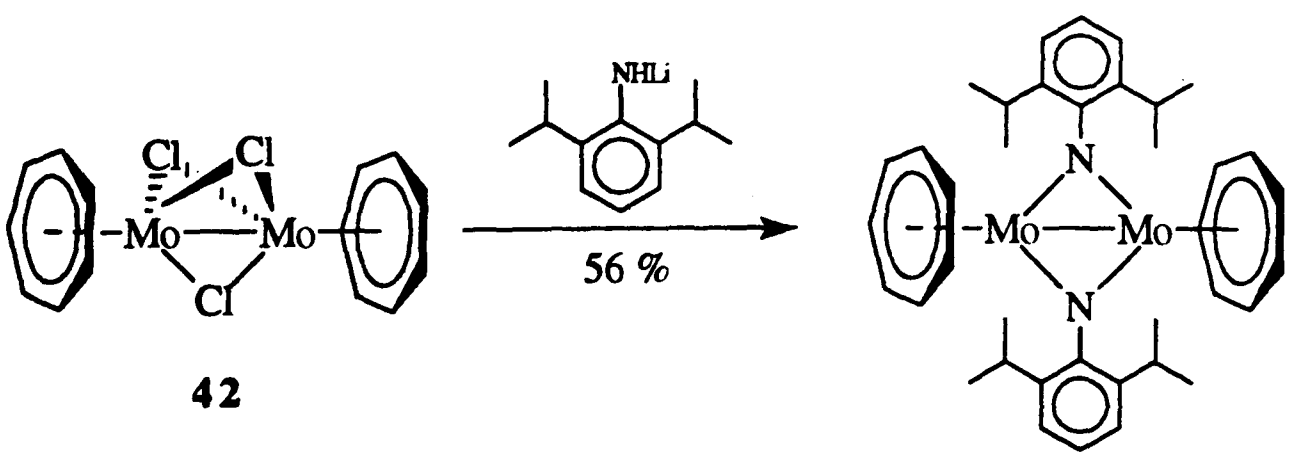

42 **41**

Scheme 5.4

The analytical and spectroscopic data characterising the compound **41** are given in Appendix A3. The compound **41** is very air-sensitive both in solid state and in solution. Nevertheless, satisfactory microanalysis were obtained. The mass spectrum (FAB) of **41** did not show a parent M+ peak. However, it gave peaks centred at m/z 362 as the base peak which is assignable to the fragment $[Mo(\eta\text{-}C_7H_7)(NAr)]^+$. The isotope pattern of these peaks was in good agreement with that obtained from simulation (Fig. 5.10). Fig. 5.11 shows the ^1H NMR spectrum of **41** in [$^2H_6$]-benzene which comprises a doublet at δ 7.24 and a triplet at δ 7.12 assignable to the phenyl protons H_m and H_p, respectively, a sharp singlet at δ 4.55 may be assigned to the $\eta\text{-}C_7H_7$ protons, and a septet at δ 2.77 and a doublet at δ 1.19 may be assigned to the isopropyl groups. The ^{13}C NMR spectrum supports the ^1H NMR assignments and shows bands at δ 160.0 (C_i), 140.4 (C_o), 124.2 (C_m), 123.1 (C_p), 88.8 ($\eta\text{-}C_7H_7$), 26.7 ($\underline{C}HMe_2$) and 26.2 (Me). The sharp bands observed in the NMR spectra indicate **41** is diamagnetic. Therefore we propose the structure for **42** shown in Scheme 5.4.

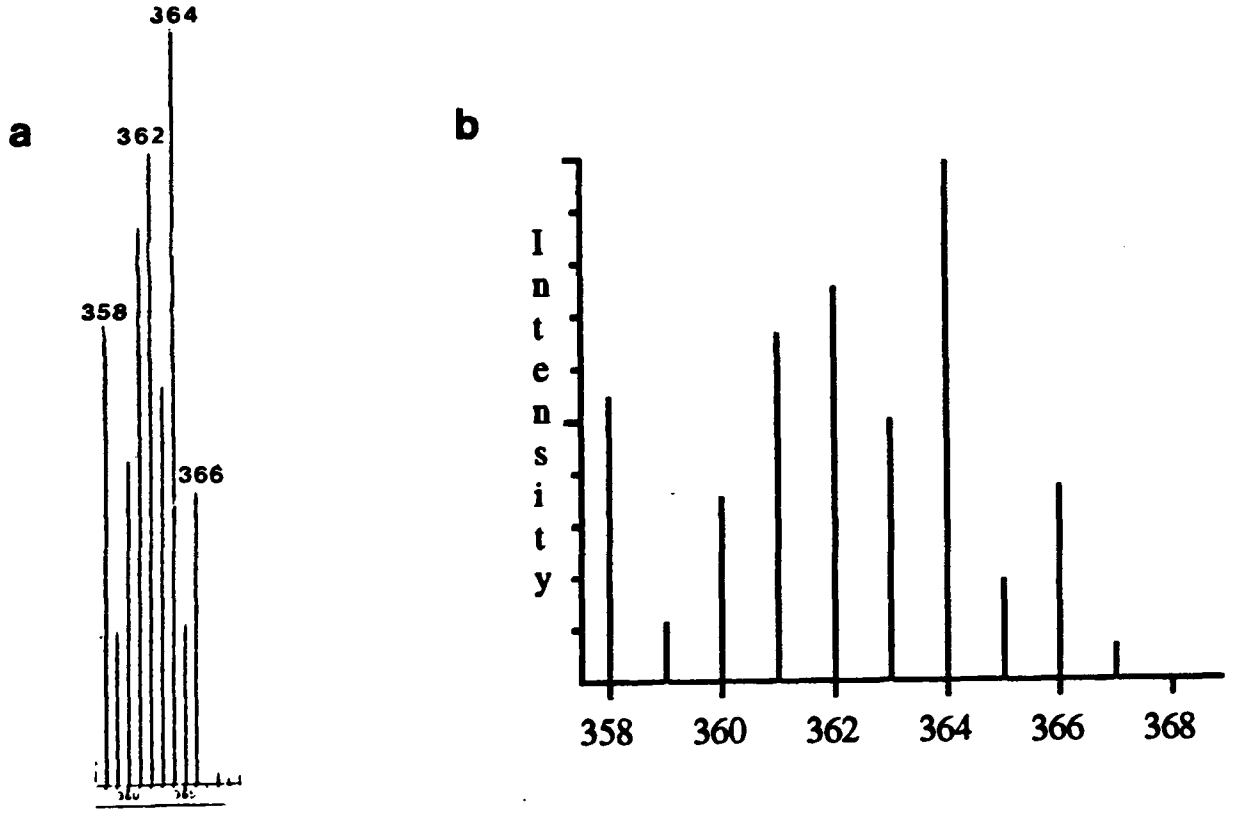

Fig. 5.10 Comparison of (a) experimental and (b) simulated isotope pattern for $[Mo(\eta\text{-}C_7H_7)(NAr)]^+$ (Ar = 2,6-diisopropylphenyl)

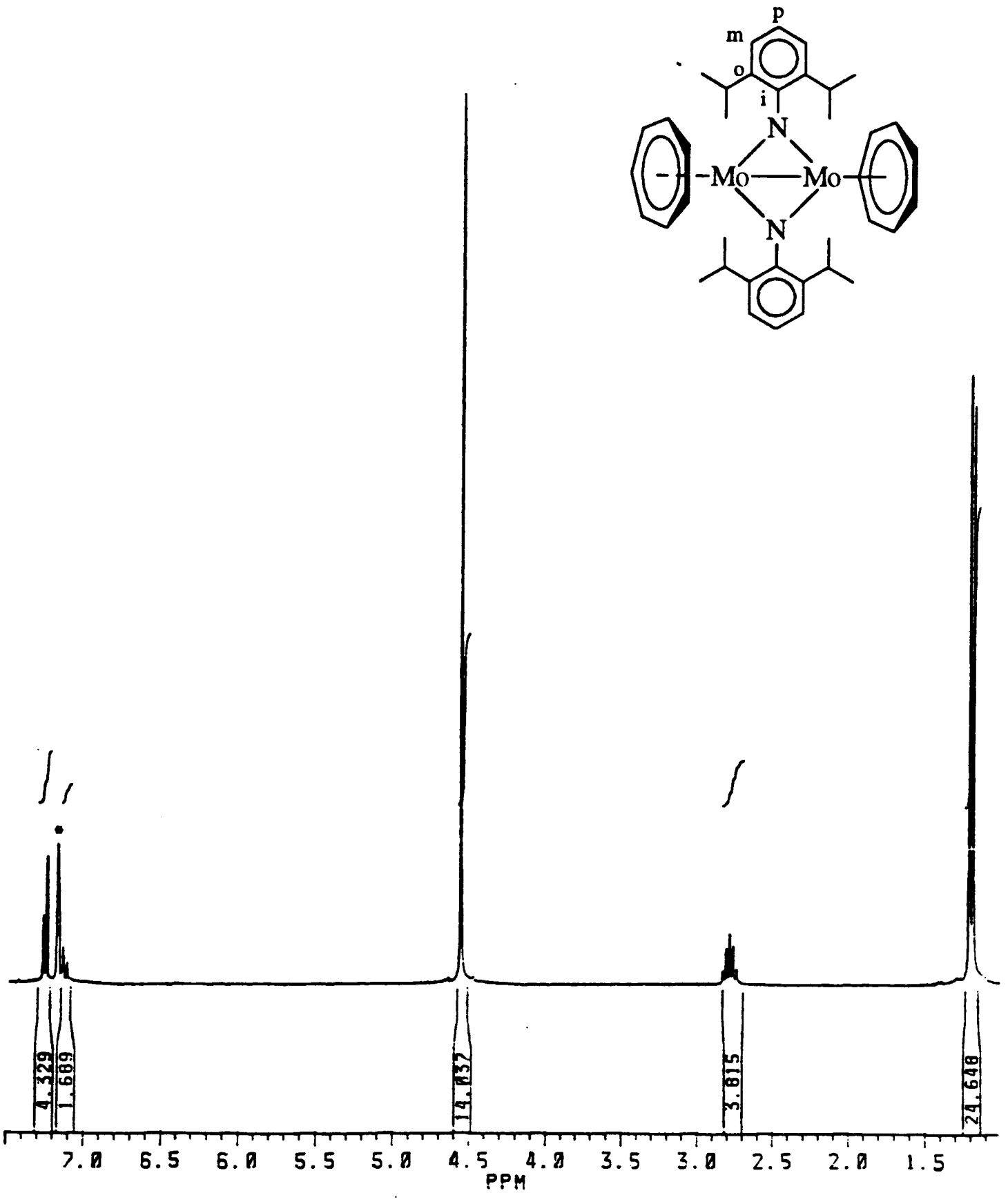

Fig. 5.11 ^1H NMR spectrum of $[(\eta\text{-}C_7H_7)Mo(\mu\text{-}NAr)_2Mo(\eta\text{-}C_7H_7)]$ (Ar = 2,6-diisopropyl-phenyl) in $[^2H_6]$-benzene : *indicates solvent

There is substantial evidence that the η-C_7H_7 ligand requires three electrons from the metal centre in the formation of the metal-ligand bond.[19] By considering that the imido ligand is a four electron donor and a metal-metal bond is involved, compound **41** should be considered as a formally d^0 compound and both metal centres have 18 electrons.

Preliminary studies on the reactivity of the bridging-imido compound **41** showed that this compound remained intact upon treatment with PMe_3 or PPh_3.

5.2.3 Summary

In summary, a novel bridging-imido η-cycloheptatrienyl-molybdenum compound **41** has been described in this section. This represents the first example of a transition-metal imido compound with η-cycloheptatrienyl ligand. The reaction and the proposed structure for **41** are shown in Scheme 5.4.

5.3 References

1 C. J. Casewit and M. Rakowski Dubois, *J. Am. Chem. Soc.* , 1986, **108**, 5482 and references therein.

2 (a) D. Coucouvanis, *Acc. Chem. Res.*, 1991, **24**, 1; (b) R. H. Holm, *Chem. Soc. Rev.*, 1981, **10**, 455.

3 (a) D. Mohr, H. Wienand and M. L. Ziegler, *J. Organomet. Chem.*, 1977, **134** , 281; (b) I. B. Benson, S. A. R. Knox, P. J. Naish and A. J. Welch, *J. Chem. Soc., Chem. Commun.*, 1978, 878.

4 (a) E. F. Ashworth, J. C. Green, M. L. H. Green, J. Knight, R. B. A. Pardy and N. J. Wainwright, *J. Chem. Soc., Dalton Trans.*, 1977, 1693; (b) M. Green, H. P. Kirsch, F. G. A. Stone and A. J. Welch, *J. Chem. Soc., Dalton Trans.*, 1977, 1755; (c) M. L. H. Green and R. B. A. Pardy, *Polyhedron*, 1985, **4**, 1035.

5 R. C. Tovey, D. Phil. Thesis, University of Oxford, 1986.

6 (a) E. W. Abel, R. P. Bush, F. J. Hopton and C. R. Jenkins, *J. Chem. Soc., Chem. Commun.*, 1966, 58; (b) P. Haake and P. C. Turley, *J. Am. Chem. Soc.* , 1967, **89**, 4611.

7 J. Sandström, *Dynamic NMR Spectroscopy*, Academic Press, New York, 1982.

8 (a) S. D. Killops and S. A. R. Knox, *J. Chem. Soc., Dalton Trans.*, 1978, 1260; (b) E. W. Abel, D. G. Evans, J. R. Koe, M. B. Hursthouse, M. Mazid, M. F. Mahon and K. C. Molloy, *J. Chem. Soc., Dalton Trans.*, 1990, 1697.

9 P. D. Frisch, M. K. Lloyd, J. A. McCleverty and D. Seddon, *J. Chem. Soc., Dalton Trans.*, 1973, 2268.

10 L. J. Lyons, M. H. Tegen, K. J. Haller, D. H. Evans and P. M. Treichel, *Organometallics*, 1988, **7**, 357.

11 D. P. S. Rodgers, D. Phil. Thesis, Oxford, 1984.

12 T. Boschi, B. Crociani, L. Toniolo and U. Belluco, *Inorg. Chem.*, 1970, **9**, 532.

13 D. Cruz-Garritz, J. Garcia-Alejandre, H. Torrens, C. Alvarez, R. A. Toscano, P. Poilblanc and A. Thorez, *Transition Met. Chem.*, 1991, **16**, 130.

14 (a) J. D. Burrington, C. Kartisek and R. K. Grasselli, *J. Catal.*, 1984, **87**, 363; (b) D. M. T. Chan, W. C. Fultz, W. A. Nugent, D. C. Roe and T. H. Tulip, *J. Am. Chem. Soc.*, 1985, **107**, 251; (c) D. M. T. Chan and W. A. Nugent, *Inorg. Chem.* , 1985, **24**, 1422; (d) D. E. Fjare and W. L. Gladfelter, *J. Am. Chem. Soc.* , 1981, **103**, 1572; (e) M. A. Andrews and H. D. Kaesz, *J. Am. Chem. Soc.*, 1979, **101**, 7255.

15 (a) J. Chatt, J. R. Dilworth and R. L. Richards, *Chem. Rev.*, 1978, **78**, 589; (b) D. Mansuy, P. Battioni and J. P. Mahy, *J. Am. Chem. Soc.*, 1982, **104**, 4487.

16 (a) J. Feldman and R. R. Schrock, *Prog. Inorg. Chem.*, 1991, **39** , 1; (b) R. R. Schrock, *Acc. Chem. Res.*, 1990, **23**, 158.

17 (a) P. J. Walsh, F. J. Hollander and R. G. Bergmann, *J. Am. Chem. Soc.*, 1988, **110**, 8729; (b) C. C. Cummins, S. M. Baxter and P. T. Wolczanski, *J. Am. Chem. Soc.*, 1988, **110**, 8731.

18 M. Bochmann, M. Green, H. P. Kirsch and F. G. A. Stone, *J. Chem. Soc., Dalton Trans.*, 1977, 714.

19 (a) C. E. Davies, I. M. Gardiner, J. C. Green, M. L. H. Green, N. J. Hazel, P. D. Grebenik, V. S. B. Mtetwa and K. Prout, *J. Chem. Soc., Dalton Trans.*, 1985, 669; (b) J. C. Green, M. L. H. Green, N. Kaltsoyannis, P. Mountford, P. Scott and S. J. Simpson, *Organometallics*, 1992, **11**, 3353; (c) N. Kaltsoyannis, D. Phil. Thesis, University of Oxford, 1992.

CHAPTER SIX

η-1,2,4,6-Tetramethylcycloheptatrienyl-

Molybdenum Chemistry

6.1 Introduction

Many studies of pentamethylcyclopentadienyl-transition metal derivatives show that ring methylation can have a considerable influence on the structure and properties of η-cyclopentadienyl-metal compounds.[1] Although considerable progress has been made in the development of η-cycloheptatrienyl-transition metal chemistry, the chemistry of highly ring-substituted η-cycloheptatrienyl analogues remains virtually unexplored. This chapter describes the syntheses and reactions of 1,2,4,6-tetramethylcycloheptatrienyl derivatives of molybdenum.

6.2 Reaction of $[Mo(CO)_6]$ with 1,3,5,7-Tetramethylcycloheptatriene

The ligand 1,3,5,7-tetramethylcycloheptatriene was prepared in two steps according to the literature procedures (Scheme 6.1).[2,3] Treatment of 1,1-dichloroethane with iodoethane in the presence of $AlCl_3$ gave 1,1-diiodoethane. But in contrast to the procedure reported previously,[2] a small amount of 1-chloro-1-iodoethane (7 %) was also produced. Compound 1,1-diiodoethane was then treated with diethylzinc in mesitylene to give the ligand as a colourless liquid.[3]

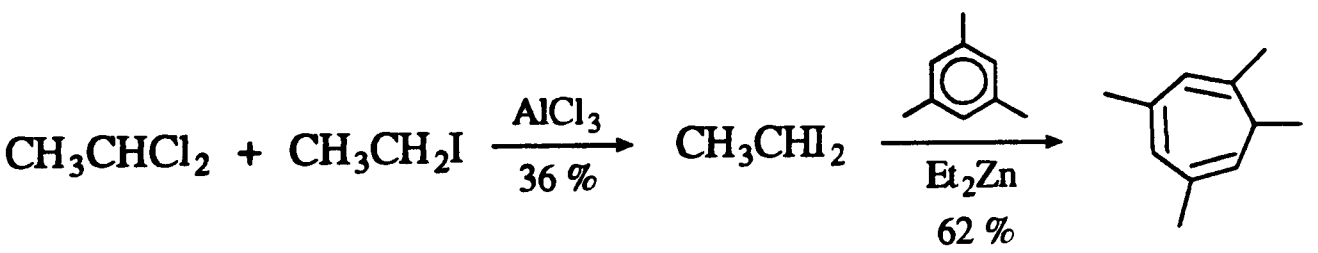

Scheme 6.1

A mixture of $[Mo(CO)_6]$ and 1,3,5,7-tetramethylcycloheptatriene in octane was heated at 140°C for 17 h to give a red suspension. A small amount of thf was also added to the reaction mixture to rinse down the sublimed $[Mo(CO)_6]$ along the Schlenk wall as it refluxed. Removal of the volatiles from the red suspension followed by extraction of the residue with light petroleum (b.p. 40-60°C) gave an orange-red solution. Cooling the

solution to -20°C produced orange crystals which were characterised as the compound [Mo(η^6-$C_7H_4Me_4$-1,3,5,7)$(CO)_3$] **43**. The mother-liquor was filtered, concentrated and cooled again to yield some further red crystals which were shown by ^1H NMR spectroscopy to be an inseparable mixture of [Mo(η^6-$C_7H_4Me_4$-1,2,4,6)$(CO)_3$] **44** and [Mo(η^6-$C_7H_4Me_4$-1,3,4,6)$(CO)_3$] **45** (Scheme 6.2).

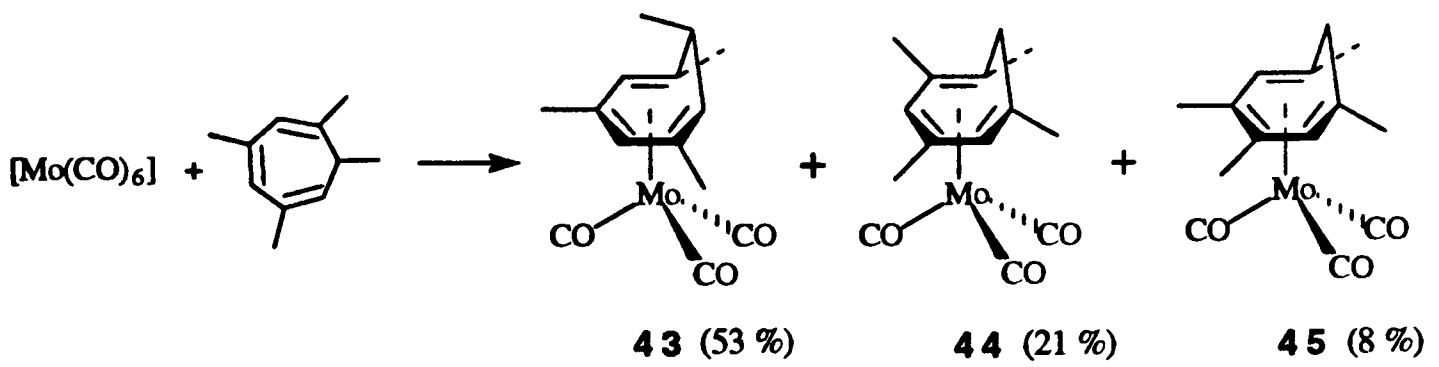

Scheme 6.2

Compound **43** was characterised by microanalysis and various spectroscopic methods. The mass spectrum (EI) showed the parent cation M^+ peak together with the signals due to successive loss of carbonyl ligand. The IR spectrum of **43** showed two rather broad and very strong bands at 1958 and 1870 cm^{-1} in the carbonyl region. These values are lower that those of the unsubstituted analogue [Mo(η^6-C_7H_8)$(CO)_3$] by about 30 cm^{-1}.[4] Predictably, the enhancement of electron density in the metal centre due to the four methyl groups increases the extent of backbonding and decreases the value of ν (CO).

By examination of models, it has been shown that the dihedral angle between the axial H_7 and $H_{1,6}$ in cycloheptatriene is *ca.* 125°, whereas the corresponding angle for the equatorial H_7 is *ca.* 4°.[5] For such angles the Karplus curve[6] predicts coupling constants of 4 and 8 Hz respectively. From the ^1H NMR spectrum of **43** in [$^2H_6$]-benzene (Fig. 6.1), it can be determined that the coupling constant between H_f and H_g is 8.4 Hz, which suggests that compound **43** is an *exo*-isomer.

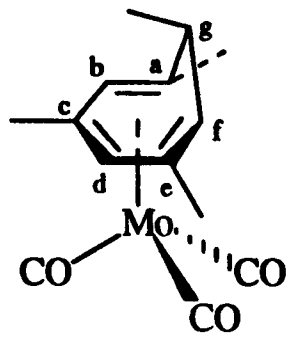

Fig. 6.1 ^{1}H NMR spectrum of [Mo(η^6-$C_7H_4Me_4$-1,3,5,7)(CO)$_3$] **43** in [$^2H_6$]-benzene : *indicates solvent

Fig. 6.2 shows the ^{13}C NMR spectra of **43**. The carbonyl absorptions were not observed due to the long relaxation time and the assignments were assisted by a series of DEPT experiments. Fig. 6.2(b) shows only the CH absorptions whilst Fig. 6.2(c) shows the CH and CH_3 absorptions with positive intensity and CH_2 absorption with negative intensity (not observed in this case). The three bands with lower intensity at δ 112.3, 109.7 and 90.6 in Fig. 6.2(a) are obviously due to the quaternary carbons C_a, C_c and C_e. Since C_a is expected to have a distinct environment, the upfield signal at δ 90.6 is assigned to it. The bands at δ 100.7 and 100.5, which are not resolved in Fig. 6.2(b) and Fig. 6.2(c), are assigned to C_b and C_d. The bands at δ 66.4 and 38.7 are attributed to C_f and C_g respectively and the remaining four signals at δ 26.62, 26.57, 26.0 and 24.0 are due to the four methyl groups.

From the NMR spectra of samples containing different proportion of the compounds **44** and **45**, it was possible to identify the bands due to each compound and to make partial assignments. The data are listed in Appendix A4.

Pauson and co-workers reported that the 7-*endo*-hydrogen atom of substituted cycloheptatriene complexed to chromium was able to migrate in a 1,5-shift manner (Scheme 1.8, p.10).[7] Based on the stepwise nature and stereospecificity of the rearrangement, the transition state **1** was postulated. On this basis, the formation of **44** and **45** may be ascribed to a series of sequential [1,5] hydrogen migrations in the initially formed compound **43**. The above assumption was tested by heating a solution of pure compound **43** in octane at 120°C for 10 h. The ^1H NMR spectrum of the resulting solution showed that it contains the compounds **43**, **44** and **45** in the ratio 6 : 2.5 : 1 respectively. This ratio is close to that found in the initial reaction (Scheme 6.2). The ratio may represent the equilibrium distribution of compounds **43**, **44** and **45**. Pauson and co-workers also reported that substituents in the 1-position might hinder the formation of the proposed transition state. As a result, compounds having 1- and 6-substitution did not undergo further rearrangement.[7] Thus, the presence of compounds **44** and **45** only but not of other isomers of **43** is understandable.

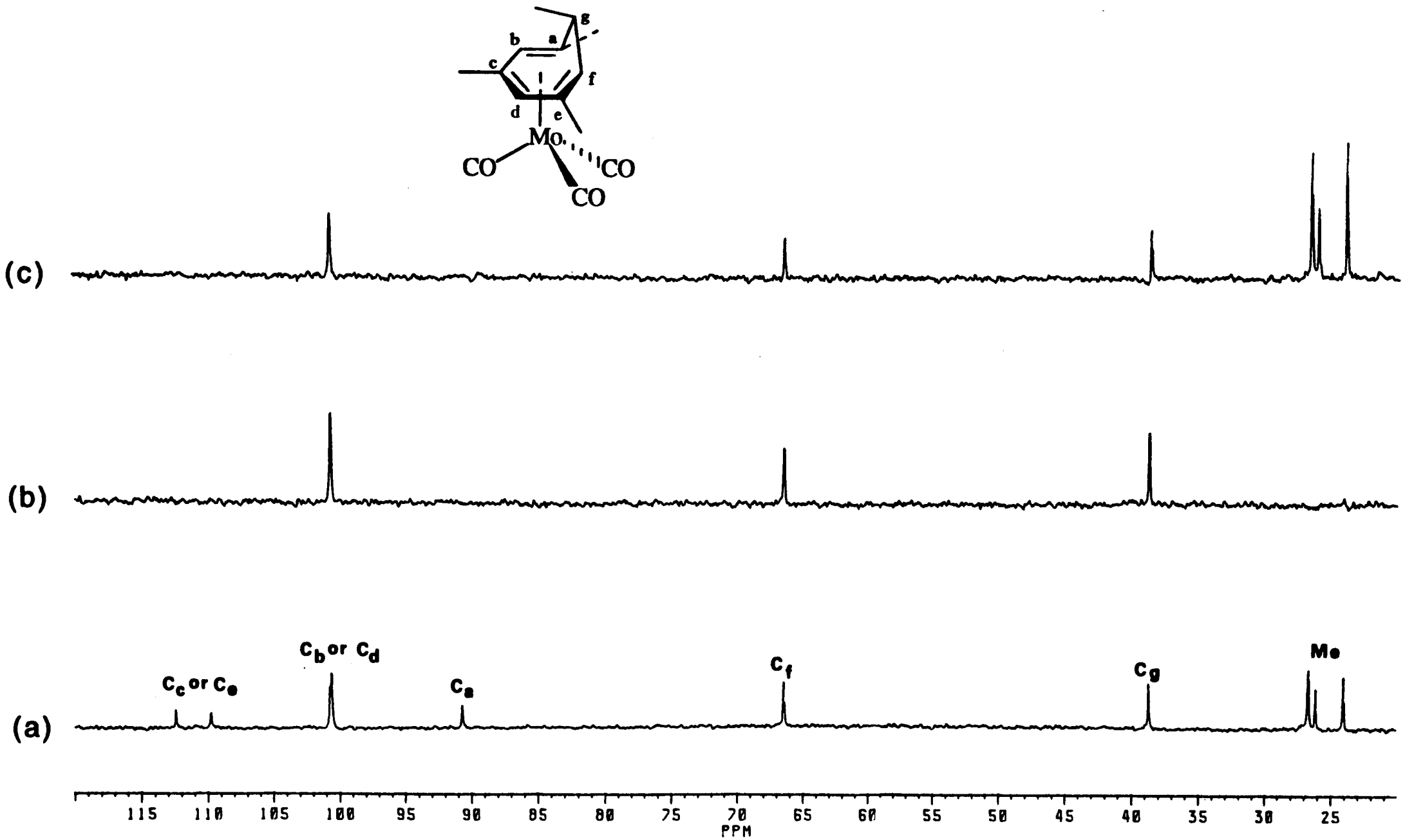

Fig. 6.2 ^{13}C NMR spectra of $[Mo(\eta^6\text{-}C_7H_4Me_4\text{-}1,3,5,7)(CO)_3]$ **43** in $[^2H_6]$-benzene. (a) $^{13}C\{^1H\}$, (b) DEPT ($\theta = \pi/2$), (c) DEPT ($\theta = 3\pi/4$)

6.3 Preparation and Characterisation of [Mo(η-$C_7H_3Me_4$-1,2,4,6)$(CO)_3$]-[BF_4]

Treatment of **43** with one equivalent of [CPh_3][BF_4] in dichloromethane at 60°C for 32 h gave the tetramethylcycloheptatrienyl-molybdenum compound [Mo(η-$C_7H_3Me_4$-1,2,4,6)$(CO)_3$][BF_4] **46** in 38 % yield and 15 % of **43** was recovered (Scheme 6.3). The reaction requires more vigorous conditions than for the unsubstituted analogue. For comparison, the unsubstituted analogue of **46**, namely [Mo(η-C_7H_7)$(CO)_3$][BF_4] can be prepared in excellent yield by treating [Mo(η^6-C_7H_8)$(CO)_3$] with [CPh_3][BF_4] in dichloromethane at room temperature for 1 h.[8] The reaction between [CPh_3][BF_4] and a mixture of **43**, **44** and **45** (2 : 3 : 1) in dichloromethane at 60°C for 7 h also afforded compound **46**. The yield was 86 % and 67 % of **43** was recovered. These results showed that **44** and **45** undergo hydride elimination much more readily than **43**. Probably, the 7-*exo*-methyl group of **43** hinders the approach of the bulky [CPh_3]+ cation.

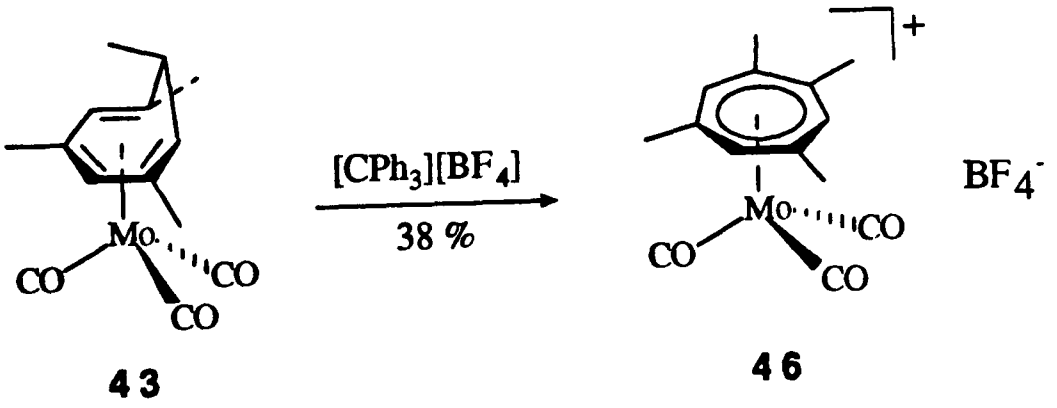

43 **46**

Scheme 6.3

Microanalysis for **46** was consistent with the proposed formulation and the mass spectrum (FAB) showed the parent cation M+ signal and peaks due to successive loss of carbonyl ligand. The IR spectrum of **46** showed two very strong carbonyl absorptions at 2055 and 2007 cm^{-1}, which are also lower than those of the unsubstituted analogue [Mo(η-C_7H_7)$(CO)_3$][BF_4].[9]

The ^1H NMR spectrum of **46** in [$^2H_6$]-acetone (Fig. 6.3) gives four singlets at δ 6.43, 6.22, 2.80 and 2.71 with relative intensity 2 : 1 : 6 : 6 assignable to the η-$C_7H_3Me_4$-1,2,4,6 group. The ^{13}C NMR spectrum exhibits an absorption at δ 210.7 for the carbonyl groups, four absorptions at δ 118.6, 116.6, 103.3 and 101.3 for the ring carbons and two absorptions at δ 26.2 and 25.0 for the methyl groups. These results clearly indicate the presence of a mirror plane in the molecule. These ^1H and ^{13}C NMR spectra are typical for all the other Mo(η-$C_7H_3Me_4$-1,2,4,6) complexes described below.

The electrochemistry of compound **46** was studied by cyclic voltammetry. A fully reversible wave at $E_{1/2}$ = +0.21 *vs.* SCE was observed in its voltammogram.

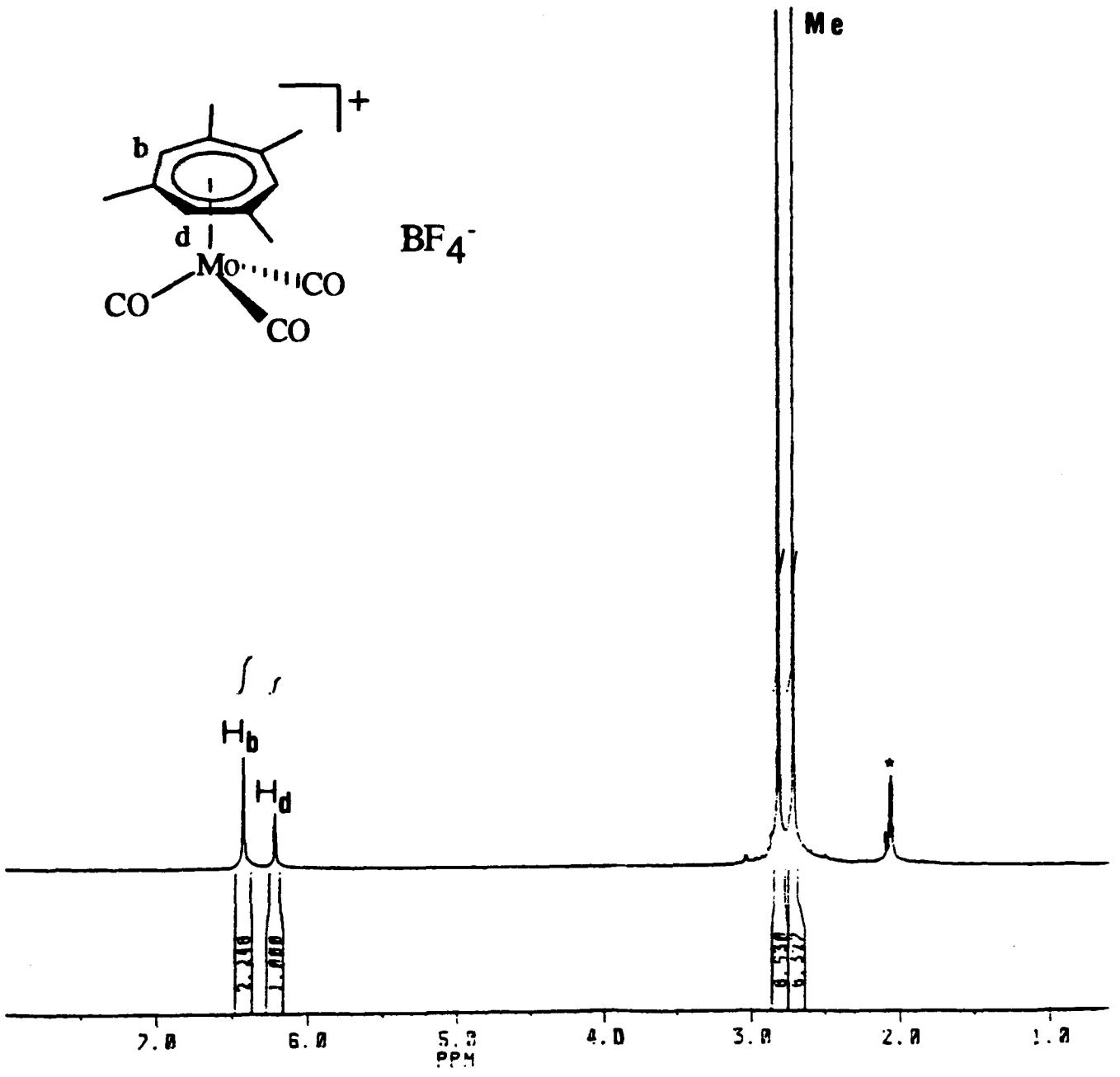

Fig. 6.3 ^1H NMR spectrum of [Mo(η-$C_7H_3Me_4$-1,2,4,6)$(CO)_3$][BF_4] **46** in [$^2H_6$]-acetone : *indicates solvent

6.4 Preparation and Characterisation of [Mo(η-$C_7H_3Me_4$-1,2,4,6)$(CO)_2Cl$]

An orange solution of **46** in acetone was treated with one equivalent of LiCl giving dark green crystals of [Mo(η-$C_7H_3Me_4$-1,2,4,6)$(CO)_2$Cl] **47** in good yield (Scheme 6.4). The NMR data of this compound were consistent with the proposed structure whilst the carbonyl stretching frequencies were lower than those of the unsubstituted analogue by about 40 cm^{-1}.[10] The mass spectrum (EI) of **47** did not show the parent cation M^+ peak, but peaks at m/z 595 and 280 (M - 2 CO) occurred in high intensity. The former peak may correspond to the species [Mo_2(η-$C_7H_3Me_4$-1,2,4,6)$_2Cl_3$] **48** formed by recombination reactions in the spectrometer. A similar result was observed for the mass spectra of the complexes [Mo(η-C_7H_7)$(CO)_2$X] (X = Cl, Br or I).[10]

It was attempted to prepare the compound **48** independently by refluxing a mixture of **46** with trimethylsilyl chloride in thf for 7 h.[10] The resulting deep green suspension was evaporated to dryness, then the residue was extracted with toluene. The ^1H NMR spectrum of the resulting green product showed that the toluene extract contained compound **47**. No compound **48** could be isolated.

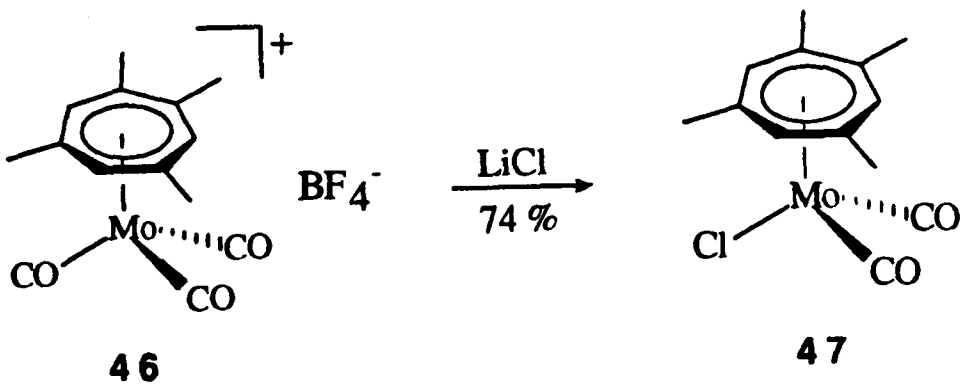

46 **47**

Scheme 6.4

6.5 Preparation and Characterisation of [Mo(η³-C₇H₃Me₄-1,2,4,6)(dmpe)(CO)₂Cl]

Addition of one equivalent of dmpe to a green solution of **47** in toluene gave a red solution from which the trihapto-bonded cycloheptatrienyl compound [Mo(η³-$C_7H_3Me_4$-1,2,4,6)(dmpe)$(CO)_2$Cl] **49** was isolated in good yield (Scheme 6.5). The related compound [Mo(η³-C_7H_7)(dppe)$(CO)_2$Cl] **50** has been prepared similarly.[11]

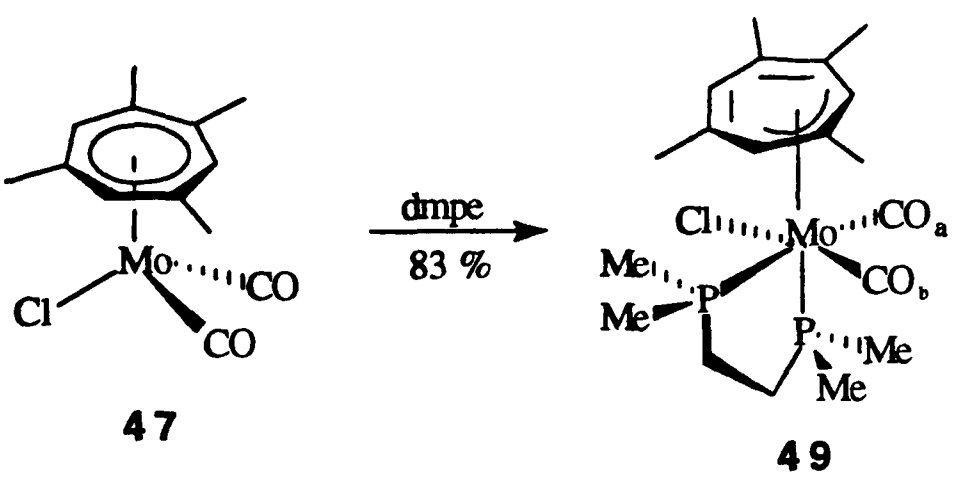

Scheme 6.5

It has been shown that some trihapto-cycloheptatrienyl complexes have extensive fluxional behaviour. The compound [Mo(η³-C_7H_7)(η-C_5H_5)$(CO)_2$] undergoes 1,2-shift of the metal group around the cycloheptatrienyl ring so that only one resonance due to the η-C_7H_7 protons is observed in the ^1H NMR spectrum at room temperature.[12] Whiteley and co-workers have reported that the compound **50** undergoes a trigonal twist process which interconverts the two P-donor atoms (Fig. 6.4).[11] The variable-temperature NMR spectra of **49** indicate that it has both fluxional properties. Thus the low temperature (230 K) $^{31}P\{^1H\}$ NMR spectrum of **49** exhibits a doublet of doublet pattern which shows that the two phosphorus atoms are inequivalent. The signals broaden at higher temperature and finally coalesce at 313 K (Fig. 6.5). The $\Delta G^{\ddagger}$ of this trigonal twist rearrangement was estimated to be 53.3 ± 0.4 kJ mol^{-1}.

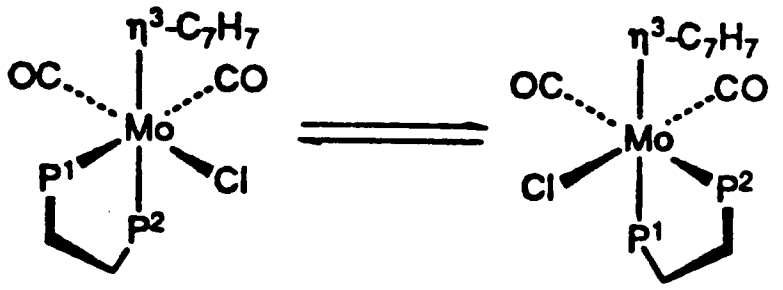

Fig. 6.4 Trigonal twist rearrangement proposed for [Mo(η3-C_7H_7)(dppe)$(CO)_2$Cl]

Fig. 6.6 shows the variable-temperature ^1H NMR spectra of **49** in [$^2H_6$]-acetone (220 K - 315 K) or [$^2H_8$]-toluene (323 K - 333 K). At the higher temperature (323 K), two doublets at δ 1.29 and 1.09 and two multiplets at *ca* . δ 1.4 and 1.0 are observed which may be assigned to the methyl and methylene groups in the dmpe ligand respectively. The presence of two methyl signals and two methylene signals reflects that a fast exchange process is operating which interconverts the two P-donor atoms. The remaining four signals may be assigned to the η3-$C_7H_3Me_4$-1,2,4,6 group. The simplicity of this pattern clearly indicates that another averaging process occurs on the C_7 ring. The rearrangement may involve 1,2-shift of the Mo atom about the cycloheptatrienyl ring as described previously.[12] Moreover, the fast trigonal twist rearrangement produces a pseudo-mirror plane across the C_7 ring so that only four signals arise for this ligand. Changing the solvent to [$^2H_6$]-acetone shifts the two methyl absorptions downfield and reduces the separation between them. At the lower temperature, the methyl absorptions overlap to become a broad signal which splits into four doublets at 230 K. Two of the doublets overlap at 220 K. The four doublets may be assigned to the four methyl groups in the dmpe ligand. The positions of the methylene absorptions are partially obscured due to their low intensity. The broad signal at δ 5.3 also splits into two signals of equal intensity at the lower temperature. It is worth noting that the two cycloheptatrienyl methyl absorptions broaden at different rates and both of them split into two signals at 240 - 250 K. The downfield signal broadens much faster than the upfield one and gives two signals with larger separation. The three broad signals for the cycloheptatrienyl protons and four broad signals for the methyl groups on C_7 ring indicate that the pseudo-mirror plane is removed at low temperature due to the slow trigonal twist process. However, the 1,2-shift of the Mo atom around the C_7 ring is still occurring even at 220 K.

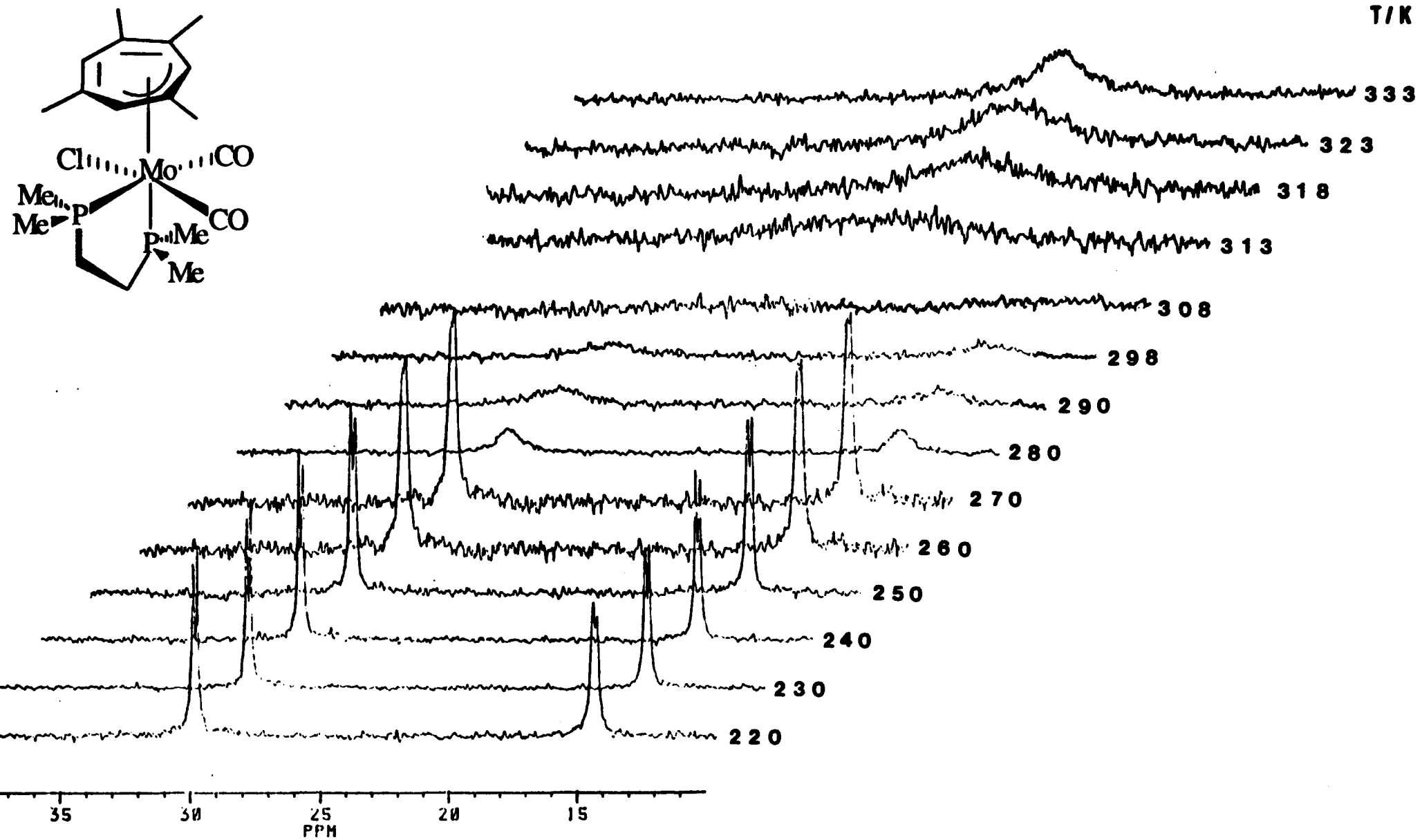

Fig. 6.5 Variable-temperature $^{31}P\{^{1}H\}$ NMR spectra of [Mo(η^3-$C_7H_3Me_4$-1,2,4,6)(dmpe)$(CO)_2Cl$] **49** in [$^2H_6$]-acetone (220 - 308 K) or [$^2H_8$]-toluene (313 - 333 K)

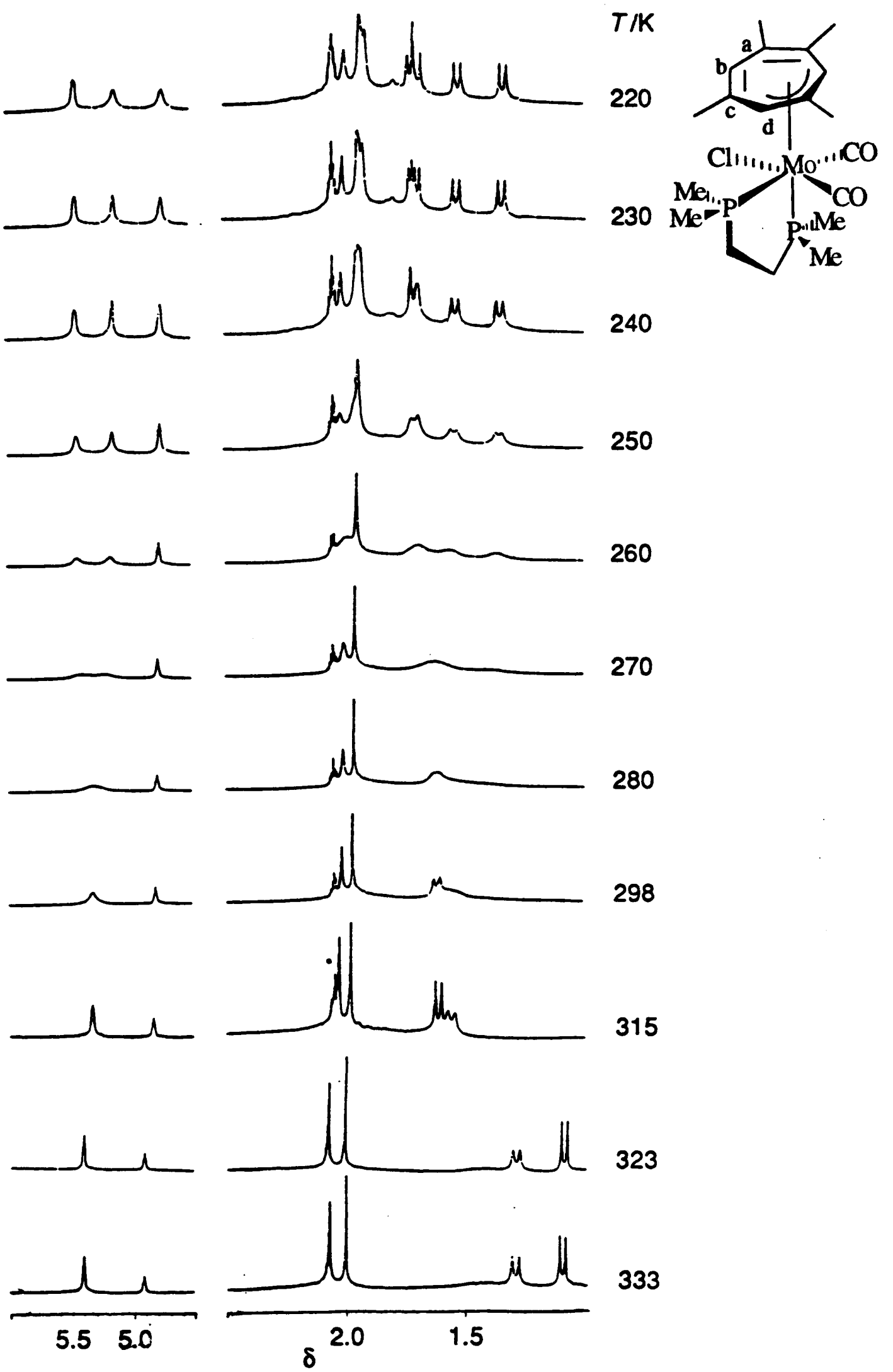

Fig. 6.6 Variable-temperature ^1H NMR spectra of [Mo(η^3-$C_7H_3Me_4$1,2,4,6)(dmpe)$(CO)_2Cl$] **49** in [$^2H_6$]-acetone (220 - 315 K) or [$^2H_8$]-toluene (323 - 333 K) : *indicates solvent

The IR and low-temperature ^{13}C NMR spectrum of **49** provide further evidence for the proposed structure. The IR spectrum of **49** shows two almost equally intense carbonyl stretching absorptions suggesting that the two carbonyl groups are *cis* to each other.[13] The ^{13}C NMR spectrum of **49** in [$^{2}H_6$]-acetone at 233 K (Fig. 6.7) exhibits a virtual triplet at δ 225.5 with average coupling constant 11 Hz and a virtual doublet of doublets at δ 229.6 with coupling constants 21 and 26 Hz. It was reported that the carbonyls *trans* to phosphorus showed a larger ^{31}P-^{13}C coupling than those oriented *cis* to phosphorus.[14] Thus the former band may be assigned to CO_b which is *cis* to both phosphorus atoms while the latter may be assigned to CO_a which is *cis* to one phosphorus atom but *trans* to the other.[11]

The parent cation M^+ peak could not be detected in the mass spectrum (EI) of **49**, but peaks at m/z 595 (**48**$^+$), 430 (M - 2 CO), 280 (M - 2 CO - dmpe) and 147 ($C_7H_3Me_4$) occurred with high intensity.

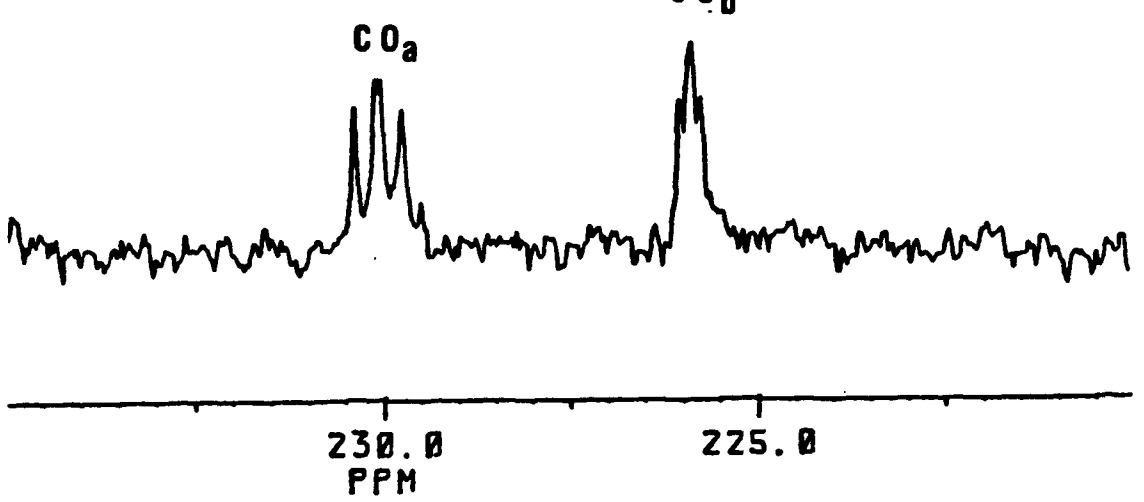

Fig. 6.7 ^{13}C {^{1}H} NMR spectrum of [Mo(η^3-$C_7H_3Me_4$-1,2,4,6)(dmpe)$(CO)_2Cl$] **49** in [$^{2}H_6$]-acetone at 233 K

6.6 Preparation and Characterisation of [Mo(η-$C_7H_3Me_4$-1,2,4,6)-(dmpe)Cl]

Heating a solution of **49** in toluene at 110°C for 8 h afforded a pale green solution from which only a mixture of unidentified products was obtained. However, photolysis of a solution of **49** in toluene at room temperature for 1 h yielded the oily green product [Mo(η-$C_7H_3Me_4$-1,2,4,6)(dmpe)Cl] **51** (Scheme 6.6). It is worth noting that this reaction has not been reported for the unsubstituted analogue.

Attempts to purify **51** by recrystallisation and sublimation were not successful, thus satisfactory microanalytical data could not be obtained. However, compound **51** was characterised by ^1H, ^{13}C and ^{31}P NMR spectroscopy. Fig. 6.8 shows the ^1H NMR spectrum of crude **51** in [$^2H_6$]-benzene, which is similar to those of [M(η-C_7H_7)(dmpe)I] (M = Mo or W). The two broad signals at δ 4.81 and 4.55 are due to H_b and H_d respectively which couple to the phosphorus atoms. The two singlets at δ 2.40 and 2.17 are attributed to the methyl groups in the C_7 ring. The spectrum also comprises two doublets at δ 1.34 and 0.94 assignable to two sets of methyl groups in dmpe, 'up' and 'down', and two multiplets at δ 1.12-1.30 and 0.56-0.82 assignable to two sets of methylene protons in dmpe. The $^{31}P\{^1H\}$ NMR spectrum showed a singlet at δ 31.4 assignable to the dmpe ligand and the ^{13}C NMR data was consistent with the proposed structure.

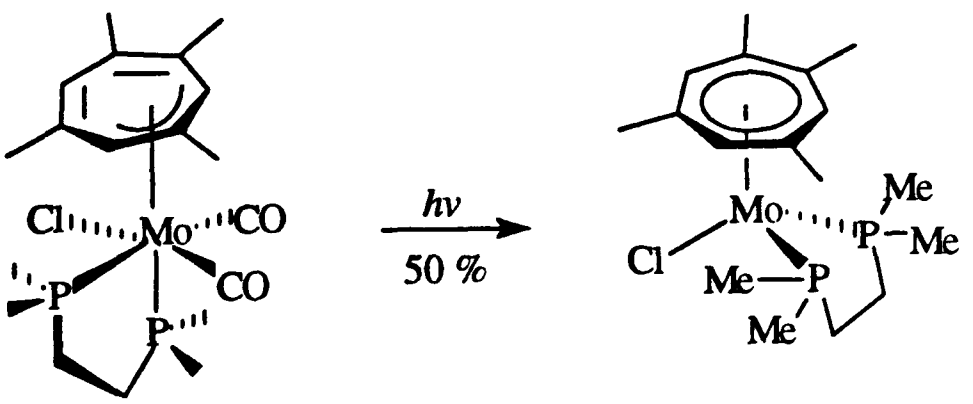

49 **51**

Scheme 6.6

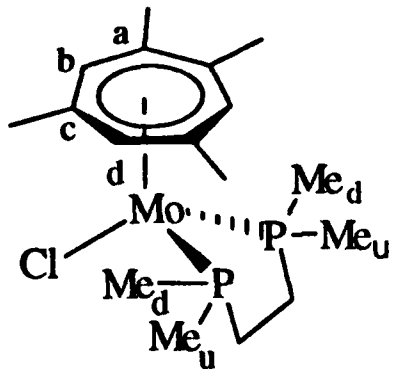

Fig. 6.8 ^{1}H NMR spectrum of [Mo(η-$C_7H_3Me_4$-1,2,4,6)(dmpe)Cl] **51** in [$^{2}H_6$]-benzene : *indicates solvent

6.7 Preparation and Characterisation of [Mo(η-$C_7H_3Me_4$-1,2,4,6)(η-C_6H_5Me)][BF_4]

Treatment of compound **46** with toluene at 120°C for 27 h led to the production of [Mo(η-$C_7H_3Me_4$-1,2,4,6)(η-C_6H_5Me)][BF_4] **52** as pale green crystals (Scheme 6.7). The microanalytical data for **52** were consistent with the proposed stoichiometry and the mass spectrum (FAB) showed the base peak at m/e 337, which could be assigned to the cation [Mo(η-$C_7H_3Me_4$-1,2,4,6)(η-C_6H_5Me)]$^+$.

The ^1H NMR spectrum of **52** in [$^2H_6$]-acetone is shown in Fig. 6.9. The two multiplets at δ 6.06-6.10 and 6.16-6.22 and the singlet at δ 2.25 are assigned to the coordinated toluene whilst the remaining four singlets at δ 5.89, 5.82, 2.49 and 2.46 with relative intensity 2 : 1 : 6 : 6 are typical for the η-$C_7H_3Me_4$-1,2,4,6 ligand.

The ^{13}C NMR data of **52** are consistent with the sandwich structure. Fig. 6.10(a) shows the $^{13}C\{^1H\}$ NMR spectrum of **52** in [$^2H_6$]-acetone. By comparing with the corresponding DEPT $^{13}C\{^1H\}$ NMR spectrum [Fig. 6.10(b)], which only displays the CH and CH_3 signals, it can be concluded that the bands at δ 113.7, 99.7 and 99.2 in Fig. 6.10(a) are quarternary carbons; the first of these is assigned to C_i while the higher field pair are assigned to C_a and C_c. Based on the characteristic chemical shifts and the relative intensity of the signals, the rest of the bands can be assigned as shown in the figure.

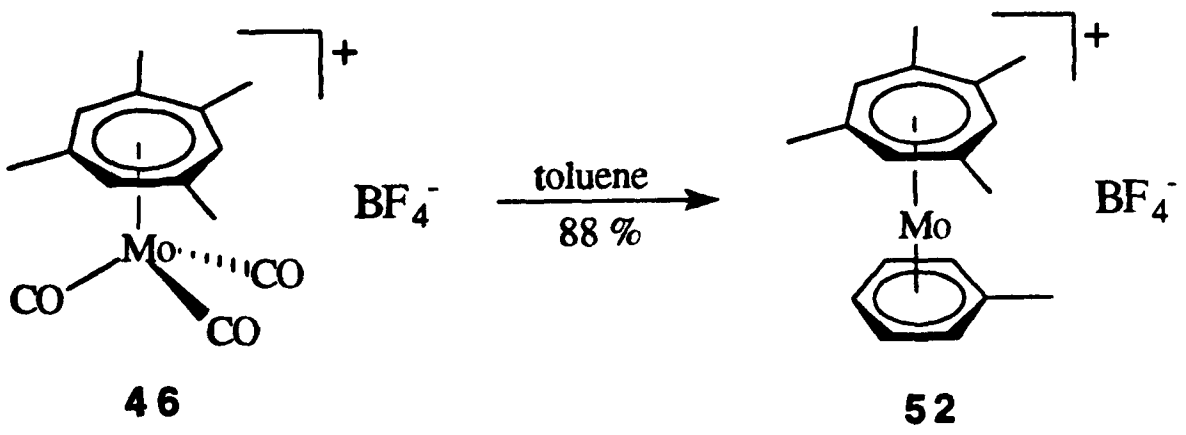

46 **52**

Scheme 6.7

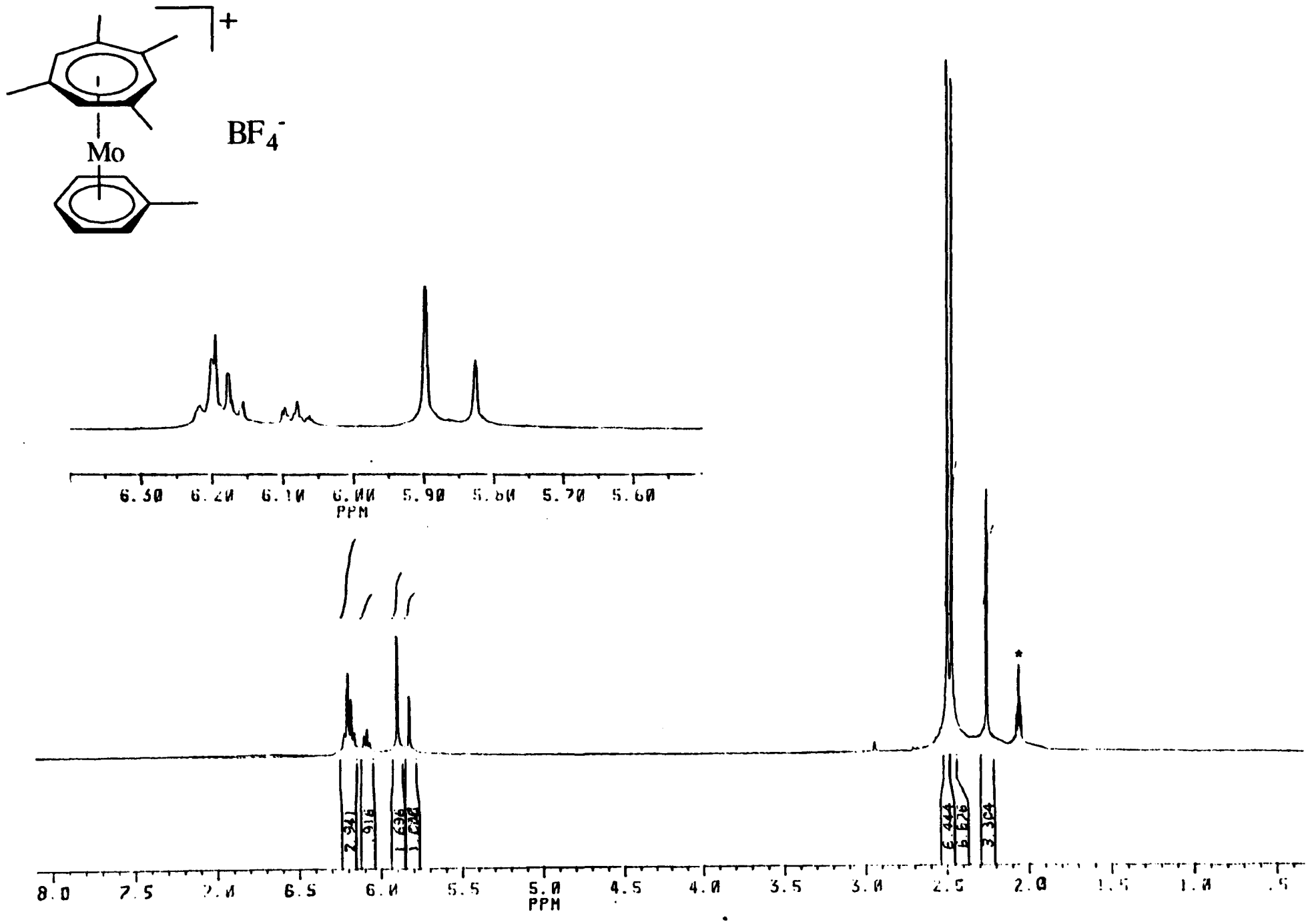

Fig. 6.9 ^{1}H NMR spectrum of $[Mo(\eta\text{-}C_7H_3Me_4\text{-}1,2,4,6)(\eta\text{-}C_6H_5Me)][BF_4]$ **52** in $[^{2}H_6]$-acetone : *indicates solvent

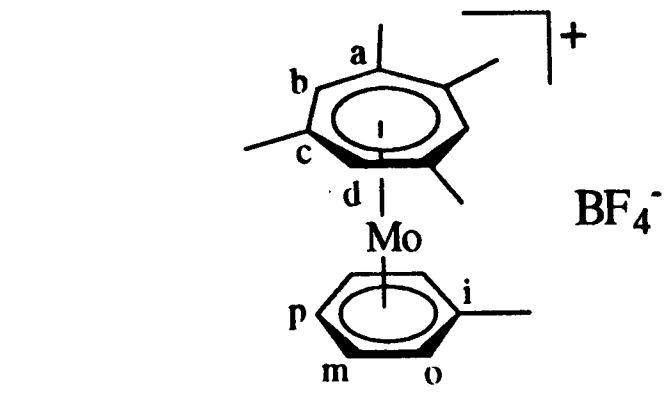

Fig. 6.10 ^{13}C NMR spectra of [Mo(η-$C_7H_3Me_4$-1,2,4,6)(η-C_6H_5Me)][BF_4] **52** in [$^2H_6$]-acetone. (a) $^{13}C\{^1H\}$, (b) DEPT ($\theta = 3\pi/4$) : *indicates solvent

6.8 Preparation and Characterisation of [Mo(η-$C_7H_3Me_4$-1,2,4,6)(acac)-(PPh_3)]

It has been shown that the unsubstituted analogue of **52**, namely [Mo(η-C_7H_7)(η-C_6H_5Me)][PF_6] is an excellent precursor of half-sandwich Mo(η-C_7H_7) compounds.[15] For example, it reacts with LiCl or ROH (R = Me or Et) to give the binuclear compounds [(η-C_7H_7)Mo(μ-Cl)$_3$Mo(η-C_7H_7)] or [(η-C_7H_7)Mo(μ-OR)$_3$Mo(η-C_7H_7)][PF_6] (R = Me or Et) respectively.[15a] However, the reactions of **52** with LiCl or PhOH failed to give the corresponding products and a significant amount of starting material **52** was recovered in both cases.

As discussed in chapter 5, compound **52** reacts with benzenethiol yielding the binuclear thiolato-bridged complex [(η-$C_7H_3Me_4$-1,2,4,6)Mo(μ-SPh)$_3$Mo(η-$C_7H_3Me_4$-1,2,4,6)][BF_4] in excellent yield. Treatment of **52** with sodium pentane-2,4-dionate and PPh_3 in MeOH gave a brown suspension from which red crystalline [Mo(η-$C_7H_3Me_4$-1,2,4,6)(acac)(PPh_3)] **53** was isolated (Scheme 6.8). Satisfactory microanalysis could not be obtained for this compound, but the mass spectrum (FAB) exhibited signals at m/z = 344 (M - PPh_3) and 147 ($C_7H_3Me_4$). This, together with the ^1H, ^{13}C and ^{31}P NMR data, suggested that **53** has the structure proposed below. The unsubstituted analogue has been prepared similarly.[15a]

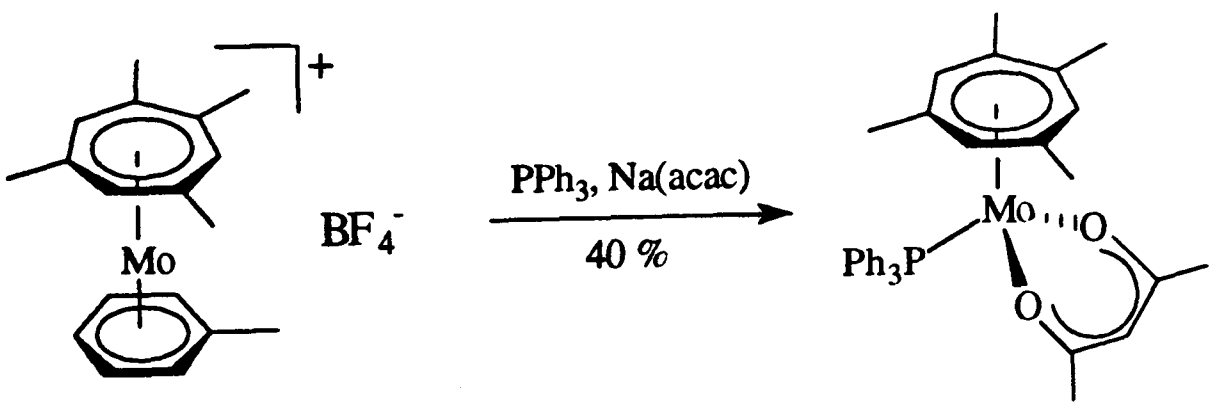

52 **53**

Scheme 6.8

The ^1H NMR spectrum of **53** in [$^2H_6$]-acetone is shown in Fig. 6.11. The two broad signals at δ 5.02 and 5.16 are attributed to H_b and H_d in the C_7 ring respectively. The occurrence of broad rather than sharp signals may indicate unresolved coupling to the phosphorus atom. Similar situation has been observed in the ^1H NMR spectra of compounds **49** and **51**. The resonance due to the methyl group in acac ligand is obscured by the solvent peaks. Changing the solvent to [$^2H_6$]-benzene reveals that these protons resonate as a sharp singlet at δ 1.97 (Fig. 6.12). The spectrum also shows that the multiplet at δ 7.26-7.54 due to the phenyl protons becomes two well-separated multiplets at δ 7.03-7.06 and 7.36-7.42 in 3 : 2 ratio and the bands due to H_d (δ 5.24) and H_e (δ 5.22) are close to each other. Spinning sidebands are also observed in the spectrum.

The ^{13}C NMR data of **53** is consistent with the proposed structure and the $^{31}P\{^1H\}$ NMR spectrum showed a singlet at δ -8.4 attributable to the PPh_3.

6.9 Reaction of $MoCl_5$ with Na/Hg and 1,3,5,7-Tetramethylcyclo-heptatriene

It has been demonstrated in chapter 2 that the compound [Mo(η-C_7H_7)(η^5-C_7H_9)] can be prepared readily by reducing $MoCl_5$ with sodium amalgam in the presence of cycloheptatriene. However, treatment of a thf suspension of $MoCl_5$ and 1,3,5,7-tetramethylcycloheptatriene with 5 equivalents of sodium amalgam failed to yield any tractable organometallic products.

6.10 Summary

The new η-1,2,4,6-tetramethylcycloheptatrienyl-molybdenum chemistry has been described in this chapter. The reactions and structures proposed for the new compounds are shown in the Scheme 6.9. The chemistry for the most part is closely similar to that of Mo(η-C_7H_7) analogues. However, the mixed ring cation **52** is clearly less reactive than [Mo(η-C_7H_7)(η-C_6H_5Me)]$^+$.

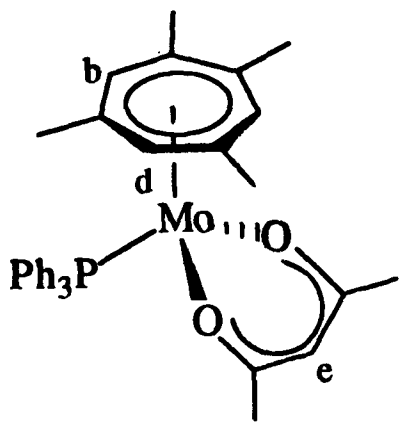

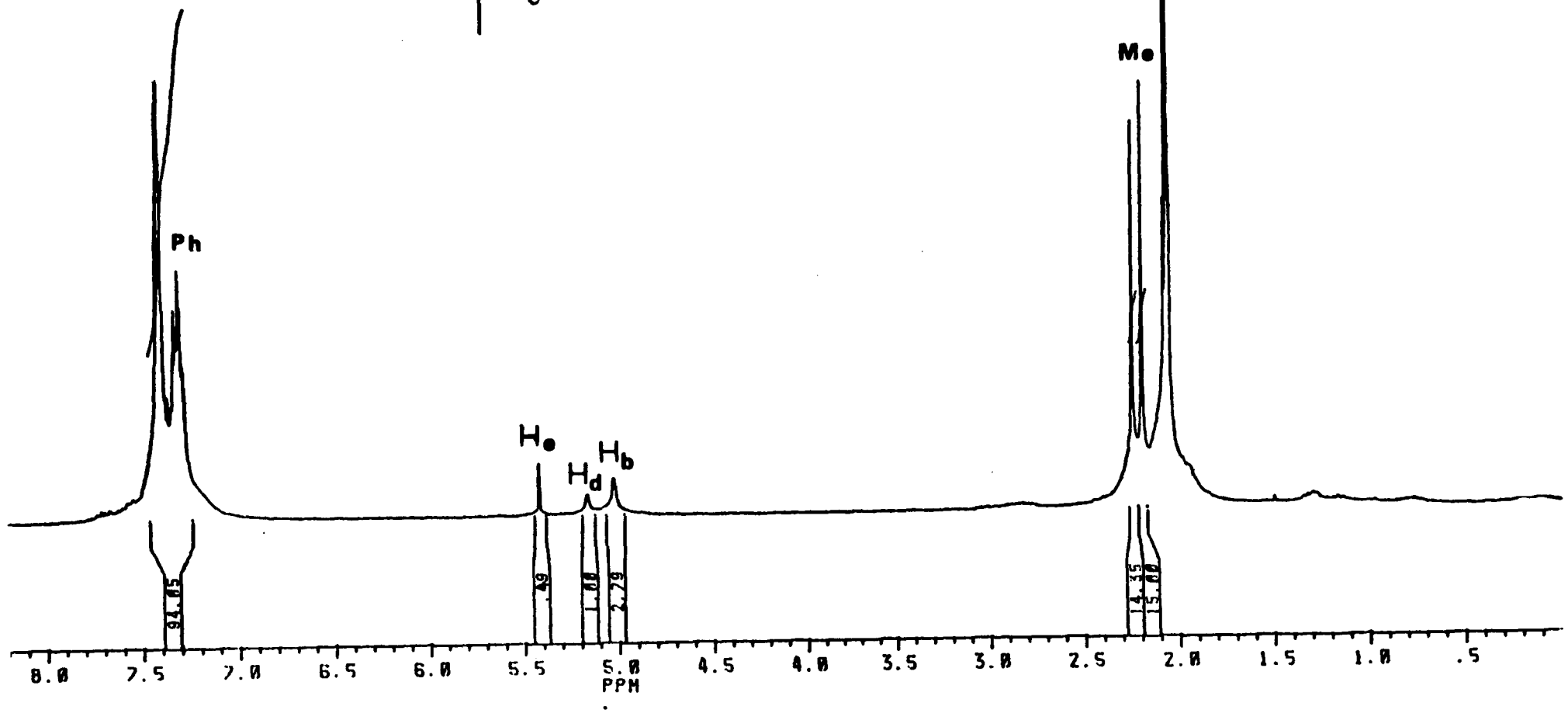

Fig. 6.11 ^{1}H NMR spectrum of $[Mo(\eta\text{-}C_7H_3Me_4\text{-}1,2,4,6)(acac)(PPh_3)]$ **53** in $[^{2}H_6]$-acetone : *indicates solvent

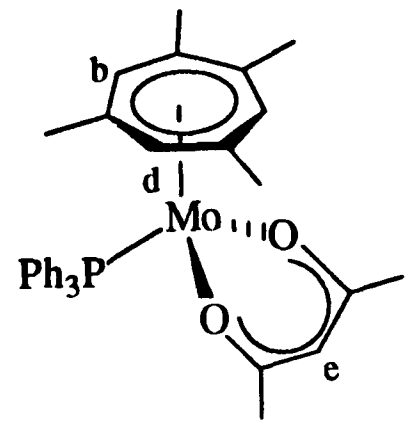

Fig. 6.12 ^{1}H NMR spectrum of [Mo(η-$C_7H_3Me_4$-1,2,4,6)(acac)(PPh_3)] **53** in [$^{2}H_6$]-benzene : *indicates solvent

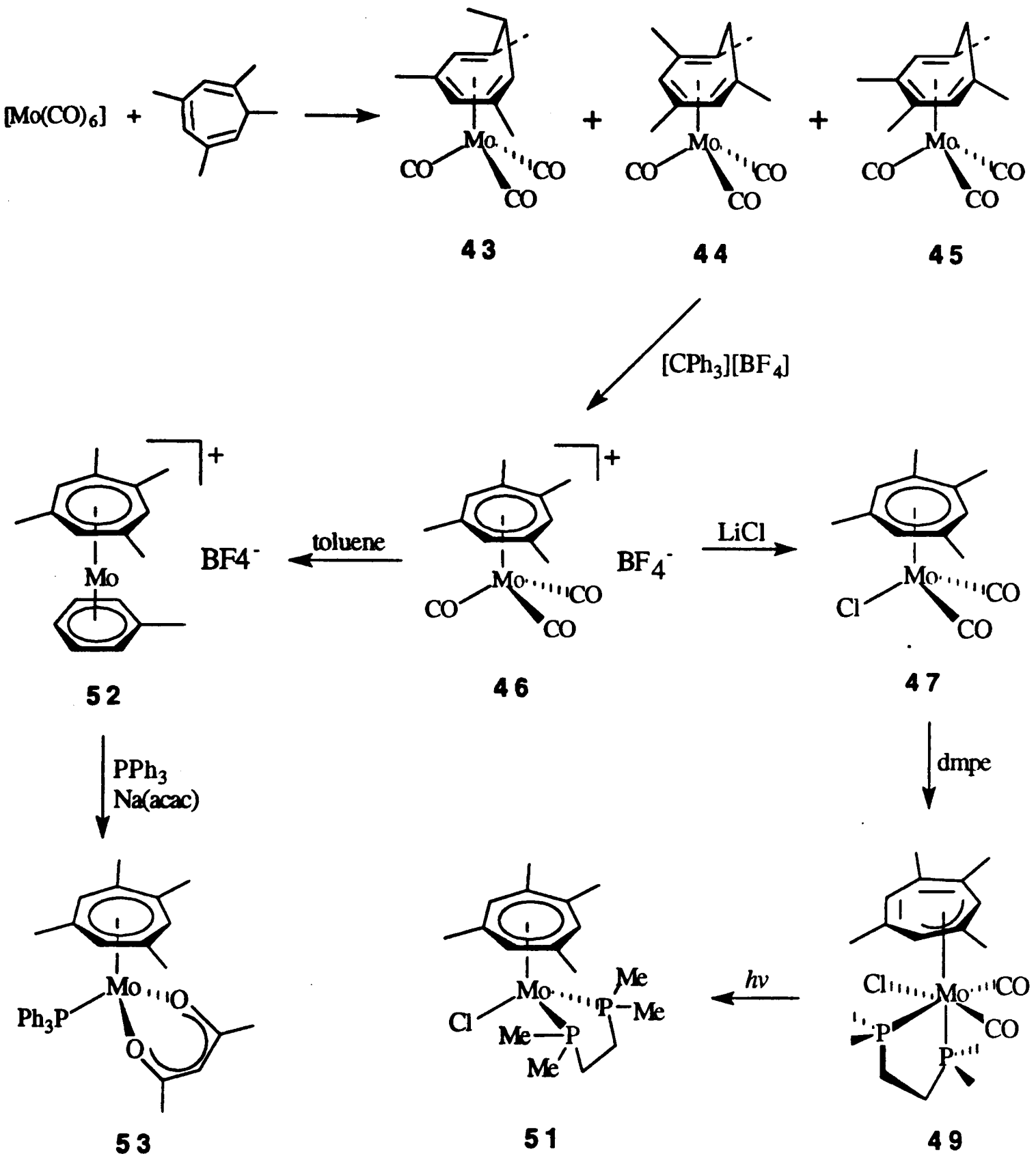
[Mo(CO)6]
43
44
45
[CPh3][BF4]
BF4-
toluene
BF4-
LiCl
52
46
47
PPh3
Na(acac)
dmpe
hv
53
51
49

Scheme 6.9

6.11 References

1 (a) F. G. N. Cloke, J. P. Day, J. C. Green, C. P. Morley and A . C. Swain, *J. Chem. Soc., Dalton Trans.*, 1991, 789; (b) J. A. Bandy, F. G. N. Cloke, G. Cooper, J. P. Day, R. B. Girling, R. G. Graham, J. C. Green, R. Grinter and R. N. Perutz, *J. Am. Chem. Soc.*, 1988, **110**, 5039 and references therein.

2 R. L. Letsinger and C. W. Kammeyer, *J. Am. Chem. Soc.*, 1951, **73**, 4476.

3 J. Nishimura, J. Furukawa, N. Kawabata and T. Fujita, *Tetrahedron*, 1970, **26**, 2229.

4 F. A. Cotton, J. A. McCleverty and J. E. White, *Inorg. Synth.*, 1967, **9**, 121.

5 P. L. Pauson, G. H. Smith and J. H. Valentine, *J. Chem. Soc. (C)*, 1967, 1057.

6 M. Karplus, *J. Chem. Phys.*, 1959, **30**, 11.

7 M. I. Foreman, G. R. Knox, P. L. Pauson, K. H. Todd and W. E. Watts, *J. Chem. Soc., Perkin Trans.*, 1972, 1141.

8 R. B. King, *Organometallic Synthesis*, Academic Press, New York, 1965, p.141.

9 P. D. Harvey, I. S. Butler and D. F. R. Gilson, *Inorg. Chem.*, 1987, **26**, 32.

10 M. Bochmann, M. Green, H. P. Kirsch and F. G. A. Stone, *J. Chem. Soc., Dalton Trans.*, 1977, 714.

11 R. A. Brown, S. Endud, J. Friend, J. M. Hill and M. W. Whiteley, *J. Organomet. Chem.*, 1988, **339**, 283.

12 (a) J. W. Faller, *Inorg. Chem.*, 1969, **8**, 767; (b) M. A. Bennett, R. Bramley and R. Watt, *J. Am. Chem. Soc.*, 1969, **91**, 3089.

13 A. T. T. Hsieh and B. O. West, *J. Organomet. Chem.*, 1976, **112**, 285.

14 P. S. Braterman, D. W. Milne, E. W. Randall and E. Rosenberh, *J. Chem. Soc., Dalton Trans.*, 1973, 1027.

15 (a) E. F. Ashworth, J. C. Green, M. L. H. Green, J. Knight, R. B. A. Pardy and N. J. Wainwright, *J. Chem. Soc., Dalton Trans.*, 1977, 1693; (b) M. Green, H. P. Kirsch, F. G. A. Stone and A. J. Welch, *J. Chem. Soc., Dalton Trans.*, 1977, 1755; (c) M. L. H. Green and R. B. A. Pardy, *Polyhedron*, 1985, **4**, 1035.

CHAPTER SEVEN
Experimental Details

7.1 General

7.1.1 Techniques

All manipulations and reactions were carried out using either standard Schlenk-line techniques under an atmosphere of dinitrogen or in an inert atmosphere dry-box containing dinitrogen. Dinitrogen was purified by passage over a BTS catalyst and 5 Å molecular sieves.

Solvents and solutions were generally transferred through stainless steel cannulae using an overpressure of dinitrogen, and filtered using cannulae modified to be fitted with filter paper.

Ultraviolet photolyses were performed using a Hanovia UVS 500 500W medium-pressure ozone-free mercury lamp with the sample contained in a quartz ampoule.

7.1.2 Solvents and general materials

Solvents were thoroughly deoxygenated by repeated evacuation followed by admission of dinitrogen before use and were pre-dried by standing over 5 Å molecular sieves and then distilled under an atmosphere of dinitrogen from potassium (tetrahydrofuran), sodium (toluene), calcium hydride (acetonitrile), phosphorus pentaoxide (dichloromethane), or sodium-potassium alloy [light petroleum (b.p. 40-60°C), diethyl ether and pentane]. Deuteriated solvents for NMR studies were stored in Young's ampoules and transferred by pipette in the dry-box.

Cycloheptatriene (tech., Aldrich) was distilled and tcne was sublimed prior to use. Tetrabutylammonium hexafluorophosphate for cyclic voltammetric studies was recrystallised from thf. All other reagents were used as received.

7.1.3 Instrumental methods

^{1}H, ^{13}C and ^{31}P NMR spectra were recorded on a Brüker AM 300 spectrometer (^{1}H, 300 MHz; ^{13}C, 75.43 MHz; ^{31}P, 121.44 MHz). Spectra were referenced internally using the residual solvent (^{1}H) and solvent (^{13}C) resonances relative to tetramethylsilane ($\delta = 0$ ppm), or externally using trimethyl phosphate [$PO(OMe)_3$] in D_2O (^{31}P). All chemical shifts are quoted in δ (ppm) and coupling constants in Hertz (Hz).

EPR spectra were obtained using an X-band Varian spectrometer and an Oxford Instruments cryostat or a Brüker ESP 300 spectrometer. The field was calibrated using 1,1-diphenyl-2-picryl hydrazyl ($g = 2.0037$). The samples were prepared under an atmosphere of dinitrogen and recorded in quartz tubes fitted with a Young's Teflon stopcock.

Infra-red spectra were recorded on a Perkin Elmer 1510 FT interferometer, a

Mattison Instruments Polaris Fourier transform spectrometer or a Perkin Elmer 457 grating spectrometer, on which spectra below 400 cm^{-1} were obtained.

Low-resolution mass spectra were obtained on an AEI MS 302 mass spectrometer or by the SERC mass spectrometry service, University College, Swansea. The m/z values quoted are based on the most abundant isotope of each element.

Cyclic voltammetry measurements were carried out using an Oxford Instruments potentiostat and recorded on a Rikadenki X-Y chart recorder. The cell used comprised a vacuum-tight chamber fitted with inlets for a platinum disc working electrode, a platinum gauze auxiliary electrode, and a silver wire pseudo-reference electrode. Typically, experiments were carried out using *ca.* 15 cm^3 of *ca.* 0.1 mol dm^{-3} tetrabutylammonium hexafluorophosphate in acetonitrile solution containing *ca.* 2 mg of sample under dinitrogen at ambient temperature. The potentials were referenced to the ferrocenium/ferrocene (Fc^+/Fc) couple at +0.355 V relative to the saturated calomel electrode (SCE), and the reversibility was judged by comparison of ΔE_p at various scan rates with that of the Fc^+/Fc internal standard.[1]

Magnetic susceptibility data were collected on a Cryogenics Consultants SCU 500 SQUID magnetometer in conjunction with a Lakeshore DRC-91C Temperature Controller. The susceptibilities were corrected for the intrinsic diamagnetism of the sample container and the diamagnetism of the electronic cores of the constituent atoms.

Photoelectron spectra were obtained using a PES laboratories 0078 spectrometer interfaced with a Research Machines 380Z microcomputer. Both He I (21.22 eV) and He II (40.81 eV) radiation were used for spectral aquisition. Data were collected by repeated scans and the spectra calibrated with He, Xe and N_2.

Powder X-ray diffraction data were obtained using Cu Kα radiation (40 kV, 30 mA) on a Philips PW1710 Powder Diffractometer. Lattice parameters were obtained by least-squares analysis of the peak positions.

Microanalyses were performed by the Microanalytical Services of the Inorganic Chemistry Laboratory, University of Oxford.

7.1.4 Literature preparations

The following compounds were prepared as described : $[MoCl_4(MeCN)_2]$,[2] $[MoCl_4(thf)_2]$,[2] $PhICl_2$,[3] ZrS_2,[4] $[Mo(\eta^6\text{-}C_7H_8)(CO)_3]$,[5] $[Mo(\eta\text{-}C_7H_7)(CO)_3][BF_4]$,[6] $[Mo(\eta\text{-}C_7H_7)(\eta\text{-}C_6H_5Me)][BF_4]$,[7] $[(\eta\text{-}C_7H_7)Mo(\mu\text{-}Cl)_3Mo(\eta\text{-}C_7H_7)]$,[8] CH_3CHI_2,[9] and 1,3,5,7-tetramethylcycloheptatriene.[10]

7.2 Reactions Discussed in Chapter 2

7.2.1 Preparation of [Mo(η-C_7H_7)(η^5-C_7H_9)] 5

(a) Cold thf (400 cm^3, -20^{0}C) was added slowly to $MoCl_5$ (10.0 g, 36.6 mmol) which was pre-cooled at -196^{0}C. The mixture was allowed to warm to -78^{0}C then degassed cycloheptatriene (20 cm^3, 0.19 mol) was added through a cannula. The suspension turned to yellow immediately. Then Na/Hg [4.2 g of Na (0.18 mol) in *ca.* 50 cm^3 of Hg] was added with stirring. The mixture was allowed to warm gradually to room temperature over 3 h, then it was kept stirring for a further 2 h at room temperature. The yellow suspension changed to brown, and then deep green during the course of the reaction. The volatiles were removed *in vacuo* and the residue was extracted with light petroleum (b.p. 40-60^{0}C) (4 x 75 cm^3). After filtration, the filtrate was cooled to -80^{0}C to give some green microcrystals which were collected by filtration. The filtrate was concentrated and cooled to give a second crop of green microcrystals. The ^{1}H NMR spectrum showed that it to be a mixture of [Mo(η^6-C_7H_8)$_2$] **4** and [Mo(η-C_7H_7)(η^5-C_7H_9)] **5** in 1.7 : 1 ratio. The combined green microcrystals were heated at 70^{0}C for 2 h to give the product as dark red microcrystals. Yield, 4.0 g (39 %).

(b) A mixture of [$MoCl_4$(thf)$_2$] (4.9 g, 12.8 mmol) and cycloheptatriene (9 cm^3) in thf (100 cm^3) was cooled to -60^{0}C, then Na/Hg [1.2 g of Na (52.2 mmol) in 20 cm^3 of Hg] was added slowly. The mixture was stirred vigorously and allowed to warm gradually to room temperature over 3 h. The mixture was kept stirring for a further 3 h at room temperature then the volatiles were removed *in vacuo*. The residue was extracted with light petroleum (b.p. 40-60^{0}C) (3 x 40 cm^3). The combined extract was then cooled to -80^{0}C and green microcrystals separated. The ^{1}H NMR spectrum showed that it to be a mixture of [Mo(η^6-C_7H_8)$_2$] **4** and [Mo(η-C_7H_7)(η^5-C_7H_9)] **5** in 3 : 2 ratio. The green microcrystals were heated at 70^{0}C for 2 h to give the product **5** as dark red microcrystals. Yield, 1.9 g (54 %).

7.2.2 Preparation of [Mo(η-C_7H_7)(MeCN)I_2] 6

A solution of iodine (0.53 g, 2.1 mmol) in MeCN (30 cm^3) was added slowly to a suspension of [Mo(η-C_7H_7)(η^5-C_7H_9)] **5** (0.59 g, 2.1 mmol) in MeCN (30 cm^3). The red suspension darkened gradually during addition. The mixture was heated at 50^{0}C for 1 h. After filtration, the residual purple solid was extracted with MeCN (3 x 30 cm^3). The combined MeCN extract was cooled to -20^{0}C and dark purple microcrystals

separated (0.54 g). The filtrate was concentrated to *ca.* 50 cm^3 then cooled to -20°C again to furnish a second crop of product (0.18 g). Combined yield, 0.72 g (71 %).

7.2.3 Preparation of [Mo(η-C_7H_7)(PMe_3)I_2] 7

The compound PMe_3 (0.1 cm^3, 1 mmol) was added to a suspension of [Mo(η-C_7H_7)(MeCN)I_2] **6** (0.48 g, 1 mmol) in thf (80 cm^3) at room temperature. The mixture was stirred for 3 h to give a red-green dichroic solution. After filtration, the filtrate was concentrated to *ca.* 30 cm^3 then cooled to -80°C to afford the product as dark red crystals. Yield, 0.41 g (79 %).

7.2.4 Preparation of [Mo(η-C_7H_7)(PMe_3)$_2$I] 8

A mixture of [Mo(η-C_7H_7)(MeCN)I_2] **6** (0.24 g, 0.5 mmol) and PMe_3 (0.1 cm^3, 1 mmol) in toluene (30 cm^3) was cooled to -60°C. Then Na/Hg [12 mg of Na (0.5 mmol) in *ca.* 0.5 cm^3 of Hg] was added with vigorous stirring. The mixture was allowed to warm to room temperature over 3 h and stirred at room temperature for a further 15 h. After filtration, the residue was washed with toluene (10 cm^3). The combined toluene solution was stripped to dryness to give the product as green microcrystals. Yield, 0.19 g (82 %).

7.2.5 Preparation of [Mo(η-C_7H_7)(dmpe)I] 9

A mixture of [Mo(η-C_7H_7)(MeCN)I_2] **6** (0.24 g, 0.5 mmol) and 1,2-bis(dimethylphosphino)ethane (0.8 cm^3 of a 0.1 g cm^{-3} solution in toluene, 0.5 mmol) in toluene (30 cm^3) was cooled to -60°C. Then Na/Hg [12 mg of Na (0.5 mmol) in *ca.* 0.5 cm^3 of Hg] was added with vigorous stirring. The mixture was allowed to warm to room temperature over 3 h and stirred at room temperature for a further 20 h. After filtration, the residue was washed with toluene (20 cm^3). The combined toluene solution was stripped to dryness to give a green solid which was purified by sublimation [*ca.* 160°C (0.02 mmHg)]. Yield, 0.14 g (61 %).

7.2.6 Preparation of [Mo(η-C_7H_7)(dppe)I] 10

A mixture of [Mo(η-C_7H_7)(MeCN)I_2] **6** (0.24 g, 0.5 mmol) and 1,2-bis(diphenylphosphino)ethane (0.20 g, 0.5 mmol) in toluene (30 cm^3) was cooled to

-60°C. Then Na/Hg [12 mg of Na (0.5 mmol) in *ca.* 0.5 cm^3 of Hg] was added with vigorous stirring. The mixture was allowed to warm to room temperature over 3 h and stirred at room temperature for a further 14 h. After filtration, the residue was washed with toluene (10 cm^3). The combined toluene solution was stripped to dryness to afford the product as a green solid. Yield, 0.23 g (65 %).

7.2.7 Preparation of [NBu_4][Mo(η-C_7H_7)I_3] 11

A mixture of [Mo(η-C_7H_7)(MeCN)I_2] **6** (0.10 g, 0.21 mmol) and tetrabutylammonium iodide (0.08 g, 0.21 mmol) in acetone (10 cm^3) was stirred at room temperature for 12 h. The volatiles were removed *in vacuo* and the residue was extracted with thf (10 cm^3) giving a purple solution. Diethyl ether was allowed to diffuse slowly into the thf solution over a few days to deposit the product as large purple crystals. Yield, 0.13 g (77 %).

7.2.8 Preparation of [Mo(η-C_7H_7)(η-C_5H_5)] 12

A mixture of [Mo(η-C_7H_7)(MeCN)I_2] **6** (0.12 g, 0.25 mmol) and NaC_5H_5 (0.09 g, 1.02 mmol) in thf (25 cm^3) was stirred at room temperature for 16 h. After removing the volatiles *in vacuo*, the residue was extracted with light petroleum (b.p. 40-60°C) (3 x 20 cm^3). The combined extract was concentrated to *ca.* 15 cm^3 then cooled to -80°C to give the product as brown crystals. Yield, 41 mg (65 %).

7.2.9 Preparation of [Mo(η-C_7H_7)(η-C_5H_4Me)] 13

A mixture of [Mo(η-C_7H_7)(MeCN)I_2] **6** (0.18 g, 0.37 mmol) and NaC_5H_4Me (0.15 g, 1.47 mmol) in thf (30 cm^3) was stirred at room temperature for 15 h. After removing the volatiles *in vacuo*, the residue was extracted with light petroleum (b.p. 40-60°C) (3 x 20 cm^3). The combined extract was concentrated to *ca.* 15 cm^3 then cooled to -80°C to give the product as green crystals. Yield, 85 mg (85 %).

7.2.10 Preparation of [Mo(η-C_7H_7)(η^5-C_9H_7)] 14

A mixture of [Mo(η-C_7H_7)(MeCN)I_2] **6** (0.12 g, 0.25 mmol) and lithium indenide (0.09 g, 0.74 mmol) in thf (20 cm^3) was stirred at room temperature for 12 h. After removing the volatiles *in vacuo*, the residue was extracted with light petroleum

(b.p. 40-60°C) (4 x 25 cm^3) to give a purple solution. The combined extract was concentrated to *ca.* 25 cm^3 then cooled to -80°C. The purple crystals formed were separated and recrystallised again from light petroleum (b.p. 40-60°C). Yield, 48 mg (64 %).

7.2.11 Polymerisation of norbornene using 6 as a catalyst

A suspension of [Mo(η-C_7H_7)(MeCN)I_2] **6** (35 mg) in toluene (50 cm^3) was treated with 300 equivalents of norbornene (2 g). There was no observable change. However, when a few drops of Me_3SiCH_2MgCl solution in diethyl ether was added, precipitation occurred almost immediately and the viscosity of the mixture increased. The mixture was stirred at room temperature for 17 h to give a yellow brown viscous solution. This was slowly poured into methanol (200 cm^3) with a small amount of N-phenyl-1-naphthylamine as a stabilizer. The jelly-like material formed was dissolved in hot toluene (*ca.* 80 cm^3) then the solution was added in dropwise to a large excess of methanol (500 cm^3) with vigorous stirring. White fibrous polymer was formed which was separated and then dried *in vacuo* (0.2 g).

7.2.12 Preparation of [Mo(η-C_7H_7)(MeCN)Cl_2] 15

A yellow suspension of $PhICl_2$ (0.45 g, 1.6 mmol) in toluene (15 cm^3) was added to a red solution of [Mo(η-C_7H_7)(η^5-C_7H_9)] **5** (0.2 g, 0.7 mmol) in toluene (15 cm^3). Precipitation occurred immediately. The mixture was stirred at room temperature for 1 h then filtered. The residue was extracted with MeCN (20 cm^3) to give a brown solution. The extract was then cooled to -20°C to afford the product as orange microcrystals. The filtrate was concentrated and cooled again to give a second crop of product. Combined yield, 0.12 g (54 %).

7.2.13 Preparation of [Mo(η-C_7H_7)(η-C_5H_4Me)][tcne] 16

A solution of tetracyanoethene (0.12 g, 0.94 mmol) in thf (5 cm^3) was added to a solution of [Mo(η-C_7H_7)(η-C_5H_4Me)] **13** (0.25 g, 0.94 mmol) in thf (20 cm^3). Precipitation occurred immediately and the solution darkened. The mixture was stirred at room temperature for *ca.* 15 min, then diethyl ether (30 cm^3) was layered. After 2 days, some black solid was deposited which was collected by filtration. The black solid was extracted with dichloromethane (3 x 10 cm^3) to give a dark red solution. The solution

was concentrated and cooled to -80°C to give the product as purple crystals. Yield, 0.12 g (32 %).

7.2.14 Preparation of {[Mo(η-C$_7$H$_7$)(η-C$_5$H$_5$)]$_2$[tcnq]} 17

A solution of [Mo(η-C_7H_7)(η-C_5H_5)] **12** (70 mg, 0.28 mmol) in dichloromethane (10 cm^3) was added to a suspension of 7,7,8,8-tetracyanoquinodimethane (57 mg, 0.28 mmol) in acetonitrile (10 cm^3). A green solution with small amount of precipitate was formed. The mixture was stirred at room temperature for *ca.* 15 min then it was filtered. Diethyl ether (40 cm^3) was layered onto the filtrate and the mixture was allowed to stand for a few days to give the product as a dark green solid. Yield, 50 mg (51 %).

7.2.15 Preparation of {ZrS$_2$[Mo(η-C$_7$H$_7$)(η-C$_5$H$_4$Me)]$_{0.22}$} 18

A mixture of [Mo(η-C_7H_7)(η-C_5H_4Me)] **13** (0.20 g, 0.75 mmol) and powdered ZrS_2 (0.22 g, 1.42 mmol) in toluene (2 cm^3) was heated at 120°C with stirring for 4 days. The mixture was allowed to settle then decanted. The residue was washed with toluene (4 x 10 cm^3) then dried *in vacuo*.

7.3 Reactions Discussed in Chapter 3

7.3.1 Preparation of [W(η-C$_7$H$_7$)(η^5-C$_7$H$_9$)] 19

Cold thf (400 cm^3, -20°C) was added slowly to WCl_6 (12.0 g, 30.3 mmol) which was pre-cooled at -196°C. The mixture was allowed to warm to -78°C then degassed cycloheptatriene (16 cm^3, 0.15 mol) was added through a cannula. Na/Hg [4.2 g of Na (0.18 mol) in *ca.* 50 cm^3 of Hg] was added slowly with stirring then the mixture was allowed to warm gradually to room temperature over 3 h. The mixture was kept stirring for a further 3 h at room temperature to give a greeenish brown suspension. The volatiles were removed *in vacuo* then the residue was extracted with light petroleum (b.p. 40-60°C) (3 x 100 cm^3). After filtration, the filtrate was concentrated to *ca.* 150 cm^3 then cooled to -80°C to afford a brown solid. This was collected by filtration and the filtrate was concentrated and cooled again to give a second crop of product. Combined yield, 3.0 g (27 %).

7.3.2 Preparation of [W(η-C_7H_7)(MeCN)I_2] 20

A solution of iodine (1.0 g, 4 mmol) in MeCN (30 cm^3) was added to a suspension of [W(η-C_7H_7)(η^5-C_7H_9)] **19** (1.5 g, 4 mmol) in MeCN (30 cm^3) over 10 min. The reddish brown suspension darkened gradually during the addition. The mixture was heated at 80^{0}C for 3 h to give a bright red solution which was filtered and the residue was washed with MeCN (5 cm^3). The combined MeCN extract was cooled to -20^{0}C to give dark red microcrystals (1.5 g). These were separated and the filtrate was concentrated to *ca*. 20 cm^3 and cooled to -20^{0}C to furnish a second crop of product (0.5 g). Combined yield, 2.0 g (86 %).

7.3.3 Preparation of [W(η-C_7H_7)(PMe_3)Br_2] 22

Bromine (0.83 g, 5.19 mmol) was added to a solution of [W(η-C_7H_7)(η^5-C_7H_9)] **19** (1.93 g, 5.24 mmol) in thf (60 cm^3). Precipitation occurred immediately. The suspension was stirred at room temperature for 15 min then PMe_3 (0.5 cm^3, 4.83 mmol) was added. The mixture was kept stirring for a further 2 h, then filtered. The residue was washed with thf (10 cm^3) and the combined filtrate was concentrated to *ca.* 50 cm^3 and cooled to -80^{0}C to give the product as orange brown crystals. Yield, 1.18 g (44 %).

7.3.4 Preparation of [W(η-C_7H_7)(PMe_3)I_2] 23

The compound PMe_3 (0.1 cm^3, 1 mmol) was added to a suspension of [W(η-C_7H_7)(MeCN)I_2] **20** (0.57 g, 1 mmol) in thf (40 cm^3). The mixture was stirred at room temperature for 1 h to give a deep red solution. After filtration, the filtrate was cooled to -20^{0}C to afford large red crystals which were collected by filtration and then dried *in vacuo*. The filtrate was concentrated to *ca.* 20 cm^3 and cooled to -80^{0}C to give a second crop of product. Combined yield, 0.42 g (70 %).

7.3.5 Preparation of [W(η-C_7H_7)(dmpe)I] 24

A mixture of [W(η-C_7H_7)(MeCN)I_2] **20** (0.43 g, 0.75 mmol) and 1,2-bis(dimethylphosphino)ethane (1.2 cm^3 of a 0.1 g cm^{-3} solution in toluene, 0.80 mmol) in thf (50 cm^3) was cooled to -60^{0}C. Then Na/Hg [18 mg of Na (0.78 mmol) in *ca.* 0.5 cm^3 of Hg] was added with vigorous stirring. The mixture was allowed to warm

to room temperature over 3 h and stirred at room temperature for a further 15 h. After filtration, the residue was washed with thf (10 cm^3). The combined thf solution was stripped to dryness and the residue was extracted with toluene (3 x 15 cm^3). Removal of the volatiles in the extract gave the product as a green solid. An analytically pure sample was obtained from sublimation [*ca.* 130°C (10^{-4} mmHg)]. Yield, 91 mg (22 %).

7.3.6 Preparation of [W(η-C_7H_7)(η-C_5H_5)] 25

(a) A mixture of [W(η-C_7H_7)(MeCN)I_2] **20** (0.11 g, 0.19 mmol) and NaC_5H_5 (0.07 g, 0.79 mmol) in thf (15 cm^3) was stirred at room temperature for 20 h. After removing the volatiles *in vacuo*, the residue was extracted with light petroleum (b.p. 40-60°C) (2 x 20 cm^3). The extract was concentrated to *ca.* 15 cm^3 and cooled to -80°C to give the product as dark brown crystals. Yield, 26 mg (40 %).

(b) To a solution of [W(η-C_7H_7)(η^5-C_7H_9)] **19** (1.3 g, 3.5 mmol) in thf (70 cm^3) was slowly added a solution of iodine (0.9 g, 3.5 mmol) in thf (70 cm^3). Precipitation occurred immediately and the resulting brown suspension was heated at 60°C for 2 h. It was then transferred to a Schlenk vessel containing NaC_5H_5 (1.2 g, 13.6 mmol). The mixture was stirred at room temperature for 16 h. The volatiles were then removed *in vacuo* and the residue was extracted with light petroleum (b.p. 40-60°C) (3 x 20 cm^3). The extract was concentrated to *ca.* 30 cm^3 and cooled to -80°C to afford the product as dark brown microcrystals. Yield, 0.17 g (14 %).

7.3.7 Preparation of [W(η-C_7H_7)(η-C_5H_4Me)] 26

(a) A mixture of [W(η-C_7H_7)(MeCN)I_2] **20** (0.15 g, 0.26 mmol) and NaC_5H_4Me (0.11 g, 1.08 mmol) in thf (20 cm^3) was stirred at room temperature for 20 h. After removing the volatiles *in vacuo*, the residue was extracted with light petroleum (b.p. 40-60°C) (3 x 20 cm^3). The extract was concentrated to *ca.* 15 cm^3 and cooled to -80°C to give the product as dark brown crystals. Yield, 74 mg (80 %).

(b) A mixture of [W(η-C_7H_7)(PMe_3)Br_2] **22** (0.20 g, 0.39 mmol) and NaC_5H_4Me (0.15 g, 1.47 mmol) in thf (30 cm^3) was stirred at room temperature for 16 h. The mixture was stripped to dryness and the residue was extracted with light petroleum (b.p. 40-60°C) (3 x 20 cm^3). The extract was concentrated to *ca.* 15 cm^3 and cooled to -80°C to afford the product as dark brown microcrystals. Yield, 83 mg (60

%).

(c) To a solution of [W(η-C_7H_7)(η^5-C_7H_9)] **19** (0.28 g, 0.76 mmol) in thf (30 cm^3) was slowly added a solution of iodine (0.19 g, 0.75 mmol) in thf (30 cm^3). The resulting brown suspension was heated at 60^{0}C for 2 h, then it was transferred to a Schlenk vessel containing NaC_5H_4Me (0.17 g, 1.66 mmol). The mixture was stirred at room temperature for 16 h. The volatiles were then removed *in vacuo* and the residue was extracted with light petroleum (b.p. 40-60^{0}C) (2 x 20 cm^3). The extract was cooled to -80^{0}C to afford the desired product. Yield, 0.13 g (50 %).

7.3.8 Preparation of [W(η-C_7H_7)(η^5-C_9H_7)] 27

A mixture of [W(η-C_7H_7)(MeCN)I_2] **20** (0.15 g, 0.26 mmol) and lithium indenide (0.10 g, 0.82 mmol) in thf (20 cm^3) was stirred at room temperature for 15 h. After removing the volatiles *in vacuo*, the residue was extracted with light petroleum (b.p. 40-60^{0}C) (3 x 15 cm^3) to give a purple solution which was filtered, concentrated to *ca.* 15 cm^3, and cooled to -80^{0}C. The purple crystals formed were recrystallised from light petroleum (b.p. 40-60^{0}C). Yield, 26 mg (25 %).

7.3.9 Polymerisation of norbornene using 20 as a catalyst

A suspension of [W(η-C_7H_7)(MeCN)I_2] **20** (20 mg) in toluene (30 cm^3) was treated with 300 equivalents of norbornene (1 g). The mixture was stirred at room temperature for 15 min without any observable change. However, when a few drops of Me_3SiCH_2MgCl solution in diethyl ether was added, precipitation occurred and the viscosity of the mixture increased. The mixture was stirred at room temperature for 24 h to give a very viscous green solution. This was slowly poured into methanol (200 cm^3) with a small amount of N-phenyl-1-naphthylamine as a stabilizer. The jelly-like material formed was dissolved in hot toluene (*ca.* 80 cm^3) then the solution was added in dropwise to a large excess of methanol (500 cm^3) with vigorous stirring. White fibrous polymer was formed which was separated and then dried *in vacuo* (0.53 g).

7.3.10 Preparation of {ZrS_2[W(η-C_7H_7)(η-C_5H_4Me)]$_{0.20}$} 28

A mixture of [W(η-C_7H_7)(η-C_5H_4Me)] **26** (0.3 g, 0.85 mmol) and powdered ZrS_2 (0.3 g, 1.93 mmol) in toluene (3 cm^3) was heated at 120^{0}C with stirring for 5 days.

The mixture was allowed to settle then decanted. The residue was washed with toluene (4 x 10 cm^3) then dried *in vacuo*.

7.4 Reactions Discussed in Chapter 5

7.4.1 Preparation of [(η-C_7H_7)Mo(μ-SBu)$_3$Mo(η-C_7H_7)][BF_4] 30

A mixture of [Mo(η-C_7H_7)(η-C_6H_5Me)][BF_4] **29** (1 g, 2.7 mmol) and butane-1-thiol (20 cm^3) was heated at 80°C for 4 h. The volatiles were removed from the resulting dark green suspension under reduced pressure and the resulting residue was extracted with thf (2 x 50 cm^3). The thf solution was concentrated to *ca.* 50 cm^3, then diethyl ether (20 cm^3) was added. Cooling to -20°C gave dark green microcrystals. These were collected by filtration. The filtrate was further concentrated and cooled to give a second crop of product. This step was repeated several times to give more product. Combined yield, 0.7 g (70 %).

7.4.2 Preparation of [(η-C_7H_7)Mo(μ-SPr)$_3$Mo(η-C_7H_7)][BF_4] 31

A suspension of green [Mo(η-C_7H_7)(η-C_6H_5Me)][BF_4] **29** (1 g, 2.7 mmol) in propane-1-thiol (30 cm^3) was heated at 75°C for 20 h. The mixture turned dark greenish red during the course of the reaction. The volatiles were removed *in vacuo*, then the residue was extracted with thf (2 x 40 cm^3) followed by acetone (2 x 30 cm^3). The combined extracts were concentrated to *ca.* 80 cm^3 and cooled to -20°C affording dark green microcrystals. After collecting the crystals by filtration, the filtrate was further concentrated and cooled to give a second crop of product. Combined yield, 0.28 g (30 %).

7.4.3 Preparation of [(η-C_7H_7)Mo(μ-SPh)$_3$Mo(η-C_7H_7)][BF_4] 32

(a) A mixture of [Mo(η-C_7H_7)(η-C_6H_5Me)][BF_4] **29** (4 g, 10.9 mmol) and benzenethiol (50 cm^3) was heated at 100°C for 6 h. After cooling to room temperature, light petroleum (b.p. 40-60°C) (150 cm^3) was added. A green solid precipitated and was collected by filtration and then washed with light petroleum (b.p. 40-60°C) (3 x 50 cm^3) to remove trace amounts of benzenethiol. The solid obtained after drying was essentially pure but it was recrystallised from an acetone-thf (1 : 2) mixture at -20°C. Yield, 3.7 g (87 %).

(b) A solution of $[Mo(\eta\text{-}C_7H_7)(\eta^5\text{-}C_7H_9)]$ **5** (0.2 g, 0.71 mmol) in diethyl ether (50 cm^3) was treated with an excess of $HBF_4{\cdot}Et_2O$ (*ca.* 1 cm^3). There was immediate precipitation of a light material and loss of colour of the solution. The solid was allowed to settle and the supernatant liquor was filtered off. The solid was washed with diethyl ether (30 cm^3) and dried *in vacuo*. Benzenethiol (5 cm^3) was then added and the mixture was heated at 80°C for 3 h. After cooling to room temperature, light petroleum (b.p. 40-60°C) (80 cm^3) was added. A dark green solid precipitated and was collected by filtration and washed with light petroleum (b.p. 40-60°C) (2 x 40 cm^3). The crude product was recrystallised from an acetone-thf mixture at -20°C. Yield, 0.2 g (71 %).

7.4.4 Preparation of $[(\eta\text{-}C_7H_7)Mo(\mu\text{-}SCH_2Ph)_3Mo(\eta\text{-}C_7H_7)][BF_4]$ 33

(a) A mixture of $[Mo(\eta\text{-}C_7H_7)(\eta\text{-}C_6H_5Me)][BF_4]$ **29** (1 g, 2.7 mmol) and phenylmethanethiol (15 cm^3) was heated at 100°C for 5 h. After cooling to room temperature, light petroleum (b.p. 40-60°C) (200 cm^3) was added to precipitate the product. The resulting greenish brown solid obtained after filtration was washed with light petroleum (b.p. 40-60°C) (2 x 50 cm^3) and dried *in vacuo*. The product was essentially pure, but it was recrystallised from an acetone-thf (1 : 2) mixture at -20°C. Yield, 1.0 g (88 %).

(b) The compound $[Mo(\eta\text{-}C_7H_7)(\eta^5\text{-}C_7H_9)]$ **5** (0.1 g, 0.36 mmol) was dissolved in diethyl ether (30 cm^3). The solution was treated with an excess of $HBF_4{\cdot}Et_2O$ (*ca.* 0.5 cm^3). There was immediate precipitation of a light material and loss of colour of the solution. The solid was allowed to settle and the supernatant liquor was filtered off. The solid was washed with diethyl ether (20 cm^3) and dried *in vacuo*. Phenylmethanethiol (3 cm^3) was then added and the mixture was heated at 90°C for 3 h. After cooling to room temperature, light petroleum (b.p. 40-60°C) (100 cm^3) was added. The brown solid precipitated was collected by filtration and then washed with light petroleum (b.p. 40-60°C) (2 x 30 cm^3). The crude product was recrystallised from an acetone-thf mixture at -20°C. Yield, 95 mg (64 %).

7.4.5 Preparation of $[(\eta\text{-}C_7H_7)Mo(\mu\text{-}SEt)_3Mo(\eta\text{-}C_7H_7)][BF_4]$ 34

A stirred suspension of $[Mo(\eta\text{-}C_7H_7)(\eta\text{-}C_6H_5Me)][BF_4]$ **29** (1 g, 2.7 mmol) and lithium thioethoxide (0.28 g, 4.1 mmol) in thf (40 cm^3) was heated at 60°C for 3 h.

The initially green suspension slowly darkened. After removing the volatiles *in vacuo*, the residue was extracted with toluene (2 x 50 cm^3). The insoluble oily material was extracted with thf (2 x 50 cm^3) followed by acetone (2 x 30 cm^3). The combined acetone-thf solution was concentrated to *ca.* 60 cm^3 and cooled to -20^{0}C. Some green solid was obtained which was recrystallised from acetone-thf to give the product as dark green microcrystals. Yield, 0.23 g (26 %).

7.4.6 Preparation of [(η-$C_7H_3Me_4$-1,2,4,6)Mo(μ-SPh)$_3$Mo(η-$C_7H_3Me_4$-1,2,4,6)][BF_4] 35

A mixture of [Mo(η-$C_7H_3Me_4$-1,2,4,6)(η-C_6H_5Me)][BF_4] **52** (0.1 g, 0.24 mmol) and benzenethiol (10 cm^3) was heated at 100^{0}C for 5 h. After cooling to room temperature, light petroleum (b.p. 40-60^{0}C) (200 cm^3) was added. The pale greenish yellow solution was decanted off and the residue was extracted with thf (3 x 20 cm^3). The thf solution was concentrated to *ca.* 40 cm^3 and cooled to -80^{0}C to give green microcrystals which were collected by filtration, washed with light petroleum (b.p. 40-60^{0}C) (10 cm^3) and dried *in vacuo*. The filtrate was concentrated and cooled again to give a second crop of product. Combined yield, 97 mg (91 %).

7.4.7 Preparation of [(η-C_7H_7)Mo(μ-NAr)$_2$Mo(η-C_7H_7)] (Ar = 2,6-diisopropylphenyl) 41

To a solution of 2,6-diisopropylaniline (0.75 cm^3, 4.0 mmol) in thf (10 cm^3) was added butyllithium (1.6 mol dm^{-3} solution in hexane, 2.5 cm^3, 4.0 mmol) giving a very pale yellow solution. This was transferred to a stirred suspension of [(η-C_7H_7)Mo(μ-Cl)$_3$Mo(η-C_7H_7)] **42** (0.5 g, 1.3 mmol) in thf (30 cm^3) which was pre-cooled at -78^{0}C. The mixture was allowed to warm to room temperature over 3 h then kept stirring overnight and gave a dark brown suspension. The volatiles were removed *in vacuo* and the residue was extracted with pentane (3 x 30 cm^3). The extract was filtered and the filtrate was cooled to -80^{0}C overnight. A small amount of precipitate separated and was filtered off. The filtrate was concentrated to *ca.* 40 cm^3 and cooled to -20^{0}C to yield dark red crystals. These were collected by filtration and dried *in vacuo*. The filtrate was further concentrated and cooled again to give a second crop of product. Combined yield, 0.26 g (56 %).

7.5 Reactions Discussed in Chapter 6

7.5.1 Reaction of [Mo(CO)$_6$] with 1,3,5,7-tetramethylcycloheptatriene

A mixture of [Mo(CO)$_6$] (1 g, 3.8 mmol), 1,3,5,7-tetramethylcycloheptatriene (0.67 g, 4.5 mmol), octane (15 cm^3) and thf (5 cm^3) was heated at 140^{0}C for 17 h. The resulting deep red solution was evaporated to dryness, then the residue was extracted with light petroleum (b.p. 40-60^{0}C) (2 x 30 cm^3). Cooling the extract to -20^{0}C gave orange needle-shaped crystals of [Mo(η^6-$C_7H_4Me_4$-1,3,5,7)(CO)$_3$] **43** which were collected by filtration. The crystals were then washed with cold light petroleum (b.p. 40-60^{0}C) (5 cm^3) and dried *in vacuo*. Yield, 0.66 g (53 %). The filtrate was concentrated to *ca.* 20 cm^3 and cooled to -20^{0}C to give red crystals of [Mo(η^6-$C_7H_4Me_4$-1,2,4,6)(CO)$_3$] **4 4** (0.26 g, 21 %) and [Mo(η^6-$C_7H_4Me_4$-1,3,4,6)(CO)$_3$] **45** (0.10 g, 8 %) as an inseparable mixture.

7.5.2 Preparation of [Mo(η-$C_7H_3Me_4$-1,2,4,6)(CO)$_3$][BF_4] 46

(a) A mixture of [Mo(η^6-$C_7H_4Me_4$-1,3,5,7)(CO)$_3$] **43** (3.94 g, 12 mmol) and triphenylcarbenium tetrafluoroborate (3.96 g, 12 mmol) in CH_2Cl_2 (50 cm^3) was heated at 60^{0}C for 32 h. After removing the volatiles, the residue was extracted with light petroleum (b.p. 40-60^{0}C) (3 x 30 cm^3). The combined extracts were evaporated to dryness and the ^{1}H NMR spectrum of the residue showed that it contained the starting [Mo(η^6-$C_7H_4Me_4$-1,3,5,7)(CO)$_3$] **43** (0.61 g). The insoluble material was extracted with acetone (3 x 25 cm^3). The combined extracts were concentrated to *ca.* 30 cm^3 and cooled to -80^{0}C to afford the product as orange-red crystals. Yield, 1.6 g (38 % based on unrecovered starting material).

(b) A mixture of [Mo(η^6-$C_7H_4Me_4$-1,3,5,7)(CO)$_3$] **43**, [Mo(η^6-$C_7H_4Me_4$-1,2,4,6)-(CO)$_3$] **44** and [Mo(η^6-$C_7H_4Me_4$-1,3,4,6)(CO)$_3$] **45** (1.4 g, 4.3 mmol) in 2 : 3 : 1 ratio was treated with triphenylcarbenium tetrafluoroborate (1.5 g, 4.5 mmol) in CH_2Cl_2 (25 cm^3) at 60^{0}C for 7 h. The volatiles were then removed *in vacuo* and the residue was extracted with light petroleum (b.p. 40-60^{0}C) (2 x 30 cm^3). The light petroleum solution was evaporated to dryness and the ^{1}H NMR spectrum of the residue showed that it contained [Mo(η^6-$C_7H_4Me_4$-1,3,5,7)(CO)$_3$] **43** (0.31 g). The insoluble material was then extracted with acetone (2 x 20 cm^3). The combined extracts

were cooled to -80°C to produce red crystals which were filtered off and then dried *in vacuo*. Yield, 1.2 g (87 % based on unrecovered starting material).

7.5.3 Preparation of [Mo(η-C$_7$H$_3$Me$_4$-1,2,4,6)(CO)$_2$Cl] 47

A mixture of [Mo(η-$C_7H_3Me_4$-1,2,4,6)$(CO)_3$][BF_4] **46** (0.50 g, 1.21 mmol) and LiCl (52 mg, 1.23 mmol) in acetone (20 cm^3) was stirred at room temperature for 1 h. The volatiles were removed *in vacuo* and the residue was extracted with toluene (2 x 25 cm^3). Concentration followed by cooling to -80°C gave dark green crystals which were collected by filtration and dried *in vacuo*. Yield, 0.3 g (74 %).

7.5.4 Preparation of [Mo(η^3-C$_7$H$_3$Me$_4$-1,2,4,6)(CO)$_2$(dmpe)Cl] 49

To a solution of [Mo(η-$C_7H_3Me_4$-1,2,4,6)$(CO)_2$Cl] **47** (50 mg, 0.15 mmol) in toluene (10 cm^3) was added a solution of 1,2-bis(dimethylphosphino)ethane in toluene (0.22 cm^3 of a 0.1 g cm^{-3} solution, 0.15 mmol). The colour changed from green to bright red during the course of the reaction. After stirring for 2 h at room temperature, the volatiles were removed *in vacuo* and the red oily material was extracted with light petroleum (b.p. 40-60°C) (2 x 20 cm^3). After filtration, the red filtrate was cooled to -20°C to give red needle-shaped crystals which were collected by filtration and dried *in vacuo*. Yield, 60 mg (83 %).

7.5.5 Preparation of [Mo(η-C$_7$H$_3$Me$_4$-1,2,4,6)(dmpe)Cl] 51

A solution of [Mo(η^3-$C_7H_3Me_4$-1,2,4,6)$(CO)_2$(dmpe)Cl] **49** (40 mg, 0.08 mmol) in toluene (20 cm^3) was photolysed for 1 h at room temperature. The resulting green solution was evaporated to dryness to give the product in an oily form containing a small amount of impurity. Yield, *ca.* 50 %.

7.5.6 Preparation of [Mo(η-C$_7$H$_3$Me$_4$-1,2,4,6)(η-C$_6$H$_5$Me)][BF$_4$] 52

A suspension of [Mo(η-$C_7H_3Me_4$-1,2,4,6)$(CO)_3$][BF_4] **46** (0.65 g, 1.57 mmol) in toluene (80 cm^3) was heated at 125°C for 27 h. After removing the volatiles *in vacuo*, a green solid was obtained which was essentially pure. Recrystallisation from an acetone-thf mixture furnished the pure product as pale green crystals. Yield, 0.58 g (88 %).

7.5.7 Preparation of [Mo(η-$C_7H_3Me_4$-1,2,4,6)(acac)(PPh_3)] 53

A mixture of pentane-2,4-dione (30 mg, 0.3 mmol) and sodium ethoxide (18 mg, 0.26 mmol) in methanol (10 cm^3) was stirred at room temperature for 30 min. The solution was then transferred to a Schlenk vessel containing PPh_3 (62 mg, 0.24 mmol) and [Mo(η-$C_7H_3Me_4$-1,2,4,6)(η-$C_6H_5CH_3$)][BF_4] **52** (0.1 g, 0.24 mmol). The mixture was heated at 60°C for 6 h to give a brown suspension. The suspension was then evaporated to dryness and the residue was extracted with light petroleum (b.p. 40-60°C) (4 x 25 cm^3). The light petroleum solution was concentrated to *ca.* 20 cm^3 and cooled to -80°C to afford the product as red crystals. Yield, 58 mg (40 %).

7.6 References

1 H. M. Koepp, H. Wendt and H. Stehlow, *Z. Electrochem.*, 1960, **64**, 483.

2 J. R. Dilworth and R. L. Richards, *Inorg. Synth.*, 1980, **20**, 119.

3 H. J. Lucas and E. R. Kennedy, *Organic Syntheses*, 1942, **22**, 69.

4 R. P. Clement, W. B. Davies, K. A. Ford, M. L. H. Green and A. J. Jacobson, *Inorg. Chem.*, 1978, **17**, 2754.

5 F. A. Cotton, J. A. McCleverty and J. E. White, *Inorg. Synth.*, 1967, **9**, 121.

6 R. B. King, *Organometallic Synthesis*, Academic Press, New York, 1965, 141.

7 M. Bochmann, M. Cooke, M. Green, H. P. Kirsch, F. G. A. Stone and A. J. Welch, *J. Chem. Soc., Chem. Commun.*, 1976, 381.

8 E. F. Ashworth, J. C. Green, M. L. H. Green, J. Knight, R. B. A. Pardy and N. J. Wainwright, *J. Chem. Soc., Dalton Trans.*, 1977, 1693.

9 R. L. Letsinger and C. W. Kammeyer, *J. Am. Chem. Soc.*, 1951, **73**, 4476.

10 J. Nishimura, J. Furukawa, N. Kawabata and T Fujita, *Tetrahedron*, 1970, **26**, 2229.

APPENDIX A

Characterising Data

A1 New Compounds Described in Chapter 2

A1.1 Data characterising [Mo(η-C_7H_7)(dmpe)I]

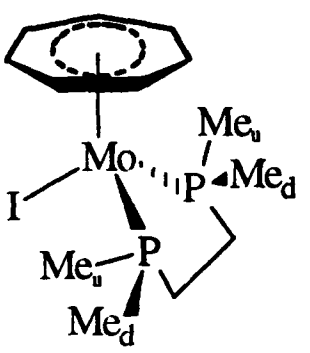

Description : green solid

Elemental Analysis for $C_{13}H_{23}IMoP_2$:

Found (Required)/% : C 34.0 (33.6), H 5.1 (5.0), I 28.4 (27.3)

Mass Spectrum (EI) :

466 (base peak) (M^+), 339 (M - I), 91(C_7H_7)

^1H NMR data : (300 MHz, [$^2H_6$]-benzene)

4.81 [t, *J* (H-P) 2.2, 7 H, η-C_7H_7]

1.61 [d, *J* (H-P) 7.9, 6 H, Me_u or Me_d]

1.19-1.34 (m, 2 H, H_u or H_d)

0.78 [d, *J* (H-P) 7.1, 6 H, Me_u or Me_d]

0.53-0.75 (m, 2 H, H_u or H_d)

^{13}C {^1H} NMR data : (75.43 MHz, [$^2H_6$]-benzene)

86.0 (s, η-C_7H_7)

28.4 [vt, *J* (C-P) 20.6, CH_2]

21.7 [vt, *J* (C-P) 14.6, Me_u or Me_d]

15.6 [vt, *J* (C-P) 9.8, Me_u or Me_d]

^{31}P {^1H} NMR data : (121.44 MHz, [$^2H_6$]-benzene)

19.9 (s, dmpe)

Infra-red data (KBr disc) :

449(m), 541(w), 653(m), 703(s), 723(m), 808(vs), 836(s), 857(m), 900(s), 934(vs), 1082(w), 1237(w), 1279(m), 1420(s), 2904(s), 2974(m), 3043(m) cm^{-1}

A1.2 Data characterising $[NBu_4][Mo(\eta\text{-}C_7H_7)I_3]$

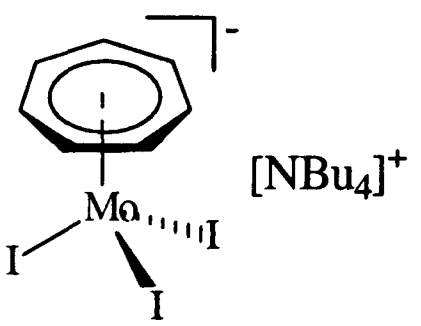

$[NBu_4]^+$

Description : purple crystals

Elemental Analysis for $C_{23}H_{43}I_3MoN$:

Found (Required)/% : C 34.1 (34.1), H 5.4 (5.4), I 49.1 (47.8), N 1.7 (1.7)

EPR data : (thf, r.t.)

g_{iso} = 2.04, A^{Mo} = 46 G, line width = 22 G

Infra-red data (KBr disc) :

737(m), 801(vs), 833(m), 844(m), 876(m), 965(m), 1028(m), 1062(m), 1105(m), 1166(m), 1379(s), 1477(vs), 2872(vs), 2930(vs), 2957(vs), 2991(m), 3041(vs) cm^{-1}

Magnetic data (1 T and 3 T) :

obey the Curie-Weiss law at 6-180 K with C = 0.31 emu-K mol^{-1},

θ = -1.2 K, μ_{eff} = 1.57 μ_B

Comment : X-ray crystal structure

A1.3 Data characterising [Mo(η-C_7H_7)(η-C_5H_4Me)]

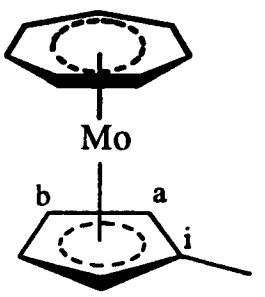

Description : green crystals

Mass Spectrum (EI) :

268 (base peak) (M^+), 189 (M - C_5H_4Me)

^{1}H NMR data : (300 MHz, [$^2H_6$]-benzene)

4.90 (s, 7 H, η-C_7H_7)

4.80 [t, *J* (H-H) 1.8, 2 H, H_a or H_b]

4.66 [t, *J* (H-H) 1.8, 2 H, H_a or H_b]

1.75 (s, 3 H, Me)

^{13}C {^{1}H} NMR data : (75.43 MHz, [$^2H_6$]-benzene)

101.7 (C_i)

86.6 (C_a or C_b)

83.7 (C_a or C_b)

80.8 (η-C_7H_7)

14.6 (Me)

Infra-red data (KBr disc) :

702(s), 748(s), 812(vs), 917(vs), 1028(s), 1098(s), 1281(s), 1457(m), 1559(w), 1653(m), 1700(m), 2924(m), 2962(m), 3092(m) cm^{-1}

Electrochemical data (in MeCN) :

one reversible oxidation at $E_{1/2}$ = -0.63 V *vs.* SCE

Comment : X-ray crystal structure

A1.4 Data characterising [Mo(η-C_7H_7)(η^5-C_9H_7)]

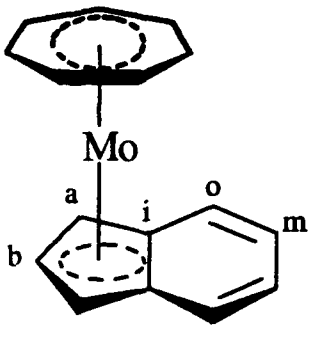

Description : purple crystals

Elemental Analysis for $C_{16}H_{14}Mo$:

Found (Required)/% : C 62.6 (63.6), H 4.6 (4.7)

Mass Spectrum (EI) :

304 (base peak) (M+)

^{1}H NMR data : (300 MHz, [$^2H_6$]-acetone)

7.38 [dd, *J* (H-H) 3.0, 6.4, 2 H, H_o or H_m]

6.78 [dd, *J* (H-H) 3.0, 6.4, 2 H, H_o or H_m]

5.50 [d, *J* (H-H) 2.6, 2 H, H_a]

5.38 [t, *J* (H-H) 2.6, 1 H, H_b]

4.75 (s, 7 H, η-C_7H_7)

^{13}C {^{1}H} NMR data : (75.43 MHz, [$^2H_6$]-acetone)

127.8 (C_o or C_m)

121.4 (C_o or C_m)

103.3 (C_i)

91.2 (C_b)

82.7 (η-C_7H_7)

78.0 (C_a)

Infra-red data (KBr disc) :

465(m), 547(m), 668(m), 729(s), 739(s), 796(vs), 823(vs), 1033(s), 1068(m), 1099(m), 1337(m), 1517(w), 1559(w), 1653(w), 2916(w), 2970(m),

3025(m) cm^{-1}

Electrochemical data (in MeCN) :

one reversible oxidation at $E_{1/2}$ = -0.48 V *vs.* SCE

A1.5 Data characterising [Mo(η-C_7H_7)(MeCN)Cl_2]

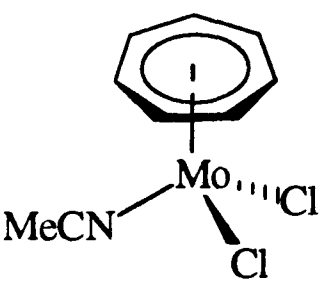

Description : orange crystals

Elemental Analysis for $C_9H_{10}Cl_2MoN$:

Found (Required)/% : C 36.0 (36.1), H 3.3 (3.4), Cl 23.6 (23.7),
N 4.7 (4.7)

EPR data : ([$^2H_3$]-acetonitrile, r.t.)

g_{iso} = 1.97, A^{Mo} = 45 G, line width = 14 G

Infra-red data (KBr disc) :

806(vs), 838(w), 961(m), 969(m), 1034(m), 1175(w), 1412(m), 1429(m), 1474(w), 1500(w), 2287(m), 2309(w), 2323(w), 2907(w), 2967(m), 3041(m) cm^{-1}

Magnetic data (1 T) :

obey the Curie-Weiss law at 6-290 K with C = 0.30 emu-K mol^{-1},

θ = -0.5 K, μ_{eff} = 1.55 μ_B

A1.6 Data characterising [Mo(η-C_7H_7)(η-C_5H_4Me)][tcne]

Description : purple crystals

Elemental Analysis for $C_{19}H_{14}MoN_4$:

Found (Required)/% : C 57.7 (57.9), H 3.3 (3.6), N 13.8 (14.2)

EPR data : (solid, r.t.)

g_{iso} = 1.995, line width = 50 G

Infra-red data (KBr disc) :

515(w), 550(w), 805(s), 831(w), 850(w), 858(w), 961(w), 1043(m), 1061(m), 1367(s), 1424(m), 1456(m), 1481(m), 1596(w), 1632(w), 2160(s), 2171(s), 2192(m), 2928(w), 2964(w), 3062(m), 3083(w) cm^{-1}

Magnetic data (0.2 T) :

obey the Curie-Weiss law at 6-300 K with C = 0.35 emu-K mol^{-1},

θ = -3.1 K, μ_{eff} = 1.67 μ_B

A1.7 Data characterising [Mo(η-C_7H_7)(η-C_5H_5)]$_2$[tcnq]

Description : dark green solid

Elemental Analysis for $C_{36}H_{28}Mo_2N_4$:

Found (Required)/% : C 57.3 (61.0), H 3.6 (4.0), N 7.5 (7.9)

EPR data : (CH_2Cl_2, r.t.)

g_{iso} = 1.982, line width = 25 G

Infra-red data (KBr disc) :

500(m), 533(w), 568(w), 810(s), 831(w), 960(w), 1170(w), 1224(m), 1298(s), 1418(m), 1500(s), 1572(m), 2104(s), 2150(s), 2964(w), 3048(m), 3089(w) cm^{-1}

A2 New Compounds Described in Chapter 3

A2.1 Data characterising $[W(\eta\text{-}C_7H_7)(MeCN)I_2]$

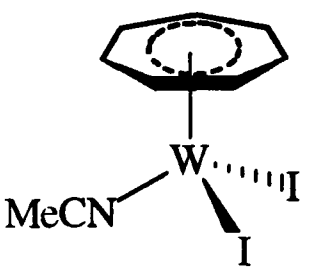

Description : dark red crystals

Elemental Analysis for $C_9H_{10}I_2NW$:

Found (Required)/% : C 18.7 (19.0), H 1.8 (1.8), I 45.1 (44.5),
N 2.5 (2.5),

Mass Spectrum (FAB) :

570 (M^+)

EPR data : ([$^2H_3$]-acetonitrile, r.t.)

g_{iso} = 1.941, line width = 56 G

Infra-red data (KBr disc) :

345(w), 392(w), 453(m), 466(m), 670(w), 813(vs), 964(m), 1353(m), 1426(m), 2280(m), 2310(m), 2903 (w), 3022(m) cm^{-1}

Magnetic data (0.2 T) :

antiferromagnetic with $T(\chi_{max})$ = 17 K, μ_{eff} = 1.44 μ_B (high temp.)

A2.2 Data characterising [W(η-C_7H_7)(MeCN)Br_2]

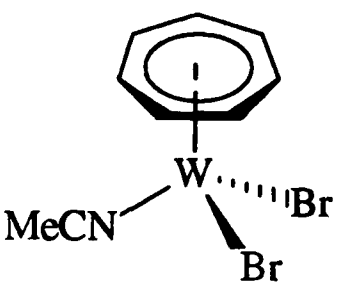

Description : green crystals

EPR data : (solid, r.t.)

g_{iso} = 1.927, line width = 630 G

Infra-red data (KBr disc) :

818(vs), 840(m), 964(m), 1027(m), 1363(w), 1407(w), 1426(m), 1501(w), 1630(m), 2279(m), 2308(m), 2907 (m), 2964(m), 3036(m) cm^{-1}

A2.3 Data characterising [W(η-C_7H_7)(PMe_3)Br_2]

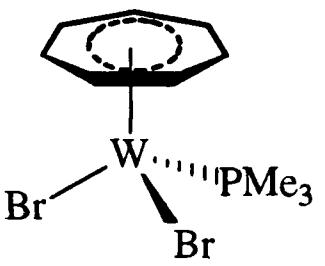

Description : orange brown crystals

Elemental Analysis for $C_{10}H_{16}Br_2PW$:

Found (Required)/% : C 23.9 (23.5), H 3.1 (3.2), Br 31.8 (31.3)

Mass Spectrum (FAB) :

509 (M+), 430 (M - Br)

EPR data : (thf, 153 K)

g_{iso} = 1.943, line width = 57 G

Infra-red data (KBr disc) :

300(w), 340(w), 457(w), 536(w), 675(m), 738(s), 816(vs), 845(s), 890(w), 905(m), 946(vs), 962(vs), 1071(m), 1174(w), 1246(w), 1280(s), 1289(s), 1305(m), 1419(vs), 1430(s), 1499(m), 2909(s), 2963(m), 2978(m), 3035(s), 3051(m) cm^{-1}

Magnetic data (0.2 T) :

antiferromagnetic with $T(\chi_{max}) = 13$ K

obey the Curie-Weiss law at 45-140 K with C = 0.20 emu-K mol^{-1},

$\theta = -3.6$ K, $\mu_{eff} = 1.27\ \mu_B$

A2.4 Data characterising $[W(\eta\text{-}C_7H_7)(PMe_3)I_2]$

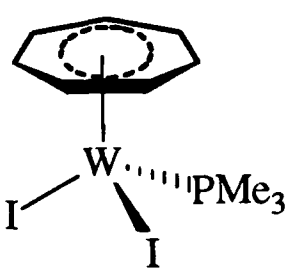

Description : red crystals

Elemental Analysis for $C_{10}H_{16}I_2PW$:

Found (Required)/% : C 20.2 (19.9), H 2.7 (2.7), I 42.5 (42.0)

EPR data : (thf, 153 K)

$g_{iso} = 1.988$, line width = 53 G

Infra-red data (KBr disc) :

454(w), 534(w), 672(m), 732(s), 815(vs), 842(s), 889(w), 905(w), 940(vs), 956(vs), 1173(w), 1244(w), 1280(s), 1303(m), 1417(s), 1428(s), 1484(w), 1499(m), 2904(s), 2963(m), 3032(s) cm^{-1}

Magnetic data (0.2 T) :

antiferromagnetic with $T(\chi_{max}) = 13$ K, $\mu_{eff} = 1.50\ \mu_B$ (high temp.)

A2.5 Data characterising [W(η-C_7H_7)(dmpe)I]

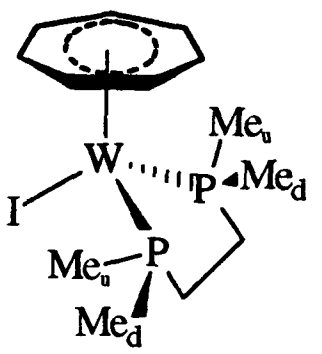

Description : green solid

Elemental Analysis for $C_{13}H_{23}IP_2W$:

Found (Required)/% : C 29.0 (28.3), H 4.2 (4.2), I 23.4 (23.0)

Mass Spectrum (EI) :

552 (M+), 402 (M - dmpe), 91 (C_7H_7)

^{1}H NMR data : (300 MHz, [$^2H_8$]-toluene)

4.99 [t, *J* (H-P) 1.9, 7 H, η-C_7H_7]

1.61 [d, *J* (H-P) 8.0, 6 H, Me_u or Me_d]

1.12-1.36 (m, 2 H, H_u or H_d)

0.88 [d, *J* (H-P) 7.6, 6 H, Me_u or Me_d]

0.72-0.98 (m, 2 H, H_u or H_d)

^{13}C {^{1}H} NMR data : (75.43 MHz, [$^2H_8$]-toluene)

81.0 (s, η-C_7H_7)

31.7 [vt, *J* (C-P) 22.0, CH_2]

21.5 [vt, *J* (C-P) 17.1, Me_u or Me_d]

17.1-18.0 (m, Me_u or Me_d)

^{31}P {^{1}H} NMR data : (121.44 MHz, [$^2H_8$]-toluene)

-7.9 [s, *J* (P-^{183}W) 346.0, dmpe]

Infra-red data (KBr disc) :

450(w), 651(m), 701(s), 727(m), 811(vs), 833(m), 941(s), 1278(m), 1293(w), 1420(m), 2896(m), 2961(m), 3034(w) cm^{-1}

A2.6 Data characterising [W(η-C_7H_7)(η-C_5H_4Me)]

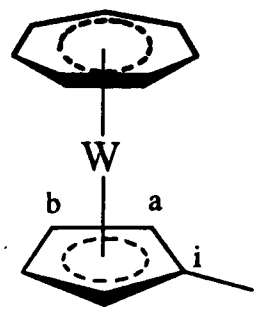

Description : dark brown crystals

Elemental Analysis for $C_{13}H_{14}W$:

Found (Required)/% : C 44.2 (44.1), H 4.0 (4.0)

^1H NMR data : (300 MHz, [$^2H_6$]-benzene)

5.28 (br s, 2 H, H_a or H_b)

5.21 (s, 7 H, η-C_7H_7)

5.16 (br s, 2 H, H_a or H_b)

1.76 (s, 3 H, Me)

^{13}C {^1H} NMR data : (75.43 MHz, [$^2H_6$]-benzene)

100.1 (C_i)

85.4 (C_a or C_b)

82.2 (C_a or C_b)

74.5 (η-C_7H_7)

16.0 (Me)

Infra-red data (KBr disc) :

702(m), 811(vs), 832(vs), 874(m), 961(m), 1023(s), 1037(s), 1455(m), 1476(m), 2916(w), 2951(w), 2968(m), 2986(m), 3017(m), 3028(m) cm^{-1}

Electrochemical data (in MeCN) :

one reversible oxidation at $E_{1/2}$ = -0.79 V *vs.* SCE

A2.7 Data characterising [W(η-C_7H_7)(η^5-C_9H_7)]

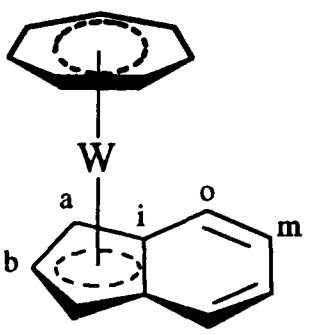

Description : purple crystals

Elemental Analysis for $C_{16}H_{14}W$:

Found (Required)/% : C 49.4 (49.3), H 3.6 (3.6)

^{1}H NMR data : (300 MHz, [$^2H_6$]-acetone)

7.29 [dd, *J* (H -H) 3.0, 6.4, 2 H, H_o or H_m]

6.77 [dd, *J* (H -H) 3.0, 6.4, 2 H, H_o or H_m]

6.08 [t, *J* (H-H) 2.4, 1 H, H_b]

6.02 [d, *J* (H-H) 2.4, 2 H, H_a]

5.11 (s, 7 H, η-C_7H_7)

^{13}C {^{1}H} NMR data : (75.43 MHz, [$^2H_6$]-benzene)

128.4 (C_o or C_m)

121.2 (C_o or C_m)

101.8 (C_i)

88.9 (C_b)

75.9 (η-C_7H_7)

75.5 (C_a)

Infra-red data (KBr disc) :

419(m), 546(w), 613(w), 727(s), 738(s), 827(vs), 873(m), 961(w), 1336(s), 2933(w), 3036(w) cm^{-1}

Electrochemical data (in MeCN) :

one reversible oxidation at $E_{1/2}$ = -0.66 V *vs.* SCE

A3 New Compounds Described in Chapter 5

A3.1 Data characterising $[(\eta\text{-}C_7H_7)Mo(\mu\text{-}SBu)_3Mo(\eta\text{-}C_7H_7)][BF_4]$

Description : Dark green crystals

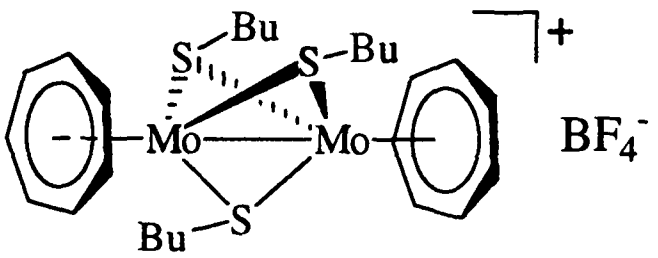

Elemental Analysis for $C_{26}H_{41}BF_4Mo_2S_3$:

Found (Required)/% : C 42.7 (42.9), H 5.7 (5.7), S 12.9 (13.2)

Mass Spectrum (FAB) :

645 (base peak) (M - BF_4), 588 (M - BF_4 - Bu), 531 (M - BF_4 - 2 Bu), 499 (M - BF_4 - 2 Bu - S), 442 (M - BF_4 - 3 Bu - S)

^{1}H NMR data : (300 MHz, [$^2H_1$]-chloroform)

5.53 (s, 14 H, η-C_7H_7)

2.58 (br s, 6 H, SCH_2)

1.68 (br s, 6 H, $SCH_2C\underline{H}_2$)

1.42-1.58 (m, 6 H, $SCH_2CH_2C\underline{H}_2$)

1.00 [t, *J* (H-H) 7.2, 9 H, Me]

Variable-temperature ^{1}H NMR data : (300 MHz, [$^2H_1$]-chloroform)

$T_{coalescence}$ ($C_7\underline{H}_7$ <=> $C'_7\underline{H}'_7$ due to the sulfur inversion) = 263 ± 5 K

$\Delta\nu$ at low temperature limit = 8.8 Hz

$\Delta G^{\ddagger}$ = 57.2 ± 1.0 kJ mol^{-1}

^{13}C NMR data : (75.43 MHz, 293 K, [$^{2}H_1$]-chloroform)

93.0 [d, *J* (C-H) 190, η-C_7H_7]

34.8 [t, *J* (C-H) 124, $SCH_2\underline{C}H_2$]

22.0 [t, *J* (C-H) 128, $SCH_2CH_2\underline{C}H_2$]

13.9 [q, *J* (C-H) 125, Me]

^{13}C {^{1}H} NMR data : (75.43 MHz, 243 K, [$^{2}H_6$]-acetone)

94.2 (η-C_7H_7)

47.5 (SCH_2)

35.2 ($SCH_2\underline{C}H_2$)

22.8 ($SCH_2CH_2\underline{C}H_2$)

14.4 (Me)

Infra-red data (KBr disc) :

343(w), 522(w), 534(w), 704(w), 732(w), 799(vs), 848(w), 964(w), 1050(vs), 1218(w), 1263(w), 1288(w), 1378(w), 1434(m), 1463(m), 1496(w), 1630(w), 2868(s), 2928(s), 2954(s), 3070(w) cm^{-1}

Electrochemical data (in MeCN) :

two reversible reductions at $E_{1/2}$ = -1.01 V and -1.59 V *vs.* SCE

A3.2 Data characterising [(η-C_7H_7)Mo(μ-SPr)$_3$Mo(η-C_7H_7)][BF_4]

Description : Dark green crystals

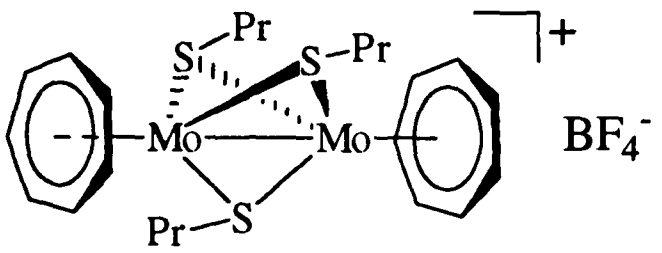

Elemental Analysis for $C_{23}H_{35}BF_4Mo_2S_3$:

Found (Required)/% : C 39.9 (40.3), H 5.1 (5.1), S 14.0 (14.0)

Mass Spectrum (FAB) :

603 (base peak) (M - BF_4), 560 (M - BF_4 - Pr), 517 (M - BF_4 - 2 Pr), 485 (M - BF_4 - 2 Pr - S), 442 (M - BF_4 - 3 Pr - S)

^1H NMR data : (300 MHz, [$^2H_1$]-chloroform)

5.53 (s, 14 H, η-C_7H_7)

2.56 (br s, 6 H, SCH_2)

1.72 (br s, 6 H, $SCH_2C\underline{H}_2$)

1.10 [t, *J* (H-H) 7.2, 9 H, Me]

Variable-temperature ^1H NMR data : (300 MHz, [$^2H_1$]-chloroform)

$T_{coalescence}$ ($C_7\underline{H}_7$ <=> $C'_7\underline{H}'_7$ due to the sulfur inversion) = 263 ± 5 K

$\Delta\nu$ at low temperature limit = 7.4 Hz

$\Delta G^{\ddagger}$ = 57.6 ± 1.0 kJ mol^{-1}

^{13}C {^1H} NMR data : (75.43 MHz, 293 K, [$^2H_1$]-chloroform)

93.0 (η-C_7H_7)

26.0 ($SCH_2\underline{C}H_2$)

13.4 (Me)

^{13}C {^1H} NMR data : (75.43 MHz, 243 K, [$^2H_6$]-acetone)

94.2 (η-C_7H_7)

49.4 (SCH_2)

26.5 ($SCH_2\underline{C}H_2$)

13.9 (Me)

Infra-red data (KBr disc) :

250(w), 343(w), 519(m), 534(w), 791(vs), 809(s), 1045(vs), 1180(w), 1227(m), 1245(m), 1283(m), 1328(w), 1382(m), 1435(m), 1458(m), 1496(w), 1626(w), 2868(m), 2926(m), 3070(w) cm^{-1}

Electrochemical data (in MeCN) :

two reversible reductions at $E_{1/2}$ = -1.02 V and -1.60 V *vs.* SCE

A3.3 Data characterising $[(\eta\text{-}C_7H_7)Mo(\mu\text{-}SPh)_3Mo(\eta\text{-}C_7H_7)][BF_4]$

Description : Dark green crystals

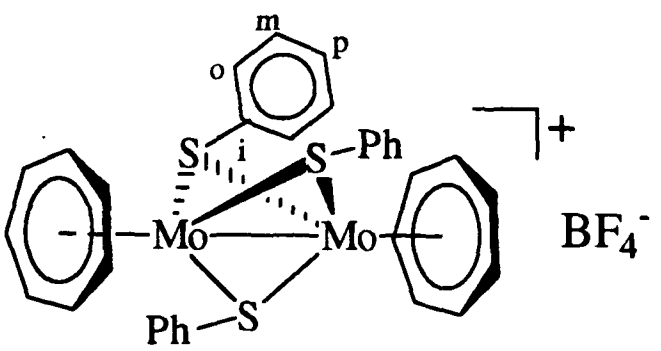

Elemental Analysis for $C_{32}H_{29}BF_4Mo_2S_3$:

Found (Required)/% : C 49.0 (48.8), H 3.6 (3.7), S 12.2 (12.2)

Mass Spectrum (FAB) :

705 (base peak) (M - BF_4), 628 (M - BF_4 - Ph), 596 (M - BF_4 - SPh), 519 (M - BF_4 - 2 Ph - S)

^1H NMR data : (300 MHz, [$^2H_6$]-acetone)

7.55-7.59 (m, 6 H, H_o)

7.41-7.49 (m, 9 H, H_m and H_p)

5.54 (s, 14 H, η-C_7H_7)

^{13}C {^1H} NMR data : (75.43 MHz, [$^2H_6$]-acetone)

143.2 (C_i)

131.9 (C_o or C_m)

130.5 (C_o or C_m)

129.3 (C_p)

96.6 (η-C_7H_7)

Infra-red data (KBr disc) :

328(w), 345(w), 372(w), 480(w), 521(w), 537(w), 695(vs), 746(vs), 803(vs), 840(w), 999(s), 1058(vs), 1181(w), 1255(w), 1286(w), 1305(w), 1436(s), 1467(s), 1496(w), 1574(s), 1639(w), 3058(m) cm^{-1}

Electrochemical data (in MeCN) :

two reversible reductions at $E_{1/2}$ = -0.79 V and -1.30 V *vs.* SCE

A3.4 Data characterising [(η-C_7H_7)Mo(μ-SCH_2Ph)$_3$Mo(η-C_7H_7)][BF_4]

Description : brown solid

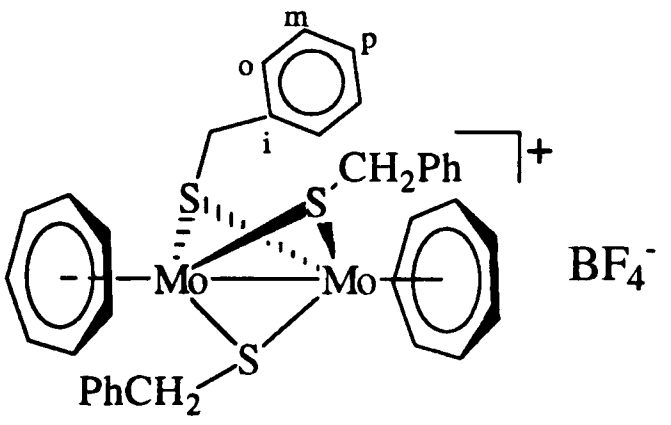

Elemental Analysis for $C_{35}H_{35}BF_4Mo_2S_3$:

Found (Required)/% : C 49.9 (50.6), H 4.4 (4.3), S 11.6 (11.6)

Mass Spectrum (FAB) :

747 (base peak) (M - BF_4), 656 (M - BF_4 - CH_2Ph), 565 (M - BF_4 - 2 CH_2Ph), 533 (M - BF_4 - 2 CH_2Ph - S), 474 (M - BF_4 - 3 CH_2Ph), 442 (M - BF_4 - 3 CH_2Ph - S)

^1H NMR data : (300 MHz, [$^2H_6$]-acetone)

7.40-7.57 (m, 15 H, Ph)

5.55 (s, 14 H, η-C_7H_7)

3.98 (br s, 6 H, SCH_2)

Variable-temperature ^1H NMR data : (300 MHz, [$^2H_6$]-acetone)

$T_{coalescence}$ ($C_7\underline{H}_7$ <=> $C'_7\underline{H}'_7$ due to the sulfur inversion) = 253 ± 5 K

Δν at low temperature limit = 24.3 Hz

$\Delta G^{\ddagger}$ = 53.0 ± 1.0 kJ mol^{-1}

^{13}C {^{1}H}NMR data : (75.43 MHz, [$^{2}H_6$]-acetone)

140.2 (C_i)

129.9 (C_o or C_m)

129.8 (C_o or C_m)

128.9 (C_p)

93.6 (η-C_7H_7)

50.8 (SCH_2)

Infra-red data (KBr disc) :

337(w), 474(w), 520(w), 665(m), 702(vs), 764(s), 799(vs), 849(w), 921(w), 1053(vs), 1175(w), 1231(m), 1435(m), 1451(s), 1493(s), 1599(m), 3026(w), 3062(m) cm^{-1}

Electrochemical data (in MeCN) :

two reversible reductions at $E_{1/2}$ = -0.95 V and -1.52 V *vs.* SCE

A3.5 Data characterising [(η-C_7H_7)Mo(μ-SEt)$_3$Mo(η-C_7H_7)][BF_4]

Description : Dark green crystals

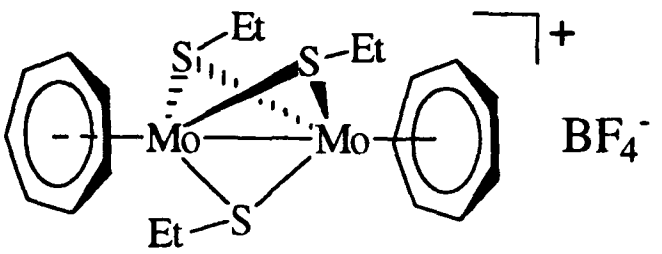

Elemental Analysis for $C_{20}H_{29}BF_4Mo_2S_3$:

Found (Required)/% : C 37.5 (37.3), H 4.6 (4.5), S 14.2 (14.9)

Mass Spectrum (FAB) :

561 (M - BF_4), 532 (M - BF_4 - Et), 500 (M - BF_4 - SEt)

^{1}H NMR data : (300 MHz, [$^{2}H_6$]-acetone)

5.79 (s, 14 H, η-C_7H_7)

2.76 (br s, 6 H, SCH_2)

1.35 (br s, 9 H, Me)

Variable-temperature ^1H NMR data : (300 MHz, [$^2H_6$]-acetone)

$T_{coalescence}$ ($C_7\underline{H}_7$ <=> $C'_7\underline{H}'_7$ due to the sulfur inversion) = 263 ± 5 K

$\Delta\nu$ at low temperature limit = 5.4 Hz

$\Delta G^{\ddagger}$ = 58.3 ± 1.0 kJ mol^{-1}

^{13}C {^1H} NMR data : (75.43 MHz, [$^2H_6$]-acetone)

94.1 (η-C_7H_7)

41.0 (SCH_2)

17.9 (Me)

Infra-red data (KBr disc) :

250(m), 340(w), 522(m), 534(m), 761(m), 799(vs), 845(m), 967(s), 1054(vs), 1248(s), 1374(s), 1434(s), 1497(w), 1630(m), 2864(m), 2922(m), 2961(m), 3044(w) cm^{-1}

Electrochemical data (in MeCN) :

two reversible reductions at $E_{1/2}$ = -0.98 V and -1.57 V *vs.* SCE

A3.6 Data characterising [(η-$C_7H_3Me_4$-1,2,4,6)Mo(μ-SEt)$_3$Mo(η-$C_7H_3Me_4$-1,2,4,6)][BF_4]

Description : green crystals

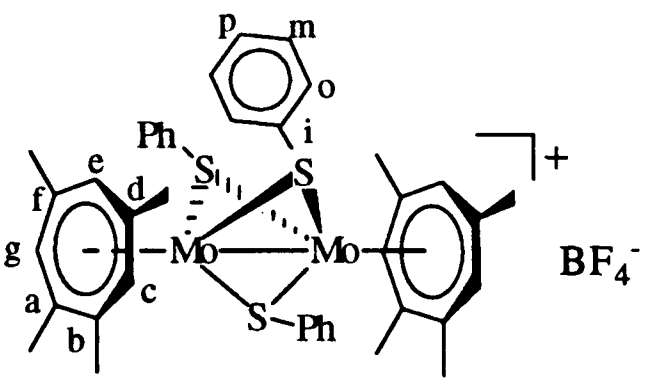

Elemental Analysis for $C_{40}H_{45}BF_4Mo_2S_3$:

Found (Required)/% : C 53.0 (53.3), H 5.1 (5.0), S 10.5 (10.7)

Mass Spectrum (FAB) :

817 (base peak) (M - BF_4)

^1H NMR data : (300 MHz, [$^2H_6$]-acetone)

7.43 (br s, 15 H, Ph)

5.14 (s, 2 H, H_c, H_e or H_g)

4.85 (s, 2 H, H_c, H_e or H_g)

4.73 (s, 2 H, H_c, H_e or H_g)

2.58 (s, 6 H, Me_a, Me_b, Me_d or Me_f)

2.40 (s, 6 H, Me_a, Me_b, Me_d or Me_f)

2.13 (s, 6 H, Me_a, Me_b, Me_d or Me_f)

1.61 (s, 6 H, Me_a, Me_b, Me_d or Me_f)

^{13}C {^1H} NMR data : (75.43 MHz, [$^2H_6$]-acetone)

143.3 (C_i)

132.7 (C_o or C_m)

130.2 (C_o or C_m)

129.2 (C_p)

109.6 (C_a, C_b, C_d or C_f)

106.2 (C_a, C_b, C_d or C_f)

103.4 (C_a, C_b, C_d or C_f)

99.4 (C_c, C_e or C_g)

98.8 (C_a, C_b, C_d or C_f)

96.6 (C_c, C_e or C_g)

94.8 (C_c, C_e or C_g)

27.8 (Me_a, Me_b, Me_d or Me_f)

27.1 (Me_a, Me_b, Me_d or Me_f)

26.1 (Me_a, Me_b, Me_d or Me_f)

23.0 (Me_a, Me_b, Me_d or Me_f)

Infra-red data (KBr disc) :

479(w), 668(m), 691(m), 743(m), 868(w), 895(w), 904(w), 1000(m), 1022(s), 1037(s), 1056(vs), 1085(s), 1094(s), 1381(m), 1438(m), 1466(m), 1473(m), 1376(m), 1653(m), 2858(m), 2917(m), 3055(w) cm^{-1}

Electrochemical data (in MeCN) :

two reversible reductions at $E_{1/2}$ = -0.99 V and -1.54 V *vs.* SCE

A3.7 Data characterising [(η-C_7H_7)Mo(μ-NAr)$_2$Mo(η-C_7H_7)] (Ar = 2,6-diisopropylphenyl)

Description : dark red crystals

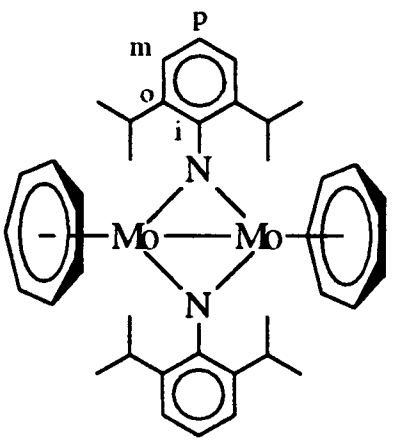

Elemental Analysis for $C_{38}H_{48}Mo_2N_2$:

Found (Required)/% : C 61.1 (63.0), H 6.7 (6.7), N 3.9 (3.9)

Mass Spectrum (FAB) :

364 (base peak) [Mo(η-C_7H_7)(NAr)]+

^{1}H NMR data : (300 MHz, [$^2H_6$]-benzene)

7.24 [d, *J* (H-H) 7.5 Hz, H_m, 4 H]

7.12 [t, *J* (H-H) 7.5 Hz, H_p, 2 H]

4.55 (s, 14 H, η-C_7H_7)

2.77 [septet, *J* (H-H) 6.8 Hz, 4 H, C<u>H</u>Me_2]

1.19 [d, *J* (H-H) 6.8 Hz, 24 H, Me]

^{13}C {^{1}H} NMR data : (75.43 MHz, [$^{2}H_6$]-benzene)

160.0 (C_i)

140.4 (C_o)

124.2 (C_m)

123.1 (C_p)

88.8 (η-C_7H_7)

26.7 ($\underline{C}HMe_2$)

26.2 (Me)

Infra-red data (KBr disc) :

524(w), 711(w), 762(vs), 783(vs), 800(m), 813(m), 857(m), 906(m), 929(m), 966(m), 1050(w), 1099(m), 1205(m), 1243(s), 1313(s), 1360(m), 1380(m), 1420(s), 1462(m), 2865(m), 2923(m), 2962(s), 3044(w) cm^{-1}

A4 New Compounds Described in Chapter 6

A4.1 Data characterising [Mo(η^6-$C_7H_4Me_4$-1,3,5,7)(CO)$_3$]

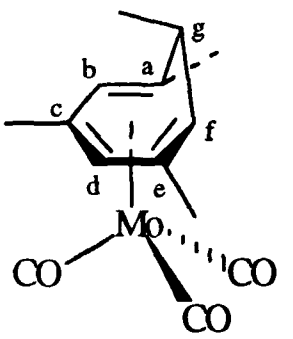

Description : orange needle-like crystals

Elemental Analysis for $C_{14}H_{16}MoO_3$:

Found (Required)/% : C 51.0 (51.2), H 5.1 (4.9)

Mass spectrum (EI) :

330 (M+), 302 (M - CO), 274 (M - 2 CO), 246 (base peak) (M - 3 CO), 148 ($C_7H_4Me_4$), 133 ($C_7H_4Me_3$)

^{1}H NMR data : (300 MHz, [$^{2}H_6$]-benzene)

5.17 (s, 1 H, H_b or H_d)

4.17 (s, 1 H, H_b or H_d)

3.24 [dd, *J* (H-H) 8.4, 1.4, 1 H, H_f]

2.20-2.24 (m, 1 H, H_g)

1.95 (s, 3 H, Me_a, Me_c or Me_e)

1.67 (s, 3 H, Me_a, Me_c or Me_e)

1.55 (s, 3 H, Me_a, Me_c or Me_e)

-0.04 [d, *J* (H-H) 7.0, 3 H, Me_g]

^{13}C {^{1}H} NMR data : (75.43 MHz, [$^{2}H_6$]-benzene)

112.3 (C_c or C_e)

109.7 (C_c or C_e)

100.7 (C_b or C_d)

100.5 (C_b or C_d)

90.6 (C_a)

66.4 (C_f)

38.7 (C_g)

26.62 (Me_a, Me_c, Me_e or Me_g)

26.57 (Me_a, Me_c, Me_e or Me_g)

26.0 (Me_a, Me_c, Me_e or Me_g)

24.0 (Me_a, Me_c, Me_e or Me_g)

Carbonyl absorptions not observed

Infra-red data (KBr disc) :

438(w), 488(m), 501(m), 561(m), 577(m), 593(m), 613(m), 626(m), 911(w), 1004(w), 1034(m), 1098(w), 1185(w), 1336(w), 1378(m), 1446(m), 1478(w), 1870(vs), 1958(vs), 2922(m), 2972(m) cm^{-1}

Electrochemical data (in MeCN) :

one quasi-reversible wave at $E_{1/2}$ = + 0.48 V *vs.* SCE

A4.2 Data characterising [Mo(η⁶-C₇H₄Me₄-1,2,4,6)(CO)₃] and [Mo(η⁶-C₇H₄Me₄-1,3,4,6)(CO)₃]

Description : bright red crystals, mixture of isomers

Elemental Analysis for $C_{14}H_{16}MoO_3$:

Found (Required)/% : C 51.8 (51.2), H 4.9 (4.9)

(A) [Mo(η⁶-$C_7H_4Me_4$-1,2,4,6)$(CO)_3$]

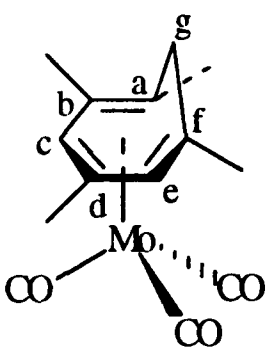

^{1}H NMR data : (300 MHz, [$^2H_6$]-benzene)

5.24 (s, 1 H, H_c or H_e)

4.34 (s, 1 H, H_c or H_e)

2.04 (s, 1 H, $H_{g\text{-}exo}$ or $H_{g\text{-}endo}$)

1.92 (s, 4 H, $H_{g\text{-}exo}$ or $H_{g\text{-}endo}$ and Me_a, Me_b, Me_d or Me_f)

1.73 (s, 3 H, Me_a, Me_b, Me_d or Me_f)

1.53 (s, 3 H, Me_a, Me_b, Me_d or Me_f)

1.49 (s, 3 H, Me_a, Me_b, Me_d or Me_f)

^{13}C {^{1}H} DEPT NMR data : (300 MHz, [$^2H_6$]-benzene)

102.2 (C_c or C_e)

101.7 (C_c or C_e)

39.0 (C_g)

27.1 (Me_a, Me_b, Me_d or Me_f)

25.7 (Me_a, Me_b, Me_d or Me_f)

25.1 (Me_a, Me_b, Me_d or Me_f)

23.4 (Me_a, Me_b, Me_d or Me_f)

(B) [Mo(η^6-$C_7H_4Me_4$-1,3,4,6)$(CO)_3$]

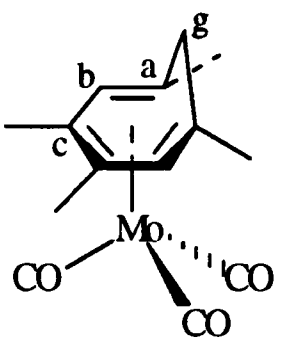

^{1}H NMR data : (300 MHz, [$^2H_6$]-benzene)

4.48 (s, 2 H, H_b)

1.87 (s, 7 H, $H_{g\text{-}exo}$ or $H_{g\text{-}endo}$ and Me_a or Me_c)

1.52 (s, 6 H, Me_a or Me_c)

a peak due to another $H_{g\text{-}exo}$ or $H_{g\text{-}endo}$ was not observed

A4.3 Data characterising [Mo(η-$C_7H_3Me_4$-1,2,4,6)$(CO)_3$][BF_4]

Description : orange-red crystals

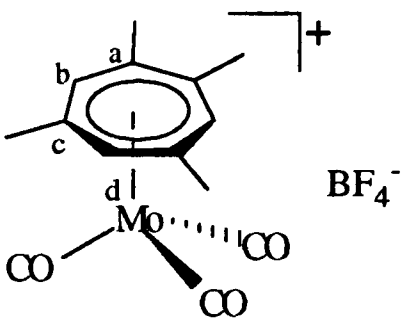

Elemental Analysis for $C_{14}H_{15}BF_4MoO_3$:

Found (Required)/% : C 40.7 (40.6), H 3.6 (3.7)

Mass Spectrum (FAB) :

416 (M^+), 329 (base peak) (M - BF_4), 301 (M - BF_4 - CO), 273 (M - BF_4 - 2 CO), 245 (M - BF_4 - 3 CO), 147 ($C_7H_3Me_4$)

^{1}H NMR data : (300 MHz, [$^{2}H_6$]-acetone)

6.43 (s, 2 H, H_b)

6.22 (s, 1 H, H_d)

2.80 (s, 6 H, Me_a or Me_c)

2.71 (s, 6 H, Me_a or Me_c)

^{13}C {^{1}H} NMR data : (75.43 MHz, [$^{2}H_6$]-acetone)

210.7 (CO)

118.6 (C_a or C_c)

116.6 (C_a or C_c)

103.3 (C_b)

101.3 (C_d)

26.2 (Me_a or Me_c)

25.0 (Me_a or Me_c)

Infra-red data (KBr disc) :

482(s), 508(w), 523(m), 565(s), 593(m), 805(w), 897(m), 1056(vs), 1184(w), 1212(m), 1288(w), 1393(s), 1455(s), 1490(w), 1545(w), 1631(w), 1864(w), 1928(s), 2007(vs), 2055 (vs), 2921(w), 2978(w), 3074(m) cm^{-1}

Electrochemical data (in MeCN) :

one reversible wave at $E_{1/2}$ = + 0.21 V *vs.* SCE

A4.4 Data characterising [Mo(η-$C_7H_3Me_4$-1,2,4,6)(CO)$_2$Cl]

Description : dark green crystals

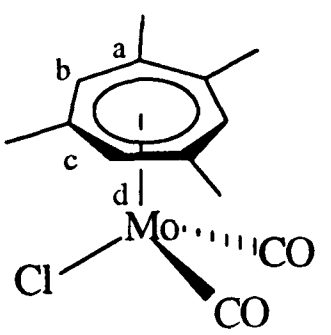

Elemental Analysis for $C_{13}H_{15}ClMoO_2$:

Found (Required)/% : C 46.8 (46.7), H 4.3 (4.5), Cl 10.6 (10.6)

Mass spectrum (EI) :

595 {[$Mo_2(\eta\text{-}C_7H_3Me_4)_2(\mu\text{-}Cl)_3$]}, 280 (M - 2 CO), 146 ($C_7H_3Me_4$ - H), 91 (base peak) (C_7H_7)

^1H NMR data : (300 MHz, [$^2H_6$]-benzene)

4.60 (s, 2 H, H_b)

3.88 (s, 1 H, H_d)

1.90 (s, 6 H, Me_a or Me_c)

1.76 (s, 6 H, Me_a or Me_c)

^{13}C {^1H} NMR data : (75.43 MHz, [$^2H_6$]-benzene)

221.4 (CO)

109.0 (C_a or C_c)

101.4 (C_a or C_c)

98.7 (C_b)

93.0 (C_d)

26.1 (Me_a or Me_c)

23.2 (Me_a or Me_c)

Infra-red data (KBr disc) :

289(w), 410(m), 481(m), 508(m), 518(m), 566(m), 875(m), 1028(m), 1177(w), 1219(w), 1377(m), 1411(w), 1452(m), 1913(vs), 1929(vs), 1980(vs), 2921(w), 2957(w) cm^{-1}

A4.5 Data characterising [Mo(η³-$C_7H_3Me_4$-1,2,4,6)(CO)$_2$(dmpe)Cl]

Description : red crystals

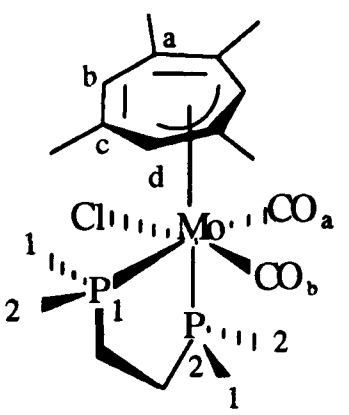

Elemental Analysis for $C_{19}H_{31}ClMoO_2P_2$:

Found (Required)/% : C 46.8 (47.1), H 6.5 (6.5), Cl 7.4 (7.3)

Mass spectrum (EI) :

595 {[$Mo_2(\eta\text{-}C_7H_3Me_4)_2(\mu\text{-}Cl)_3$]}, 430 (M - 2 CO), 280 (M - 2 CO - dmpe), 147 (base peak) ($C_7H_3Me_4$)

^{1}H NMR data : (300 MHz, 298 K, [$^2H_6$]-acetone)

5.32 (br s, 2 H, H_b)

4.80 [vt, *J* (H-P) 1.7, 1 H, H_d]

2.02 (s, 6 H, Me_a or Me_c)

1.97 (s, 6 H, Me_a or Me_c)

1.62 [d, *J* (H-P) 7.5, 12 H, Me]

1.55 (br s, 4 H, CH_2)

^{1}H NMR data : (300 MHz, 323 K, [$^2H_8$]-toluene)

5.42 (br s, 2 H, H_b)

4.92 (br s, 1 H, H_d)

2.08 (s, 6 H, Me_a or Me_c)

2.01 (s, 6 H, Me_a or Me_c)

1.25-1.55 (m, 2 H, H^1 or H^2)

1.29 [d, *J* (H-P) 8.6, 6 H, Me^1 or Me^2]

1.09 [d, *J* (H-P) 7.3, 6 H, Me^1 or Me^2]

0.88-1.18 (m, 2 H, H^1 or H^2)

Variable-temperature ^1H NMR data : (300 MHz, $[^2H_6]$-acetone)

$T_{coalescence}$ (Me^1 <=> $Me^{1'}$ or Me^2 <=> $Me^{2'}$ due to the trigonal twist rearrangment) = 270 ± 5 K

$\Delta\nu$ at low temperature limit = 56.65 Hz

$\Delta G^{\ddagger}$ = 53.5 ± 1.0 kJ mol^{-1}

^{13}C {^1H} NMR data : (75.43 MHz, 233 K, $[^2H_6]$-acetone)

229.6 [dd, *J* (C-P) 20.8, 25.6, CO_a]

225.5 [vt, *J* (C-P) 11.0, CO_b]

129.9 (br s, C on C_7 ring)

104.3 (br s, C on C_7 ring)

78.6 (br s, C on C_7 ring)

28.6 [d, *J* (C-P) 16.2, CH_2]

28.3 [d, *J* (C-P) 16.2, CH_2]

24.4-26.4 (Me on C_7 ring)

14.7 [d, *J* (C-P) 20.3, PMe]

14.5 [d, *J* (C-P) 26.4, PMe]

13.3 [d, *J* (C-P) 29.1, PMe]

10.3 [d, *J* (C-P) 14.4, PMe]

^{31}P {^1H} NMR data : (121.44 MHz, 230 K, $[^2H_6]$-acetone)

30.2 [d, *J* (P-P) 18.6, P_1 or P_2]

14.6 [d, *J* (P-P) 18.6, P_1 or P_2]

Variable-temperature ^{31}P NMR data : (121.44 MHz, $[^2H_6]$-acetone)

$T_{coalescence}$ (P_1 <=> P_2 due to the trigonal twist rearrangment) = 313 ± 2.5 K

$\Delta\nu$ at low temperature limit = 1887 Hz

$\Delta G^{\ddagger}$ = 53.3 ± 0.4 kJ mol^{-1}

Infra-red data (KBr disc) :

470(w), 487(w), 536(m), 568(m), 601(w), 618(w), 656(m), 710(m), 721(w), 741(m), 768(w), 798(w), 840(w), 857(w), 891(s), 935(s), 948(s), 1016(m), 1081(m), 1134(m), 1279(m), 1368(m), 1416(s), 1545(w), 1612(w), 1828(vs), 1910(vs), 2907(m), 2965(w) cm^{-1}

A4.6 Data characterising [Mo(η-$C_7H_3Me_4$-1,2,4,6)(dmpe)Cl]

Description : green oil

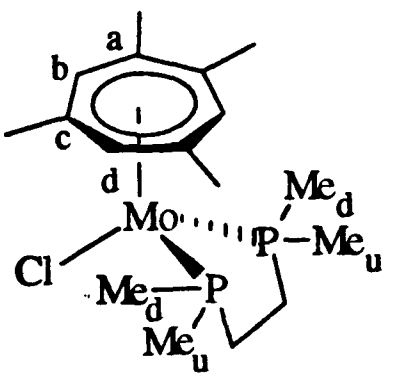

^{1}H NMR data : (300 MHz, [$^2H_6$]-benzene)

4.81 (br s, 2 H, H_b)

4.55 (br s, 1 H, H_d)

2.40 (s, 6 H, Me_a or Me_c)

2.17 (s, 6 H, Me_a or Me_c)

1.34 [d, *J* (H-P) 7.9, 6 H, Me_u or Me_d]

1.12-1.30 (m, 2 H, H_u or H_d)

0.94 [d, *J* (H-P) 8.1, 6 H, Me_u or Me_d]

0.56-0.82 (m, 2 H, H_u or H_d)

DEPT (θ = 3π/4) ^{13}C {^{1}H} NMR data : (75.43 MHz, [$^2H_6$]-benzene)

91.1 (s, C_b)

82.7 (s, C_d)

27.6 [vt, *J* (C-P) 20.4, CH_2]

26.3 (s, Me_a or Me_c)

23.9 (s, Me_a or Me_c)

17.1 [vt, *J* (C-P) 9.7, Me_u or Me_d]

12.8 [vt, *J* (C-P) 12.0, Me_u or Me_d]

^{31}P {^{1}H} NMR data : (121.44 MHz, [$^2H_6$]-benzene)

31.4 (dmpe)

A4.7 Data characterising [Mo(η-$C_7H_3Me_4$-1,2,4,6)(η-C_6H_5Me)][BF_4]

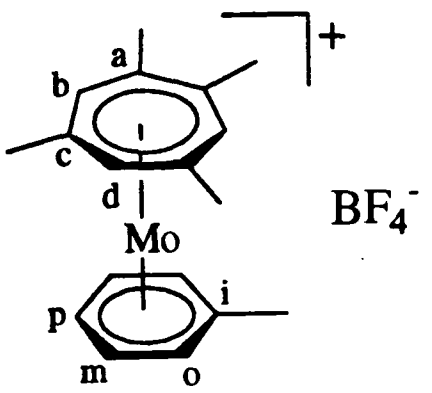

Description : pale green needle-like crystals

Elemental Analysis for $C_{18}H_{23}BF_4Mo$:

Found (Required)/% : C 51.1 (51.2), H 5.6 (5.5)

Mass Spectrum (FAB) :

337 (base peak) (M - BF_4)

^{1}H NMR data : (300 MHz, [$^2H_6$]-acetone)

6.16-6.22 (m, 4 H, H_o and H_m)

6.06-6.10 (m, 1 H, H_p)

5.89 (s, 2 H, H_b)

5.82 (s, 1 H, H_d)

2.49 (s, 6 H, Me_a or Me_c)

2.46 (s, 6 H, Me_a or Me_c)

2.25 (s, 3 H, Me)

^{13}C {^{1}H} NMR data : (75.43 MHz, [$^2H_6$]-acetone)

113.7 (C_i)

100.0 (C_o or C_m)

99.7 (C_a or C_c)

99.2 (C_a or C_c)

98.8 (C_o or C_m)

97.7 (C_p)

91.2 (C_b)

89.1 (C_d)

25.2 (Me_a or Me_c)

24.2 (Me_a or Me_c)

20.4 (Me)

Infra-red data (KBr disc) :

407(m), 522(m), 534(w), 773(w), 824(w), 895(m), 1055(vs), 1204(w), 1284(w), 1385(s), 1455(s), 1536(w), 1627(w), 2919(m), 2970(m) cm^{-1}

A4.8 Data characterising [Mo(η-$C_7H_3Me_4$-1,2,4,6)(acac)(PPh_3)]

Description : red crystals

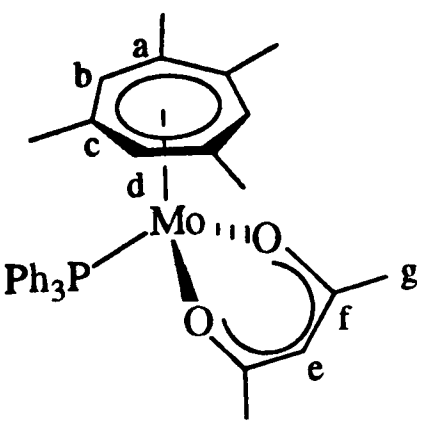

^1H NMR data : (300 MHz, [$^2H_6$]-acetone)

7.26-7.54 (m, 15 H, Ph)
5.41 (s, 1 H, H_e)
5.16 (br s, 1 H, H_d)
5.02 (br s, 2 H, H_b)
2.23 (s, 6 H, Me_a or Me_c)
2.18 (s, 6 H, Me_a or Me_c)
2.04 (s, 6 H, H_g)

^{13}C {^1H} NMR data : (75.43 MHz, [$^2H_6$]-acetone)

187.4 (s, C_f)
138.2 [d, *J* (C-P) 11.6, Ph]
134.5 (s, Ph)
134.3 (s, Ph)
132.7 (s, C_e)
129.7 (s, Ph)
129.5 (s, Ph)
129.4 (s, Ph)
99.4 (s, C_a or C_c)
96.4 (s, C_a or C_c)
91.9 (s, C_b)
87.2 (s, C_d)
27.7 (s, Me_a, Me_c or Me_g)

27.6 (s, Me_a, Me_c or Me_g)

25.5 (s, Me_a, Me_c or Me_g)

$^{31}P\{^1H\}$ NMR data : (121.44 MHz, $[^2H_6]$-acetone)

-8.4 (s, PPh_3)

Infra-red data (KBr disc) :

404(m), 446(w), 494(m), 515(m), 544(m), 564(w), 700(s), 709(s), 744(s), 749(s), 753(s), 778(m), 848(m), 858(m), 921(m), 1155(m), 1191(m), 1369(vs), 1400(s), 1432(vs), 1477(m), 1516(vs), 1578(vs), 2865(m), 2915(m), 2959(m), 3042(w) cm^{-1}

A5 Previously Unreported Data for Known Compounds

A5.1 Data characterising $[Mo(\eta\text{-}C_7H_7)(MeCN)I_2]$

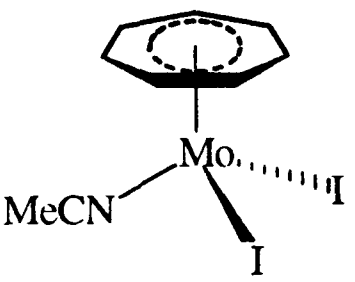

Magnetic data (1 T) :

antiferromagnetic with $T(\chi_{max}) = 16$ K

obey the Curie-Weiss law at 50-300 K with $C = 0.29$ emu-K mol^{-1},

$\theta = -5.2$ K, $\mu_{eff} = 1.53\ \mu_B$

Comment : X-ray crystal structure

A5.2 Data characterising [Mo(η-C_7H_7)(PMe_3)$_2$I]

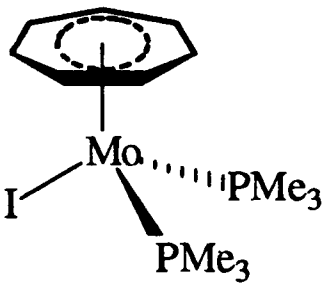

^{1}H NMR data : (300 MHz, [$^2H_6$]-benzene)

4.74 [t, *J* (H-P) 2.2, 7 H, η-C_7H_7]

1.05 [vt, *J* (H-P) 3.3, 18 H, Me]

^{13}C {^{1}H} NMR data : (75.43 MHz, [$^2H_6$]-benzene)

86.6 (s, η-C_7H_7)

20.8 [vt, *J* (C-P) 12.1, Me]

^{31}P {^{1}H} NMR data : (121.44 MHz, [$^2H_6$]-benzene)

-24.5 (br s, PMe_3)

Infra-red spectrum (KBr disc) :

667(s), 712(s), 809(vs), 845(m), 855(m), 870(w), 941(vs), 951(sh), 1099(w), 1282(s), 1299(m), 1419(s), 1507(w), 1653(w), 2901(m), 2972(m), 2993(w), 3025(w) cm^{-1}

A5.3 Data characterising [Mo(η-C_7H_7)(dppe)I]

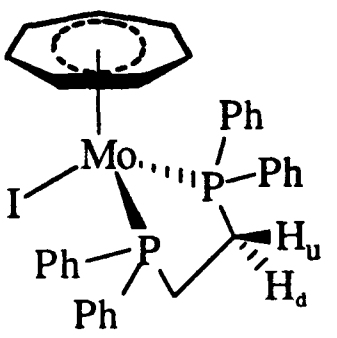

^{1}H NMR data : (300 MHz, [$^2H_6$]-benzene)

7.88 [t, *J* (H-H) 8.3, 4 H, Ph]

7.00-7.24 (m, 16 H, Ph)

4.91 [t, *J* (H-P) 1.9, 7 H, η-C_7H_7]

2.40-2.62 (m, 2 H, H_u or H_d)

1.73-2.00 (m, 2 H, H_u or H_d)

^{13}C {^{1}H} NMR data : (75.43 MHz, [$^2H_6$]-benzene)

141.4 [d, *J* (C-P) 27.0, Ph]

127.6-134.8 (Ph)

87.3 (s, η-C_7H_7)

27.2 [vt, *J* (C-P) 19.4, CH_2]

^{31}P {^{1}H} NMR data : (121.44 MHz, [$^2H_6$]-benzene)

53.5 (s, dppe)

A5.4 Data characterising [Mo(η-C_7H_7)(η-C_5H_5)]

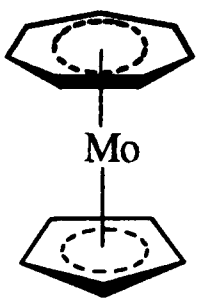

^{1}H NMR data : (300 MHz, [$^2H_6$]-benzene)

4.93 (s, 7 H, η-C_7H_7)

4.72 (s, 5 H, η-C_5H_5)

Electrochemical data (in MeCN) :

one reversible oxidation at $E_{1/2}$ = -0.60 V *vs.* SCE

A5.5 Data characterising [W(η-C_7H_7)(η-C_5H_5)]

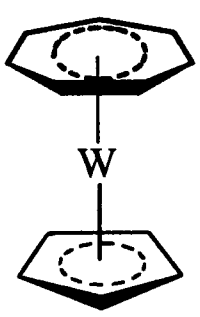

^{1}H NMR data : (300 MHz, [$^2H_6$]-benzene)

5.25 (s, 7 H, η-C_7H_7)

5.19 (s, 5 H, η-C_5H_5)

^{13}C {^{1}H} NMR data : (75.43 MHz, [$^2H_6$]-benzene)

82.5 (η-C_5H_5)

73.8 (η-C_7H_7)

Electrochemical data (in MeCN) :

one reversible oxidation at $E_{1/2}$ = -0.77 V *vs.* SCE

APPENDIX B

Crystallographic Details

B1 X-ray Crystal Structure Data for [Mo(η-C_7H_7)(MeCN)I_2]

B1.1 Crystal data, data collection and refinement

Formula	$C_9H_{10}I_2MoN$
M	481.93
Crystal Size / mm	0.20 x 0.40 x 0.50
Crystal System	Triclinic
Space Group	$P\bar{1}$
a / Å	7.219 (2)
b / Å	6.643 (2)
c / Å	13.149 (3)
α / °	96.95 (2)
β / °	94.31 (2)
γ / °	101.78 (2)
U / Å^3	609.6
Z	2
D_c / gcm^{-3}	2.626
μ / cm^{-1}	60.26
F(000)	438
Radiation (λ / Å)	0.71069 (Mo-Kα)
2θ limits / °	3-60
ω scan width	1.00 + 0.35 tan θ
Zone	0 - h, ± k, ± l
Scan Mode	ω - 2θ
Total data collected	4183
No. of Observations (I>3σ(I))	2606
R(merge)	0.014
No. of Variables	119
Obs. / Variables	21.9
Weighting Scheme	Chebyshev
Weighting Coefficients	51.6, -75.0, 50.1, -19.8, 5.59
Max / min peaks in final difference map / eÅ^{-3}	0.79, -0.02
r.m.s. shift / e.s.d. in final l.s. cycle	0.454
R[a]	0.029
R'[b]	0.033

[a] $R = \Sigma(|Fo - Fc|) / \Sigma|Fo|$; [b] $R' = \{\Sigma w(|Fo| - |Fc|)^2 / \Sigma w|Fo|^2\}^{1/2}$

B1.2 Bond length (Å) and angles (⁰)

MO(1)	- I(1)	2.8210(4)		MO(1)	- I(2)	2.8003(4)	
MO(1)	- N(1)	2.166(3)		MO(1)	- C(1)	2.264(4)	
MO(1)	- C(2)	2.271(5)		MO(1)	- C(3)	2.272(5)	
MO(1)	- C(4)	2.258(5)		MO(1)	- C(5)	2.280(5)	
MO(1)	- C(6)	2.260(5)		MO(1)	- C(7)	2.270(5)	
N(1)	- C(8)	1.135(6)		C(1)	- C(2)	1.389(8)	
C(1)	- C(7)	1.389(9)		C(2)	- C(3)	1.409(8)	
C(3)	- C(4)	1.392(9)		C(4)	- C(5)	1.41(1)	
C(5)	- C(6)	1.42(1)		C(6)	- C(7)	1.404(9)	
C(8)	- C(9)	1.450(6)					

I(2)	- MO(1)	- I(1)	87.47(1)	N(1)	- MO(1)	- I(1)	84.1(1)		
N(1)	- MO(1)	- I(2)	84.6(1)	C(1)	- MO(1)	- I(1)	88.2(1)		
C(1)	- MO(1)	- I(2)	118.9(2)	C(1)	- MO(1)	- N(1)	155.0(2)		
C(2)	- MO(1)	- I(1)	85.0(2)	C(2)	- MO(1)	- I(2)	153.5(2)		
C(2)	- MO(1)	- N(1)	119.7(2)	C(2)	- MO(1)	- C(1)	35.7(2)		
C(3)	- MO(1)	- I(1)	104.1(2)	C(3)	- MO(1)	- I(2)	167.2(2)		
C(3)	- MO(1)	- N(1)	91.1(2)	C(3)	- MO(1)	- C(1)	67.8(2)		
C(3)	- MO(1)	- C(2)	36.1(2)	C(4)	- MO(1)	- I(1)	136.3(2)		
C(4)	- MO(1)	- I(2)	131.4(2)	C(4)	- MO(1)	- N(1)	81.3(2)		
C(4)	- MO(1)	- C(1)	88.1(2)	C(4)	- MO(1)	- C(2)	67.5(2)		
C(4)	- MO(1)	- C(3)	35.8(2)	C(5)	- MO(1)	- I(1)	171.8(2)		
C(5)	- MO(1)	- I(2)	100.7(2)	C(5)	- MO(1)	- N(1)	96.4(2)		
C(5)	- MO(1)	- C(1)	88.0(2)	C(5)	- MO(1)	- C(2)	87.7(2)		
C(5)	- MO(1)	- C(3)	67.8(3)	C(6)	- MO(1)	- I(1)	146.4(2)		
C(6)	- MO(1)	- I(2)	85.1(2)	C(6)	- MO(1)	- N(1)	127.5(2)		
C(6)	- MO(1)	- C(1)	67.3(2)	C(6)	- MO(1)	- C(2)	87.2(2)		
C(6)	- MO(1)	- C(3)	88.0(2)	C(7)	- MO(1)	- I(1)	111.9(2)		
C(7)	- MO(1)	- I(2)	92.5(2)	C(7)	- MO(1)	- N(1)	163.6(2)		
C(7)	- MO(1)	- C(1)	35.7(2)	C(7)	- MO(1)	- C(2)	67.1(2)		
C(7)	- MO(1)	- C(3)	88.2(2)	C(5)	- MO(1)	- C(4)	36.3(3)		
C(6)	- MO(1)	- C(4)	68.2(2)	C(6)	- MO(1)	- C(5)	36.4(3)		
C(7)	- MO(1)	- C(4)	88.7(2)	C(7)	- MO(1)	- C(5)	68.3(2)		
C(7)	- MO(1)	- C(6)	36.1(2)	C(8)	- N(1)	- MO(1)	173.8(4)		
C(2)	- C(1)	- MO(1)	72.4(3)	C(7)	- C(1)	- MO(1)	72.4(3)		
C(7)	- C(1)	- C(2)	129.3(5)	C(1)	- C(2)	- MO(1)	71.9(3)		
C(3)	- C(2)	- MO(1)	72.0(3)	C(3)	- C(2)	- C(1)	129.4(5)		
C(2)	- C(3)	- MO(1)	71.9(3)	C(4)	- C(3)	- MO(1)	71.6(3)		
C(4)	- C(3)	- C(2)	127.7(5)	C(3)	- C(4)	- MO(1)	72.6(3)		
C(5)	- C(4)	- MO(1)	72.7(3)	C(5)	- C(4)	- C(3)	129.3(5)		
C(4)	- C(5)	- MO(1)	71.0(3)	C(6)	- C(5)	- MO(1)	71.0(3)		
C(6)	- C(5)	- C(4)	126.9(5)	C(5)	- C(6)	- MO(1)	72.6(3)		
C(7)	- C(6)	- MO(1)	72.3(3)						
C(7)	- C(6)	- C(5)	129.7(5)	C(1)	- C(7)	- MO(1)	71.9(3)		
C(6)	- C(7)	- MO(1)	71.5(3)	C(6)	- C(7)	- C(1)	127.6(5)		

B1.3 Fractional atomic coordinates and thermal parameters

Atom	x/a	y/b	z/c	U(iso)
MO(1)	0.82446(4)	0.36101(5)	0.22056(2)	0.0278
I(1)	0.49591(4)	0.04065(5)	0.20510(3)	0.0444
I(2)	0.96352(5)	0.19735(6)	0.38988(2)	0.0493
N(1)	0.6794(6)	0.5214(6)	0.3320(3)	0.0404
C(1)	0.8758(9)	0.2306(9)	0.0605(4)	0.0489
C(2)	0.7482(9)	0.359(1)	0.0497(4)	0.0531
C(3)	0.7557(9)	0.5607(9)	0.1003(4)	0.0543
C(4)	0.897(1)	0.6811(8)	0.1732(5)	0.0529
C(5)	1.0690(9)	0.635(1)	0.2136(5)	0.0593
C(6)	1.1327(7)	0.449(1)	0.1904(5)	0.0574
C(7)	1.0471(8)	0.268(1)	0.1224(4)	0.0534
C(8)	0.6089(8)	0.6211(7)	0.3865(4)	0.0440
C(9)	0.519(1)	0.752(1)	0.4545(5)	0.0585
H(11)	0.8389(9)	0.0965(9)	0.0194(4)	0.0702
H(21)	0.6400(9)	0.303(1)	-0.0000(4)	0.0685
H(31)	0.6513(9)	0.6227(9)	0.0816(4)	0.0832
H(41)	0.873(1)	0.8124(8)	0.2013(5)	0.0787
H(51)	1.1519(9)	0.744(1)	0.2607(5)	0.0867
H(61)	1.2513(7)	0.445(1)	0.2275(5)	0.0806
H(71)	1.1149(8)	0.158(1)	0.1180(4)	0.0826
H(91)	0.563(1)	0.746(1)	0.5246(5)	0.0947
H(92)	0.549(1)	0.892(1)	0.4405(5)	0.0947
H(93)	0.384(1)	0.700(1)	0.4435(5)	0.0947

B1.3 Fractional atomic coordinates and thermal parameters (continued)

Atom	U(11)	U(22)	U(33)	U(23)	U(13)	U(12)
MO(1)	0.0300(2)	0.0254(1)	0.0279(1)	0.0023(1)	0.0044(1)	0.0055(1)
I(1)	0.0341(1)	0.0385(2)	0.0628(2)	0.0050(1)	0.0016(1)	-0.0022(1)
I(2)	0.0617(2)	0.0560(2)	0.0397(2)	0.0119(1)	-0.0064(1)	0.0177(1)
N(1)	0.052(2)	0.037(2)	0.038(2)	0.003(1)	0.011(2)	0.015(2)
C(1)	0.078(4)	0.054(3)	0.034(2)	-0.003(2)	0.022(2)	0.014(3)
C(2)	0.065(3)	0.073(3)	0.032(2)	0.012(2)	0.001(2)	0.010(3)
C(3)	0.071(3)	0.066(3)	0.055(3)	0.030(3)	0.018(3)	0.032(3)
C(4)	0.086(4)	0.031(2)	0.068(3)	0.016(2)	0.029(3)	0.009(2)
C(5)	0.065(4)	0.064(3)	0.063(3)	0.005(3)	0.019(3)	-0.025(3)
C(6)	0.031(2)	0.100(5)	0.070(4)	0.027(3)	0.014(2)	0.007(3)
C(7)	0.058(3)	0.072(4)	0.060(3)	0.018(3)	0.031(2)	0.031(3)
C(8)	0.065(3)	0.039(2)	0.039(2)	0.006(2)	0.013(2)	0.018(2)
C(9)	0.111(5)	0.060(3)	0.056(3)	0.013(3)	0.038(3)	0.048(3)

B2 X-ray Crystal Structure Data for $[NBu_4][Mo(\eta\text{-}C_7H_7)I_3]$

B2.1 Crystal data, data collection and refinement

Formula	$C_{23}H_{43}I_3MoN$
M	810.26
Crystal Size / mm	0.20 x 0.22 x 0.84
Crystal System	Orthorhombic
Space Group	Pnma
a / Å	17.137 (2)
b / Å	11.365 (1)
c / Å	15.943 (1)
U / Å^3	3105.2
Z	4
D_c / gcm^{-3}	1.73
μ / cm^{-1}	33.74
F(000)	1556
Radiation (λ / Å)	0.71069 (Mo-Kα)
Scan Mode	ω - 2θ
Total data collected	3528
No. of Observations (I>4σ(I))	1967
R(merge)	0.013
No. of Variables	145
Obs. / Variables	13.6
Weighting Scheme	Chebyshev
Weighting Coefficients	11.7, -6.00, 9.15
Max / min peaks in final difference map / eÅ^{-3}	0.57, -0.63
R[a]	0.035
R'[b]	0.041

[a] $R = \Sigma(|Fo| - |Fc|) / \Sigma|Fo|$; [b] $R' = \{\Sigma w(|Fo| - |Fc|)^2 / \Sigma w|Fo|^2\}^{1/2}$

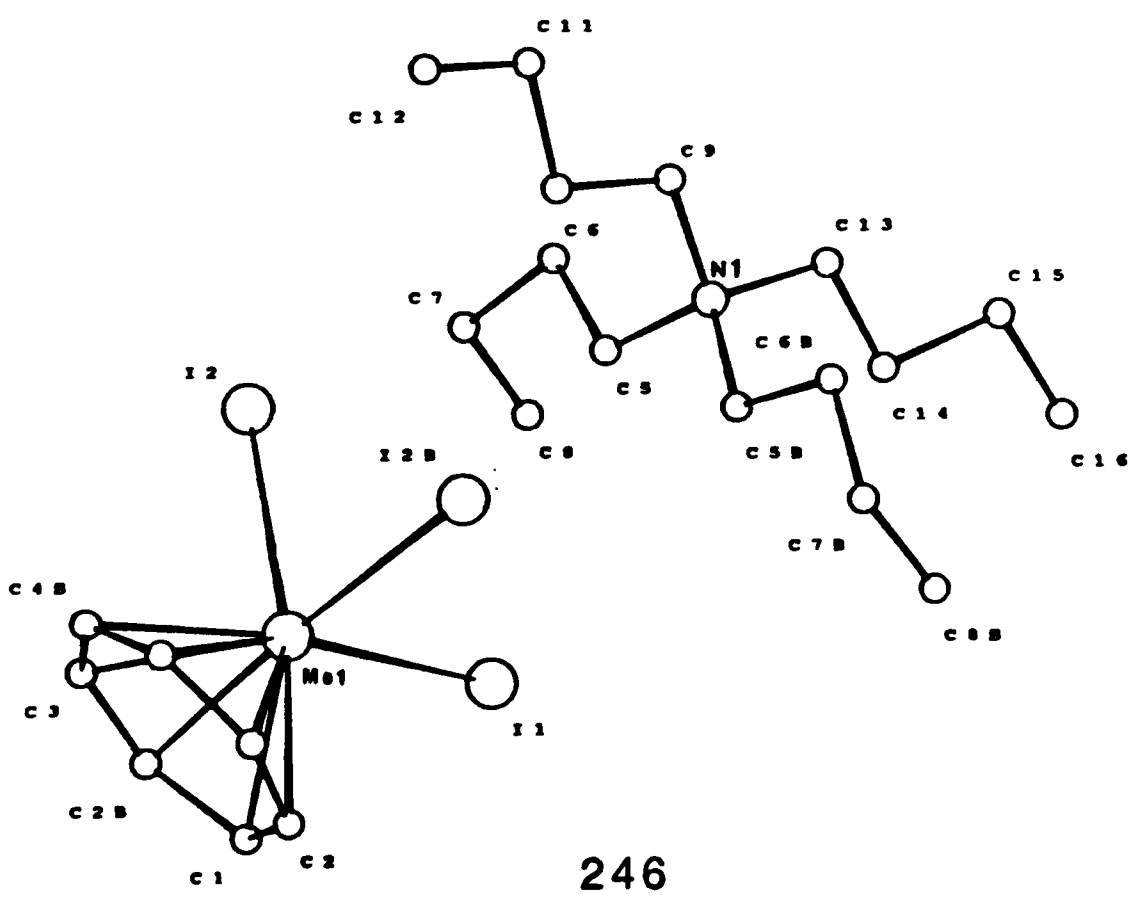

B2.2 Bond length (Å) and angles (⁰)

I(1)	- MO(1)	2.8386(9)	
I(2)	- MO(1)	2.8394(7)	
MO(1)	- C(1)	2.22(1)	
MO(1)	- C(2)	2.21(1)	
MO(1)	- C(2)	2.21(1)	
MO(1)	- C(3)	2.22(1)	
MO(1)	- C(3)	2.22(1)	
MO(1)	- C(4)	2.236(8)	
MO(1)	- C(4)	2.236(8)	
N(1)	- C(5)	1.514(8)	
N(1)	- C(5)	1.514(8)	
N(1)	- C(9)	1.52(1)	
N(1)	- C(13)	1.52(1)	
C(1)	- C(2)	1.36(2)	
C(1)	- C(2)	1.36(2)	
C(2)	- C(3)	1.34(2)	
C(3)	- C(4)	1.34(2)	
C(4)	- C(4)	1.32(2)	
C(5)	- C(6)	1.49(1)	
C(6)	- C(7)	1.52(1)	
C(7)	- C(8)	1.47(2)	
C(9)	- C(10)	1.50(2)	
C(10)	- C(11)	1.47(3)	
C(11)	- C(12)	1.23(6)	
C(13)	- C(14)	1.45(2)	
C(14)	- C(15)	1.48(2)	
C(15)	- C(16)	1.36(3)	

I(2)	- MO(1)	- I(1)	87.47(2)
I(2)	- MO(1)	- I(1)	87.47(2)
I(2)	- MO(1)	- I(2)	86.33(3)
C(1)	- MO(1)	- I(1)	82.6(5)
C(1)	- MO(1)	- I(2)	135.76(9)
C(1)	- MO(1)	- I(2)	135.76(9)
C(2)	- MO(1)	- I(1)	95.6(4)
C(2)	- MO(1)	- I(2)	169.7(4)
C(2)	- MO(1)	- I(2)	103.6(5)
C(2)	- MO(1)	- C(1)	35.7(6)
C(2)	- MO(1)	- I(1)	95.6(4)
C(2)	- MO(1)	- I(2)	103.6(5)
C(2)	- MO(1)	- I(2)	169.7(4)
C(2)	- MO(1)	- C(1)	35.7(6)
C(2)	- MO(1)	- C(2)	66.3(10)
C(3)	- MO(1)	- I(1)	124.3(5)
C(3)	- MO(1)	- I(2)	84.6(4)
C(3)	- MO(1)	- I(2)	146.3(6)
C(3)	- MO(1)	- C(1)	66.7(6)
C(3)	- MO(1)	- C(2)	85.6(5)
C(3)	- MO(1)	- C(2)	35.1(6)
C(3)	- MO(1)	- I(1)	124.3(5)
C(3)	- MO(1)	- I(2)	146.3(6)
C(3)	- MO(1)	- I(2)	84.6(4)
C(3)	- MO(1)	- C(1)	66.7(6)
C(3)	- MO(1)	- C(2)	35.1(6)
C(3)	- MO(1)	- C(2)	85.6(5)

C(4)	- MO(1)	- I(1)	159.4(3)
C(4)	- MO(1)	- I(2)	112.5(3)
C(4)	- MO(1)	- I(2)	88.9(3)
C(4)	- MO(1)	- C(1)	85.9(5)
C(4)	- MO(1)	- C(2)	65.7(5)
C(4)	- MO(1)	- C(2)	84.8(4)
C(4)	- MO(1)	- I(1)	159.4(3)
C(4)	- MO(1)	- I(2)	88.9(3)
C(4)	- MO(1)	- I(2)	112.5(3)
C(4)	- MO(1)	- C(1)	85.9(5)
C(4)	- MO(1)	- C(2)	84.8(4)
C(4)	- MO(1)	- C(2)	65.7(5)
C(3)	- MO(1)	- C(3)	85.3(6)
C(4)	- MO(1)	- C(3)	65.2(6)
C(4)	- MO(1)	- C(3)	35.1(5)
C(4)	- MO(1)	- C(3)	35.1(5)
C(4)	- MO(1)	- C(3)	65.2(6)
C(4)	- MO(1)	- C(4)	34.3(7)
C(5)	- N(1)	- C(5)	104.6(7)
C(9)	- N(1)	- C(5)	111.0(5)
C(9)	- N(1)	- C(5)	111.0(5)
C(13)	- N(1)	- C(5)	112.4(5)
C(13)	- N(1)	- C(5)	112.4(5)
C(13)	- N(1)	- C(9)	105.5(8)
C(2)	- C(1)	- MO(1)	71.7(8)
C(2)	- C(1)	- MO(1)	71.7(8)
C(2)	- C(1)	- C(2)	125.8(17)
C(1)	- C(2)	- MO(1)	72.6(8)
C(3)	- C(2)	- MO(1)	72.9(7)
C(3)	- C(2)	- C(1)	129.9(14)
C(2)	- C(3)	- MO(1)	71.9(7)
C(4)	- C(3)	- MO(1)	73.1(6)
C(4)	- C(3)	- C(2)	128.1(13)
C(3)	- C(4)	- MO(1)	71.9(6)
C(4)	- C(4)	- MO(1)	72.9(3)
C(4)	- C(4)	- C(3)	129.1(9)

C(6)	- C(5)	- N(1)	116.2(6)
C(7)	- C(6)	- C(5)	109.6(8)
C(8)	- C(7)	- C(6)	114.0(12)
C(10)	- C(9)	- N(1)	116.6(9)
C(11)	- C(10)	- C(9)	113.4(13)
C(12)	- C(11)	- C(10)	123.4(28)
C(14)	- C(13)	- N(1)	116.4(9)
C(15)	- C(14)	- C(13)	112.2(13)
C(16)	- C(15)	- C(14)	120.4(20)

B2.3 Fractional atomic coordinates and thermal parameters

Atom	x/a	y/b	z/c	U(iso)
I(1)	0.01829(4)	0.2500	0.12328(4)	0.0619
I(2)	0.18459(3)	0.07909(4)	0.00571(3)	0.0688
MO(1)	0.07321(4)	0.2500	-0.04470(5)	0.0545
N(1)	0.2448(5)	0.2500	0.2916(5)	0.0662
C(1)	-0.0535(8)	0.2500	-0.074(1)	0.1231
C(2)	-0.0238(9)	0.356(2)	-0.0956(9)	0.1090
C(3)	0.040(1)	0.118(1)	-0.1407(8)	0.1017
C(4)	0.0899(6)	0.308(1)	-0.1775(5)	0.0980
C(5)	0.1988(4)	0.1446(7)	0.2610(5)	0.0713
C(6)	0.2343(6)	0.0269(8)	0.2773(6)	0.0969
C(7)	0.1754(9)	-0.069(1)	0.2566(9)	0.1272
C(8)	0.109(1)	-0.075(1)	0.315(1)	0.1551
C(9)	0.3266(6)	0.2500	0.2557(8)	0.0839
C(10)	0.3332(8)	0.2500	0.1621(9)	0.1141
C(11)	0.415(2)	0.2500	0.132(1)	0.1883
C(12)	0.432(2)	0.2500	0.057(4)	0.3637
C(13)	0.2552(7)	0.2500	0.3865(6)	0.0710
C(14)	0.1842(9)	0.2500	0.4363(9)	0.1100
C(15)	0.200(1)	0.2500	0.5273(9)	0.1229
C(16)	0.141(2)	0.2500	0.584(2)	0.2530

Atom	U(11)	U(22)	U(33)	U(23)	U(13)	U(12)
I(1)	0.0565(3)	0.0743(4)	0.0575(3)	0.0000	0.0080(3)	0.0000
I(2)	0.0735(3)	0.0648(3)	0.0732(3)	-0.0102(2)	-0.0016(2)	0.0146(2)
MO(1)	0.0543(4)	0.0605(5)	0.0495(4)	0.0000	-0.0021(3)	0.0000
N(1)	0.075(5)	0.062(5)	0.072(5)	0.0000	-0.027(4)	0.0000
C(1)	0.041(6)	0.70(5)	0.072(9)	0.0000	-0.016(6)	0.0000
C(2)	0.21(1)	0.30(2)	0.12(1)	-0.11(1)	-0.091(9)	0.21(1)
C(3)	0.30(2)	0.053(6)	0.13(1)	0.005(7)	-0.12(1)	-0.04(1)
C(4)	0.134(8)	0.15(1)	0.065(4)	0.037(5)	-0.021(5)	-0.047(7)
C(5)	0.088(5)	0.060(4)	0.078(4)	-0.007(4)	-0.026(4)	0.001(4)
C(6)	0.125(7)	0.072(5)	0.115(7)	-0.007(5)	-0.039(6)	0.012(5)
C(7)	0.21(2)	0.084(7)	0.15(1)	0.009(8)	-0.08(1)	-0.021(9)
C(8)	0.26(2)	0.105(9)	0.20(2)	0.03(1)	-0.08(1)	-0.07(1)
C(9)	0.059(6)	0.12(1)	0.101(8)	0.0000	-0.028(6)	0.0000
C(10)	0.074(8)	0.25(2)	0.084(8)	0.0000	-0.018(7)	0.0000
C(11)	0.12(2)	0.45(5)	0.12(2)	0.0000	-0.02(1)	0.0000
C(12)	0.09(2)	1.3(2)	0.42(8)	0.0000	-0.05(3)	0.0000
C(13)	0.094(7)	0.065(6)	0.066(6)	0.0000	-0.026(5)	0.0000
C(14)	0.10(1)	0.17(2)	0.079(8)	0.0000	-0.018(7)	0.0000
C(15)	0.19(2)	0.14(1)	0.074(8)	0.0000	-0.01(1)	0.0000
C(16)	0.21(3)	0.8(1)	0.10(2)	0.0000	-0.02(2)	0.0000

B3 X-ray Crystal Structure Data for [Mo(η-C_7H_7)(η-C_5H_4Me)]

B3.1 Crystal data, data collection and refinement

Formula	$C_{13}H_{14}Mo$
M	266.19
Crystal Size / mm	0.30 x 0.40 x 0.50
Crystal System	Monoclinic
Space Group	$P2_1/C$
a / Å	12.512 (10)
b / Å	8.018 (7)
c / Å	11.521 (12)
β / °	112.82 (8)
U / Å^3	1065.2
Z	4
D_c / gcm^{-3}	1.66
μ / cm^{-1}	11.58
F(000)	536
Radiation (λ / Å)	0.71069 (Mo-Kα)
2θ limits / °	2 - 50
ω scan width	1.20 + 0.35 tan θ
Scan Mode	ω - 2θ
Total data collected	2689
No. of Observations (I>3σ(I))	1446
R(merge)	0.086
No. of Variables	128
Obs. / Variables	11.3
Weighting Scheme	Chebyshev
Weighting Coefficients	25.1, -33.9, 27.0, -11.1, 4.13
Max / min peaks in final difference map / eÅ^{-3}	0.61, -0.03
r.m.s. shift / e.s.d. in final l.s. cycle	0.0437
R[a]	0.035
R'[b]	0.039

[a] $R = \Sigma(|Fo - Fc|) / \Sigma|Fo|$; [b] $R' = \{\Sigma w(|Fo| - |Fc|)^2 / \Sigma w|Fo|^2\}^{1/2}$

B3.2 Bond length (Å) and angles (⁰)

MO(1) - C(1)	2.334(4)	MO(1) - C(2)	2.312(5)
MO(1) - C(3)	2.306(5)	MO(1) - C(4)	2.304(5)
MO(1) - C(5)	2.317(5)	MO(1) - C(11)	2.255(5)
MO(1) - C(12)	2.246(5)	MO(1) - C(13)	2.269(5)
MO(1) - C(14)	2.247(5)	MO(1) - C(15)	2.247(5)
MO(1) - C(16)	2.243(6)	MO(1) - C(17)	2.241(6)
C(1) - C(2)	1.417(7)	C(1) - C(5)	1.409(7)
C(1) - C(6)	1.497(7)	C(2) - C(3)	1.393(8)
C(3) - C(4)	1.393(8)	C(4) - C(5)	1.417(7)
C(11) - C(12)	1.357(9)	C(11) - C(17)	1.36(1)
C(12) - C(13)	1.381(9)	C(13) - C(14)	1.391(9)
C(14) - C(15)	1.42(1)	C(15) - C(16)	1.42(1)
C(16) - C(17)	1.39(1)		

B3.2 Bond length (Å) and angles (⁰) (continued)

C(2)	- MO(1) -	C(1)	35.5(2)	C(3)	- MO(1) -	C(1)	59.0(2)
C(3)	- MO(1) -	C(2)	35.1(2)	C(4)	- MO(1) -	C(1)	59.3(2)
C(4)	- MO(1) -	C(2)	58.7(2)	C(4)	- MO(1) -	C(3)	35.2(2)
C(5)	- MO(1) -	C(1)	35.3(2)	C(5)	- MO(1) -	C(2)	58.6(2)
C(5)	- MO(1) -	C(3)	58.8(2)	C(5)	- MO(1) -	C(4)	35.7(2)
C(11)	- MO(1) -	C(1)	104.5(2)	C(11)	- MO(1) -	C(2)	110.8(2)
C(11)	- MO(1) -	C(3)	141.9(2)	C(11)	- MO(1) -	C(4)	163.5(2)
C(11)	- MO(1) -	C(5)	128.8(2)	C(12)	- MO(1) -	C(1)	119.5(2)
C(12)	- MO(1) -	C(2)	103.7(2)	C(12)	- MO(1) -	C(3)	118.9(2)
C(12)	- MO(1) -	C(4)	153.4(2)	C(12)	- MO(1) -	C(5)	154.3(2)
C(12)	- MO(1) -	C(11)	35.1(2)	C(13)	- MO(1) -	C(1)	144.3(2)
C(13)	- MO(1) -	C(2)	112.7(2)	C(13)	- MO(1) -	C(3)	105.5(2)
C(13)	- MO(1) -	C(4)	128.0(2)	C(13)	- MO(1) -	C(5)	163.2(2)
C(13)	- MO(1) -	C(11)	66.6(2)	C(14)	- MO(1) -	C(1)	166.1(2)
C(14)	- MO(1) -	C(2)	133.8(2)	C(14)	- MO(1) -	C(3)	107.2(2)
C(14)	- MO(1) -	C(4)	108.8(2)	C(14)	- MO(1) -	C(5)	138.2(2)
C(14)	- MO(1) -	C(11)	87.7(2)	C(15)	- MO(1) -	C(1)	147.6(3)
C(15)	- MO(1) -	C(2)	160.0(3)	C(15)	- MO(1) -	C(3)	124.9(3)
C(15)	- MO(1) -	C(4)	104.2(2)	C(15)	- MO(1) -	C(5)	114.8(2)
C(15)	- MO(1) -	C(11)	88.1(2)	C(16)	- MO(1) -	C(1)	121.6(2)
C(16)	- MO(1) -	C(2)	157.1(2)	C(16)	- MO(1) -	C(3)	150.8(3)
C(16)	- MO(1) -	C(4)	116.8(3)	C(16)	- MO(1) -	C(5)	103.7(2)
C(16)	- MO(1) -	C(11)	67.3(3)	C(17)	- MO(1) -	C(1)	105.6(2)
C(17)	- MO(1) -	C(2)	131.3(3)	C(17)	- MO(1) -	C(3)	164.6(2)
C(17)	- MO(1) -	C(4)	140.5(3)	C(17)	- MO(1) -	C(5)	110.0(2)
C(17)	- MO(1) -	C(11)	35.1(3)	C(13)	- MO(1) -	C(12)	35.6(2)
C(14)	- MO(1) -	C(12)	67.4(2)	C(14)	- MO(1) -	C(13)	35.9(2)
C(15)	- MO(1) -	C(12)	88.0(2)	C(15)	- MO(1) -	C(13)	68.1(3)
C(15)	- MO(1) -	C(14)	36.8(3)	C(16)	- MO(1) -	C(12)	87.2(2)
C(16)	- MO(1) -	C(13)	88.0(2)	C(16)	- MO(1) -	C(14)	68.9(3)
C(16)	- MO(1) -	C(15)	36.8(3)	C(17)	- MO(1) -	C(12)	65.9(3)
C(17)	- MO(1) -	C(13)	86.6(2)				
C(17)	- MO(1) -	C(14)	88.1(2)	C(17)	- MO(1) -	C(15)	68.2(3)
C(17)	- MO(1) -	C(16)	36.1(3)	C(2)	- C(1) -	MO(1)	71.4(3)
C(5)	- C(1) -	MO(1)	71.7(3)	C(5)	- C(1) -	C(2)	106.5(5)
C(6)	- C(1) -	MO(1)	125.9(4)	C(6)	- C(1) -	C(2)	126.0(5)
C(6)	- C(1) -	C(5)	127.3(5)	C(1)	- C(2) -	MO(1)	73.1(3)
C(3)	- C(2) -	MO(1)	72.2(3)	C(3)	- C(2) -	C(1)	108.9(5)
C(2)	- C(3) -	MO(1)	72.7(3)	C(4)	- C(3) -	MO(1)	72.3(3)
C(4)	- C(3) -	C(2)	108.5(5)	C(3)	- C(4) -	MO(1)	72.5(3)
C(5)	- C(4) -	MO(1)	72.6(3)	C(5)	- C(4) -	C(3)	107.6(5)
C(1)	- C(5) -	MO(1)	73.0(3)	C(4)	- C(5) -	MO(1)	71.7(3)
C(4)	- C(5) -	C(1)	108.5(5)	C(12)	- C(11) -	MO(1)	72.1(3)
C(17)	- C(11) -	MO(1)	71.9(4)	C(17)	- C(11) -	C(12)	128.3(6)
C(11)	- C(12) -	MO(1)	72.8(3)	C(13)	- C(12) -	MO(1)	73.1(3)
C(13)	- C(12) -	C(11)	130.3(6)	C(12)	- C(13) -	MO(1)	71.3(3)
C(14)	- C(13) -	MO(1)	71.2(3)	C(14)	- C(13) -	C(12)	128.1(6)
C(13)	- C(14) -	MO(1)	72.9(3)	C(15)	- C(14) -	MO(1)	71.6(3)
C(15)	- C(14) -	C(13)	128.1(6)	C(14)	- C(15) -	MO(1)	71.6(3)
C(16)	- C(15) -	MO(1)	71.4(4)	C(16)	- C(15) -	C(14)	127.2(6)
C(15)	- C(16) -	MO(1)	71.8(4)	C(17)	- C(16) -	MO(1)	71.9(4)
C(17)	- C(16) -	C(15)	127.6(6)	C(11)	- C(17) -	MO(1)	73.0(3)
C(16)	- C(17) -	MO(1)	72.0(4)	C(16)	- C(17) -	C(11)	130.3(6)

B3.3 Fractional atomic coordinates and thermal parameters

Atom	x/a	y/b	z/c	U(iso)
MO(1)	0.77378(3)	0.01311(4)	0.04739(3)	0.0316
C(1)	0.7035(4)	-0.1145(6)	-0.1502(4)	0.0428
C(2)	0.8237(4)	-0.0835(7)	-0.1140(5)	0.0449
C(3)	0.8850(5)	-0.1769(7)	-0.0067(5)	0.0493
C(4)	0.8059(5)	-0.2663(6)	0.0270(5)	0.0491
C(5)	0.6933(5)	-0.2284(6)	-0.0620(5)	0.0437
C(6)	0.6082(6)	-0.050(1)	-0.2661(5)	0.0669
C(11)	0.7064(6)	0.2767(7)	0.0095(6)	0.0585
C(12)	0.8238(6)	0.2838(6)	0.0637(6)	0.0514
C(13)	0.9007(5)	0.2052(7)	0.1699(6)	0.0511
C(14)	0.8763(7)	0.0911(8)	0.2472(5)	0.0594
C(15)	0.7663(9)	0.0334(8)	0.2386(7)	0.0593
C(16)	0.6565(7)	0.077(1)	0.1466(9)	0.0635
C(17)	0.6332(5)	0.1869(9)	0.0464(7)	0.0616
H(11)	0.6690(6)	0.3421(7)	-0.0652(6)	0.0769
H(12)	0.8581(6)	0.3573(6)	0.0220(6)	0.0741
H(13)	0.9812(5)	0.2299(7)	0.1911(6)	0.0751
H(14)	0.9421(7)	0.0477(8)	0.3162(5)	0.0747
H(15)	0.7659(9)	-0.0431(8)	0.3026(7)	0.1013
H(16)	0.5902(7)	0.024(1)	0.1531(9)	0.1110
H(17)	0.5522(5)	0.2019(9)	-0.0042(7)	0.0931
H(2)	0.8569(4)	-0.0103(7)	-0.1569(5)	0.0679
H(3)	0.9676(5)	-0.1770(7)	0.0380(5)	0.0665
H(4)	0.8252(5)	-0.3426(6)	0.0964(5)	0.0641
H(5)	0.6218(5)	-0.2711(6)	-0.0615(5)	0.0636
H(61)	0.5354(6)	-0.090(1)	-0.2682(5)	0.0803
H(62)	0.6191(6)	-0.086(1)	-0.3402(5)	0.0803
H(63)	0.6084(6)	0.070(1)	-0.2636(5)	0.0803

B3.3 Fractional atomic coordinates and thermal parameters (continued)

Atom	U(11)	U(22)	U(33)	U(23)	U(13)	U(12)
MO(1)	0.0330(2)	0.0309(2)	0.0312(2)	-0.0029(2)	0.0125(2)	-0.0012(2)
C(1)	0.046(3)	0.048(3)	0.036(2)	-0.011(2)	0.013(2)	-0.003(2)
C(2)	0.048(3)	0.055(3)	0.051(3)	-0.017(2)	0.029(2)	-0.011(2)
C(3)	0.040(3)	0.056(3)	0.058(3)	-0.016(3)	0.015(3)	0.007(2)
C(4)	0.065(4)	0.037(3)	0.046(3)	-0.004(2)	0.008(3)	0.010(2)
C(5)	0.045(3)	0.044(3)	0.054(3)	-0.016(2)	0.025(2)	-0.013(2)
C(6)	0.066(4)	0.097(5)	0.041(3)	-0.001(3)	0.009(3)	-0.002(4)
C(11)	0.077(5)	0.047(3)	0.060(4)	-0.000(3)	0.018(3)	0.023(3)
C(12)	0.083(5)	0.036(3)	0.063(4)	-0.006(2)	0.044(3)	-0.010(3)
C(13)	0.045(3)	0.054(3)	0.069(4)	-0.027(3)	0.019(3)	-0.015(3)
C(14)	0.094(5)	0.058(4)	0.038(3)	-0.012(3)	0.001(3)	0.018(4)
C(15)	0.178(9)	0.049(3)	0.060(4)	-0.011(3)	0.084(6)	-0.015(5)
C(16)	0.084(5)	0.079(5)	0.112(6)	-0.045(5)	0.076(5)	-0.034(4)
C(17)	0.040(4)	0.082(5)	0.089(5)	-0.030(4)	0.015(3)	0.017(3)

APPENDIX C

X-ray Powder Diffraction Data

	$\{ZrS_2[Mo(\eta\text{-}C_7H_7)(\eta\text{-}C_5H_4Me)]_{0.22}\}$		$\{ZrS_2[W(\eta\text{-}C_7H_7)(\eta\text{-}C_5H_4Me)]_{0.20}\}$	
hkl	*d* (obs), Å	*d* (calc), Å	*d* (obs), Å	*d* (calc), Å
001	11.7464	11.7435	11.8250	11.8310
002	5.9608	5.9186	5.9270	5.9202
003	3.9510	3.9564	3.9693	3.9479
004	2.9782	2.9713	2.9786	2.9613
005	2.3639	2.3790	2.3699	2.3692
006	1.9822	1.9837	1.9672	1.9745
007	1.7011	1.7010	1.6885	1.6925
008	1.4899	1.4889	1.4840	1.4810